MODULATION OF THE CRITICAL SMALL VENTROLATERAL PACEMAKER NEURONS IN DROSOPHILA

by

Katherine R. Lelito

A dissertation submitted in partial fulfillment
of the requirements for the degree of
Doctor of Philosophy
(Molecular, Cellular and Developmental Biology)
in the University of Michigan
2014

Doctoral Committee:

Assistant Professor Orie T. Shafer, Chair
Assistant Professor Catherine A. Collins
Professor Richard I. Hume
Assistant Professor Scott Pletcher

© Katherine R. Lelito

All Rights Reserved

2014

To the women of the world

May you, too, have the opportunity and motivation to pursue your dreams, whatever they may be.

ACKNOWLEDGEMENTS

I owe so much gratitude to advisors, colleagues, friends and family, who helped me during my doctoral studies. I extend my deepest gratitude to my mentor, Dr. Orie Shafer, whose enthusiasm and expertise in circadian biology made me fall in love with the field. Orie fosters an exciting and collegial lab environment that preserves the "fun" in scientific research that draws most scholars into academia. I also thank the members of my thesis committee: Dr. Rich Hume, for always having an open door and time to discuss my project; Dr. Catherine Collins, for applying her eye for detail to my thesis work and asking difficult questions; Dr. Scott Pletcher, for his insightful outsider's critique of my work– his passion for science and commitment to his department continues to inspire me.

To my very closest friends and colleagues here at University of Michigan- now Dr. Mohammad Samie, Dr. Marcelo Pires de Oliveira, and Qi Zhang: I'm thankful to have had your companionship and advice through the years. Many thanks to Marcelo, especially, who was my pharmacology spiritual leader throughout this journey. I am also grateful to the current and former members of the Shafer lab for assistance in the lab, critical input on my research at lab meetings, and their time listening to hours of my practice talks with such patience, especially Tammy Minosyan, Aaron Talsma, Zepeng Yao, Charles Williams VI, Ann Marie Macara, Jennifer Denike, Andrew Bahl, Veronica Rios, Harper Jocque, and Sara Lennox. I would like to recognize the work of several programmers who I worked closely with to develop a data-processing program that has become critically important to the lab and my research: Alok Talekar, Ashish Farmer, Mary Hemmeter, and Chris Broussard. Special thanks to Dr. Susan Klinedinst, Dr. Isabel Martinez-Pena y Valenzuela and Sara Lennox for their friendship and support inside and outside of

the lab. I would also like to thank Sukanya Punthambaker, Sara Parker, Xin Xiong, and Xin Wang. These wonderful women helped me early on to stay afloat in a challenging department and helped me determine the best lab environment for rotations and doctoral study.

I would like to express my great appreciation to the many members of the MCDB department, especially the Xu Lab, Hume Lab, Denver Lab, Akaaboune Lab, Kuwada Lab, Aton lab, Buttita lab, Cadigan Lab, and Ye Lab. Their critiques of my work were invaluable and they generously shared resources and time to assist me with my project. Many thanks to Mary Carr and the MCDB administrative team for personally looking out for me and keeping me on track to get my degree.

Thank you to Dr. Charlotte Helrich-Förster, Dr. Taishi Yoshii, Dr. Christiane Hermann and members of the Helrich-Förster Lab at the University of Würzburg, Germany for taking the time to train me in their lab's expertise. To Dr. Charlotte Helrich-Förster, especially, for being my personal role model for a powerful woman and leader in science.

I must acknowledge my very first scientific mentors, Dr. Roy Kaspi and Dr. Katayoon (Katie) Dehesh at the University of California, Davis, whose high expectations and meticulous training built the foundation for my scientific career. Very special thanks to Katie Dehesh, who saw power in me before I did and helped me to recognize my potential.

I am extremely thankful and fortunate for the hard work and sacrifice by my parents, Karen Reed-Szulewski and Paul Szulewski, who taught me the values of independence and hard work so that I could continually better my community and myself. Without their love and support, I would not have achieved my scholarly and personal goals. Special thanks to my aunt, Janet Pitcher, who provides daily support and advice with transcontinental phone calls. Lastly, I thank my loving husband, Jon Lelito, for support that cannot be fully accounted for with words. Most of all his humor and ability to continually make me happy got me through so many hurdles in my studies.

PREFACE

This work consists of both original and published work carried out by K.R. Lelito and members of the Shafer laboratory.

All of the content in Chapter 2 is published in the Neuromethods series, Genetically Encoded Functional Indicators, volume 72. Katherine R. Lelito (K.R.L.) and Orie T. Shafer (O.T.S.) designed the experiments and K.R.L. carried out experiments, analyzed the data and prepared the figures. OT.S. and K.R.L. prepared the manuscript.

Chapter 3 is published in the Journal of Neurophysiology 107:2096-2108. K.R.L. and O.T.S. designed the experiments and K.R.L. carried out experiments, analyzed the data and prepared the figures. O.T.S. and K.R.L. prepared the manuscript.

The content in Chapter 4 is published in the Journal of Neurophysiology 108: 684-696. Zepeng Yao (Z.Y.), Ann Marie Macara (A.M.M.), and K.R.L. are co-first authors. Z.Y, A.M.M., K.R.L., Tamara Minosyan (T.M.) and O.T.S. designed the experiments. Z.Y., A.M.M., K.R.L., and T.M. performed experiments Z.Y., A.M.M., K.R.L., and T.M. analyzed data. K.R.L. specifically generated the data for figure 4.6. Z.Y., A.M.M., K.R.L., T.M., and O.T.S. interpreted results of experiments; Z.Y., A.M.M., and K.R.L. prepared figures; Z.Y., A.M.M., K.R.L., and O.T.S. drafted manuscript; O.T.S. edited and revised manuscript; O.T.S. approved final version of manuscript.

Chapters 1,5, and 6 have not yet been published. K.R.L. and O.T.S. planned experiments and K.R.L. performed all experiments. Jennifer Denike assisted in the generation of a critical fly line and assisted in GRASP studies (Chapter 5). The content was generated by K.R.L. and edited by O.T.S. Shafer.

TABLE OF CONTENTS

LIST OF FIGURES

ABSTRACT

Almost every organism on earth carries with it a timepiece that bestows a critical sense of time. In many organisms, including humans, that timepiece is a network of neurons that each expresses an ancient molecular circadian clock. Like setting a clock, modulation of clock neurons adjusts the timing of an organism's daily rhythms. However, it is not well understood how neuronal modulation of clock neuron activity translates into adjustments of molecular clocks and synchronization of daily rhythms to environment cycles. To investigate this question, I looked to the fruit fly's small ventral lateral clock neurons (s-LN_v), which are not only located in a rich medulla of environmental and interneuronal inputs, but are critical components of the fly's timepiece. To survey these small clock neurons, I employed, validated and expanded a burgeoning method of genetically encoded circuit interrogation to determine s-LN_v receptivity and connectivity. Acetylcholine and GABA are neuromodulators from the visual system and sleep/arousal circuits, respectively. I found that cholinergic agonists and GABA inversely modulate Ca^{2+} and cAMP levels in the s-LN_v. Cholinergic modulation likely comes from the fly's eyelets, as I further showed that activation of the larval and adult eyelets lead to increases in Ca^{2+} and cAMP from the s-LN_v. The results of my studies identify concrete neuronal connections between the s-LN_v and the visual system. My work also suggests that the mechanism by which environmental and interneuronal modulation adjusts the clock is through modulation of critical signaling molecules like cAMP. Overall, this work contributes to a growing body of evidence that shows cAMP to be a conserved signaling molecule involved in clock resetting in mammals and insects. Furthermore, the results of this study support continued investigation into the

simple fruit fly to understand the more complex circuitry that underlies the rhythms of our life.

CHAPTER 1
GENERAL INTRODUCTION

The circadian clock is so seamlessly adapted to the environment that under normal conditions, one would never suspect that our clock naturally runs longer than the twenty-four hour day. The focus of my work is to understand how brain clocks integrate environmental and internal signals to maintain synchronization of the body's behavior and physiology with the twenty-four hour cycling world. The following introduction will describe what is known about how brain clocks generate rhythmic output and technological advances that are allowing investigation of brain clock activity. The first section focuses on the network of cells, or clock neurons, that each express a molecular clock that cycles on with a near twenty-four hour endogenous rhythm. Both molecular clock expression and neural communication between ventrally and dorsally separated clock neurons are required for rhythmic behavior in an animal. The second section describes the central circadian clock in the fruit fly, *Drosophila melanogaster*, and it's ventral clock neurons that are critically important for rhythmicity. The fly's brain clock and these critical ventral neurons have highly analogous counterparts in mammals. My thesis research focuses on understanding how neuromodulatory input effects the activity of the ventral clock neurons and their timekeeping ability. The final part of this chapter describes the relatively recent advances in genetically encoded sensors and activators of neural activity that have finally made functional interrogation of these neurons possible. In particular, they allow circuit interrogation when use of electrophysiology is impracticable such as when evaluating intact circuits of the fly's

brain or neuronal activity in live, freely moving animals. With these tools, I have shown how specific neuromodulatory inputs alter Ca^{2+} and cAMP signaling in the ventral neurons, and I have identified specific neuronal inputs that alone are able to shift the rhythm of circadian behaviors. My thesis work contributes to a greater understanding of the pathways between the modulation of clock neurons and the adjustment of rhythmic output.

1.1 CIRCADIAN CLOCKS AND RHYTHMS

Biological mechanisms that orchestrate daily rhythms are defined as circadian systems, and can be cell autonomous oscillators as found in single celled organisms, or networks of cells expressing oscillators as found the vertebrate suprachiasmatic nucleus (SCN) or the invertebrate circadian clock neuron network (CCNN). To date, all studied circadian oscillations arise from molecular feedback loops within single cells and do not require interaction with other cells in order to generate a near 24-h periodicity. Below, the principles of circadian oscillations and their molecular components will be examined before describing the networks of neurons expressing circadian oscillators that are required for daily rhythms in behavior in vertebrates and invertebrates.

The fruit fly has become a widely used model to study the genetic, molecular and neural basis of circadian timekeeping in part because of its robust circadian locomotor activity. Under controlled laboratory conditions, flies that are subjected to a 12-hour light: 12-dark cycle in constant temperature, exhibit a stereotyped bimodal locomotor activity rhythm (Hamblen-Coyle et al., 1992; Helfrich-Förster, 2000). Wildtype flies display a peak in activity in the morning, exhibit sleep-like activity or a siesta in the mid-day, increase activity towards evening and are relatively inactive, or sleeping, throughout the dark period of the night (Fig. 1A). The two locomotor activity peaks are centered on the light-dark transitions, but increased locomotor activity is observed *before* the transitions indicating that they are not merely passive responses to the change in light. The rhythmic locomotor behavior is “entrained” to the light cycle, as the times at which the behavioral peaks occur are phase-locked to a specific time of day. In a 12:12 LD cycle, Zeitgeber Time

0 (ZT0, Zeitgeber meaning "time-giver" in German) denotes when the lights turn on and ZT12 when the lights turn off. Anticipatory locomotor activity is observed in wildtype flies preceding both ZT0 and ZT12 (Fig. 1A). When flies are released into constant darkness and temperature (DD) where there are no cycling environmental indicators of a 24-h day, the hours are denoted as Circadian Time (CT). Rhythmic locomotor behavior persists with a period or "τ" that is nearly 24-hs, or circadian (Circa- about, dian- day) (Fig. 1B). This behavioral rhythm is generated endogenously, as it persists in the absence of a cycling environment. Using this rhythm as a marker for circadian timekeeping and entrainment, the role of specific molecules, genes and cells can be determined by manipulating their activities and observing the effects on this robust behavior.

1.1.1 MOLECULAR CLOCKS

At the core of generating 24-h behavioral and physiological rhythms are molecular feedback loops occurring at the level of single cells. In common with other biological oscillators, a circadian oscillator has both positive and negative elements that modulate the rate of a molecular chain reaction. This review focuses on transcription-translation feedback loops (TTFL) common to circadian oscillators in mammals and insects, even though other molecular oscillatory loops are known, for example, post-transcriptional oscillators (PTO) in cyanobacteria (reviewed by (Dunlap, 1999).

The Eukaryotic molecular circadian clock is composed of a set genes that negatively regulate their own expression on a near 24-h cycle. There are several genes in *Drosophila* that function to generate the near 24-h feedback loop: *clock* (*clk*), *cycle* (*cyc*), *period* (*per*), *timeless* (*tim*), *double-time* (*dbt*), and *shaggy* (*sgg*) (reviewed by (Dunlap, 1999; Allada et al., 2001; Stanewsky, 2003)). *Clk* and *cyc* encode transcription factors that heterodimerize and promote the expression of *per*, *tim* and other circadian clock controlled genes (ccgs) (Hao et al., 1997; Allada et al., 1998; Darlington et al., 1998a; Rutila et al., 1998; McDonald et al., 2001). PERIOD (PER) and TIMELESS (TIM) proteins accumulate in the cytoplasm and at high

enough levels can heterodimerize to enter the nucleus (Lee et al., 1999). Their heterodimerization and translocation to the nucleus is regulated by the activities of cytoplasmic DOUBLE-TIME (DBT) and SHAGGY (SGG) kinases (Kloss et al., 1998; Price et al., 1998; Martinek et al., 2001; Kim and Edery, 2006; Yu et al., 2006). Once in the nucleus, the PER-TIM heterodimer represses the transcriptional activity of CLK and CYC, thereby negatively regulating their own expression (Darlington et al., 1998a; Lee et al., 1999). It is predicted that the cyclic regulation of clock-controlled gene expression orchestrates rhythmic metabolic and behavioral programs.

The mammalian molecular clock cycles with a feedback loop similar to that of the fly, including a family of *per* genes, (*mPer1*, *mPer2*, and *mPer3*), as well as *mClk*, *Bmal1* (homolog of *Drosophila cyc*), and *CKI*ε (homolog of the DBT kinase) (reviewed by (Dunlap, 1999; Allada et al., 2001; Stanewsky, 2003)). The genes encoding CRYPTOCHROME, *mCry1* and *mCry2*, play a role similar to that of *Drosophila tim* as transcriptional repressors, while CLK and BMAL promote *mCry* and *mPer* gene expression. Interestingly, *Drosophila* CRY interacts with the molecular clock to degrade TIM in response to light, a function that is not performed by mammalian CRY (see below). Despite gene duplications and differing molecular partners, the negative feedback loop functions in a similar way to *Drosophila*: CKIε phosphorylates cytoplasmic mPER and delays it's pairing with mCRY. Upon eventual nuclear entry, a complex of mPER, mCRY and CKIe blocks transcriptional activity of mCLK and BMAL (Lee et al., 2001).

Molecular clock cycling is entrained to the 24-h environmental cycles that an organism experiences. Insects have evolved a "night-phase" clock, where the positive and negative elements of the clock act in the subjective evening, whereas mammals have a "day-phase" clock (Dunlap, 1999) (Fig. 2). In *Drosophila*, *Clk* is rhythmically expressed with peak mRNA and protein expression phase-locked near dawn (Bae et al., 1998; Darlington et al., 1998b). *Cyc*, however is constitutively expressed without rhythmicity (Rutila et al., 1998). When CLK reaches high enough levels to heterodimerize with CYC, the complex promotes *per* and *tim* expression (Allada et al., 1998; Darlington et al., 1998b; Rutila et al., 1998). *Per* and *tim* mRNA rise in the subjective day and peak after dusk ((Hardin et al., 1990; Sehgal et al.,

1995). PER and TIM protein are expressed at high enough levels halfway through the night to enter the nucleus *en masse* (Curtin et al., 1995). The transcriptional repression by PER-TIM acting on their own promoters through interaction with CLK-CYC, leads to the lowest levels of *per* and *tim* mRNA during subjective morning. Whereas most of the negative molecular clock elements are active during the subjective night for *Drosophila*, the case is reversed for mammalian circadian oscillators (Fig. 2B). *mPer* mRNA levels begin to increase before subjective dawn and mRNA levels of *mPer1*, *mPer3* and *mPer2*, peak sequentially throughout the day (Shearman et al., 1997; Tei et al., 1997; Zylka et al., 1998). Mechanisms that phase-lock molecular clock cycling with environmental cycling may be very different between insects and mammals due to the differences in the phasing of their clock components.

Light is the strongest environmental signal known to synchronize molecular clocks with environmental cycles. In mammals, light activates transcription of *per* genes (Shearman et al., 1997; Tei et al., 1997; Zylka et al., 1998). A suggested mechanism for light entrainment is that light exposure in the early evening (>ZT12) would increase in *per* expression when *per* transcripts are declining, which would result in delaying the cycle, or a negative phase-shift (Fig. 2B). An increase in *per* levels in the late evening (>ZT0), when *per* transcripts are increasing would result in an advance of the cycle. In Drosophila, the molecular clock target of light appears to be TIM. In *Drosophila*, light induces CRY-dependent proteasomal degradation of TIM protein (Ceriani et al., 1999; Naidoo et al., 1999; Busza et al., 2004). Light exposure in early evening when TIM levels are increasing, would cause an apparent delay in molecular clock cycle (Fig. 2A). Alternatively, a light pulse and TIM degradation in the late evening when TIM levels were starting to decline would advance the clock in its cycle. The role of CRY in TIM modulation and phase shifting is well understood, however, there are non-CRY mediated light inputs to clock cells where by the mechanism of phase-shifting is not known.

The description of the molecular clock presented here is highly simplified. There are additional interlocked feedback loops and modulators that are outside of the scope of this introduction (Dunlap, 1999; Allada et al., 2001; Stanewsky, 2003;

Zheng and Sehgal, 2012). These other molecules and oscillatory loops interact with this core molecular clock to influence the phasing and length of the cycle. The basic description here emphasizes the concept of cell autonomous molecular clocks that are phase-locked with environmental cycles. Throughout the bodies of vertebrates and invertebrates, many tissues express cycling molecular clocks as described above, but in the next section I will describe networks of clock expressing neurons that control rhythmic behavior in vertebrates and invertebrates.

1.1.2 CIRCADIAN NEURAL NETWORKS

Complex multicellular animals, from mammals to insects, rely on communication between clock expressing neurons in the brain to coordinate daily rhythms in synchronicity with events occurring throughout the 24-h day (Helfrich-Förster, 2004). In mammals, the "master" circadian clock in the brain is in the suprachiasmatic nuclei (SCN). The SCN forms two small, symmetrical wing-like structures from roughly 20,000 neurons depending on the species (Van den Pol, 1980). In the fruit fly, the clock network in the brain is more dispersed, with just 150 clock neurons arranged symmetrically around the perimeter of the central brain (Kaneko and Hall, 2000; Helfrich-Förster, 2003). These two networks are not homologous but share many similarities (reviewed by (Helfrich-Förster, 2004)): 1) the clock neurons can be distinguished by their expression of a conserved molecular clock; 2) The clock networks are located close to and receive input from the visual system; 3) Information from the visual system is funneled through select classes of neurons and travels to the rest of the clock network to regulate circadian cycling behaviors; 4) Neuropeptide communication between the light receiving neurons and the other clock neurons, as well as neuropeptide communication between the two hemispheres is required for endogenous circadian rhythms (Helfrich-Förster and Homberg, 1993; Aton et al., 2005). The circadian network in flies and mammals have similar features, but the simplicity of the fruit fly clock network and genetic tools available to investigate it, make the fly a valuable model in understanding the importance of neuronal modulation of clock neurons in circadian timekeeping and entrainment.

1.2 THE CIRCADIAN CLOCK NETWORK IN DROSOPHILA

Although molecular clock expression is observed throughout the body, only 150 of the ~100,000 neurons in the adult fruit fly brain express the molecular clock (Kaneko and Hall, 2000; Helfrich-Förster, 2003). They have been classified into (at least) 9 groups based on relative location in the brain, cell body size, projection pattern, and peptide expression (Fig. 3A). The left and right hemispheres each house the 9 groups of clock neurons and their distribution is roughly mirrored on each side (reviewed by (Helfrich-Förster, 2005)). The cell bodies of 3 groups are found in the ventral lateral portion of the brain. In one hemisphere there are 4 large ventrolateral (l-LN_v) and 4 small ventrolateral neurons (s-LN_v) that both express the PDF neuropeptide (PDF^+) (Helfrich-Förster, 1995; Park and Hall, 1998). There is also one 5^{th} s-LN_v per hemisphere that does not express PDF and it therefore is classified as a separate class of clock neuron (Kaneko et al., 1997). The cell body of the 5^{th} s-LN_v is usually found clustered nearer to the l-LN_v cell bodies, dorsal to the other s-N_v cell bodies. The remaining 6 classes of clock neurons are distributed in the dorsal brain. In the most dorsal and medial regions of the brain are two groups of dorsal clocks: DN1a and DN1p. The DN1a include two cell bodies per hemisphere that are anteriorly located, while the DN1p include 12-15 cells that are posteriorly located. Within the dorsal protocerebrum are two cell bodies that make up the DN2 clock class. At the lateral edge of the dorsal protocerebrum is a cluster of ~40 dorsal neurons, called DN3's (Shafer et al., 2006). There are three neurons located laterally and posteriorly in the brain, called the LPNs. Lastly, there is a group six of anteriorly and laterally clustered dorsal neuron cell bodies called the LNd. Although the role of each class in time keeping is not completely understood, distinct classes have been shown to play different roles in circadian timekeeping and entrainment (Muraro et al., 2013).

The circadian locomotor rhythm of *Drosophila* requires molecular clock expression in distinct neuronal classes. Flies that do not express PER, a core molecular clock protein, do not exhibit anticipatory activity in light:dark (LD) cycles and nor do they display rhythmic bouts of locomotor activity in constant darkness

(DD)(Konopka and Benzer, 1971; Dowse et al., 1987). However, restoration of PER expression to only the ventral neurons, specifically the s-LN_v, rescues morning anticipatory activity in LD cycles (Grima et al., 2004; Stoleru et al., 2004). A dual oscillator model has emerged to explain the coordinated activity of the ventral and dorsal clock neurons in mediating a bimodal circadian locomotor activity rhythm (Grima et al., 2004; Stoleru et al., 2004).

In addition to molecular clock expression in specific neurons, there is evidence that communication between clock neuron classes is required for rhythmic behaviors (reviewed by (Taghert and Shafer, 2006)). Pigment Dispersing Factor (PDF) is a neuropeptide expressed in the central brain by only 16 neurons: the 8 l-LN_v and 8 s-LN_v (Helfrich-Förster, 1995; Park and Hall, 1998). Receptivity to PDF is widespread throughout the clock neuron classes (Hyun et al., 2005; Mertens et al., 2005; Shafer et al., 2008; Lear et al., 2009; Im and Taghert, 2010). Flies mutant for PDF lack the morning activity peak in LD cycles, and increased arrhythmicity in their locomotor activity and a shortening of τ in constant darkness (Renn et al., 1999). More recently, Yao & Shafer (2014) showed that altering the molecular clocks in the PDF neurons so that they cycled slower or faster than the remaining network, induced a slower cycling of the molecular clocks in subsets of unaltered dorsal clock classes in a PDFR dependent manner (Yao and Shafer, 2014). The likely source of the PDF signaling is the s-LN_v via their dorsal projections. The l-LN_v do not project dorsally, and l-LN_v molecular clock oscillations do not persist under DD as do the oscillations of the s-LN_v and other dorsal clock neurons. Therefore, s-LN_v PDF signaling adjusts molecular clock cycling in dorsal clock neurons and is critical for the maintenance of circadian behavioral rhythms.

Although the l-LN_v do not likely play a critical role in circadian time keeping, their activity is important in regulating sleep and arousal. Sleep, like circadian rhythms, is a ubiquitous phenomenon in animals (Campbell and Tobler, 1984). The timing of sleep is orchestrated by the circadian clock, but is also homeostatically regulated by an animal's need for sleep. The circadian locomotor rhythm of the fruit fly is characterized by states of activity and inactivity, and since the first locomotor

activity recordings, inactive periods were considered "sleep" (Benzer, 1971). Later it was shown that these inactive periods were "sleep-like" states, where flies showed increased arousal thresholds and increased need for sleep if the sleep-like states were prevented (Hendricks et al., 2000; Shaw et al., 2000). Chronic excitation of the l-LN_v leads to a substantial decrease in night-time sleep, while reduction in the number of l-LN_v lead to increases in daytime-sleep and lower daytime locomotor activity (Shang et al., 2008). Knockdown of PDF or its receptor induces somnolence (Parisky et al., 2008), but whether the s-LN_v are also involved is controversial (Sheeba et al., 2008a). Based on l-LN_v light sensitivity and projection pattern over the eye, one model suggests that the l-LN_v integrate arousal signals, such as light, and signal to the s-LN_v to increases locomotor activity output (Parisky et al., 2008).

The anatomical positions of the ventral neurons suggest a role in circadian photoreception and synchronization of clock neurons across dorsal and contralateral hemispheres. The l-LN_v make net-like projections over the optic lobe in the distal medulla and project contralaterally via the posterior optic tract (POT) (Figure 3A&B, adapted from (Helfrich-Förster, 2005)). There are two "shells" of l-LN_v projections at the distal medulla made from ipsilateral and contralateral l-LN_v terminals (Helfrich-Förster et al., 2007), but it is not known if some terminals are sensory. The receptor for PDF has been detected in the distal medulla near visual system neurons whose morphology cycles with a daily rhythm (Pyza and Meinertzhagen, 1999; Im and Taghert, 2010); therefore it is possible that the l-LN_v projections in the optic lobe may strictly be output terminals and not receptive to optic lobe modulation. Both the s- and l-LN_v project to the secondary optic neuropil called the accessory medulla (aMe) (Helfrich-Förster et al., 2007). Among the nine classes of clock neuron, only the LN_v are located near the aMe and optic lobe, suggesting that the LN_v are modulated by light information from these visual system centers. Interestingly the accessory medulla is densely packed with more than just visual system projections; it potentially hosts projections from the dorsal clock neuron classes (DN1, DN3, LPN, (Helfrich-Förster, 2005)) and other yet to be characterized neuronal input. The s-LN_v each send a long branch into the dorsal brain where the rest of the clock neurons (DN1, DN2, DN3, LPN, and the LNd) reside

(Fig.3A, (Helfrich-Förster et al., 2007)). Overall, the PDF neurons are well positioned to receive light information and other modulation and distribute that information to PDF receptive dorsal clock neurons.

The fruit fly larva has also served as a useful model to evaluate the network properties of circadian rhythms as they have a relatively simple clock neuron network compared to the adult fly. The ventral portion of larval clock neuron network includes only 4 PDF^+ LN_v, which are the progenitors of the adult s-LN_v (Fig. 3C, reviewed in (Helfrich-Förster, 2005)). As in the adult clock network, there is also a 5^{th} s-LN_v that does not express PDF (reviewed in (Keene and Sprecher, 2012)). The dorsal clock classes include only 2 DN1s and 2 DN2s. The relative simplicity of the clock neuron network would be advantageous for circuit interrogation of circadian neurons that control circadian rhythms, however, larvae exhibit less obvious circadian rhythms in behavior than adult flies. When subjected to a choice assay between light and dark, larvae will, on average, crawl towards darkness and away from light (Mazzoni et al., 2005). The magnitude of the photophobic response varies on a circadian cycle and requires the molecular clock expression in clock neurons. Despite their subtle circadian behavioral phenotype, the larval clock has been increasingly used as a model for the mechanisms of clock network timekeeping and entrainment.

1.3 CIRCADIAN PHOTORECEPTION IN DROSOPHILA

The visual system in the fly is complex and likely consists of photoreceptive mechanisms with overlapping circadian function. The visual system in *Drosophila* includes cryptochrome (CRY), retinal photoreceptors, ocelli, extra-retinal eyelets, and potentially a set of unidentified photoreceptors to the dorsal clock neurons (reviewed (Helfrich-Förster, 2002)). CRY is a cell-autonomous molecular blue-light sensor expressed throughout the brain and by many of the clock neuron classes: all s-LN_v, l-LN_v, DN1a and some LNd and DN1p (Stanewsky et al., 1998; Emery et al., 2000; Yoshii et al., 2008). As a molecular light sensor expressed by clock neurons, CRY entrains the autonomous molecular clock cycling to environmental light cycles by targeting TIM for degradation upon light activation (Ceriani et al., 1999; Naidoo

et al., 1999; Busza et al., 2004). CRY is only one environmental coupling mechanism however, as flies lacking CRY activity show relatively good entrainment to moderate to long photoperiods (Rieger et al., 2003). CRY mutants do show difficulty in entraining to short photoperiods (LD4:20) and slower re-entrainment relative to wildtype flies (Helfrich-Förster et al., 2001; Rieger et al., 2003). Interestingly, after entrainment to short or long days, the free-running period from CRY mutants was unchanged, where as wild-type flies showed so-called "after effects" or a free running period that was altered by the previous entrainment condition. This suggests that CRY activity is required for day length to alter the timekeeping of the internal clock (Rieger et al., 2003). CRY clearly interacts directly with the molecular clock but other photoreceptors besides CRY can transmit phase information to the clock.

Less is known about the mechanism of circadian photoreception by non-CRY or external photoreceptors. The compound eyes of the fruit fly are tiled with retinal photoreceptors terminating in the lamina or optic lobe medulla while the ocelli are a set of 3 photoreceptive cell clusters at the top of the head, with no obvious projections near clock neurons (Helfrich-Förster, 2002; Rieger et al., 2003). Retinal photoreceptors terminating the in lamina express Rhodopsin1 (Rh1) and those terminating in the optic lobe use Rh3-6 giving the compound eye spectral sensitivity to 350-650 nm light (Helfrich-Förster, 2002). The ocelli express Rh2, a photopigment with light sensitivity between 400-450 nm (Helfrich-Förster, 2002). Mutant flies lacking the compound eyes and ocelli (cli^{eya}, or sine $occulus^{1}$ mutants) exhibit difficulty entraining only to very long or short ("extreme") photoperiods, and do not show the typical masking responses to the light:dark or dark:light transitions seen in the wild type (Rieger et al., 2003). These masking responses have been hypothesized to mediate immediate appropriate behavioral responses to changes in light conditions, before the clock has been entrained to a new light cycle (Rietveld et al., 1993). The role of the retinal photoreceptors and the ocelli are to mediate immediate changes in locomotor activity in response to light and to enhance sensitivity of the clock to extreme photoperiods.

The extra-retinal eyelets are perhaps the most obvious circadian photoreceptor yet have the least well-understood role in circadian photoreception. Each eyelet, or Hofbauer-Bucher (HB)-eyelet, is a cluster of four photoreceptive neurons that project over the optic lobe under the retina to the accessory medulla in the central brain (Hofbauer and Buchner, 1989). Uniquely among the external photoreceptors, they project seemingly directly to the ventral neurons of the clock network (Helfrich-Förster et al., 2002). In an entrainment study of locomotor rhythms from visual system mutants, Rieger, Stanewsky and Forster compared mutants that maintained only the HB-eyelet and the unidentified DN photoreceptor to mutants that only retain the DN photoreceptor (Rieger et al., 2003). Comparatively, without the HB-eyelet, significantly fewer flies entrained to extreme day-length protocols (short to long, long to short), indicating a role for the HB-eyelet in entrainment sensitivity. The HB-eyelets express Rh6, and provide the clock with sensitivity to 500 nm light (Yasuyama and Meinertzhagen, 1999; Helfrich-Förster et al., 2002). Interestingly, the free-running period of mutants lacking the HB-eyelet, compound eyes and ocelli showed no after-effects from the previous photoperiod, whereas the period of mutants lacking only compound eyes and ocelli did show after effects. Therefore the HB-eyelet, like CRY, can mediate period adjustment of the internal clock in addition to providing the clock with enhanced sensitivity for entrainment.

To further investigate the role of the HB-eyelet in circadian entrainment, Veleri and colleagues silenced the HB-eyelet neurons but found no impairment to entrainment in bright light:dark cycles (Veleri et al., 2003). If the authors used combined HB-eyelet silencing with a visual system mutation (in the *norpa*^{1} phototransduction cascade) and subjected flies to dim light cycles, they found that flies could not re-entrain to a shifted light cycle. This suggests that, like other photoreceptive inputs, the HB-eyelet provides the clock with enhanced sensitivity in extreme entrainment conditions. However, in another study that used a very similar protocol (norpa1,cryb mutations in low light) in silencing the HB eyelet, found no effect on entrainment ability (Mealey-Ferrara et al., 2003). Therefore the function of the HB-eyelet in circadian photoreception is still enigmatic. In lieu of combinatorial

mutants or selective silencing of redundant sets of neurons, acute excitation of discrete photoreceptive neurons may be more successful in determining their contribution in circadian photoreception (Chapter 5).

The larval precursor to the HB-eyelet, Bolwig's organ (BO), has a more defined role in circadian photoreception. The BO can be separated into 2 groups of 12 photoreceptive neurons: eight expressing Rh6 (green) and four expressing Rh5 (blue) (reviewed by (Keene and Sprecher, 2012)). Keene and colleagues studied light mediated degradation of TIM in larval LN_v from single or double mutants of the larval eyelet rhodopsins (Keene et al., 2011). Two-hour light pulses were given to larvae just after lights off in a 12:12 LD cycle, when TIM levels are high. Each of the single mutants showed TIM degradation; whereas the double mutant (*rh5*^{5}*;rh6*^{1}) did not (Keene et al., 2011). *cry* mutants showed TIM degradation similar to wildtype larvae. This suggests that either Rh6 or Rh5 is sufficient for TIM degradation and presumably entrainment, and that CRY is not required or sufficient to degrade TIM in the early evening in larval LN_v. In BO, neurotransmission, presumably through ACh, was required for the function of either BO cell type in light-mediated TIM-degradation. Interestingly, photoreception from Rh5-expressing neurons was sufficient to mediate another light-induced behavior, phototaxis away from light, whereas photoreception by Rh6-expressing neurons was not. In larvae, there appears to be a division of roles for these two types of BO neurons, despite having overlapping circadian function.

One of the more nuanced properties of light is its ability to both phase advance and delay circadian rhythms. Light entrainment, in essence, is the effect of subtle phase advancing and delaying effects of light on a non-24-h endogenous rhythm, stabilizing it in phase with environmental cycles (Johnson et al., 2004). For example, in *Drosophila*, light elongates and phase-locks the 23.5-hr endogenous circadian rhythm to the 24-h cycling environment. More specifically, the phase-shifting effects of light allow the clock to consolidate locomotor activity into day lengths that change seasonally. To measure the phase-shifting effects of light on a circadian rhythm, a phase-response curve is generated. Animals are entrained to a 12:12 LD cycle and released into constant darkness (DD). Over the course of a day in

constant darkness, individual animals are exposed to a brief light pulse at various times throughout the day. The phase of their rhythm following the light pulse is compared to the phase of the rhythm before the light pulse or compared to the phase measured in animals that were not exposed to light (Dushay et al., 1990; Emery et al., 1998; Rutila et al., 1998; Stanewsky et al., 1998; Suri et al., 1998). Compiling the data from many animals exposed to light at different times of day allows one to observe the time dependent effects of light on the phase of a circadian rhythm. For *Drosophila*, light pulses given throughout the subjective day (CT0-12) have very little phase shifting effects. Light pulses early in subjective night phase delay rhythms, while light pulses late in subjective night (nearing the next subjective dawn) are advancing (Emery et al., 1998; Rutila et al., 1998; Stanewsky et al., 1998; Suri et al., 1998). Thus, when day length is changing, for example occurring later in the day, the animal's rhythm can be delayed. Broadly, most organisms show remarkably similar response profiles to light as the one described here for *Drosophila* (reviewed by (Johnson et al., 2004)).

External photoreceptors are sufficient to mediate phase-shifts of circadian locomotor rhythms in fruit flies (Kistenpfennig et al., 2012). The phase of circadian locomotor rhythms of CRY mutant flies can be delayed by a brief light pulse at early subjective night (ZT15) and advanced with a light pulse at late subjective night (ZT 21) (Kistenpfennig et al., 2012). Little is known about circadian photoreception by external, or non-CRY mediated photoreception, whereas the mechanism of circadian photoreception by CRY is well understood. It is not known whether each of the external photoreceptor components is capable of both delaying and advancing the phase of a circadian rhythm. One of the main aims of this thesis is to determine specific external photoreceptor connections to the clock network and whether their input is sufficient to shift circadian rhythms (Chapter 5).

1.4 PREDICTED INPUT AND RECEPTIVITY OF THE VENTRAL NEURONS

The activity of PDF neurons may be modulated by several modalities in the densely innervated neuropil of the optic lobe and in the aMe. However, electrophysiological analysis of connectivity and receptivity of the LN_v have proved

to be very difficult, especially with respect to multi-electrode recordings. The majority of input and receptivity data summarized below is based on immunohistochemical localization of receptors and neuromodulators, promoter based expression of receptors and enzymes required for neurotransmitter synthesis, and visualization of proximal projections of other cell types. There is very little functional information about the input and connectivity of the adult LN_v, especially the s-LN_v.

Pigment Dispersing Factor

PDF is a neuropeptide critical for the maintenance of circadian behavioral rhythms (Park and Hall, 1998; Renn et al., 1999). PDF is released by both the s- and l-LN_v (Helfrich-Förster, 1995). Although the neuropeptide receptor has been localized to both classes of PDF neurons (Im and Taghert, 2010), it appears that only the s-LN_v respond with increases cAMP (Shafer et al., 2008). One model suggests that the l-LN_v relay light information to the s-LN_v by PDF signaling and that the s-LN_v distribute synchronizing and arousal signals to the $PDFR^+$ dorsal clock and locomotor control centers (Shang et al., 2008).

Acetylcholine

Acetylcholine (ACh) is employed broadly in the fly nervous system (Bossy et al., 1988; Schuster et al., 1993; Yasuyama and Salvaterra, 1999; Littleton and Ganetzky, 2000) and there are several sources that might modulate the LN_v. Lamina neurons in the secondary optic neuropil that are immunoreactive to antibodies raised against Choline-acetyltransferase (ChAT-IR) could communicate with l-LN_v terminals in the optic lobe (Kolodziejczyk et al., 2008). Johard and colleges isolated the promoter region preceding the ChAT gene sequence and analyzed its expression pattern based by using the promoter to drive the expression of a reported gene (Johard et al., 2009). Based on that promoter expression study, the 5^{th} small LN_v express ChAT and are likely cholinergic (Johard et al., 2009). Neuroanatomically, the 5^{th} s-LN_v have indistinguishable projection patterns relative to the PDF^+ s LN_v, and could modulate the dorsal s-LN_v projections. ChAT-IR also localizes to the neurons

of the HB-eyelet, which project near LN_v terminals in the aMe (Yasuyama and Salvaterra, 1999). It is predicted that light information is relayed directly to the clock network from the HB-eyelet via the PDF neurons at the aMe, but functional connectivity of the PDF neurons to this source of light input has not been shown. Dissociated and cultured larval LN_v respond directly to ACh with an increase in Ca^{2+} mediated by nicotinic receptors and the subsequent activation of voltage gated Ca^{2+} channels (Wegener et al., 2004; Dahdal et al., 2010). Treatment of intact adult brains with ACh and the specific nAChR agonist, nicotine, elicited increases in neuronal firing from the l-LN_v (McCarthy et al., 2011), one of the only electrophysiologically accessible neurons in the fly's clock network. Therefore, the l-LN_v have endogenous receptivity to ACh, and it is predicted that the s-LN_v are receptive to ACh based on the receptivity of the larval LN_v. In chapter three, I will examine whether the s-LN_v are responsive to this important neurotransmitter.

Histamine

Histamine (HA) is best known as a neurotransmitter of retinal photoreceptors in *Drosophila* (Hardie, 1989). Light entrainment can be mediated by photoreceptor input, and histamine modulation may directly act on LN_v to relay light information to the clock network (Helfrich-Förster et al., 2001, 2002; Rieger et al., 2003). HA activity is inhibitory, acting on histamine-gated chloride channels (Hardie, 1989; Gengs et al., 2002; Pantazis et al., 2008). A subset of the histaminergic retinal photoreceptors, R7 and R8, terminate in the distal medulla (Fig.3B) and may relay light information to the clock via inhibition of the l-LN_v via their optic lobe projections (Nässel et al., 1988; Pollack and Hofbauer, 1991; Sarthy, 1991). HA-immunoreactivity (HA-IR) localizes with LN_v projections at the aMe (Hamasaka and Nässel, 2006) and the likely sources of this HA are the terminals of the HA-immunoreactive HB-eyelet (Pollack and Hofbauer, 1991). As the eyelet also stains against ChAT (Yasuyama and Meinertzhagen, 1999), it is not known whether individual eyelet neurons use one or both of these neurotransmitters. Of the two known types of HA-receptors, only HisCl1 is known to localize to the l-LN_v (Hong et al., 2006) but so far responses of the LN_v to HA have not been recorded. In chapter

five, I examine whether the s-LN_v and l-LN_v respond to this visual system neurotransmitter.

γ-Amino Butyric Acid (GABA)

Immunoreactivity to GABA (GABA-IR) is found in the aMe and in many visual system neurons innervating the optic lobe (Hamasaka et al., 2005; Kolodziejczyk et al., 2008). Modulation of GABAergic neurons in flies alters circadian rhythms and sleep patterns (Parisky et al., 2008; Sheeba et al., 2008a; Chung et al., 2009; Dahdal et al., 2010). Both metabotropic ($GABA_BR$) and ionotropic ($GABA_AR$) GABA receptors have been implicated in the modulation of *Drosophila* sleep-wake activity. In larval LN_v, application of GABA and a $GABA_BR$ agonist reduced Ca^{2+} levels, whereas GABA responses could not be blocked by a $GABA_AR$ antagonist. Thus GABA receptivity in adult s-LN_v is predicted be mediated by metabotropic $GABA_B$ receptors (Hamasaka et al., 2005; Dahdal et al., 2010). Perfusion of GABA over explanted brains induces a chloride current in the l-LN_v and decreases spontaneous firing frequency, while picrotoxin, a $GABA_AR$ antagonist, increased action potential firing rates (Chung et al., 2009; McCarthy et al., 2011). While ionotropic $GABA_A$ receptors mediate GABA inhibition in the L-LN_v, their modulation by $GABA_BRs$ has not been excluded. In chapter three, I examine whether GABA affects neural activity and intracellular signaling in the s- and l-LN_v.

Glutamate

Glutamate is another widespread neurotransmitter in the fruit fly nervous system, most notably released by motor neurons at the neuromuscular junction (Jan and Jan, 1976; Ultsch et al., 1992; Littleton and Ganetzky, 2000; Völkner et al., 2000). Glutamatergic projections are found in the aMe, and may be terminals of dorsal clock neurons (Hamasaka et al., 2007; Daniels et al., 2008). Glutamate receptors in *Drosophila* can mediate both excitatory and inhibitory responses through either ionotropic or metabotropic receptors, respectively (Anwyl, 1999; Dingledine et al., 1999). The metabotropic glutamate receptor, mGluRA, localizes to the aMe and knockdown of mGluRA in adult LN_v disrupted normal circadian locomotor rhythms

and lengthened the phase of free-running rhythms (Hamasaka et al., 2007). Therefore, glutamate signaling to LN_v, potentially from dorsal neurons, modulate timekeeping by the clock neuron network. In explanted adult brains, glutamate inhibits spontaneous firing from the l-LN_v and voltage clamp experiments implicate a glutamate-gated chloride channel (McCarthy et al., 2011). Larval LN_v are inhibited by glutamate as well, but the metabotropic glutamate receptor has been implicated in this inhibition (Hamasaka et al., 2007; Dahdal et al., 2010). Based on the receptivity of the adult l-LN_v and the larval LN_v to glutamate, it is predicted that the adult s-LN_v are also inhibited by glutamate (Hamasaka et al., 2007). In a collaborative study, I examined the responsivity of the s-LN_v to glutamate and the role of glutamate signaling in timekeeping (Collins et al., *submitted*).

Other Neuromodulatory Input

Adding to the list of known and potential modulators described above, are a host of other neurochemicals that may be involved in circadian photoreception and modulation of adult PDF neuron activity. In flies, octopamine and dopamine modulate locomotor activity, sleep and arousal, and at least in the l-LN_v they induce cAMP increases (Andretic and Hirsh, 2000; Friggi-Grelin et al., 2003; Crocker and Sehgal, 2008; Shang et al., 2011). The serotonin receptor d5-HT1B localizes to the adult LN_v and reduces circadian photosensitivity (Yuan et al., 2005). The LN_v may be modulated by the neuropeptides of the dorsal clock neurons: ITP, NPF, sNPF (Johard et al., 2009; Hermann et al., 2012). These neuromodulators, although potentially important for circadian rhythms, are outside of the scope of this work.

The response profiles of the more accessible larval LN_v or adult l-LN_v have been used to predict the receptivity of the adult s-LN_v. However, several differences exist between these sets of neurons that suggest these predictions may not be true for the adult s-LN_v. First, the fly undergoes complete metamorphosis from larva to adult, changing its body plan, ecology, and behavior. The adult clock network becomes more complex: the ventral clock classes double, while the dorsal clock classes expand 2.5 times (reviewed by (Helfrich-Förster, 2005)). Additionally, the

visual system adds the compound eye and ocelli to the existing extra-retinal eyelet. The adult eyelet further gains histaminergic identity (Pollack and Hofbauer, 1991). Taking into account the multitude of potential inputs to the adult s-LN_v in the adult, the response profile of the adult s-LN_v are likely to differ from their precursor cells. In the adult, the s- and l-LN_v may express a common neuropeptide, but their highly diversified morphologies suggest very different functions. Already, there is evidence that histamine receptors localize to the l-LN_v and not the s-LN_v (Hong et al., 2006), suggesting the intriguing hypothesis that histaminergic input from the HB-eyelet targets the l-LN_v. The increased complexity of adult circadian clock network may require new and diversified sensitivities between the s- and l-LN_v. In this work, I examine the modulation of the critical s-LN_v pacemaker cells.

1.5 CIRCUIT INTERROGATION TECHNIQUES IN THE INTACT BRAIN

1.5.1 ELECTROPHYSIOLOGY OF THE VENTRAL LATERAL CLOCK NEURONS

Of the various clock neuron classes, only the l-LN_v have been routinely recorded from with electrophysiological techniques. Recording success is likely due to their large cell bodies and relatively superficial location in the brain. The resting membrane potential (RMP) of the l-LN_v fluctuates on a daily rhythm and is modulated by light (Park and Griffith, 2006; Cao and Nitabach, 2008; Sheeba et al., 2008b). The RMP of the l-LN_v peaks near dawn and troughs midday in 12:12 LD cycles (Cao and Nitabach, 2008). Light exposure to whole-cell patched l-LN_v in intact brains increases RMP and spontaneous firing frequency in a CRY dependent manner (Fogle et al., 2011). McCarthy et al. (2011) further showed that nicotine, a nAChR agonist, elicits increases in firing rates from the l-LN_v, while GABA and Glutamate blocked spontaneous firing. While the l-LN_v are important for the regulation of sleep and arousal, they are less critical to circadian time keeping than the s-LN_v.

Electrophysiological interrogation of the s-LN_v has proved to be technically difficult due to the deep location of their cell bodies within the brain and their small size. Cao and Nitabach (2008) were able to patch the s-LN_v but very little spontaneous activity was recorded likely because of technical issues patching such

small cells. They did, however, show that RMP of the s-LN_v cycled much like the l-LN_v: most depolarized at dawn with increasing variability at midday. As the s-LN_v are thought to orchestrate the morning locomotor activity peak of the bimodal circadian locomotor rhythm (Grima et al., 2004; Stoleru et al., 2004), increases in s-LN_v membrane excitability at dawn may be linked to increases in locomotor activity. Most of the clock neurons and other important circuits in the fly brain are similarly inaccessible with electrodes; therefore many developments have been made to adopt genetically encoded sensors and activators of neural activity to accomplish circuit interrogation in the intact fly brain.

1.5.2 GENETICALLY ENCODED SENSORS OF NEURAL ACTIVITY

Genetically encoded sensors of neural activity have several advantages over electrophysiology. First, because they are genetically targeted, their use is non-invasive and allows for the preservation of intact circuits, cell membranes and ionic distributions. Second, by virtue of the signal they detect, they allow researchers to not only observe neuronal activity events but also further downstream signaling changes, such as Ca^{2+} and cAMP changes. Third, genetically encoded sensors allow visualization of neural activity along the length of an entire cell. Multiple electrodes would be required to record from discrete locations of one cell and electrode tips are often too large to record from dendrites. Lastly, widespread sensor expression can provide a high-throughput method for screening responsivity of thousands of neurons at once. Historically, genetically encoded sensors lack temporal signal resolution of electrophysiological recording (Miesenböck, 2009); so for all of the potential gains acquired using genetically encoded neural activity sensors, inability to discern and quantify changes in high frequency neuronal activity is a potential disadvantage to this technique.

Ca^{2+} is a particularly relevant signal for neural activity, as large increases in Ca^{2+} occur after depolarization of neurons. The Ca^{2+} sensor, GCaMP, has been the most widely used sensor for neural activity in the *Drosophila* brain. GCaMP is a fusion of a circularly permutated Green Fluorescent Protein (GFP) to the Ca^{2+} binding domain of calmodulin (CaM) and the CaM-binding peptide (M13pep) of

myosin light chain kinase (Akerboom et al., 2009). Ca^{2+} binding induces a conformational change in the GFP structure into a more highly fluorescing state. The first version of GCaMP used in *Drosophila* brain had relatively low basal florescence and a limited response range to Ca^{2+} changes (Nakai et al., 2001; Wang et al., 2003). Since then several improvements to the sensor have been made to increase the baseline florescence making cells easier to image. Additionally, the dynamic range and sensitivity was increased, and the photostability was improved (Tian et al., 2009; Akerboom et al., 2012). The latest versions of the GCaMP sensors (GCaMP6) can detect Ca^{2+} changes from single action potentials and Ca^{2+} transients within individual dendritic spines (Chen et al., 2013). Several versions of GCaMP6 were created in this study to detect changes in Ca^{2+} over different time scales. However, the optimization of GCaMP has focused on detection of excitatory and not inhibitory responses. Inhibitory neuromodulation may not result in changes in Ca^{2+}, and therefore may not be detectable with this sensor.

Cyclic Adenosine Monophosphate (cAMP) signaling may be evoked by neural activation of voltage-gated adenylyl cyclases or by metabotropic G-protein signaling. The cAMP sensor Epac1-cAMPs was developed for mammalian cell culture (Nikolaev et al., 2004), and was introduced into *Drosophila* in 2008 by Shafer et al. The Epac protein based on the exchange protein directly activated by cAMP (EPAC) whose cAMP binding domain is flanked by Cyan Fluorescent Protein (CFP) and Yellow Fluorescent Protein (YFP). Florescence resonance energy transfer (FRET) from CFP to YFP is decreased when cAMP binds to Epac. The ratio of fluorescence intensities of CFP and YPF can be recorded as measurement of relative cAMP levels. Shafer et al., (2008) recorded increases in cAMP in response to PDF peptide application in the s-LN_v, and many other clock neuron classes. Several other studies have successfully utilized this sensor in the fly brain and body (Tomchik and Davis, 2009; Crocker et al., 2010; Beckwith et al., 2011; Duvall and Taghert, 2012; Talsma et al., 2012). As with GCaMP, very few studies have detected or evaluated inhibitory neuron modulation using this sensor, and not all neuromodulation is coupled to changes in cAMP. In the following chapters, I provide a detailed review of the methods for using the Epac1-cAMPs sensor in live-imaging of *Drosophila* neurons,

establish that the sensor can detect some forms of inhibitory neuromodulation, and show that it is compatible with genetically encoded circuit interrogation (Lelito and Shafer, 2012a, 2012b; Yao et al., 2012).

1.5.3 GENETICALLY ENCODED ACTUATORS OF NEURAL ACTIVITY

Targeted genetically encoded activators allow for control of neural activity in cell types that are inaccessible to stimulating electrodes. For circuit interrogation, actuators can be employed to manipulate neurons while simultaneously live-imaging neuronal activity in post-synaptic neurons, or can used independently to manipulate neural activity in freely moving animals. Actuators are traditionally made from ion channels that can be temporally opened to excite or inhibit neurons expressing the channel (Miesenböck and Kevrekidis, 2005). Most activators are made using channels that do not endogenously occur in the model organism whose circuits are being evaluated. This ensures that only targeted neurons of interest are manipulated. The activator should not be active at the neuron's resting state or during development to avoid unintended changes in neural activity and developmental defects. Depolarizing, or excitatory actuators have the widest range of activation options, such as by light, temperature and ligand application. There are fewer functional options for inhibitory control of neurons by genetically encoded actuators. Temporal control of the activator is critical for inducing defined changes in neural activity (Miesenböck, 2009). Light-activated channels offer the most temporal precision, while ligand-gated channels are limited by diffusion rate of the ligand. For this work, the description of actuators will be limited to ones that are compatible with circuit interrogation of the circadian clock network in *Drosophila*.

P2X2

In 2005, Lima and Miesenböck generated a targetable P2X2 ion channel for expression in *Drosophila*, taking advantage of the lack of this ATP-gated cation channel sequence in the fly genome (Littleton and Ganetzky, 2000; Lima and Miesenböck, 2005). When P2X2 was expressed in motor neurons, ATP application induced full-scale excitatory junction potentials (EJP) in larval muscle fibers,

whereas only mini-EJPs were seen in response to GTP application. Lima & Misenböck also investigated the potential for P2X2-mediated excitation of neurons in freely moving flies by injecting the flies with caged ATP that could be released by exposing the flies to a light pulse. P2X2 was targeted to dopaminergic neurons and uncaging ATP elicited an increase in locomotor activity as well as a change in locomotor pattern, which required P2X2 expression and injection with caged ATP but was not elicited by the phototrigger alone. Use of P2X2 will be vetted for use with live-imaging in circadian neurons in Chapter 4, but the use of photo-uncaging of ATP in the investigation of circadian behavioral circuitry is impractical due to the extreme sensitivity of the clock to light.

TRPA1

Thermosensitive channels have also been used for temperature-mediated activation of neurons. Viswanath et al. (2003) showed that the *Drosophila* ortholog of the mammalian TRPA1 cation channel responds to increasing temperatures (24-29°C) (Viswanath et al., 2003). Based on the expression pattern of the promoter, only 12 neurons express *trpa1* in the *Drosophila* brain and they are non-circadian (Hamada et al., 2008). Hamada et al. generated a targetable TRPA1 expression construct and expressed it widely in the nervous system. With temperature increases flies could be incapacitated completely by 1 minute of warming, and recovered within minutes. Therefore, desensitization of the TRPA1 channel did not occur over 1 minute of continuous activation. Hamada et al. also attempted to perform live-imaging from TRPA1 cells of explanted brains expressing the GCaMP Ca^{2+} sensor. Due to the substantial movement artifacts induced by temperature changes, the brains had to be mounted on sylgard-coated cover slips and glued down near the optic lobes with VetBond. They were eventually able to visualize increases in Ca^{2+} to temperatures over 25°C. The TRPA1 channel is not optimal for live-imaging, but has been used widely for neuronal activation in freely moving flies (see examples below).

Pulver et al. characterized the effect of temperature-mediated excitation of fly neurons heterologously expressing TRPA1(Pulver et al., 2009). Whole cell patch

clamp recordings were made on MNISN-Is neurons (motor neurons synapsing on larval body wall muscle six) expressing TRPA1. Over a 5-minute temperature ramp from 22 to 27°C, the cells fired tonically with little desensitization. This response did not require the cell bodies and genetic controls did not show significant increases in firing during temperature ramps. Resting membrane potential and responses to depolarizing current injection were not different between WT and TRAP1 expression neurons, but input resistance was significantly higher when TRPA1 was expressed. They also measured the decay of excitatory junction potential (EJP) frequency over 20-minutes in constantly activated TRPA1 expressing cells and found that there was very little spike frequency adaptation. Additionally, they activated both larval sensory and motor neurons with temperature activated TRPA1 and measured crawling speed to see if TRP activation and behavioral modification could be sustained over minutes. They found that over a 2-minute increase in temperature, TRPA1 activation was able to stop the larvae from crawling whereas the controls were almost completely unaffected. The TRPA1 channel appears to be a promising tool compatible with behavioral assays and capable of producing sustained activation of neurons.

Parisky and colleagues targeted TRPA1 expression to PDF neurons to examine the effects of PDF neuron activity on sleep (Parisky et al., 2008). To prevent developmental effects of TRPA1 activity, flies were reared at 22°C and adults experienced a temperature step to 27°C for 3 days. Initially, when the temperature is raised to 27°C all genotypes exhibit an increase in overall sleep, especially during the day. However, in the early night (ZT 12-15), flies expressing TRP in PDF neurons at 27°C show increased wakefulness over control flies, where wakefulness was measured by the relative length of wake and sleep bouts between ZT12-15. No significant effect on daytime sleep was observed. The authors showed that the effect on sleep was specifically mediated by the l-LN_v and not the s-LN_v blocking TRPA1 expression in the s-LN_v neurons, and observing that the effect on sleep persisted. These results implicate a specific role for the l-LN_v in arousal, shown by use of the genetically targeted TRPA1.

Temperature activated TRPA1 has been an effective tool to evaluate the function of PDF neurons, but temperature alone modulates circadian behaviors. In constant darkness, flies subjected to a 3°C temperature cycle (12-hr at 25°C, 12-hour 28°C) showed anticipation (increased locomotor activity) of the temperature transition (Wheeler et al., 1993). Additionally, in constant light, when fly locomotor activity is arrhythmic under constant temperature, similar 24-h temperature cycles produce rhythmic locomotor activity that requires the molecular clock expression in clock neurons (Yoshii et al., 2005). The PDF neurons are likely involved in mediating the thermocycle induced rhythm, as the anticipatory behavior associated with the temperature transition was largely lost when PDF neurons were eliminated or when flies were mutant for the peptide. Kaushik et al. measured the phase response of circadian locomotor rhythms to heat (Kaushik et al., 2007).. Exposure to 37°C for 30-min in the early night (ZT 12-15) was sufficient to induce ~2.5hr delays in the phase of locomotor rhythms. The same heat exposures given at other times of the day induced small or non-existent shifts in phase. Lower temperature exposure at early night, such as 30°C and 34°C, produced little or no phase shifts. Therefore, temperature mediated neuronal excitation may interact with the circadian clock at temperatures near 37°C, and exposures in the early evening.

1.5.4 EXPRESSION SYSTEMS

Utilization of even the most sophisticated sensors and activators for circuit interrogation in the *Drosophila* brain will always be limited by the specificity of the expression system used to drive their expression. Targeting activators and sensors to discrete, identifiable and non-overlapping cell types is critical for determining network connectivity and neuronal sensitivity. The Gal4/UAS system is currently the most well developed binary expression system for the fruit fly, with thousands of publicly available stocks. Gal4 is a transcriptional activator of the UAS (Upstream Activating Sequence), whose sequences were isolated from yeast and are not found in the *Drosophila* genome endogenously (Brand and Perrimon, 1993). The Gal4 sequence can placed under the control selected fly enhancer/promoter sequences, so that when inserted into the genome of a fruit fly, the expression of the Gal4 will

be targeted only in cells where the selected enhancer/promoter is endogenously utilized in gene expression. This results in expression of the Gal4 in a reproducible but normally broadly distributed set of cells. Since its introduction by Brand and Perrimon in 1993, thousands of Gal4 stocks have been created from known promoters or by random insertions of the Gal4 sequence into the genome. The Gal4 transcription factor, or driver, is used in combination with UAS elements. The UAS sequence is cloned upstream of a gene of interest, for example, a genetically encoded fluorescent sensor. Through straightforward genetic methods, both Gal4 and UAS elements can be combined in the genome of a single fly, thereby ensuring that the gene of interest will be expressed in cells where Gal4 expression is present.

Circuit interrogation using targeted sensors and activators requires knowing exactly which cells express the transgenes, and limiting the expression to cells of interest. However, of the publicly available Gal4 stocks, many are unusable for circuit interrogation because they are expressed too broadly or express in unidentified cell types. The circadian neurobiology field has been fortunate to have access to the Pdf-gal4 driver that has very limited expression in only the 16 PDF^{+} ventrolateral clock neurons in the mature brain (Park et al., 2000). Yet even with this remarkably specific driver, it is still difficult to functionally separate the roles of the two distinct PDF neuron cell types. Furthermore, the field of circadian biology is interested in the neural populations that modulate and are modulated by the clock network. Recently, many labs are taking advantage of genetic techniques to reduce the expression patterns of existing Gal4 drivers, or making ultra-specific drivers based on smaller portions of known promoter regions (Wu and Luo, 2006; Pfeiffer et al., 2010; Jenett et al., 2012). These techniques may bring much needed specificity to genetically encoded circuit interrogation, and *Drosophila* biology on the whole.

In order to independently stimulate one cell type and simultaneously record neuronal activity in another, another binary expression is required for genetically encoded circuit interrogation. The LexA/LexAop system works in the same way as the Gal4/UAS system, where the LexA transcription factor induces expression of the sequence downstream of LexAop (Lai and Lee, 2006). The LexA/LexAop system is

now being developed more extensively for complementation of the Gal4/UAS system.

The combinatorial use of various drivers with UAS and LexAop lines will allow the field of neurobiology to overcome many of the limitations of electrophysiology techniques in the *Drosophila* brain. An additional limitation to electrophysiological analysis in the small neurons of the fly brain is that traditionally only one neuron can be investigated at a time. The advantage of widely expressed sensors allows investigators to record responses to many potential post-synaptic cells at once. However, in the same vein, precise stimulation of a distinct cell or cell type is limited by the specificity of the driver directing the expression of the activator. Despite these limitations, there are many Gal4 and LexA drivers available with reasonable specificity to make genetically encoded circuit interrogation feasible in many circuits. In chapter 4, I explore the utility of genetically encoded circuit interrogation in *Drosophila*, and in chapter 5, I employ the technique to investigate the predicted connectivity of the HB-eyelet to the LN_v.

1.6 FIGURES

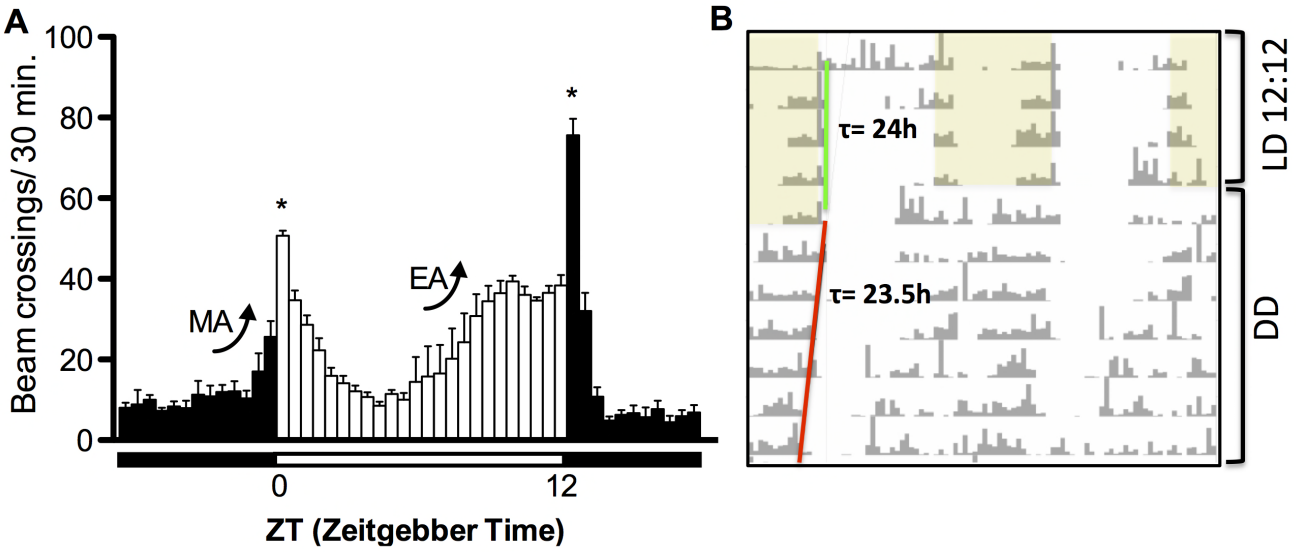

Figure 1.1 Fruit flies exhibit a robust circadian locomotor activity rhythm. A) An eduction plot of locomotor activity averaged from 32 flies over 5 consecutive days in a 12:12 Light: Dark (LD) cycle. Black bars indicate intervals of darkness and white bars indicate intervals of light. A typical fly is diurnal, and has two activity peaks (bimodal). Morning anticipation (MA) and evening anticipation (EA) are increases in locomotor activity observed before the LD transitions. Asterisks indicate peaks of activity due to the LD transitions, so-called "masking" behavior. B) Locomotor activity recorded from a single fly entrained to a LD cycle (yellow shading is light exposure) and then released into constant darkness (DD). In a typical fly, the period, or tau (τ), of the rhythm is 24h when entrained to the 12:12 LD cycle and changes to 23.5h in constant darkness.

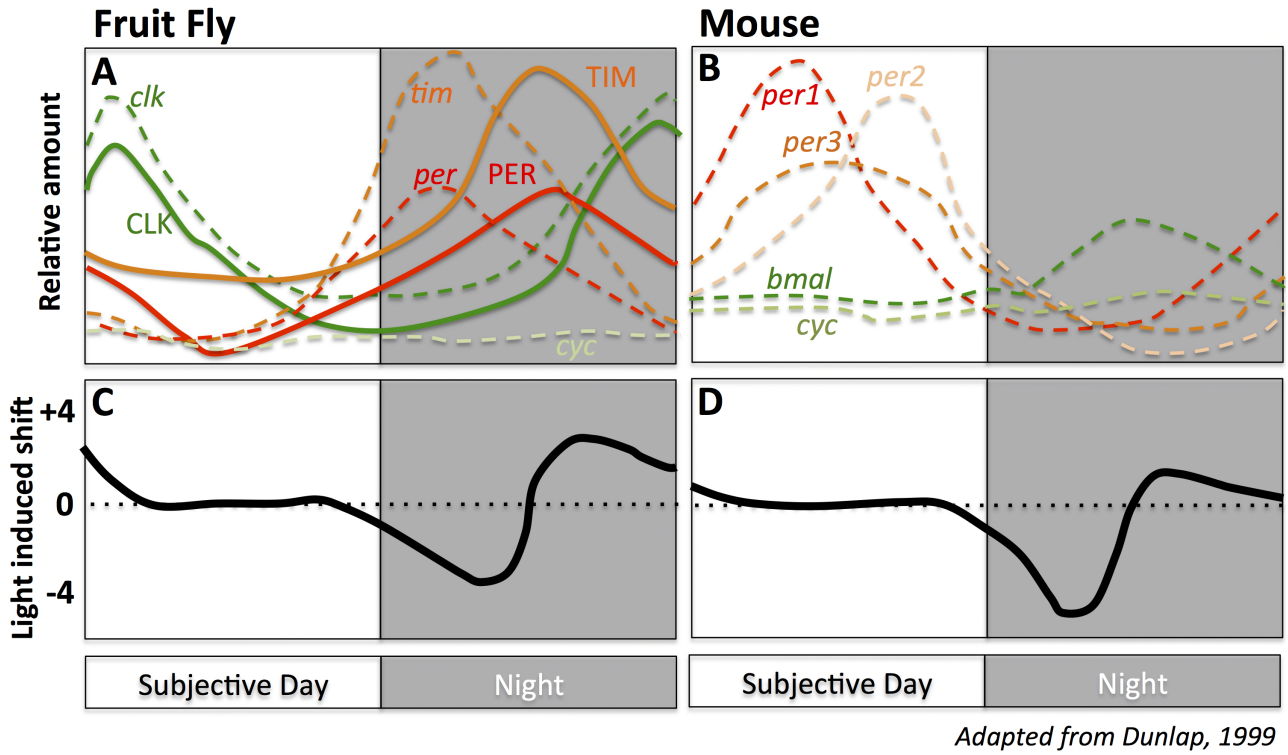

Figure 1.2. Daily cycling of molecular clock mRNA and protein plotted with Phase-Response profile to light. A-B) Relative abundance of molecular clock component mRNA (dotted line) and protein (solid line) plotted over a day (Protein levels of the mouse omitted for simplicity). The protein components of the fruit fly circadian clock are mostly present at night ("night-phase" clock): Period (per, PER); Timeless (tim, TIM); Clock (clk, CLK); Cycle (cyc, CYC). Shaggy (SGG) and Doubletime (DBT) kinases are not shown. The mouse clock is a "day-phase" clock with 3 genes for Period (mPer1, mPer2, and mPer3), bmal (homolog of CLK), cycle (cyc). Cryptochrome (CRY) and CK1e are not shown. C&D) Phase-response curves of a circadian rhythm for each animal in response to light. Light exposure during subjective day is relatively ineffective in changing the phase of a circadian cycle. Light exposure in the early evening results in delays, whereas light exposure in the late even results in advances to the phase of a circadian rhythm.

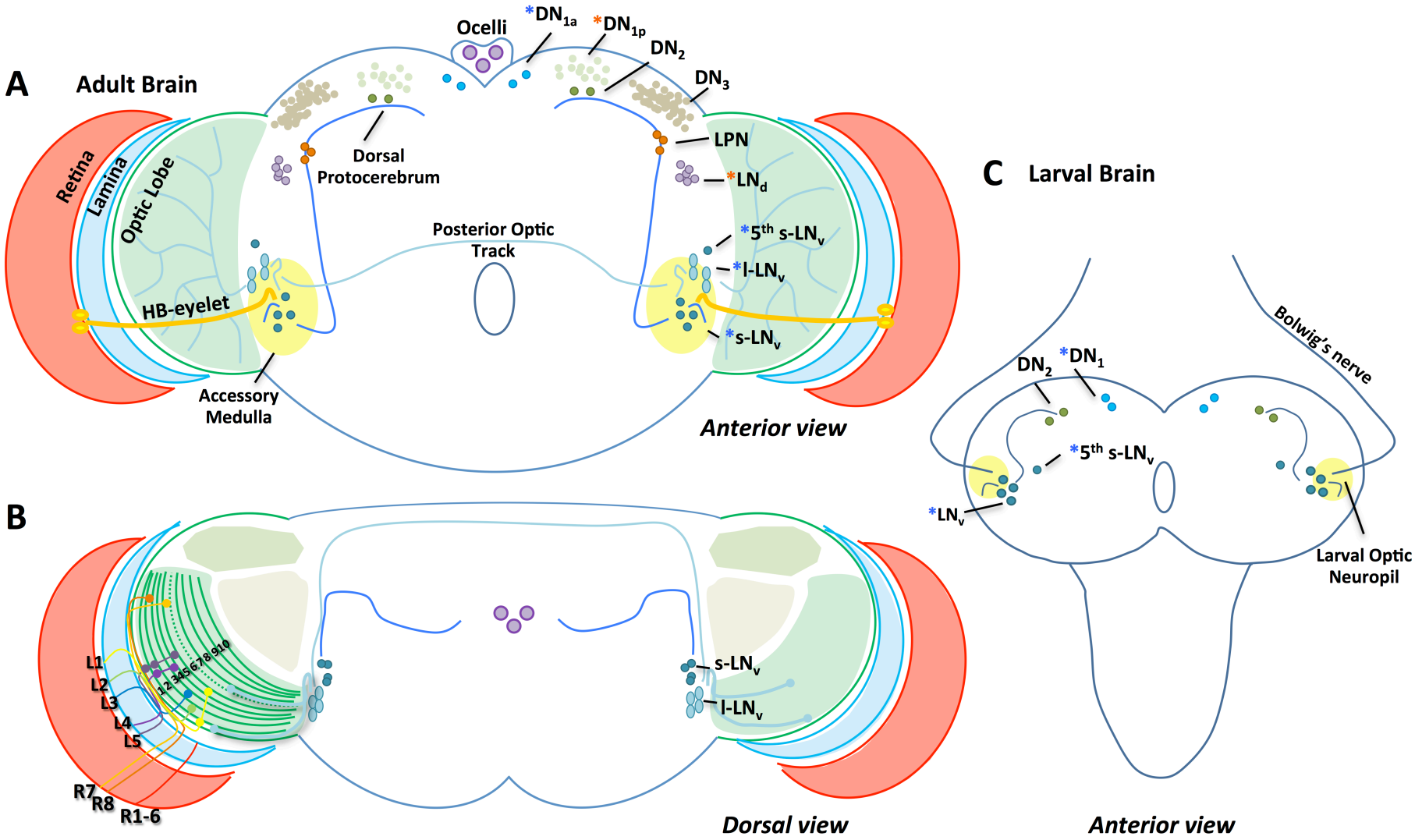
A
Adult Brain
Ocelli
*DN1a
*DN1p
DN2
DN3
Retina
Lamina
Optic Lobe
Dorsal Protocerebrum
LPN
*LNd
Posterior Optic Track
*5th s-LNv
*l-LNv
HB-eyelet
*s-LNv
Accessory Medulla
Anterior view
B
L1
L2
L3
L4
L5
1 2 3 4 5 6 7 8 9 10
R7
R8
R1-6
s-LNv
l-LNv
Dorsal view
C
Larval Brain
Bolwig's nerve
DN2
*DN1
*5th s-LNv
*LNv
Larval Optic Neuropil
Anterior view

F**igure 1.3. Clock neurons and the visual system.** A) The distribution of clock neuron cell bodies are shown from an anterior view of the adult brain: DN1a (Anterior Dorsal neurons); DN1p (Posterior Dorsal Neurons); DN2 (Dorsal Neurons 2); DN3 (Dorsal Neurons 3); LPN (Lateral Posterior Neurons); 5^{th} s-LN_v (Small Ventrolateral Neuron); l-LN_v (Large Ventrolateral Neurons); s-LN_v (Small Ventrolateral Neuron). Components of the visual system are shown in relation to the clock neurons: the retina, lamina, HB-eyelet, and ocelli. The optic lobe and accessory medulla are neuropil wherein visual system input is directed. B) A dorsal view of the brain shows l-LN_v projection pattern relative to visual system neurons: R1-6 (Retinal Photoreceptors 1-6 terminate in the lamina); R7 and R8 (Retinal Photoreceptors 7 and 8 terminate in the optic lobe medulla); L1-L5 (Lamina Cells that terminate to different layers of the medulla). Numbers 1-10 denote the layers of the optic lobe medulla. C) Clock neurons of the larval brain are shown from an anterior view: LN_v, 5^{th} s-LN_v; DN2, DN1. The LN_v, Larval Optic Neuropil, and Bolwig's Nerve are the larval counterparts to the adult s-LN_v, accessory medulla and HB-eyelet, respectively. Asterisks indicate the expression of Cryptochrome, a blue light sensor, by all (blue) or some (red) neurons in a class of clock neurons (Adapted from Helfrich-Förster, et al. 2007).

1.7 REFERENCES

Akerboom J, Chen T-W, Wardill TJ, Tian L, Marvin JS, Mutlu S, Calderón NC, Esposti F, Borghuis BG, Sun XR, Gordus A, Orger MB, Portugues R, Engert F, Macklin JJ, Filosa A, Aggarwal A, Kerr RA, Takagi R, Kracun S, Shigetomi E, Khakh BS, Baier H, Lagnado L, Wang SS-H, Bargmann CI, Kimmel BE, Jayaraman V, Svoboda K, Kim DS, Schreiter ER, Looger LL. Optimization of a GCaMP calcium indicator for neural activity imaging. *J. Neurosci.* 32: 13819–13840, 2012.

Akerboom J, Rivera JDV, Guilbe MMR, Malavé ECA, Hernandez HH, Tian L, Hires SA, Marvin JS, Looger LL, Schreiter ER. Crystal structures of the GCaMP calcium sensor reveal the mechanism of fluorescence signal change and aid rational design. *J. Biol. Chem.* 284: 6455–6464, 2009.

Allada R, Emery P, Takahashi JS, Rosbash M. Stopping time: the genetics of fly and mouse circadian clocks. *Annu. Rev. Neurosci.* 24: 1091–1119, 2001.

Allada R, White NE, So WV, Hall JC, Rosbash M. A mutant Drosophila homolog of mammalian Clock disrupts circadian rhythms and transcription of period and timeless. *Cell* 93: 791–804, 1998.

Andretic R, Hirsh J. Circadian modulation of dopamine receptor responsiveness in Drosophila melanogaster. *Proc. Natl. Acad. Sci. U. S. A.* 97: 1873–1878, 2000.

Anwyl R. Metabotropic glutamate receptors: electrophysiological properties and role in plasticity. *Brain Res. Brain Res. Rev.* 29: 83–120, 1999.

Aton SJ, Colwell CS, Harmar AJ, Waschek J, Herzog ED. Vasoactive intestinal polypeptide mediates circadian rhythmicity and synchrony in mammalian clock neurons. *Nat. Neurosci.* 8: 476–483, 2005.

Bae K, Lee C, Sidote D, Chuang KY, Edery I. Circadian regulation of a Drosophila homolog of the mammalian Clock gene: PER and TIM function as positive regulators. *Mol. Cell. Biol.* 18: 6142–6151, 1998.

Beckwith EJ, Lelito KR, Hsu Y-WA, Medina BM, Shafer O, Ceriani MF, de la Iglesia HO. Functional conservation of clock output signaling between flies and intertidal crabs. *J. Biol. Rhythms* 26: 518–529, 2011.

Benzer S. From the gene to behavior. *JAMA J. Am. Med. Assoc.* 218: 1015–1022, 1971.

Bossy B, Ballivet M, Spierer P. Conservation of neural nicotinic acetylcholine receptors from Drosophila to vertebrate central nervous systems. *EMBO J.* 7: 611–618, 1988.

Brand AH, Perrimon N. Targeted gene expression as a means of altering cell fates and generating dominant phenotypes. *Dev. Camb. Engl.* 118: 401–415, 1993.

Busza A, Emery-Le M, Rosbash M, Emery P. Roles of the two Drosophila CRYPTOCHROME structural domains in circadian photoreception. *Science* 304: 1503–1506, 2004.

Campbell SS, Tobler I. Animal sleep: a review of sleep duration across phylogeny. *Neurosci. Biobehav. Rev.* 8: 269–300, 1984.

Cao G, Nitabach MN. Circadian control of membrane excitability in Drosophila melanogaster lateral ventral clock neurons. *J. Neurosci.* 28: 6493–6501, 2008.

Ceriani MF, Darlington TK, Staknis D, Más P, Petti AA, Weitz CJ, Kay SA. Light-dependent sequestration of TIMELESS by CRYPTOCHROME. *Science* 285: 553–556, 1999.

Chen T-W, Wardill TJ, Sun Y, Pulver SR, Renninger SL, Baohan A, Schreiter ER, Kerr RA, Orger MB, Jayaraman V, Looger LL, Svoboda K, Kim DS. Ultrasensitive fluorescent proteins for imaging neuronal activity. *Nature* 499: 295–300, 2013.

Chung BY, Kilman VL, Keath JR, Pitman JL, Allada R. The GABA(A) receptor RDL acts in peptidergic PDF neurons to promote sleep in Drosophila. *Curr. Biol. CB* 19: 386–390, 2009.

Crocker A, Sehgal A. Octopamine regulates sleep in drosophila through protein kinase A-dependent mechanisms. *J. Neurosci.* 28: 9377–9385, 2008.

Crocker A, Shahidullah M, Levitan IB, Sehgal A. Identification of a neural circuit that underlies the effects of octopamine on sleep:wake behavior. *Neuron* 65: 670–681, 2010.

Curtin KD, Huang ZJ, Rosbash M. Temporally regulated nuclear entry of the Drosophila period protein contributes to the circadian clock. *Neuron* 14: 365–372, 1995.

Dahdal D, Reeves DC, Ruben M, Akabas MH, Blau J. Drosophila pacemaker neurons require g protein signaling and GABAergic inputs to generate twenty-four hour behavioral rhythms. *Neuron* 68: 964–977, 2010.

Daniels RW, Gelfand MV, Collins CA, DiAntonio A. Visualizing glutamatergic cell bodies and synapses in Drosophila larval and adult CNS. *J. Comp. Neurol.* 508: 131–152, 2008.

Darlington TK, Wager-Smith K, Ceriani MF, Staknis D, Gekakis N, Steeves TD, Weitz CJ, Takahashi JS, Kay SA. Closing the circadian loop: CLOCK-induced transcription of its own inhibitors per and tim. *Science* 280: 1599–1603, 1998a.

Darlington TK, Wager-Smith K, Ceriani MF, Staknis D, Gekakis N, Steeves TD, Weitz CJ, Takahashi JS, Kay SA. Closing the circadian loop: CLOCK-induced transcription of its own inhibitors per and tim. *Science* 280: 1599–1603, 1998b.

Dingledine R, Borges K, Bowie D, Traynelis SF. The glutamate receptor ion channels. *Pharmacol. Rev.* 51: 7–61, 1999.

Dowse HB, Hall JC, Ringo JM. Circadian and ultradian rhythms in period mutants of Drosophila melanogaster. *Behav. Genet.* 17: 19–35, 1987.

Dunlap JC. Molecular bases for circadian clocks. *Cell* 96: 271–290, 1999.

Dushay MS, Konopka RJ, Orr D, Greenacre ML, Kyriacou CP, Rosbash M, Hall JC. Phenotypic and genetic analysis of Clock, a new circadian rhythm mutant in Drosophila melanogaster. *Genetics* 125: 557–578, 1990.

Duvall LB, Taghert PH. The circadian neuropeptide PDF signals preferentially through a specific adenylate cyclase isoform AC3 in M pacemakers of Drosophila. *PLoS Biol.* 10: e1001337, 2012.

Emery P, So WV, Kaneko M, Hall JC, Rosbash M. CRY, a Drosophila clock and light-regulated cryptochrome, is a major contributor to circadian rhythm resetting and photosensitivity. *Cell* 95: 669–679, 1998.

Emery P, Stanewsky R, Helfrich-Förster C, Emery-Le M, Hall JC, Rosbash M. Drosophila CRY is a deep brain circadian photoreceptor. *Neuron* 26: 493–504, 2000.

Fogle KJ, Parson KG, Dahm NA, Holmes TC. CRYPTOCHROME is a blue-light sensor that regulates neuronal firing rate. *Science* 331: 1409–1413, 2011.

Friggi-Grelin F, Coulom H, Meller M, Gomez D, Hirsh J, Birman S. Targeted gene expression in Drosophila dopaminergic cells using regulatory sequences from tyrosine hydroxylase. *J. Neurobiol.* 54: 618–627, 2003.

Gengs C, Leung H-T, Skingsley DR, Iovchev MI, Yin Z, Semenov EP, Burg MG, Hardie RC, Pak WL. The target of Drosophila photoreceptor synaptic transmission is a histamine-gated chloride channel encoded by ort (hclA). *J. Biol. Chem.* 277: 42113–42120, 2002.

Grima B, Chélot E, Xia R, Rouyer F. Morning and evening peaks of activity rely on different clock neurons of the Drosophila brain. *Nature* 431: 869–873, 2004.

Hamada FN, Rosenzweig M, Kang K, Pulver SR, Ghezzi A, Jegla TJ, Garrity PA. An internal thermal sensor controlling temperature preference in Drosophila. *Nature* 454: 217–220, 2008.

Hamasaka Y, Nässel DR. Mapping of serotonin, dopamine, and histamine in relation to different clock neurons in the brain of Drosophila. *J. Comp. Neurol.* 494: 314–330, 2006.

Hamasaka Y, Rieger D, Parmentier M-L, Grau Y, Helfrich-Förster C, Nässel DR. Glutamate and its metabotropic receptor in Drosophila clock neuron circuits. *J. Comp. Neurol.* 505: 32–45, 2007.

Hamasaka Y, Wegener C, Nässel DR. GABA modulates Drosophila circadian clock neurons via GABAB receptors and decreases in calcium. *J. Neurobiol.* 65: 225–240, 2005.

Hamblen-Coyle MJ, Wheeler DA, Rutila JE, Rosbash M, Hall JC. Behavior of period-altered circadian rhythm mutants ofDrosophila in light: Dark cycles (Diptera: Drosophilidae). *J. Insect Behav.* 5: 417–446, 1992.

Hao H, Allen DL, Hardin PE. A circadian enhancer mediates PER-dependent mRNA cycling in Drosophila melanogaster. *Mol. Cell. Biol.* 17: 3687–3693, 1997.

Hardie RC. A histamine-activated chloride channel involved in neurotransmission at a photoreceptor synapse. *Nature* 339: 704–706, 1989.

Hardin PE, Hall JC, Rosbash M. Feedback of the Drosophila period gene product on circadian cycling of its messenger RNA levels. *Nature* 343: 536–540, 1990.

Helfrich-Förster C, Edwards T, Yasuyama K, Wisotzki B, Schneuwly S, Stanewsky R, Meinertzhagen IA, Hofbauer A. The extraretinal eyelet of Drosophila: development, ultrastructure, and putative circadian function. *J. Neurosci.* 22: 9255–9266, 2002.

Helfrich-Förster C, Homberg U. Pigment-dispersing hormone-immunoreactive neurons in the nervous system of wild-type Drosophila melanogaster and of several mutants with altered circadian rhythmicity. *J. Comp. Neurol.* 337: 177–190, 1993.

Helfrich-Förster C, Winter C, Hofbauer A, Hall JC, Stanewsky R. The circadian clock of fruit flies is blind after elimination of all known photoreceptors. *Neuron* 30: 249–261, 2001.

Helfrich-Förster C, Yoshii T, Wülbeck C, Grieshaber E, Rieger D, Bachleitner W, Cusamano P, Rouyer F. The lateral and dorsal neurons of Drosophila melanogaster: new insights about their morphology and function. *Cold Spring Harb. Symp. Quant. Biol.* 72: 517–525, 2007.

Helfrich-Förster C. The period clock gene is expressed in central nervous system neurons which also produce a neuropeptide that reveals the projections of circadian pacemaker cells within the brain of Drosophila melanogaster. *Proc. Natl. Acad. Sci. U. S. A.* 92: 612–616, 1995.

Helfrich-Förster C. Differential control of morning and evening components in the activity rhythm of Drosophila melanogaster--sex-specific differences suggest a different quality of activity. *J. Biol. Rhythms* 15: 135–154, 2000.

Helfrich-Förster C. The circadian system of Drosophila melanogaster and its light input pathways. *Zool. Jena Ger.* 105: 297–312, 2002.

Helfrich-Förster C. The neuroarchitecture of the circadian clock in the brain of Drosophila melanogaster. *Microsc. Res. Tech.* 62: 94–102, 2003.

Helfrich-Förster C. The circadian clock in the brain: a structural and functional comparison between mammals and insects. *J. Comp. Physiol. A Neuroethol. Sens. Neural. Behav. Physiol.* 190: 601–613, 2004.

Helfrich-Förster C. Neurobiology of the fruit fly's circadian clock. *Genes Brain Behav.* 4: 65–76, 2005.

Hendricks JC, Sehgal A, Pack AI. The need for a simple animal model to understand sleep. *Prog. Neurobiol.* 61: 339–351, 2000.

Hermann C, Yoshii T, Dusik V, Helfrich-Förster C. Neuropeptide F immunoreactive clock neurons modify evening locomotor activity and free-running period in Drosophila melanogaster. *J. Comp. Neurol.* 520: 970–987, 2012.

Hofbauer A, Buchner E. Does Drosophila have seven eyes? *Naturwissen* 76: 335–336, 1989.

Hong S-T, Bang S, Paik D, Kang J, Hwang S, Jeon K, Chun B, Hyun S, Lee Y, Kim J. Histamine and its receptors modulate temperature-preference behaviors in Drosophila. *J. Neurosci.* 26: 7245–7256, 2006.

Hyun S, Lee Y, Hong S-T, Bang S, Paik D, Kang J, Shin J, Lee J, Jeon K, Hwang S, Bae E, Kim J. Drosophila GPCR Han is a receptor for the circadian clock neuropeptide PDF. *Neuron* 48: 267–278, 2005.

Im SH, Taghert PH. PDF receptor expression reveals direct interactions between circadian oscillators in Drosophila. *J. Comp. Neurol.* 518: 1925–1945, 2010.

Jan LY, Jan YN. L-glutamate as an excitatory transmitter at the Drosophila larval neuromuscular junction. *J. Physiol.* 262: 215–236, 1976.

Jenett A, Rubin GM, Ngo T-TB, Shepherd D, Murphy C, Dionne H, Pfeiffer BD, Cavallaro A, Hall D, Jeter J, Iyer N, Fetter D, Hausenfluck JH, Peng H, Trautman ET, Svirskas RR, Myers EW, Iwinski ZR, Aso Y, DePasquale GM, Enos A, Hulamm P, Lam SCB, Li H-H, Laverty TR, Long F, Qu L, Murphy SD, Rokicki K, Safford T, Shaw K, Simpson JH, Sowell A, Tae S, Yu Y, Zugates CT. A GAL4-driver line resource for Drosophila neurobiology. *Cell Rep.* 2: 991–1001, 2012.

Johard HAD, Yoishii T, Dircksen H, Cusumano P, Rouyer F, Helfrich-Förster C, Nässel DR. Peptidergic clock neurons in Drosophila: ion transport peptide and short neuropeptide F in subsets of dorsal and ventral lateral neurons. *J. Comp. Neurol.* 516: 59–73, 2009.

Johnson C, Elliot J, Foster RG, Ken-Ichi H, Kronauer R. Fundemental properties of circadian rhythms. In: *Chronobiology: biological timekeeping*, edited by Dunlap JC, Loros JJ, Decoursey PJ. Massachusetts: Sinauer Associates, Inc., 2004.

Kaneko M, Hall JC. Neuroanatomy of cells expressing clock genes in Drosophila: transgenic manipulation of the period and timeless genes to mark the perikarya of circadian pacemaker neurons and their projections. *J. Comp. Neurol.* 422: 66–94, 2000.

Kaneko M, Helfrich-Förster C, Hall JC. Spatial and temporal expression of the period and timeless genes in the developing nervous system of Drosophila: newly identified pacemaker candidates and novel features of clock gene product cycling. *J. Neurosci.* 17: 6745–6760, 1997.

Kaushik R, Nawathean P, Busza A, Murad A, Emery P, Rosbash M. PER-TIM interactions with the photoreceptor cryptochrome mediate circadian temperature responses in Drosophila. *PLoS Biol.* 5: e146, 2007.

Keene AC, Mazzoni EO, Zhen J, Younger MA, Yamaguchi S, Blau J, Desplan C, Sprecher SG. Distinct visual pathways mediate Drosophila larval light avoidance and circadian clock entrainment. *J. Neurosci.* 31: 6527–6534, 2011.

Keene AC, Sprecher SG. Seeing the light: photobehavior in fruit fly larvae. *Trends Neurosci.* 35: 104–110, 2012.

Kim EY, Edery I. Balance between DBT/CKIepsilon kinase and protein phosphatase activities regulate phosphorylation and stability of Drosophila CLOCK protein. *Proc. Natl. Acad. Sci. U. S. A.* 103: 6178–6183, 2006.

Kistenpfennig C, Hirsh J, Yoshii T, Helfrich-Förster C. Phase-shifting the fruit fly clock without cryptochrome. *J. Biol. Rhythms* 27: 117–125, 2012.

Kloss B, Price JL, Saez L, Blau J, Rothenfluh A, Wesley CS, Young MW. The Drosophila clock gene double-time encodes a protein closely related to human casein kinase Iepsilon. *Cell* 94: 97–107, 1998.

Kolodziejczyk A, Sun X, Meinertzhagen IA, Nässel DR. Glutamate, GABA and acetylcholine signaling components in the lamina of the Drosophila visual system. *PloS One* 3: e2110, 2008.

Konopka RJ, Benzer S. Clock mutants of Drosophila melanogaster. *Proc. Natl. Acad. Sci. U. S. A.* 68: 2112–2116, 1971.

Lai S-L, Lee T. Genetic mosaic with dual binary transcriptional systems in Drosophila. *Nat. Neurosci.* 9: 703–709, 2006.

Lear BC, Zhang L, Allada R. The neuropeptide PDF acts directly on evening pacemaker neurons to regulate multiple features of circadian behavior. *PLoS Biol.* 7: e1000154, 2009.

Lee C, Bae K, Edery I. PER and TIM inhibit the DNA binding activity of a Drosophila CLOCK-CYC/dBMAL1 heterodimer without disrupting formation of the heterodimer: a basis for circadian transcription. *Mol. Cell. Biol.* 19: 5316–5325, 1999.

Lee C, Etchegaray JP, Cagampang FR, Loudon AS, Reppert SM. Posttranslational mechanisms regulate the mammalian circadian clock. *Cell* 107: 855–867, 2001.

Lelito KR, Shafer OT. Reciprocal cholinergic and GABAergic modulation of the small ventrolateral pacemaker neurons of Drosophila's circadian clock neuron network. *J. Neurophysiol.* 107: 2096–2108, 2012a.

Lelito KR, Shafer OT. Imaging cAMP Dynamics in the Drosophila Brain with the Genetically Encoded Sensor Epac1-Camps. In: *Genetically Encoded Functional Indicators*, edited by Martin J-R. Humana Press, p. 149–168.

Lima SQ, Miesenböck G. Remote control of behavior through genetically targeted photostimulation of neurons. *Cell* 121: 141–152, 2005.

Littleton JT, Ganetzky B. Ion channels and synaptic organization: analysis of the Drosophila genome. *Neuron* 26: 35–43, 2000.

Martinek S, Inonog S, Manoukian AS, Young MW. A role for the segment polarity gene shaggy/GSK-3 in the Drosophila circadian clock. *Cell* 105: 769–779, 2001.

Mazzoni EO, Desplan C, Blau J. Circadian pacemaker neurons transmit and modulate visual information to control a rapid behavioral response. *Neuron* 45: 293–300, 2005.

McCarthy EV, Wu Y, Decarvalho T, Brandt C, Cao G, Nitabach MN. Synchronized bilateral synaptic inputs to Drosophila melanogaster neuropeptidergic rest/arousal neurons. *J. Neurosci.* 31: 8181–8193, 2011.

McDonald MJ, Rosbash M, Emery P. Wild-type circadian rhythmicity is dependent on closely spaced E boxes in the Drosophila timeless promoter. *Mol. Cell. Biol.* 21: 1207–1217, 2001.

Mealey-Ferrara ML, Montalvo AG, Hall JC. Effects of combining a cryptochrome mutation with other visual-system variants on entrainment of locomotor and adult-emergence rhythms in Drosophila. *J. Neurogenet.* 17: 171–221, 2003.

Mertens I, Vandingenen A, Johnson EC, Shafer OT, Li W, Trigg JS, De Loof A, Schoofs L, Taghert PH. PDF receptor signaling in Drosophila contributes to both circadian and geotactic behaviors. *Neuron* 48: 213–219, 2005.

Miesenböck G, Kevrekidis IG. Optical imaging and control of genetically designated neurons in functioning circuits. *Annu. Rev. Neurosci.* 28: 533–563, 2005.

Miesenböck G. The optogenetic catechism. *Science* 326: 395–399, 2009.

Muraro NI, Pírez N, Ceriani MF. The circadian system: Plasticity at many levels. *Neuroscience* 247: 280–293, 2013.

Naidoo N, Song W, Hunter-Ensor M, Sehgal A. A role for the proteasome in the light response of the timeless clock protein. *Science* 285: 1737–1741, 1999.

Nakai J, Ohkura M, Imoto K. A high signal-to-noise Ca(2+) probe composed of a single green fluorescent protein. *Nat. Biotechnol.* 19: 137–141, 2001.

Nässel DR, Holmqvist MH, Hardie RC, Håkanson R, Sundler F. Histamine-like immunoreactivity in photoreceptors of the compound eyes and ocelli of the flies Calliphora erythrocephala and Musca domestica. *Cell Tissue Res.* 253: 639–646, 1988.

Nikolaev VO, Bünemann M, Hein L, Hannawacker A, Lohse MJ. Novel single chain cAMP sensors for receptor-induced signal propagation. *J. Biol. Chem.* 279: 37215–37218, 2004.

Pantazis A, Segaran A, Liu C-H, Nikolaev A, Rister J, Thum AS, Roeder T, Semenov E, Juusola M, Hardie RC. Distinct roles for two histamine receptors (hclA and hclB) at the Drosophila photoreceptor synapse. *J. Neurosci.* 28: 7250–7259, 2008.

Parisky KM, Agosto J, Pulver SR, Shang Y, Kuklin E, Hodge JJL, Kang K, Kang K, Liu X, Garrity PA, Rosbash M, Griffith LC. PDF cells are a GABA-responsive wake-promoting component of the Drosophila sleep circuit. *Neuron* 60: 672–682, 2008.

Park D, Griffith LC. Electrophysiological and anatomical characterization of PDF-positive clock neurons in the intact adult Drosophila brain. *J. Neurophysiol.* 95: 3955–3960, 2006.

Park JH, Hall JC. Isolation and chronobiological analysis of a neuropeptide pigment-dispersing factor gene in Drosophila melanogaster. *J. Biol. Rhythms* 13: 219–228, 1998.

Park JH, Helfrich-Förster C, Lee G, Liu L, Rosbash M, Hall JC. Differential regulation of circadian pacemaker output by separate clock genes in Drosophila. *Proc. Natl. Acad. Sci. U. S. A.* 97: 3608–3613, 2000.

Pfeiffer BD, Ngo T-TB, Hibbard KL, Murphy C, Jenett A, Truman JW, Rubin GM. Refinement of tools for targeted gene expression in Drosophila. *Genetics* 186: 735–755, 2010.

Van den Pol AN. The hypothalamic suprachiasmatic nucleus of rat: intrinsic anatomy. *J. Comp. Neurol.* 191: 661–702, 1980.

Pollack I, Hofbauer A. Histamine-like immunoreactivity in the visual system and brain of Drosophila melanogaster. *Cell Tissue Res.* 266: 391–398, 1991.

Price JL, Blau J, Rothenfluh A, Abodeely M, Kloss B, Young MW. double-time is a novel Drosophila clock gene that regulates PERIOD protein accumulation. *Cell* 94: 83–95, 1998.

Pulver SR, Pashkovski SL, Hornstein NJ, Garrity PA, Griffith LC. Temporal dynamics of neuronal activation by Channelrhodopsin-2 and TRPA1 determine behavioral output in Drosophila larvae. *J. Neurophysiol.* 101: 3075–3088, 2009.

Pyza E, Meinertzhagen IA. Daily rhythmic changes of cell size and shape in the first optic neuropil in Drosophila melanogaster. *J. Neurobiol.* 40: 77–88, 1999.

Renn SC, Park JH, Rosbash M, Hall JC, Taghert PH. A pdf neuropeptide gene mutation and ablation of PDF neurons each cause severe abnormalities of behavioral circadian rhythms in Drosophila. *Cell* 99: 791–802, 1999.

Rieger D, Stanewsky R, Helfrich-Förster C. Cryptochrome, compound eyes, Hofbauer-Buchner eyelets, and ocelli play different roles in the entrainment and masking pathway of the locomotor activity rhythm in the fruit fly Drosophila melanogaster. *J. Biol. Rhythms* 18: 377–391, 2003.

Rietveld WJ, Minors DS, Waterhouse JM. Circadian rhythms and masking: an overview. *Chronobiol. Int.* 10: 306–312, 1993.

Rutila JE, Suri V, Le M, So WV, Rosbash M, Hall JC. CYCLE is a second bHLH-PAS clock protein essential for circadian rhythmicity and transcription of Drosophila period and timeless. *Cell* 93: 805–814, 1998.

Sarthy PV. Histamine: a neurotransmitter candidate for Drosophila photoreceptors. *J. Neurochem.* 57: 1757–1768, 1991.

Schuster R, Phannavong B, Schröder C, Gundelfinger ED. Immunohistochemical localization of a ligand-binding and a structural subunit of nicotinic acetylcholine receptors in the central nervous system of Drosophila melanogaster. *J. Comp. Neurol.* 335: 149–162, 1993.

Sehgal A, Rothenfluh-Hilfiker A, Hunter-Ensor M, Chen Y, Myers MP, Young MW. Rhythmic expression of timeless: a basis for promoting circadian cycles in period gene autoregulation. *Science* 270: 808–810, 1995.

Shafer OT, Helfrich-Förster C, Renn SCP, Taghert PH. Reevaluation of Drosophila melanogaster's neuronal circadian pacemakers reveals new neuronal classes. *J. Comp. Neurol.* 498: 180–193, 2006.

Shafer OT, Kim DJ, Dunbar-Yaffe R, Nikolaev VO, Lohse MJ, Taghert PH. Widespread receptivity to neuropeptide PDF throughout the neuronal circadian clock network of Drosophila revealed by real-time cyclic AMP imaging. *Neuron* 58: 223–237, 2008.

Shang Y, Griffith LC, Rosbash M. Light-arousal and circadian photoreception circuits intersect at the large PDF cells of the Drosophila brain. *Proc. Natl. Acad. Sci. U. S. A.* 105: 19587–19594, 2008.

Shang Y, Haynes P, Pírez N, Harrington KI, Guo F, Pollack J, Hong P, Griffith LC, Rosbash M. Imaging analysis of clock neurons reveals light buffers the wake-promoting effect of dopamine. *Nat. Neurosci.* 14: 889–895, 2011.

Shaw PJ, Cirelli C, Greenspan RJ, Tononi G. Correlates of sleep and waking in Drosophila melanogaster. *Science* 287: 1834–1837, 2000.

Shearman LP, Zylka MJ, Weaver DR, Kolakowski LF Jr, Reppert SM. Two period homologs: circadian expression and photic regulation in the suprachiasmatic nuclei. *Neuron* 19: 1261–1269, 1997.

Sheeba V, Fogle KJ, Kaneko M, Rashid S, Chou Y-T, Sharma VK, Holmes TC. Large Ventral Lateral Neurons Modulate Arousal and Sleep in Drosophila. *Curr. Biol.* 18: 1537–1545, 2008a.

Sheeba V, Gu H, Sharma VK, O'Dowd DK, Holmes TC. Circadian- and light-dependent regulation of resting membrane potential and spontaneous action potential firing of Drosophila circadian pacemaker neurons. *J. Neurophysiol.* 99: 976–988, 2008b.

Stanewsky R, Kaneko M, Emery P, Beretta B, Wager-Smith K, Kay SA, Rosbash M, Hall JC. The cryb mutation identifies cryptochrome as a circadian photoreceptor in Drosophila. *Cell* 95: 681–692, 1998.

Stanewsky R. Genetic analysis of the circadian system in Drosophila melanogaster and mammals. *J. Neurobiol.* 54: 111–147, 2003.

Stoleru D, Peng Y, Agosto J, Rosbash M. Coupled oscillators control morning and evening locomotor behaviour of Drosophila. *Nature* 431: 862–868, 2004.

Suri V, Qian Z, Hall JC, Rosbash M. Evidence that the TIM light response is relevant to light-induced phase shifts in Drosophila melanogaster. *Neuron* 21: 225–234, 1998.

Taghert PH, Shafer OT. Mechanisms of clock output in the Drosophila circadian pacemaker system. *J. Biol. Rhythms* 21: 445–457, 2006.

Talsma AD, Christov CP, Terriente-Felix A, Linneweber GA, Perea D, Wayland M, Shafer OT, Miguel-Aliaga I. Remote control of renal physiology by the intestinal neuropeptide pigment-dispersing factor in Drosophila. *Proc. Natl. Acad. Sci. U. S. A.* 109: 12177–12182, 2012.

Tei H, Okamura H, Shigeyoshi Y, Fukuhara C, Ozawa R, Hirose M, Sakaki Y. Circadian oscillation of a mammalian homologue of the Drosophila period gene. *Nature* 389: 512–516, 1997.

Tian L, Hires SA, Mao T, Huber D, Chiappe ME, Chalasani SH, Petreanu L, Akerboom J, McKinney SA, Schreiter ER, Bargmann CI, Jayaraman V, Svoboda K, Looger LL. Imaging neural activity in worms, flies and mice with improved GCaMP calcium indicators. *Nat. Methods* 6: 875–881, 2009.

Tomchik SM, Davis RL. Dynamics of learning-related cAMP signaling and stimulus integration in the Drosophila olfactory pathway. *Neuron* 64: 510–521, 2009.

Ultsch A, Schuster CM, Laube B, Schloss P, Schmitt B, Betz H. Glutamate receptors of Drosophila melanogaster: cloning of a kainate-selective subunit expressed in the central nervous system. *Proc. Natl. Acad. Sci. U. S. A.* 89: 10484–10488, 1992.

Veleri S, Brandes C, Helfrich-Förster C, Hall JC, Stanewsky R. A self-sustaining, light-entrainable circadian oscillator in the Drosophila brain. *Curr. Biol. CB* 13: 1758–1767, 2003.

Viswanath V, Story GM, Peier AM, Petrus MJ, Lee VM, Hwang SW, Patapoutian A, Jegla T. Opposite thermosensor in fruitfly and mouse. *Nature* 423: 822–823, 2003.

Völkner M, Lenz-Böhme B, Betz H, Schmitt B. Novel CNS glutamate receptor subunit genes of Drosophila melanogaster. *J. Neurochem.* 75: 1791–1799, 2000.

Wang JW, Wong AM, Flores J, Vosshall LB, Axel R. Two-photon calcium imaging reveals an odor-evoked map of activity in the fly brain. *Cell* 112: 271–282, 2003.

Wegener C, Hamasaka Y, Nässel DR. Acetylcholine increases intracellular Ca2+ via nicotinic receptors in cultured PDF-containing clock neurons of Drosophila. *J. Neurophysiol.* 91: 912–923, 2004.

Wheeler DA, Hamblen-Coyle MJ, Dushay MS, Hall JC. Behavior in light-dark cycles of Drosophila mutants that are arrhythmic, blind, or both. *J. Biol. Rhythms* 8: 67–94, 1993.

Wu JS, Luo L. A protocol for dissecting Drosophila melanogaster brains for live imaging or immunostaining. *Nat. Protoc.* 1: 2110–2115, 2006.

Yao Z, Macara AM, Lelito KR, Minosyan TY, Shafer OT. Analysis of functional neuronal connectivity in the Drosophila brain. *J. Neurophysiol.* 108: 684–696, 2012.

Yao Z, Shafer OT. The Drosophila circadian clock is a variably coupled network of multiple peptidergic units. *Science* 343: 1516–1520, 2014.

Yasuyama K, Meinertzhagen IA. Extraretinal photoreceptors at the compound eye's posterior margin in Drosophila melanogaster. *J. Comp. Neurol.* 412: 193–202, 1999.

Yasuyama K, Salvaterra PM. Localization of choline acetyltransferase-expressing neurons in Drosophila nervous system. *Microsc. Res. Tech.* 45: 65–79, 1999.

Yoshii T, Heshiki Y, Ibuki-Ishibashi T, Matsumoto A, Tanimura T, Tomioka K. Temperature cycles drive Drosophila circadian oscillation in constant light that otherwise induces behavioural arrhythmicity. *Eur. J. Neurosci.* 22: 1176–1184, 2005.

Yoshii T, Todo T, Wülbeck C, Stanewsky R, Helfrich-Förster C. Cryptochrome is present in the compound eyes and a subset of Drosophila's clock neurons. *J. Comp. Neurol.* 508: 952–966, 2008.

Yu W, Zheng H, Houl JH, Dauwalder B, Hardin PE. PER-dependent rhythms in CLK phosphorylation and E-box binding regulate circadian transcription. *Genes Dev.* 20: 723–733, 2006.

Yuan Q, Lin F, Zheng X, Sehgal A. Serotonin modulates circadian entrainment in Drosophila. *Neuron* 47: 115–127, 2005.

Zheng X, Sehgal A. Speed control: cogs and gears that drive the circadian clock. *Trends Neurosci.* 35: 574–585, 2012.

Zylka MJ, Shearman LP, Weaver DR, Reppert SM. Three period homologs in mammals: differential light responses in the suprachiasmatic circadian clock and oscillating transcripts outside of brain. *Neuron* 20: 1103–1110, 1998.

CHAPTER 2
IMAGING cAMP DYNAMICS IN THE DROSOPHILA BRAIN WITH THE GENETICALLY ENCODED SENSOR EPAC1-CAMPS

2.1 ABSTRACT

Cyclic adenosine monophosphate (cAMP) is a critical second messenger signaling molecule, the modulation of which is a central mode of nervous system function. The development of genetically encoded sensors for cAMP has made it possible to measure cAMP dynamics within living cells with high temporal and spatial resolution. In this chapter, we review live-imaging methods for the measurement of relative cAMP levels within single neurons of the explanted adult Drosophila brain. Specifically, we describe a detailed protocol for the monitoring of neuronal cAMP dynamics during bath application of neurotransmitters and neuromodulators using the genetically encoded cAMP sensor Epac1-camps and scanning laser confocal microscopy.

2.2 INTRODUCTION

Despite the relative simplicity of its nervous system, Drosophila melanogaster is capable of producing a remarkable repertoire of complex behaviors (Weiner, 2000). This, coupled with its remarkable genetic malleability, has made the fly a valuable model system for the molecular and genetic basis of animal behavior. The discovery of genes that govern specific behaviors in Drosophila has allowed neurobiologists to identify the putative neural substrates of those behaviors through the mapping of behavioral gene expression within the central nervous system (Simpson and Stephen, 2009). However, the electrophysiological inaccessibility of many of the fly's

central brain neurons presents a fundamental challenge for the Drosophila neurobiologist. Understanding how networks of genetically defined neurons produce specific behavioral outputs requires the ability to measure the physiological responses of these networks to sensory and neurochemical stimuli. In this regard, the development of genetically encoded sensors for neuronal activity represents a critical technical development (Guerrero and Isacoff, 2001).

The creation of green fluorescent protein (GFP)-based Ca2+ sensors whose expression can be driven within genetically defined neural networks of the fly has made it possible to measure the activity of neuronal populations in response to sensory input and neurochemical modulation (Fiala et al., 2002). The optimization of GCaMP, a GFP-based Ca^{2+} sensor, has produced a robust and sensitive sensor for the detection of neuronal excitation in the fly brain (Tian et al., 2009). Nevertheless, many important neuromodulators act through second messenger signaling cascades that may have little or no acute effects on Ca^{2+}. For example, cyclic adenosine monophosphate (cAMP) is a ubiquitous signaling molecule, the modulation of which underlies many important physiological processes (Spaulding, 1993; Beavo and Brunton, 2002; Borland et al., 2009). In both flies and mammals cAMP signaling is critical for the formation of long-term memories (Yin and Tully, 1996), the transduction of olfactory cues (Schild and Restrepo, 1998; Nakagawa and Vosshall, 2009), and the maintenance of endogenous circadian rhythms (Levine et al., 1994; O'Neill et al., 2008). The ability to measure cAMP dynamics within neural networks of Drosophila would allow for the measurement of behaviorally relevant neuromodulatory cascades that might not be easily detected using Ca^{2+} sensors.

Recently, several genetically encoded sensors for cAMP have been developed (reviewed in ref. (Vincent et al., 2008)). Two of these, GFP-PKA and Epac1-camps, have been successfully used to measure relative cAMP levels within neural networks of the fly brain with high spatial and temporal resolution (Lissandron et al., 2007; Gervasi et al., 2010). Another sensor designed to specifically measure protein kinase A (PKA) activation has also been successfully employed in the fly brain (Gervasi et al., 2010). In this chapter, we describe methods for measuring relative cAMP levels in single Drosophila neurons in the explanted brain using the

Epac1-camps sensor and scanning laser confocal microscopy. We direct the reader to the excellent protocol of Börner et al. (Börner et al., 2011) for the measurement of cAMP concentrations in cell culture using Epac1-camps and epifluourescent microscopy.

Epac1-camps was created in the laboratory of Martin Lohse, one of several labs to develop a sensor based on Epac (exchange protein activated by cAMP) (DiPilato et al., 2004; Nikolaev et al., 2004; Ponsioen et al., 2004). Epac is a guanine nucleotide exchange factor of Rap1, a Ras-like GTPase that mediates PKA-independent effects of cAMP (Gloerich and Bos, 2010). The Epac-based cAMP sensors all rely on Förster resonance energy transfer (FRET) for the detection of changing cAMP levels. These sensors consist of Epac sequences flanked by the GFP variants cyan fluorescent protein (CFP) and yellow fluorescent protein (YFP) (DiPilato et al., 2004; Nikolaev et al., 2004; Ponsioen et al., 2004). When unbound to cAMP the proximity of CFP and YFP allows for energy transfer from CFP to YFP so that the excitation of CFP with 440 nm light results in relatively high YPF emission and low CFP emission in the absence of bound cAMP. Upon the binding of a single molecule of cAMP, Epac-based sensors undergo a conformational change that increases the distance between CFP and YFP, thereby reducing energy transfer. Thus, when cAMP levels rise, Epac-based sensors display concomitant increases in CFP and decreases in YFP emission. In this manner, the FRET ratio (YFP/CFP) of Epac-based sensors is inversely proportional to cAMP levels. Figure 2.1 schematizes the general structure and function of Epac-based cAMP sensors.

Unlike the PKA-based cAMP sensor GFP-PKA, Epac1-camps is well tolerated by fly neurons (15, 16). This is likely a reflection of the fact that GFP-PKA contains functional domains of PKA that may perturb cAMP/PKA signaling while Epac1-camps has been stripped of Epac's catalytic domains (discussed in refs. (Vincent et al., 2008; Willoughby and Cooper, 2008)). Furthermore, the invariant 1:1 CFP to YFP stoichiometry of the single molecule Epac1-camps makes its measurement of relative cAMP levels more straightforward than that of the GFP-PKA sensor, which consists of separate CFP-bound regulatory and YFP-bound catalytic subunits of PKA (Xia and Liu, 2001; Nikolaev et al., 2004; Lissandron et al., 2005). Several

laboratories have used Epac1-camps to measure cAMP dynamics within the neural networks of the fly that govern circadian rhythms (Shafer et al., 2008; Kula-Eversole et al., 2010), olfactory learning (Tomchik and Davis, 2009), and sleep (Wu et al., 2009; Crocker et al., 2010). It is important to note that despite that fact that Epac1-camps is nearly ten-times more sensitive to cAMP than to cyclic guanosine monophosphate (cGMP) in vitro (Nikolaev et al., 2004), it appears to be sensitive to physiologically relevant cGMP levels in fly neurons (Shakiryanova and Levitan, 2008). Therefore, when using Epac1-camps, conclusions regarding cAMP must be tempered by the possibility that changes in cGMP have caused or contributed to observed changes in Epac1-camps FRET.

In this chapter we present a detailed protocol for using Epac1-camps to measure relative cAMP levels within single neurons of the explanted Drosophila brain during the administration of bath-applied neurotransmitters. We describe the use of the GAL4/UAS binary system to drive Epac1-camps expression within defined neuronal networks, the dissection and preparation of the brain for imaging, the collection of time-course imaging data, the delivery of neurochemical stimuli, and the processing and analysis of Epac1-camps time-course data.

2.3 MATERIALS

Fly Crosses and Rearing

Protocols for the rearing of Drosophila in the laboratory have been described in detail by Ashburner and Roote (Ashburner and Roote, 2000) and are not discussed in detail here. Three UAS-Epac1-camps lines are available as independent insertions in chromosomes one, two, and three from the Bloomington Drosophila Stock Center (http://flystocks. bio.indiana.edu/) and GAL4 driver lines are available from labs and stock centers around the world. The reader is directed to the appendix of Greenspan's introduction of Drosophila genetics for stock center information (Greenspan, 2004). A simple cross between a UAS- Epac1-camps line and an appropriate GAL4 line will yield offspring with UAS-Epac1-camps expression in GAL4 expressing neurons (see below). We recommend using brains from 3- to 7-day-old adult flies for live imaging experiments.

Dissection and Mounting

Adult brain dissection requires a dissecting stereomicroscope, a sylgard dissecting dish, an insect pin, two sets of sharp fine forceps and ice-cold fly Ringer's solution consisting of (in mM): 128 NaCl, 2 KCl, 1.8 CaCl2, 4 MgCl2, 35.5 sucrose, 5 HEPES, pH 7.1 (Jan and Jan, 1976b). Fly saline can be autoclaved and stored at room temperature. After complete dissection of the brain, it should be transferred to the bottom of a 35 mm plastic culture dish containing the hemolymph-like saline HL3 consisting of (in mM): 70 NaCl, 5 KCl, 1.5 CaCl2, 20 MgCl2, 10 NaHCO3, 5 D(+) Trehelose, 115 sucrose, 5 HEPES, pH 7.1 (Stewart et al., 1994). HL3 should be vacuum filtered and frozen in small (~50 ml) aliquots. We recommend using freshly thawed HL3 for each day's experiments.

Recording and Data Analysis

This protocol requires a scanning laser confocal microscope with its associated command computer and software. The confocal must be capable of scanning optical sections using a laser with a wavelength at or near 440 nm and separating CFP and YFP emission centered around 480 and 530 nm, respectively. The microscope should also be equipped with epifluorescence optics for CFP and GFP or YFP visualization. The precise nature of the lenses, laser lines, and dichroic mirrors used for FRET time-course experiments will vary among imaging systems. Details of time-course acquisition, data collection and analysis will also vary among acquisition and analysis programs.

Solutions and Bath-Application

HL3 saline and dissolved compounds can be administered using a gravity fed-perfusion system. These systems typically comprise a series of elevated reservoirs fed via small gauge plastic tubes to a rubber chamber that directs fluid flow across the preparation and make possible a rapid switching between reservoirs. Fluid is removed from the dish via peristaltic or vacuum pumping. Alternatively, compounds can be prepared as 10× solutions and directly

micropipetted into a predetermined volume of HL3 within the dish to create a 1× final concentration of compound. This is the suggested method for compounds that cannot be perfused at high volumes due to scarcity or expense. Forskolin can be prepared as a 10 mM stock solution in DMSO and frozen in small (10–100 ml) aliquots. These aliquots can be freshly diluted in HL3 for imaging experiments. We recommend dissolving neurotransmitters, agonists, and antagonists in freshly made or freshly thawed HL3 immediately before conducting live imaging experiments. Researchers should strive to minimize the amount of time a compound sits in aqueous solution before being applied to brains.

2.4 METHODS

The procedures we describe in this chapter are designed specifically for monitoring cAMP dynamics within neurons of the explanted Drosophila brain in response to bath-application of neurochemical stimuli. Nevertheless, many aspects of this protocol may be applied to other tissues, organisms, and types of stimuli.

Tissue Preparation

In *Drosophila*, the targeted expression of genetically encoded sensors is most easily achieved using the GAL4/UAS system (Brand and Perrimon, 1993). In this system the yeast transcription factor GAL4 is driven by endogenous fly enhancers, so that GAL4 is expressed in a manner that resembles the expression of the fly gene controlled by the enhancer in question. Transgenes, such as genetically encoded sensors, are placed downstream of the upstream activating sequence (UAS), GAL4's target promoter sequence in yeast. The generation of flies expressing the UAS-Epac1-camps under the control of GAL4 elements is the most time consuming aspect of this protocol, taking about 2 weeks for adult GAL4/UAS-Epac1-camps flies to develop. Such flies can be easily created by crossing virgin UAS- Epac1-camps flies to male flies carrying a GAL4 element that is expressed in neurons of interest (Fig. 2.2a). We direct the reader unfamiliar with fly genetics to Greenspan's excellent introduction to Drosophila (Greenspan, 2004). Several UAS-Epac1-camps lines were created in the laboratory of Paul Taghert (Shafer et al., 2008), and are available

through the Bloomington Drosophila Stock Center at Indiana University (see above). Hundreds of GAL4 lines are available from stock centers and laboratories around the world. The GAL4 element selected should allow for reliable identification of the neuron classes of interest across individuals. For example, we have used a Clock-GAL4 element (Gummadova et al., 2009) to drive UAS-Epac1-camps expression specifically in the clock neuron network of the adult fly brain. Using the most specific GAL4 line possible will minimize the chances of recording Epac1-camps FRET from nontarget neurons and will make the identification of neurons of interest relatively easy. Nevertheless, given the high Z-resolution of the confocal microscope, even widely expressed GAL4 elements can be used if the experimenter is able to reliably identify and optically isolate the target neurons of interest within the brain. It is possible to create lines of flies that stably maintain both GAL4 and UAS-Epac1-camps elements using standard fly genetic methods (Greenspan, 2004), thereby obviating the need to set up crosses for each experiment (but see note 1).

Three to five days after the GAL4/UAS-bearing flies emerge, brains may be dissected and used for live imaging experiments. To dissect brains, immobilize adult flies on ice. Pin individual flies down under ice-cold Ringer's solution within a sylgard lined dissecting dish using a single insect pin through the thorax. Carefully disrupt the head cuticle using two fine forceps and gently remove all cuticle and (if desired) compound eye tissue from the underlying brain (Fig. 2.2b). A detailed protocol for Drosophila brain dissection and a description of the necessary materials has been described in detail (Wu and Luo, 2006). Once isolated, the brain can be adhered to the bottom of a clean 35 mm culture dish beneath a large drop of HL3. In our experience, the fly brain adheres sufficiently to plastic culture dishes, eliminating the need for poly-lysine or other treatments (Fig. 2.2b, c; see note 2). When immobilizing flies on ice for dissections, it is important to never use brains from flies that have been on ice for more than an hour. Dissected brains can be kept alive in HL3 for several hours, though we caution the reader from extending experiments beyond an hour following dissection and mounting. For experiments using a perfusion system, a perfusion insert can be lowered around the brain (Fig. 2.2c). For simple pipette-based application, the brain can simply be submerged in a

predetermined volume of HL3.

It is critical to have an intact brain for Epac1-camps imaging experiments and it is important that only cleanly dissected brains that have not been punctured or otherwise disrupted be used for experiments. It is therefore critical that the mounted brain be carefully inspected for disruptions and that disrupted brains be discarded. After a cleanly dissected brain is mounted, it should be allowed to stabilize for 10–20 min before the experiment is conducted. This will prevent the experimenter from recording fluctuations in cAMP levels that are a direct response to the trauma of the dissection. This wait also allows the brain to settle onto the culture dish, which will minimize settling movements during imaging (see note 3).

In our experience, moderate to moderately high expression levels of the Epac1-camps sensor are needed to reliably measure the changes in Epac1-camps FRET associated with changes in cAMP. However, extremely high Epac1-camps expression can be problematic (Börner et al., 2011) and it is critical that positive controls are used to insure that cAMP dependent FRET changes can be measured for each neuron class and GAL4/UAS combination used (see below). Expression levels will depend on the strength of GAL4 expression by the cell type in question (see note 4). The level of Epac1-camps expression can be determined visually by observing the YPF fluorescence under epifluorescent illumination using standard YFP or GFP optics. Expression levels are typically sufficient when the Epac1-camps expressing neurons are easily visible under epifluorescent illumination and when relatively low laser powers are required to visualize CFP and YFP emission using the scanning laser confocal (Fig. 2.2d–f). The absolute values of the laser power will vary among imaging systems, but should be low enough as to not cause a rapid photobleaching of CFP or YFP.

Recording Parameters

Optics for CFP/YFP FRET should be used for Epac1-camps imaging experiments, whereby the tissue is scanned with a 440 nm laser and CFP and YFP emission wavelengths are collected at 480 and 530 nm, respectively (Xia and Liu, 2001). Epac1-camps-expressing cell bodies and neurites can typically be imaged

using a ×20 or higher magnification objective. For upright microscopes, dipping cone objectives should be used. For inverted microscopes, standard objectives can be used, but in this case culture dishes with coverglass bottoms should be employed for optimal image quality. In this case the bottoms of the dishes should be coated with poly-lysine to insure brain adherence. Neurons of interest can be located first using epifluorescent illumination followed by rapid laser scanning and fine focal adjustment. Upon determining the focal plane and imaging field for a particular set of neurons, regions of interest (ROIs) can be placed over the cell bodies or neurites contained in the imaging plane for collection of fluorescent intensity values over time. This is easily accomplished using the software controlling most imaging systems.

Changes in cAMP generally occur over timescales of tens of seconds to several minutes. Therefore, scanning frequencies of 0.1–1 Hz are usually sufficient to measure the kinetics of cAMP responses to bath-applied neurotransmitter in the fly brain (Shafer et al., 2008; Tomchik and Davis, 2009). Sampling at higher frequencies will typically reveal very little and can result in photobleaching of Epac1-camp's fluorophores. YFP is usually more sensitive to such photobleaching, which results in an apparent decrease in the YFP/CFP FRET ratio (Börner et al., 2011). Therefore, to ensure consistency of baseline Epac1-Camps FRET profiles between samples, laser power, dwell time, and scanning frequency should remain constant between the samples of a given experiment (see note 5). We favor a strategy in which these settings are optimized for a given GAL4/UAS combination and neuron type based on several 10-min forskolin and vehicle control time-course experiments (see below). Settings should make possible the detection of FRET changes in response to the former but should not result in significant changes in FRET for the latter. Once these settings have been determined, they may be used repeatedly for specific bath- application experiments. Note: these settings may differ among cell types, even when the same GAL4/UAS combination is used, due to variation in GAL4/UAS expression and the different depths in which the cell types reside.

It is best to determine the length of the recording time for a particular

experiment empirically by testing response latencies during trial experiments. In our experience, response and recovery times range between 1 and 10 min, depending on the nature of transmitters and receptors underlying the response. Ionotropic responses are often relatively rapid (tens of seconds) while metabotropic responses can take many minutes (see note 6). Thus, 10-min time-courses will be sufficient for most bath-application experiments, though shorter experiments will suffice for some responses. Several factors likely influence the latency of an Epac1-camps FRET response. For example, bath-applied neurotransmitter must diffuse through the neurolemma into the brain and various transmitters likely differ in their permeability and diffusion rates. The application of neurotransmitters via directional perfusion or picosprtizer puffing minimizes variability in response latency. Variability in dissection quality may also lead to differential diffusion rates of compounds through the tissues of different brains. Thus, it is important to strive for exact and consistent dissections when conducting such live imaging experiments.

Applying Stimuli

To determine the effects of a bath-applied compound on the cAMP dynamics of a particular neuron type, changes in Epac1-camps FRET can be recorded before, during, and after the controlled application of the compound. We favor the use of a perfusion system to deliver compounds to the dissected brain. Perfusion flow allows for the precise timing of application, for rapid removal of the compound, and for the application of several test compounds in series. Alternatively, for compounds that cannot be perfused in large volumes, such as synthesized peptides or expensive compounds, a concentrated aliquot can be directly applied to the bath during the recording using a micropipette (Shafer et al., 2008). Alternatively, discrete regions of the brain can be stimulated using a picosprtizer positioned directly over a brain area of interest (Tomchik and Davis, 2009). Each of these methods of application can cause movement in the specimen that can cause detectable changes in FRET values (e.g., Fig. 2.3). These movement artifacts should be minimized through the adjustment of stimulation parameters during initial trials of vehicle administration.

Nevertheless, some level of movement artifact will likely be unavoidable and the inclusion of vehicle controls, the filtering of time-course data (see below), and the ratiometric nature of Epac1-camps measurement can all serve to minimize the impact of such artifacts on the final analysis of cAMP dynamics (see note 3).

The establishment of a stable FRET baseline is necessary before the effects of a bath-applied compound can be accessed. When cAMP levels are stable, the baseline FRET ratio should be relatively flat, though some drift in the ratio due to slow YPF bleaching is sometimes unavoidable. If drastic ratio fluctuations are occurring in the moments leading to compound application it is difficult, if not impossible, to determine the compound's effects on cAMP dynamics (see note 7). In such cases, the specimen may require more time to equilibrate or may be damaged and therefore unsuitable for imaging. Nevertheless, some fly neuron classes do appear to support rhythmic cAMP fluctuations and it is possible to measure cAMP responses despite such fluctuations (Shafer et al., 2008).

It is possible to record multiple time-courses from the same neurons in response to a series of treatments. In these cases, the complete removal of compounds must be ensured before subsequent applications, either by perfusing vehicle until the stimulus is removed or changing the bath solution multiple times. To gauge the required perfusion duration or number of rinses, one can perfuse or apply a colored dye and proceed to wash it out while taking aliquots of the liquid at regular intervals from the dish for several minutes. The amount of colored dye in each aliquot can be measured by a spectrophotometer and a time course of the washout can be constructed. The brain should be allowed to recover for 1–3 min after the wash out before being stimulated again. The recovery duration will depend on the time it takes for the neurons to recover a stable baseline of FRET values. If using a dipping cone objective, we recommend cleaning the dipping cone objective between recordings with deionized water and lens paper in order to remove possible residual compounds before imaging the next time-course.

Before initiating an experiment using Epac1-camps for a given GAL4/UAS combination and neuron class, it is important to confirm that the sensor produces measurable FRET changes in response to increased cAMP under the imaging

parameters chosen and that these parameters support stable baseline FRET levels in vehicle controls. Stimulation of the dissected brain with 20 mM forskolin is a convenient method of confirming the appropriate conditions for successful Epac1-camps imaging. Forskolin directly activates most adenylate cyclases, thereby acutely and potently increasing cAMP production (de Souza et al., 1983). If the brain is intact and the sensor is expressed at adequate levels, bath-applied 20 mM forskolin typically yields greater than 20% changes in the Epac1-camps FRET ratio (Fig. 2.3). For all bath-application experiments, it is also imperative to confirm that cAMP changes are not elicited in response to application of the vehicle in which a test compound is dissolved (Fig. 2.4). This serves as both a negative vehicle control for the compound of interest and as a control to insure that laser power, dwell time, and sampling frequency parameters support a relatively stable baseline FRET time-course (see note 8).

Compounds of interest should be dissolved solely in HL3 saline when possible. However, low final concentrations (typically around 0.1% Volume/Volume) of dimethyl sulfoxide (DMSO) are commonly used to dissolve insoluble peptides and compounds. This concentration of DMSO does not typically evoke Epac1- camps FRET changes (Shafer et al., 2008). Vehicle and other negative controls must be applied in precisely the same manner as test compounds to insure that they may serve as comparable controls for movement artifacts and basal FRET changes over time. In addition to controlling for the expected pharmacological effect of a particular compound, it is equally important to control for the possible changes in pH and osmolarity that often accompany bath application of a compound. This can be accomplished through the addition of chemically similar compounds that are not predicted to have pharmacological activity.

Data Analysis

It is critical that all putative Epac1-camps FRET responses should be positively confirmed as true FRET changes as opposed to photobleaching artifacts (see note 9). One can check this by aligning the raw values for the CFP and YFP traces and visually checking for the antiphasic changes in CFP and YFP values that underlie true FRET responses (Fig. 2.3a). True FRET responses will be characterized

by increasing CFP intensities with a concomitant and simultaneous decrease in YFP values or vice versa (Fig. 2.3a). Only simultaneous and opposing changes in CFP and YFP intensities signify a bonafide FRET response. Changes in the FRET ratio caused by unequal but unidirectional changes of CFP and YFP emission indicate an instance of false FRET change. In practice, this is usually caused by the uneven photobleaching of YPF and CFP, with the more rapid loss of YFP emission causing a reduction in YFP/CFP FRET values (Börner et al., 2011). Such FRET ratio drift may be unavoidable at times, but such changes should also be apparent in matched negative controls and should therefore not be mistaken for a significant cAMP response (see note 10).

Due to overlap in the emission spectra of CFP and YFP, a considerable amount of CFP emission will "spillover" into the YFP channel during FRET imaging. This spillover does not preclude the measurement of Epac1-camps FRET changes or measurement of relative cAMP changes (Vincent et al., 2008). Nevertheless, many investigators use the so-called "corrected FRET method" to correct for this spillover (Xia and Liu, 2001), which often serves to increase the magnitude of the FRET response (Fig. 2.3d). For most imaging systems, the only significant spillover consists of CFP emission spillover into the YFP channel. The spillover coefficient (i.e., the proportion of CFP emission detected by the YFP channel) is unique to every imaging system. One can measure an imaging system's CFP spillover coefficient by imaging cells that strongly express CFP but not YFP using optics for YFP/CFP FRET. Under these conditions the cells will be visible in both the CFP and YFP channels despite the absence of YFP. The ratio of the mean pixel intensity of the YFP image and the CFP image is the CFP spillover coefficient. Mean pixel intensities can be measured in real time using the confocal acquisition software or using programs such as Image J (The National Institutes of Health, http://rsbweb.nih.gov/ij/), Metamorph (Molecular Devices, Inc., Sunnyvale, CA), MatLab (Mathworks, Natick, MA), or others. The CFP spillover coefficient value typically ranges from 0.5 to 0.9 for most imaging systems (Börner et al., 2011). We do not currently know of a UAS-CFP line that drives sufficient CFP in fly neurons for use in spillover measurements. As an alternative approach, one can transfect cell lines with CFP plasmids and use

CFP expressing cells to determine spillover. Once the spillover coefficient value has been determined, the YFP intensities at each point can be spillover corrected in the following manner:

$$YFP_{SOC} = YFP - (CFP \times SO^{CFP}),$$

where YFP_{SOC} is the spillover corrected YFP intensity, CFP and YFP are the intensities from each imaging channel at a given time point, and SO^{CFP} is the spillover coefficient.

The spillover-corrected FRET ratio is then determined for each time-point as the value of YFP_{SOC}/CFP. The time-course traces of these values can be filtered and normalized in order to more easily pool data and compare the effects of different treatments (Fig. 2.4). We typically normalize the baseline FRET for each ROI to 1.0 by dividing all of the time-points by the FRET ratio value of the first time-point (Fig. 2.4a, b). For most cAMP responses, FRET ratio traces can be filtered with a moving average, whereby each ratio value is averaged with a number of values surrounding that point (Fig. 2.3d). The number of time-points included in the moving average, usually between five and ten data points, will depend on the nature of the data and should be determined empirically. When calculated using the standard FRET ratio of YFPSOC/CFP, Epac1-camps FRET is inversely proportional to cAMP levels (Nikolaev and Lohse, 2006). Thus, some researchers have preferred to express Epac1-camps data in terms of the inverse FRET ratio CFP/YFPSOC (Figs. 2.3e and 2.4), thereby making the relationship between Epac1- camps FRET plots and cAMP more intuitive (Tomchik and Davis, 2009). Pooled Epac1-camps data can be expressed as mean traces, wherein the mean Epac1-camps FRET value is determined for each time-point (Fig. 2.4c). Furthermore, mean maximum changes in the FRET ratio can then be determined for each treatment and compared statistically (Fig. 2.4d).

If the data are normally distributed, Student's t-tests can be used to compare the maximum FRET changes between a compound and its vehicle control. In the absence of a normal distribution, the Mann–Whitney U-test can be used. For the comparison of more than two treatments, an analysis of variance (ANOVA) with a Kruskal–Wallis test for nonparametric data can be used. Comparisons of mean traces can also be performed using a repeat measures ANOVA.

Example Experiment

Figure 2.4 displays a simple representative Epac1-camps experiment. In this example, we have tested whether the large ventrolateral neurons (l-LN_v) of Drosophila's circadian clock neuron network, display cAMP responses in response to bath-applied carbachol, a cholinergic receptor agonist. The adult l-LN_v are known to express nicotinic acetylcholine receptors (McCarthy et al., 2011). We therefore asked if bath- applied carbachol, a potent cholinergic agonist, would have measureable effects on cAMP levels in the adult l-LN_v neurons. Thirty-second perfusions of carbachol caused a consistent increase in the Epac1-camps inverse FRET ratio for the majority of neurons tested (Fig. 2.4a), consistent with cAMP increases. In contrast, 30-s vehicle perfusions were associated with stable inverse FRET values or a linear decrease in inverse FRET over time (Fig. 2.4b). Mean plots for carbachol and vehicle treated controls are shown in Fig. 2.4c and clearly indicate an effect of carbachol on the cAMP levels in l-LN_v neurons relative to controls. In Fig. 2.4d the effects of cabachol and vehicle treatments are expressed as maximum percent change in the inverse FRET ratio following bath-application. We conclude from these data that bath-applied carbachol results in increased cAMP levels in the l-LN_v.

Time Required

Once flies expressing the sensor are obtained (see note 11), productive recording sessions can be performed over the course of a few hours. The dissection, mounting, and recovery of each brain can take less than 15 min, while recording intervals can vary from 3 to 30 min depending on the nature of the experiment. For many experiments, one specimen can be prepared while another is being imaged. Given the variable nature of physiological experiments, we feel that seven to ten replicates should be taken for each treatment condition at minimum. Thus, for a given neuron type, testing for cAMP changes in response to one compound and its vehicle control can take less than 6 h, even for relatively long time-course experiments. In our experience, the subsequent processing and analysis of time-

course data typically require an additional day's work, though such analysis can be greatly streamlined with experience and the application of appropriate software.

2.5 NOTES

1. It is often convenient to create fly lines that stably express GAL4-driven UAS-Epac1-camps expression. Such lines obviate the need to conduct new crosses for every experiment. Any sensor that binds critical signaling molecules has the potential to interfere with cellular function, and there are unpublished reports that fly lines that widely express genetically encoded sensors can develop suppressors of sensor function. Such suppressors would be expected to interfere with Epac1-camps binding of cAMP, and thereby decrease the sensitivity of the sensor to cAMP fluctuations. Therefore, stable lines of flies expressing the sensor should be checked for sensitivity to forskolin and remade if sensitivity is determined to have diminished.
2. The brain can be most securely mounted to the bottom of the dish when all the large tracheal sacs have been removed from the exterior surface of the brain. Furthermore, the brain will adhere most securely to the dish if it is stuck down in its proper orientation on its first or second encounter with the bottom of the dish. Repeated adherence and detachment of the brain will reduce the stability of the mount. Allowing the brain to settle for 10–20 min will increase the chances of a strong adherence during live-imaging experiments. If brains fail to consistently stick securely to the bottom of the culture dish, a poly-lysine coated cover slip can be placed in the dish as an adherent surface upon which to mount the brain. The use of a coated coverslip will likely be necessary to securely mount brains if they have been treated with papain or collagenase.
3. For experiments involving a living brain, some movement of the preparation will be inevitable. The challenge is to minimize this movement so that the measurement of CFP and YFP intensities are not unduly effected by cAMP-independent events. Movement of the brain can be minimized using several approaches. The first and most critical means of minimizing movement is the strong adherence of the brain to the bottom of the culture dish (see note 2). If this does not work, other physical

devices can be constructed to immobilize brains for live-imaging experiments (Gu and O'Dowd, 2006). Filtering the FRET ratios with moving averages will minimize the effects of the unavoidable subtle movements that accompany most live imaging experiments. Lastly, the method of bath-application should be optimized to result in minimal detectable movement of the preparation. For perfusion systems this will largely be a question of flow rate and smooth transitions between reservoirs.

4. There are times when GAL4 elements may drive UAS-Epac1- camps expression weakly, making the measurement of FRET changes difficult. In instances when there are no alternative, more strongly expressed GAL4 lines, there are several options available to the researcher to increase Epac1-Camps signals. In some cases using older flies (2–3 weeks old) can yield neurons with higher Epac1-camps expression, though these brains will likely be less robust than younger brains. In cases when the GAL4 expression pattern is relatively sparse, the diameter of confocal aperture can be increased to increase the thickness of the optical section, thereby allowing more light to be collected. This approach has the advantage of not requiring increased light stimulation. In this case the increased signal comes at the cost of Z-resolution, which might be a problem if the GAL4 element drives UAS-Epac1-camps in nontarget neurons residing just above or below the image's optical section. Laser powers can be increased as a means of increasing Epac1-camps brightness. But this can often result in marked false FRET changes due to an unequal bleaching of YFP and CFP. Increasing the scanning laser's dwell time (i.e., by slowing down the rate of laser scanning) is another way to increase the brightness of Epac1-camps. This approach might require a lower frequency of scans, which would decrease the temporal resolution of timecourse experiments and may also result in increased photobleaching. Regardless of the adjustment made for weak sensor expression, researchers must be sure to use the same imaging parameters for both experimental and control time-courses. In general, one can maximize the apparent brightness of a neuron class's Epac1-camps expression by mounting the dissected brain in an optimal orientation. For example, if the neuron class of interest is situated just below the anterior surface of the brain, it is best to mount the brain with the anterior surface situated toward the microscope objective.

5. At some laser powers, scanning neurons too frequently can result in rapid and uneven photobleaching of CFP and YFP. For many types of cAMP responses there is no need for extremely rapid scanning. For example, scanning frequencies of one frame every 5 s or slower were sufficient to detect the G-protein-coupled receptor signaling in the explanted fly brain (Shafer et al., 2008). When high frequency scanning is necessary, care should be taken to minimize laser power to the greatest possible extent.
6. The lack of a measurable response to a given transmitter does not necessarily mean that the neuron of interest does not express receptors to the transmitter in question. There are several alternative explanations for the lack of a response. For example, the bath-applied transmitter may fail to reach the neuron of interest or the neuronal response, though biologically significant, may be below the limits of detection by the sensor. Treatment with enzymes such as papain or collagenase can be used to make the brain more permeable to bath-applied compound, but at the cost of some level of additional damage to the dissected brain. Alternatively, some compounds may be degraded or removed from extracellular spaces by endogenous mechanisms, thereby decreasing the effective concentration of the bath-applied compound. Employing high concentrations, blocking endogenous degradation/reuptake mechanisms, or using agonists not recognized by these mechanisms are all potential ways of overcoming this issue.
7. Fluctuations in the Epac1-camps FRET ratio before the stimulus is introduced are likely due to cAMP changes in response to the trauma of dissection and transfer to HL3 saline. To prevent this occurrence, always allow the mounted brain to recover for at least 10 min in HL3 before initiating a recording sequence.
8. Improper balance of ionic concentrations in saline can adversely affect the stability of the explanted brain and its neuronal activity. Saline should be made fresh or filtered and stored at −20°C to maintain the quality of the solution. Improperly made or spoiled HL3 saline can result in poor cAMP responses and/or inconsistent recordings.
9. For some neuronal types and GAL4/UAS-Epac1-camps combinations, a baseline drift in FRET ratios will be unavoidable (e.g., Fig. 2.4b). In these cases negative

controls will show significant changes in FRET over time, though these will likely be false FRET changes caused by unequal loss of YFP and CFP emission. In these cases we suggest displaying figures containing the individual plots of a given experiment. In cases where there are significant effects of a compound, the difference between compound-treated and vehicle-treated neurons will be apparent when the individual plots are compared (Fig. 2.4a, b). Alternatively, a mean plot of the vehicle control can be determined and the values for this plot shows over time can be subtracted from each compound-treated plot. This is a convenient means of removing FRET drift from experimental data.

10. There will be instances when rapid false FRET changes caused by a precipitous and uneven photobleaching of YFP and CFP can be easily mistaken for a significant change in Epac1-camps FRET. It is therefore extremely important that the raw CFP and YFP intensities are routinely inspected to confirm the simultaneous and opposite changes in CFP and YFP intensity that underlie bona-fide FRET responses (Fig. 2.3a).
11. Due to the fact that the majority of GAL4 lines were created through the random integration of P-elements into the fly genome, there are times when the very presence of the GAL4 will be accompanied by a mutation that decreases the general health of the fly or perhaps even interferes with the very neuronal circuitry one is trying to examine. Researchers should be mindful of the potential for such P-element effects.

2.6 FIGURES

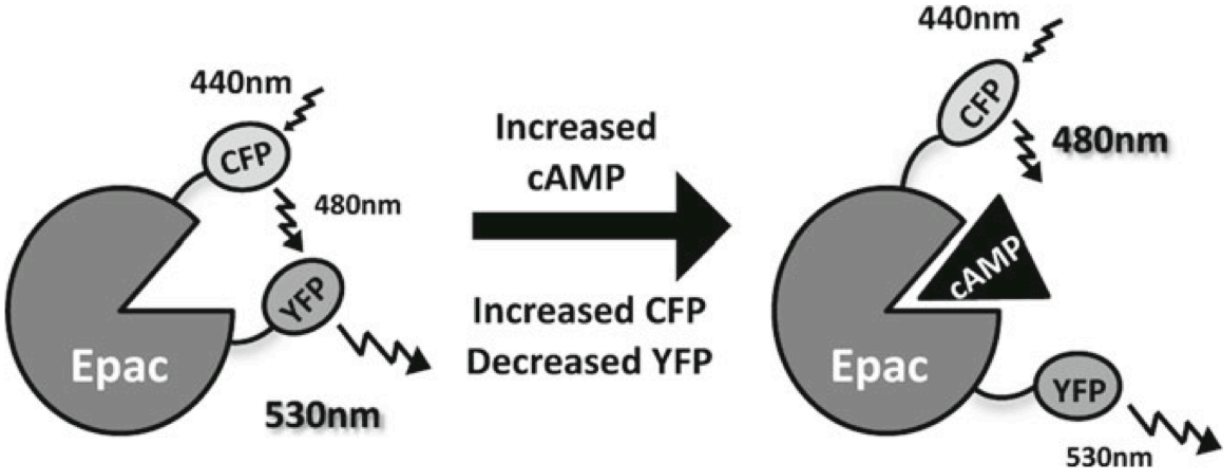

Figure 2.1. The Epac1-cAMPs sensor. The genetically encoded cAMP sensor Epac1-camps: the Epac1-camps is derived from the cAMP binding domain of Epac, a guanine nucleotide exchange factor of Rap1, a Ras-like GTPase. This Epac domain is flanked by cyan fluorescent protein (CFP) and yellow fluorescent protein (YFP) and reports cAMP changes through fluorescence resonance energy transfer (FRET) between CFP and YFP. When unbound to cAMP, the proximity of CFP and YFP allows for energy transfer from CFP to YFP so that the excitation of CFP with 440 nm light results in relatively high YPF emission at 530 nm and low CFP emission and 480 nm. Binding of a single molecule of cAMP results in a conformational change of the Epac1-camps sensor that increases the distance between CFP and YFP, thereby reducing energy transfer. Epac1-camps therefore displays concomitant increases in CFP and decreases in YFP emission upon increased cAMP levels. Thus, the FRET ratio (YFP/CFP) of Epac-based sensors is inversely proportional to cAMP levels (Nikolaev et al., 2004).

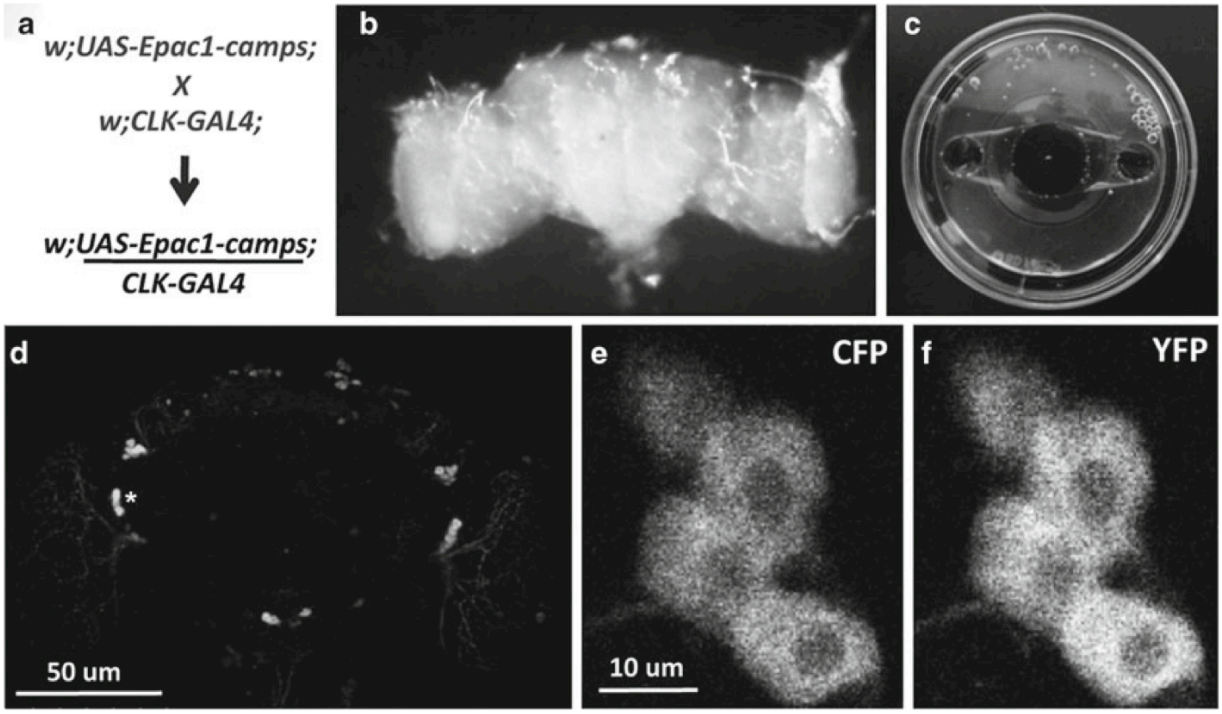

Figure 2.2. Expression of the Epac1-cAMPs sensor. Imaging Epac1-camps expression in the *Drosophila* brain for cAMP time-course experiments. (**a**) A simple cross scheme for the expression of *UAS-Epac1-camps* within the clock neuron network of the adult fly. (**b**) A dissected brain adhered to the bottom of a culture dish under HL3 saline. (**c**) An adult *Drosophila* brain mounted in a 35 mm culture dish within a perfusion insert. The brain is the *white dot* in the center of the large middle hole. The small left and right holes are the input and output of the perfusion line. (**d**) A projected confocal Z-series reconstruction of Epac1-camps expression in the clock neurons of an adult *w*;*UAS-Epac1camps*/*Clock-GAL4* brain. An *asterisk* indicates the cluster of large ventrolateral neurons (l-LN_v) in the left hemisphere. (**e**) A single optical section of CFP expression through a cluster of l-LN_v of an adult *w*;*UAS-Epac1camps*/*Clock-GAL4* brain. (**f**) YFP expression from the same optical section as shown in (**e**). When scanned with a 440 nm laser, the ratio of YFP/CFP emission intensities is inversely proportional to cAMP levels.

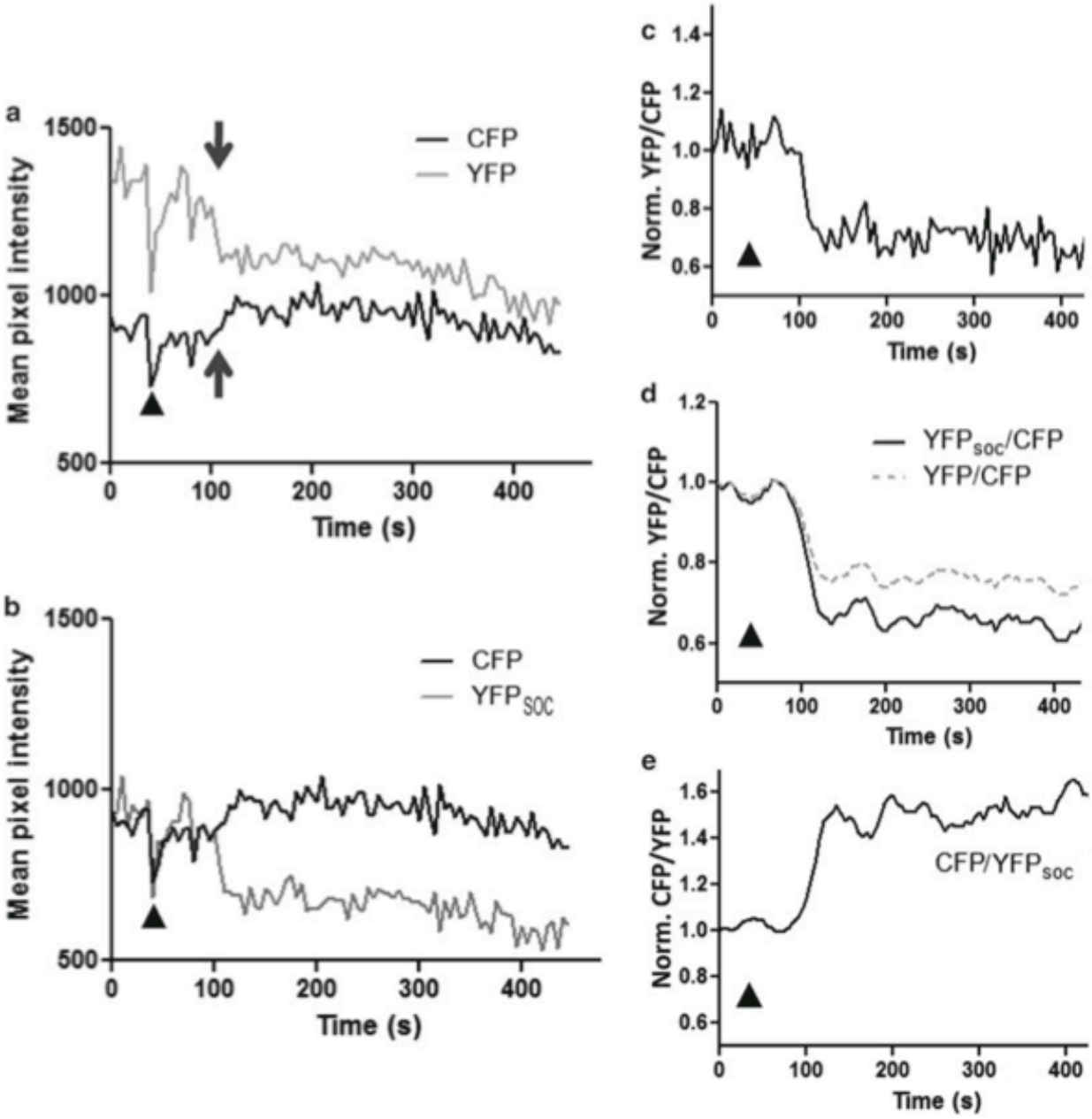

Figure 2.3. Data processing of FRET responses from Epac1-camps. (**a**) CFP and YFP emission from a single large ventrolateral clock neuron within a *w*;*UAS-Epac1camps*/*Clock-GAL4* brain before, during, and after the addition of pipetted forskolin (final concentration 20 mM) . CFP emission is plotted in *black* and YFP in *grey*. The application of forskolin is indicated by the *black triangle*. The *arrows* indicate the simultaneous decrease in YFP and increase in CFP associated with true FRET responses. (**b**) The same data as for (**a**) but using spillover-corrected YFP

values. (**c**) The raw spillover corrected (SOC) YFP/ CFP ratio from the data in (**b**). (**d**) Normalized FRET ratio plots that have been filtered using a five-point moving average. The ratio values using SOC YFP are plotted in *black*. Broken *grey lines* represent the uncorrected values. (**e**) Inversion of the normalized Epac1-camps FRET ratio makes the ratio change proportional to relative cAMP levels.

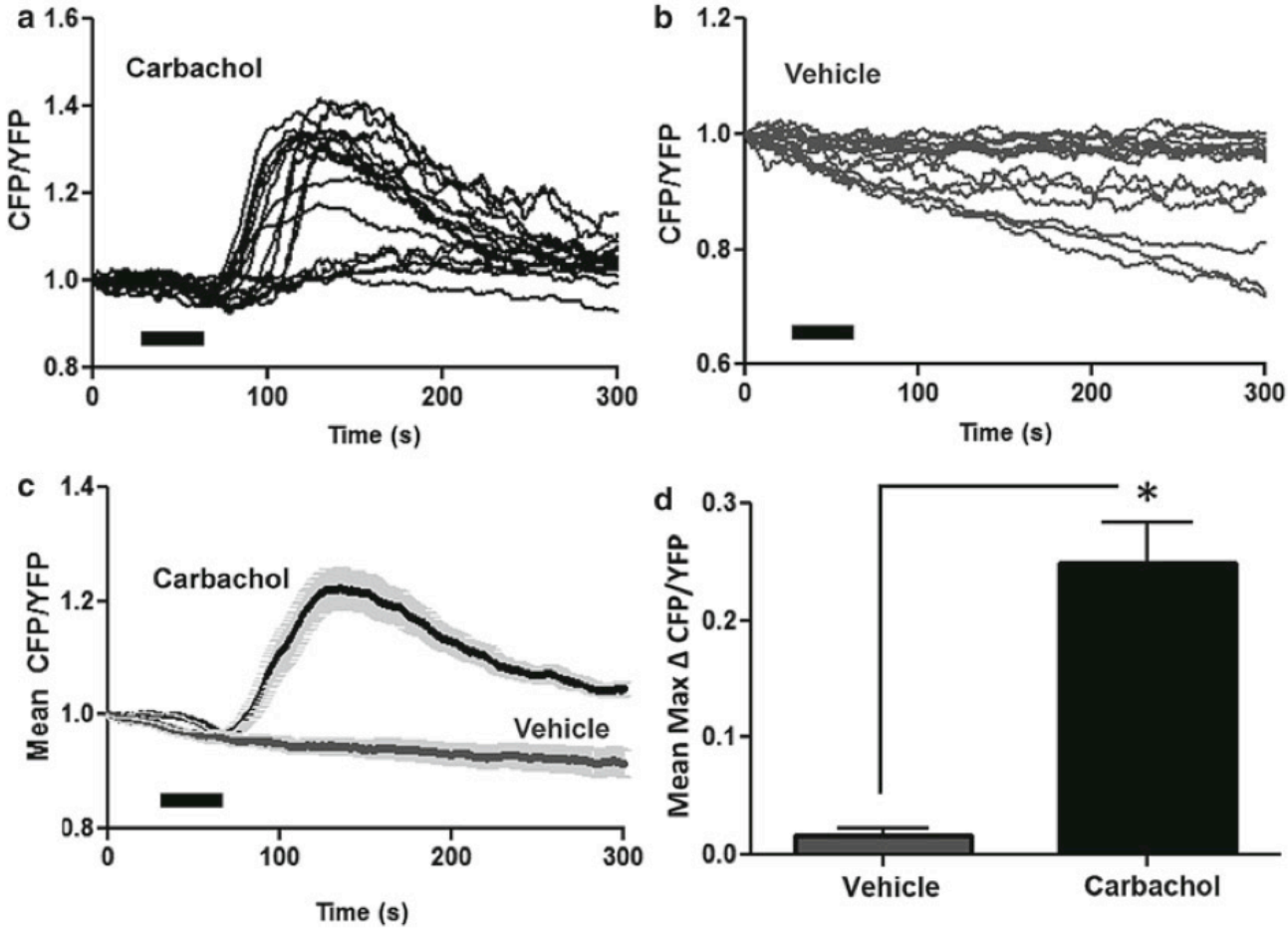

Figure 2.4. cAMP responses of the large ventrolateral clock neurons (l-LN$_v$) to a cholinergic agonist. (**a**) Individual inverse Epac1-camps FRET ratio traces recorded from single l-LN$_v$ from *w*;*UAS-Epac1camps*/*Clock-GAL4* brains before, during and after a 30 s perfusion of 10^{-4} M carbachol. The *black bar* indicates the time of carbachol perfusion. (**b**) Inverse FRET ratio traces for 30-s vehicle perfusions, HL3. Genotype, neuron type, and imaging parameters where identical to those for (**a**). (**c**) Averaged inverse FRET ratio traces for carbachol (*black*) and HL3 (*grey*). The *shaded* regions represent the standard error of the mean for each time-point. (**d**) Mean maximum changes in the inverse Epac1-camps FRET ratio plotted for the vehicle controls (*grey*) and carbachol treated brains (*black*). A Student's *t*-test revealed a significant difference between the two treatments ($P < 0.0001$).

2.7 REFERENCES

Akerboom J, Chen T-W, Wardill TJ, Tian L, Marvin JS, Mutlu S, Calderón NC, Esposti F, Borghuis BG, Sun XR, Gordus A, Orger MB, Portugues R, Engert F, Macklin JJ, Filosa A, Aggarwal A, Kerr RA, Takagi R, Kracun S, Shigetomi E, Khakh BS, Baier H, Lagnado L, Wang SS-H, Bargmann CI, Kimmel BE, Jayaraman V, Svoboda K, Kim DS, Schreiter ER, Looger LL. Optimization of a GCaMP calcium indicator for neural activity imaging. *J. Neurosci.* 32: 13819–13840, 2012.

Allada R, Emery P, Takahashi JS, Rosbash M. Stopping time: the genetics of fly and mouse circadian clocks. *Annu. Rev. Neurosci.* 24: 1091–1119, 2001.

Allada R, White NE, So WV, Hall JC, Rosbash M. A mutant Drosophila homolog of mammalian Clock disrupts circadian rhythms and transcription of period and timeless. *Cell* 93: 791–804, 1998.

Andretic R, Hirsh J. Circadian modulation of dopamine receptor responsiveness in Drosophila melanogaster. *Proc. Natl. Acad. Sci. U. S. A.* 97: 1873–1878, 2000.

Anwyl R. Metabotropic glutamate receptors: electrophysiological properties and role in plasticity. *Brain Res. Brain Res. Rev.* 29: 83–120, 1999.

Ashburner M, Roote J. Laboratory culture of Drosophila. In: *Drosophila protocols*, edited by Sullivan W, Ashburner M, Hawley S. Cold Spring Harbor, NY: Cold Spring Harbor Laboratory Press, 2000.

Aton SJ, Colwell CS, Harmar AJ, Waschek J, Herzog ED. Vasoactive intestinal polypeptide mediates circadian rhythmicity and synchrony in mammalian clock neurons. *Nat. Neurosci.* 8: 476–483, 2005.

Bae K, Lee C, Sidote D, Chuang KY, Edery I. Circadian regulation of a Drosophila homolog of the mammalian Clock gene: PER and TIM function as positive regulators. *Mol. Cell. Biol.* 18: 6142–6151, 1998.

Beavo JA, Brunton LL. Cyclic nucleotide research -- still expanding after half a century. *Nat. Rev. Mol. Cell Biol.* 3: 710–718, 2002.

Beckwith EJ, Lelito KR, Hsu Y-WA, Medina BM, Shafer O, Ceriani MF, de la Iglesia HO. Functional conservation of clock output signaling between flies and intertidal crabs. *J. Biol. Rhythms* 26: 518–529, 2011.

Benzer S. From the gene to behavior. *JAMA J. Am. Med. Assoc.* 218: 1015–1022, 1971.

Borland G, Smith BO, Yarwood SJ. EPAC proteins transduce diverse cellular actions of cAMP. *Br. J. Pharmacol.* 158: 70–86, 2009.

Börner S, Schwede F, Schlipp A, Berisha F, Calebiro D, Lohse MJ, Nikolaev VO. FRET measurements of intracellular cAMP concentrations and cAMP analog permeability in intact cells. *Nat. Protoc.* 6: 427–438, 2011.

Bossy B, Ballivet M, Spierer P. Conservation of neural nicotinic acetylcholine receptors from Drosophila to vertebrate central nervous systems. *EMBO J.* 7: 611–618, 1988.

Brand AH, Perrimon N. Targeted gene expression as a means of altering cell fates and generating dominant phenotypes. *Dev. Camb. Engl.* 118: 401–415, 1993.

Busza A, Emery-Le M, Rosbash M, Emery P. Roles of the two Drosophila CRYPTOCHROME structural domains in circadian photoreception. *Science* 304: 1503–1506, 2004.

Campbell SS, Tobler I. Animal sleep: a review of sleep duration across phylogeny. *Neurosci. Biobehav. Rev.* 8: 269–300, 1984.

Cao G, Nitabach MN. Circadian control of membrane excitability in Drosophila melanogaster lateral ventral clock neurons. *J. Neurosci.* 28: 6493–6501, 2008.

Cao G, Platisa J, Pieribone VA, Raccuglia D, Kunst M, Nitabach MN. Genetically targeted optical electrophysiology in intact neural circuits. *Cell* 154: 904–913, 2013.

Ceriani MF, Darlington TK, Staknis D, Más P, Petti AA, Weitz CJ, Kay SA. Light-dependent sequestration of TIMELESS by CRYPTOCHROME. *Science* 285: 553–556, 1999.

Chen T-W, Wardill TJ, Sun Y, Pulver SR, Renninger SL, Baohan A, Schreiter ER, Kerr RA, Orger MB, Jayaraman V, Looger LL, Svoboda K, Kim DS. Ultrasensitive fluorescent proteins for imaging neuronal activity. *Nature* 499: 295–300, 2013.

Chou WH, Huber A, Bentrop J, Schulz S, Schwab K, Chadwell LV, Paulsen R, Britt SG. Patterning of the R7 and R8 photoreceptor cells of Drosophila: evidence for induced and default cell-fate specification. *Dev. Camb. Engl.* 126: 607–616, 1999.

Chung BY, Kilman VL, Keath JR, Pitman JL, Allada R. The GABA(A) receptor RDL acts in peptidergic PDF neurons to promote sleep in Drosophila. *Curr. Biol. CB* 19: 386–390, 2009.

Crocker A, Sehgal A. Octopamine regulates sleep in drosophila through protein kinase A-dependent mechanisms. *J. Neurosci.* 28: 9377–9385, 2008.

Crocker A, Shahidullah M, Levitan IB, Sehgal A. Identification of a neural circuit that underlies the effects of octopamine on sleep:wake behavior. *Neuron* 65: 670–681, 2010.

Curtin KD, Huang ZJ, Rosbash M. Temporally regulated nuclear entry of the Drosophila period protein contributes to the circadian clock. *Neuron* 14: 365–372, 1995.

Dahdal D, Reeves DC, Ruben M, Akabas MH, Blau J. Drosophila pacemaker neurons require g protein signaling and GABAergic inputs to generate twenty-four hour behavioral rhythms. *Neuron* 68: 964–977, 2010.

Daniels RW, Gelfand MV, Collins CA, DiAntonio A. Visualizing glutamatergic cell bodies and synapses in Drosophila larval and adult CNS. *J. Comp. Neurol.* 508: 131–152, 2008.

Darlington TK, Wager-Smith K, Ceriani MF, Staknis D, Gekakis N, Steeves TD, Weitz CJ, Takahashi JS, Kay SA. Closing the circadian loop: CLOCK-induced transcription of its own inhibitors per and tim. *Science* 280: 1599–1603, 1998a.

Darlington TK, Wager-Smith K, Ceriani MF, Staknis D, Gekakis N, Steeves TD, Weitz CJ, Takahashi JS, Kay SA. Closing the circadian loop: CLOCK-induced transcription of its own inhibitors per and tim. *Science* 280: 1599–1603, 1998b.

Dingledine R, Borges K, Bowie D, Traynelis SF. The glutamate receptor ion channels. *Pharmacol. Rev.* 51: 7–61, 1999.

DiPilato LM, Cheng X, Zhang J. Fluorescent indicators of cAMP and Epac activation reveal differential dynamics of cAMP signaling within discrete subcellular compartments. *Proc. Natl. Acad. Sci. U. S. A.* 101: 16513–16518, 2004.

Dowse HB, Hall JC, Ringo JM. Circadian and ultradian rhythms in period mutants of Drosophila melanogaster. *Behav. Genet.* 17: 19–35, 1987.

Dunlap JC. Molecular bases for circadian clocks. *Cell* 96: 271–290, 1999.

Dushay MS, Konopka RJ, Orr D, Greenacre ML, Kyriacou CP, Rosbash M, Hall JC. Phenotypic and genetic analysis of Clock, a new circadian rhythm mutant in Drosophila melanogaster. *Genetics* 125: 557–578, 1990.

Duvall LB, Taghert PH. The circadian neuropeptide PDF signals preferentially through a specific adenylate cyclase isoform AC3 in M pacemakers of Drosophila. *PLoS Biol.* 10: e1001337, 2012.

Emery P, So WV, Kaneko M, Hall JC, Rosbash M. CRY, a Drosophila clock and light-regulated cryptochrome, is a major contributor to circadian rhythm resetting and photosensitivity. *Cell* 95: 669–679, 1998.

Emery P, Stanewsky R, Helfrich-Förster C, Emery-Le M, Hall JC, Rosbash M. Drosophila CRY is a deep brain circadian photoreceptor. *Neuron* 26: 493–504, 2000.

Feinberg EH, Vanhoven MK, Bendesky A, Wang G, Fetter RD, Shen K, Bargmann CI. GFP Reconstitution Across Synaptic Partners (GRASP) defines cell contacts and synapses in living nervous systems. *Neuron* 57: 353–363, 2008.

Fiala A, Spall T, Diegelmann S, Eisermann B, Sachse S, Devaud J-M, Buchner E, Galizia CG. Genetically expressed cameleon in Drosophila melanogaster is used to visualize olfactory information in projection neurons. *Curr. Biol. CB* 12: 1877–1884, 2002.

Fogle KJ, Parson KG, Dahm NA, Holmes TC. CRYPTOCHROME is a blue-light sensor that regulates neuronal firing rate. *Science* 331: 1409–1413, 2011.

Friggi-Grelin F, Coulom H, Meller M, Gomez D, Hirsh J, Birman S. Targeted gene expression in Drosophila dopaminergic cells using regulatory sequences from tyrosine hydroxylase. *J. Neurobiol.* 54: 618–627, 2003.

Gengs C, Leung H-T, Skingsley DR, Iovchev MI, Yin Z, Semenov EP, Burg MG, Hardie RC, Pak WL. The target of Drosophila photoreceptor synaptic transmission is a histamine-gated chloride channel encoded by ort (hclA). *J. Biol. Chem.* 277: 42113–42120, 2002.

Gervasi N, Tchénio P, Preat T. PKA dynamics in a Drosophila learning center: coincidence detection by rutabaga adenylyl cyclase and spatial regulation by dunce phosphodiesterase. *Neuron* 65: 516–529, 2010.

Gloerich M, Bos JL. Epac: defining a new mechanism for cAMP action. *Annu. Rev. Pharmacol. Toxicol.* 50: 355–375, 2010.

Gordon MD, Scott K. Motor control in a Drosophila taste circuit. *Neuron* 61: 373–384, 2009.

Greenspan RJ. *Fly pushing, the theory and practice of Drosophila genetics*. 2nd ed. Cold Spring Harbor, NY: Cold Spring Harbor Press, 2004.

Grima B, Chélot E, Xia R, Rouyer F. Morning and evening peaks of activity rely on different clock neurons of the Drosophila brain. *Nature* 431: 869–873, 2004.

Gu H, O'Dowd DK. Cholinergic synaptic transmission in adult Drosophila Kenyon cells in situ. *J. Neurosci.* 26: 265–272, 2006.

Guerrero G, Isacoff EY. Genetically encoded optical sensors of neuronal activity and cellular function. *Curr. Opin. Neurobiol.* 11: 601–607, 2001.

Gummadova JO, Coutts GA, Glossop NRJ. Analysis of the Drosophila Clock promoter reveals heterogeneity in expression between subgroups of central oscillator cells and identifies a novel enhancer region. *J. Biol. Rhythms* 24: 353–367, 2009.

Hamada FN, Rosenzweig M, Kang K, Pulver SR, Ghezzi A, Jegla TJ, Garrity PA. An internal thermal sensor controlling temperature preference in Drosophila. *Nature* 454: 217–220, 2008.

Hamasaka Y, Nässel DR. Mapping of serotonin, dopamine, and histamine in relation to different clock neurons in the brain of Drosophila. *J. Comp. Neurol.* 494: 314–330, 2006.

Hamasaka Y, Rieger D, Parmentier M-L, Grau Y, Helfrich-Förster C, Nässel DR. Glutamate and its metabotropic receptor in Drosophila clock neuron circuits. *J. Comp. Neurol.* 505: 32–45, 2007.

Hamasaka Y, Wegener C, Nässel DR. GABA modulates Drosophila circadian clock neurons via GABAB receptors and decreases in calcium. *J. Neurobiol.* 65: 225–240, 2005.

Hamblen-Coyle MJ, Wheeler DA, Rutila JE, Rosbash M, Hall JC. Behavior of period-altered circadian rhythm mutants ofDrosophila in light: Dark cycles (Diptera: Drosophilidae). *J. Insect Behav.* 5: 417–446, 1992.

Hao H, Allen DL, Hardin PE. A circadian enhancer mediates PER-dependent mRNA cycling in Drosophila melanogaster. *Mol. Cell. Biol.* 17: 3687–3693, 1997.

Hardie RC. Is histamine a neurotransmitter in insect photoreceptors? *J. Comp. Physiol. [A]* 161: 201–213, 1987.

Hardie RC. A histamine-activated chloride channel involved in neurotransmission at a photoreceptor synapse. *Nature* 339: 704–706, 1989a.

Hardie RC. A histamine-activated chloride channel involved in neurotransmission at a photoreceptor synapse. *Nature* 339: 704–706, 1989b.

Hardin PE, Hall JC, Rosbash M. Feedback of the Drosophila period gene product on circadian cycling of its messenger RNA levels. *Nature* 343: 536–540, 1990.

Helfrich-Förster C, Edwards T, Yasuyama K, Wisotzki B, Schneuwly S, Stanewsky R, Meinertzhagen IA, Hofbauer A. The extraretinal eyelet of Drosophila: development, ultrastructure, and putative circadian function. *J. Neurosci.* 22: 9255–9266, 2002.

Helfrich-Förster C, Homberg U. Pigment-dispersing hormone-immunoreactive neurons in the nervous system of wild-type Drosophila melanogaster and of several mutants with altered circadian rhythmicity. *J. Comp. Neurol.* 337: 177–190, 1993.

Helfrich-Förster C, Winter C, Hofbauer A, Hall JC, Stanewsky R. The circadian clock of fruit flies is blind after elimination of all known photoreceptors. *Neuron* 30: 249–261, 2001.

Helfrich-Förster C, Yoshii T, Wülbeck C, Grieshaber E, Rieger D, Bachleitner W, Cusamano P, Rouyer F. The lateral and dorsal neurons of Drosophila melanogaster: new insights about their morphology and function. *Cold Spring Harb. Symp. Quant. Biol.* 72: 517–525, 2007.

Helfrich-Förster C. The period clock gene is expressed in central nervous system neurons which also produce a neuropeptide that reveals the projections of circadian pacemaker cells within the brain of Drosophila melanogaster. *Proc. Natl. Acad. Sci. U. S. A.* 92: 612–616, 1995.

Helfrich-Förster C. Differential control of morning and evening components in the activity rhythm of Drosophila melanogaster--sex-specific differences suggest a different quality of activity. *J. Biol. Rhythms* 15: 135–154, 2000.

Helfrich-Förster C. The circadian system of Drosophila melanogaster and its light input pathways. *Zool. Jena Ger.* 105: 297–312, 2002.

Helfrich-Förster C. The neuroarchitecture of the circadian clock in the brain of Drosophila melanogaster. *Microsc. Res. Tech.* 62: 94–102, 2003.

Helfrich-Förster C. The circadian clock in the brain: a structural and functional comparison between mammals and insects. *J. Comp. Physiol. A Neuroethol. Sens. Neural. Behav. Physiol.* 190: 601–613, 2004.

Helfrich-Förster C. Neurobiology of the fruit fly's circadian clock. *Genes Brain Behav.* 4: 65–76, 2005.

Hendricks JC, Sehgal A, Pack AI. The need for a simple animal model to understand sleep. *Prog. Neurobiol.* 61: 339–351, 2000.

Hermann C, Yoshii T, Dusik V, Helfrich-Förster C. Neuropeptide F immunoreactive clock neurons modify evening locomotor activity and free-running period in Drosophila melanogaster. *J. Comp. Neurol.* 520: 970–987, 2012.

Hofbauer A, Buchner E. Does Drosophila have seven eyes? *Naturwissen* 76: 335–336, 1989.

Hong S-T, Bang S, Paik D, Kang J, Hwang S, Jeon K, Chun B, Hyun S, Lee Y, Kim J. Histamine and its receptors modulate temperature-preference behaviors in Drosophila. *J. Neurosci.* 26: 7245–7256, 2006.

Huber A, Schulz S, Bentrop J, Groell C, Wolfrum U, Paulsen R. Molecular cloning of Drosophila Rh6 rhodopsin: the visual pigment of a subset of R8 photoreceptor cells. *FEBS Lett.* 406: 6–10, 1997.

Hyun S, Lee Y, Hong S-T, Bang S, Paik D, Kang J, Shin J, Lee J, Jeon K, Hwang S, Bae E, Kim J. Drosophila GPCR Han is a receptor for the circadian clock neuropeptide PDF. *Neuron* 48: 267–278, 2005.

Im SH, Taghert PH. PDF receptor expression reveals direct interactions between circadian oscillators in Drosophila. *J. Comp. Neurol.* 518: 1925–1945, 2010.

Jan LY, Jan YN. L-glutamate as an excitatory transmitter at the Drosophila larval neuromuscular junction. *J. Physiol.* 262: 215–236, 1976a.

Jan LY, Jan YN. Properties of the larval neuromuscular junction in Drosophila melanogaster. *J. Physiol.* 262: 189–214, 1976b.

Jenett A, Rubin GM, Ngo T-TB, Shepherd D, Murphy C, Dionne H, Pfeiffer BD, Cavallaro A, Hall D, Jeter J, Iyer N, Fetter D, Hausenfluck JH, Peng H, Trautman ET, Svirskas RR, Myers EW, Iwinski ZR, Aso Y, DePasquale GM, Enos A, Hulamm P, Lam SCB, Li H-H, Laverty TR, Long F, Qu L, Murphy SD, Rokicki K, Safford T, Shaw K, Simpson JH, Sowell A, Tae S, Yu Y, Zugates CT. A GAL4-driver line resource for Drosophila neurobiology. *Cell Rep.* 2: 991–1001, 2012.

Johard HAD, Yoishii T, Dircksen H, Cusumano P, Rouyer F, Helfrich-Förster C, Nässel DR. Peptidergic clock neurons in Drosophila: ion transport peptide and short neuropeptide F in subsets of dorsal and ventral lateral neurons. *J. Comp. Neurol.* 516: 59–73, 2009.

Johnson C, Elliot J, Foster RG, Ken-Ichi H, Kronauer R. Fundemental properties of circadian rhythms. In: *Chronobiology: biological timekeeping*, edited by Dunlap JC, Loros JJ, Decoursey PJ. Massachusetts: Sinauer Associates, Inc., 2004.

Kaneko M, Hall JC. Neuroanatomy of cells expressing clock genes in Drosophila: transgenic manipulation of the period and timeless genes to mark the perikarya of circadian pacemaker neurons and their projections. *J. Comp. Neurol.* 422: 66–94, 2000.

Kaneko M, Helfrich-Förster C, Hall JC. Spatial and temporal expression of the period and timeless genes in the developing nervous system of Drosophila: newly identified pacemaker candidates and novel features of clock gene product cycling. *J. Neurosci.* 17: 6745–6760, 1997.

Kaushik R, Nawathean P, Busza A, Murad A, Emery P, Rosbash M. PER-TIM interactions with the photoreceptor cryptochrome mediate circadian temperature responses in Drosophila. *PLoS Biol.* 5: e146, 2007.

Keene AC, Mazzoni EO, Zhen J, Younger MA, Yamaguchi S, Blau J, Desplan C, Sprecher SG. Distinct visual pathways mediate Drosophila larval light avoidance and circadian clock entrainment. *J. Neurosci.* 31: 6527–6534, 2011.

Keene AC, Sprecher SG. Seeing the light: photobehavior in fruit fly larvae. *Trends Neurosci.* 35: 104–110, 2012.

Kim EY, Edery I. Balance between DBT/CKIepsilon kinase and protein phosphatase activities regulate phosphorylation and stability of Drosophila CLOCK protein. *Proc. Natl. Acad. Sci. U. S. A.* 103: 6178–6183, 2006.

Kistenpfennig C, Hirsh J, Yoshii T, Helfrich-Förster C. Phase-shifting the fruit fly clock without cryptochrome. *J. Biol. Rhythms* 27: 117–125, 2012.

Kloss B, Price JL, Saez L, Blau J, Rothenfluh A, Wesley CS, Young MW. The Drosophila clock gene double-time encodes a protein closely related to human casein kinase Iepsilon. *Cell* 94: 97–107, 1998.

Koh K, Zheng X, Sehgal A. JETLAG resets the Drosophila circadian clock by promoting light-induced degradation of TIMELESS. *Science* 312: 1809–1812, 2006.

Kolodziejczyk A, Sun X, Meinertzhagen IA, Nässel DR. Glutamate, GABA and acetylcholine signaling components in the lamina of the Drosophila visual system. *PloS One* 3: e2110, 2008.

Konopka RJ, Benzer S. Clock mutants of Drosophila melanogaster. *Proc. Natl. Acad. Sci. U. S. A.* 68: 2112–2116, 1971.

Kula-Eversole E, Nagoshi E, Shang Y, Rodriguez J, Allada R, Rosbash M. Surprising gene expression patterns within and between PDF-containing circadian neurons in Drosophila. *Proc. Natl. Acad. Sci. U. S. A.* 107: 13497–13502, 2010.

Lai S-L, Lee T. Genetic mosaic with dual binary transcriptional systems in Drosophila. *Nat. Neurosci.* 9: 703–709, 2006.

Lear BC, Zhang L, Allada R. The neuropeptide PDF acts directly on evening pacemaker neurons to regulate multiple features of circadian behavior. *PLoS Biol.* 7: e1000154, 2009.

Lee C, Bae K, Edery I. PER and TIM inhibit the DNA binding activity of a Drosophila CLOCK-CYC/dBMAL1 heterodimer without disrupting formation of the heterodimer: a basis for circadian transcription. *Mol. Cell. Biol.* 19: 5316–5325, 1999.

Lee C, Etchegaray JP, Cagampang FR, Loudon AS, Reppert SM. Posttranslational mechanisms regulate the mammalian circadian clock. *Cell* 107: 855–867, 2001.

Lelito KR, Shafer OT. Reciprocal cholinergic and GABAergic modulation of the small ventrolateral pacemaker neurons of Drosophila's circadian clock neuron network. *J. Neurophysiol.* 107: 2096–2108, 2012a.

Lelito KR, Shafer OT. Imaging cAMP Dynamics in the Drosophila Brain with the Genetically Encoded Sensor Epac1-Camps. In: *Genetically Encoded Functional Indicators*, edited by Martin J-R. Humana Press, p. 149–168.

Levine JD, Casey CI, Kalderon DD, Jackson FR. Altered circadian pacemaker functions and cyclic AMP rhythms in the Drosophila learning mutant dunce. *Neuron* 13: 967–974, 1994.

Lima SQ, Miesenböck G. Remote control of behavior through genetically targeted photostimulation of neurons. *Cell* 121: 141–152, 2005.

Lin FJ, Song W, Meyer-Bernstein E, Naidoo N, Sehgal A. Photic signaling by cryptochrome in the Drosophila circadian system. *Mol. Cell. Biol.* 21: 7287–7294, 2001.

Lissandron V, Rossetto MG, Erbguth K, Fiala A, Daga A, Zaccolo M. Transgenic fruit-flies expressing a FRET-based sensor for in vivo imaging of cAMP dynamics. *Cell. Signal.* 19: 2296–2303, 2007.

Lissandron V, Terrin A, Collini M, D'alfonso L, Chirico G, Pantano S, Zaccolo M. Improvement of a FRET-based indicator for cAMP by linker design and stabilization of donor-acceptor interaction. *J. Mol. Biol.* 354: 546–555, 2005.

Littleton JT, Ganetzky B. Ion channels and synaptic organization: analysis of the Drosophila genome. *Neuron* 26: 35–43, 2000.

Malpel S, Klarsfeld A, Rouyer F. Larval optic nerve and adult extra-retinal photoreceptors sequentially associate with clock neurons during Drosophila brain development. *Dev. Camb. Engl.* 129: 1443–1453, 2002.

Martinek S, Inonog S, Manoukian AS, Young MW. A role for the segment polarity gene shaggy/GSK-3 in the Drosophila circadian clock. *Cell* 105: 769–779, 2001.

Mazzoni EO, Desplan C, Blau J. Circadian pacemaker neurons transmit and modulate visual information to control a rapid behavioral response. *Neuron* 45: 293–300, 2005.

McCarthy EV, Wu Y, Decarvalho T, Brandt C, Cao G, Nitabach MN. Synchronized bilateral synaptic inputs to Drosophila melanogaster neuropeptidergic rest/arousal neurons. *J. Neurosci.* 31: 8181–8193, 2011.

McDonald MJ, Rosbash M, Emery P. Wild-type circadian rhythmicity is dependent on closely spaced E boxes in the Drosophila timeless promoter. *Mol. Cell. Biol.* 21: 1207–1217, 2001.

Mealey-Ferrara ML, Montalvo AG, Hall JC. Effects of combining a cryptochrome mutation with other visual-system variants on entrainment of locomotor and adult-emergence rhythms in Drosophila. *J. Neurogenet.* 17: 171–221, 2003.

Mertens I, Vandingenen A, Johnson EC, Shafer OT, Li W, Trigg JS, De Loof A, Schoofs L, Taghert PH. PDF receptor signaling in Drosophila contributes to both circadian and geotactic behaviors. *Neuron* 48: 213–219, 2005.

Miesenböck G, Kevrekidis IG. Optical imaging and control of genetically designated neurons in functioning circuits. *Annu. Rev. Neurosci.* 28: 533–563, 2005.

Miesenböck G. The optogenetic catechism. *Science* 326: 395–399, 2009.

Naidoo N, Song W, Hunter-Ensor M, Sehgal A. A role for the proteasome in the light response of the timeless clock protein. *Science* 285: 1737–1741, 1999.

Nakagawa T, Vosshall LB. Controversy and consensus: noncanonical signaling mechanisms in the insect olfactory system. *Curr. Opin. Neurobiol.* 19: 284–292, 2009.

Nakai J, Ohkura M, Imoto K. A high signal-to-noise Ca(2+) probe composed of a single green fluorescent protein. *Nat. Biotechnol.* 19: 137–141, 2001.

Nässel DR, Holmqvist MH, Hardie RC, Håkanson R, Sundler F. Histamine-like immunoreactivity in photoreceptors of the compound eyes and ocelli of the flies Calliphora erythrocephala and Musca domestica. *Cell Tissue Res.* 253: 639–646, 1988.

Nässel DR. Histamine in the brain of insects: a review. *Microsc. Res. Tech.* 44: 121–136, 1999.

Nikolaev VO, Bünemann M, Hein L, Hannawacker A, Lohse MJ. Novel single chain cAMP sensors for receptor-induced signal propagation. *J. Biol. Chem.* 279: 37215–37218, 2004.

Nikolaev VO, Lohse MJ. Monitoring of cAMP synthesis and degradation in living cells. *Physiol. Bethesda Md* 21: 86–92, 2006.

O'Neill JS, Maywood ES, Chesham JE, Takahashi JS, Hastings MH. cAMP-dependent signaling as a core component of the mammalian circadian pacemaker. *Science* 320: 949–953, 2008.

Pantazis A, Segaran A, Liu C-H, Nikolaev A, Rister J, Thum AS, Roeder T, Semenov E, Juusola M, Hardie RC. Distinct roles for two histamine receptors (hclA and hclB) at the Drosophila photoreceptor synapse. *J. Neurosci.* 28: 7250–7259, 2008.

Parisky KM, Agosto J, Pulver SR, Shang Y, Kuklin E, Hodge JJL, Kang K, Kang K, Liu X, Garrity PA, Rosbash M, Griffith LC. PDF cells are a GABA-responsive wake-promoting component of the Drosophila sleep circuit. *Neuron* 60: 672–682, 2008.

Park D, Griffith LC. Electrophysiological and anatomical characterization of PDF-positive clock neurons in the intact adult Drosophila brain. *J. Neurophysiol.* 95: 3955–3960, 2006.

Park JH, Hall JC. Isolation and chronobiological analysis of a neuropeptide pigment-dispersing factor gene in Drosophila melanogaster. *J. Biol. Rhythms* 13: 219–228, 1998.

Park JH, Helfrich-Förster C, Lee G, Liu L, Rosbash M, Hall JC. Differential regulation of circadian pacemaker output by separate clock genes in Drosophila. *Proc. Natl. Acad. Sci. U. S. A.* 97: 3608–3613, 2000.

Peschel N, Veleri S, Stanewsky R. Veela defines a molecular link between Cryptochrome and Timeless in the light-input pathway to Drosophila's circadian clock. *Proc. Natl. Acad. Sci. U. S. A.* 103: 17313–17318, 2006.

Pfeiffer BD, Ngo T-TB, Hibbard KL, Murphy C, Jenett A, Truman JW, Rubin GM. Refinement of tools for targeted gene expression in Drosophila. *Genetics* 186: 735–755, 2010.

Pichaud F, Desplan C. A new visualization approach for identifying mutations that affect differentiation and organization of the Drosophila ommatidia. *Dev. Camb. Engl.* 128: 815–826, 2001.

Van den Pol AN. The hypothalamic suprachiasmatic nucleus of rat: intrinsic anatomy. *J. Comp. Neurol.* 191: 661–702, 1980.

Pollack I, Hofbauer A. Histamine-like immunoreactivity in the visual system and brain of Drosophila melanogaster. *Cell Tissue Res.* 266: 391–398, 1991.

Ponsioen B, Zhao J, Riedl J, Zwartkruis F, van der Krogt G, Zaccolo M, Moolenaar WH, Bos JL, Jalink K. Detecting cAMP-induced Epac activation by fluorescence resonance energy transfer: Epac as a novel cAMP indicator. *EMBO Rep.* 5: 1176–1180, 2004.

Price JL, Blau J, Rothenfluh A, Abodeely M, Kloss B, Young MW. double-time is a novel Drosophila clock gene that regulates PERIOD protein accumulation. *Cell* 94: 83–95, 1998.

Pulver SR, Pashkovski SL, Hornstein NJ, Garrity PA, Griffith LC. Temporal dynamics of neuronal activation by Channelrhodopsin-2 and TRPA1 determine behavioral output in Drosophila larvae. *J. Neurophysiol.* 101: 3075–3088, 2009.

Pyza E, Meinertzhagen IA. Daily rhythmic changes of cell size and shape in the first optic neuropil in Drosophila melanogaster. *J. Neurobiol.* 40: 77–88, 1999.

Renn SC, Park JH, Rosbash M, Hall JC, Taghert PH. A pdf neuropeptide gene mutation and ablation of PDF neurons each cause severe abnormalities of behavioral circadian rhythms in Drosophila. *Cell* 99: 791–802, 1999.

Rieger D, Stanewsky R, Helfrich-Förster C. Cryptochrome, compound eyes, Hofbauer-Buchner eyelets, and ocelli play different roles in the entrainment and masking pathway of the locomotor activity rhythm in the fruit fly Drosophila melanogaster. *J. Biol. Rhythms* 18: 377–391, 2003.

Rietveld WJ, Minors DS, Waterhouse JM. Circadian rhythms and masking: an overview. *Chronobiol. Int.* 10: 306–312, 1993.

Rutila JE, Suri V, Le M, So WV, Rosbash M, Hall JC. CYCLE is a second bHLH-PAS clock protein essential for circadian rhythmicity and transcription of Drosophila period and timeless. *Cell* 93: 805–814, 1998.

Salvaterra PM, Kitamoto T. Drosophila cholinergic neurons and processes visualized with Gal4/UAS-GFP. *Brain Res. Gene Expr. Patterns* 1: 73–82, 2001.

Sarthy PV. Histamine: a neurotransmitter candidate for Drosophila photoreceptors. *J. Neurochem.* 57: 1757–1768, 1991.

Schild D, Restrepo D. Transduction mechanisms in vertebrate olfactory receptor cells. *Physiol. Rev.* 78: 429–466, 1998.

Schuster R, Phannavong B, Schröder C, Gundelfinger ED. Immunohistochemical localization of a ligand-binding and a structural subunit of nicotinic acetylcholine receptors in the central nervous system of Drosophila melanogaster. *J. Comp. Neurol.* 335: 149–162, 1993.

Sehgal A, Rothenfluh-Hilfiker A, Hunter-Ensor M, Chen Y, Myers MP, Young MW. Rhythmic expression of timeless: a basis for promoting circadian cycles in period gene autoregulation. *Science* 270: 808–810, 1995.

Shafer OT, Helfrich-Förster C, Renn SCP, Taghert PH. Reevaluation of Drosophila melanogaster's neuronal circadian pacemakers reveals new neuronal classes. *J. Comp. Neurol.* 498: 180–193, 2006a.

Shafer OT, Helfrich-Förster C, Renn SCP, Taghert PH. Reevaluation of Drosophila melanogaster's neuronal circadian pacemakers reveals new neuronal classes. *J. Comp. Neurol.* 498: 180–193, 2006b.

Shafer OT, Kim DJ, Dunbar-Yaffe R, Nikolaev VO, Lohse MJ, Taghert PH. Widespread receptivity to neuropeptide PDF throughout the neuronal circadian

clock network of Drosophila revealed by real-time cyclic AMP imaging. *Neuron* 58: 223–237, 2008.

Shafer OT, Rosbash M, Truman JW. Sequential nuclear accumulation of the clock proteins period and timeless in the pacemaker neurons of Drosophila melanogaster. *J. Neurosci.* 22: 5946–5954, 2002.

Shakiryanova D, Levitan ES. Prolonged presynaptic posttetanic cyclic GMP signaling in Drosophila motoneurons. *Proc. Natl. Acad. Sci. U. S. A.* 105: 13610–13613, 2008.

Shang Y, Griffith LC, Rosbash M. Light-arousal and circadian photoreception circuits intersect at the large PDF cells of the Drosophila brain. *Proc. Natl. Acad. Sci. U. S. A.* 105: 19587–19594, 2008.

Shang Y, Haynes P, Pírez N, Harrington KI, Guo F, Pollack J, Hong P, Griffith LC, Rosbash M. Imaging analysis of clock neurons reveals light buffers the wake-promoting effect of dopamine. *Nat. Neurosci.* 14: 889–895, 2011.

Shaw PJ, Cirelli C, Greenspan RJ, Tononi G. Correlates of sleep and waking in Drosophila melanogaster. *Science* 287: 1834–1837, 2000.

Shearman LP, Zylka MJ, Weaver DR, Kolakowski LF Jr, Reppert SM. Two period homologs: circadian expression and photic regulation in the suprachiasmatic nuclei. *Neuron* 19: 1261–1269, 1997.

Sheeba V, Fogle KJ, Kaneko M, Rashid S, Chou Y-T, Sharma VK, Holmes TC. Large Ventral Lateral Neurons Modulate Arousal and Sleep in Drosophila. *Curr. Biol.* 18: 1537–1545, 2008a.

Sheeba V, Gu H, Sharma VK, O'Dowd DK, Holmes TC. Circadian- and light-dependent regulation of resting membrane potential and spontaneous action potential firing of Drosophila circadian pacemaker neurons. *J. Neurophysiol.* 99: 976–988, 2008b.

Shiga Y, Tanaka-Matakatsu M, Hayashi S. A nuclear GFP/β-galactosidase fusion protein as a marker for morphogenesis in living Drosophila. *Dev. Growth Differ.* 38: 99–106, 1996.

Shigeyoshi Y, Taguchi K, Yamamoto S, Takekida S, Yan L, Tei H, Moriya T, Shibata S, Loros JJ, Dunlap JC, Okamura H. Light-induced resetting of a mammalian circadian clock is associated with rapid induction of the mPer1 transcript. *Cell* 91: 1043–1053, 1997.

Simpson JH, Stephen F. Genetic dissection of neural circuits and behavior. In: *Advances in genetics*, edited by Goodwin SF. San Diego, CA: Academic Press (Elsevier), 2009.

De Souza NJ, Dohadwalla AN, Reden J. Forskolin: a labdane diterpenoid with antihypertensive, positive inotropic, platelet aggregation inhibitory, and adenylate cyclase activating properties. *Med. Res. Rev.* 3: 201–219, 1983.

Spaulding SW. The ways in which hormones change cyclic adenosine 3',5'-monophosphate-dependent protein kinase subunits, and how such changes affect cell behavior. *Endocr. Rev.* 14: 632–650, 1993.

Sprecher SG, Desplan C. Switch of rhodopsin expression in terminally differentiated Drosophila sensory neurons. *Nature* 454: 533–537, 2008.

Sprecher SG, Pichaud F, Desplan C. Adult and larval photoreceptors use different mechanisms to specify the same Rhodopsin fates. *Genes Dev.* 21: 2182–2195, 2007.

Stanewsky R, Kaneko M, Emery P, Beretta B, Wager-Smith K, Kay SA, Rosbash M, Hall JC. The cryb mutation identifies cryptochrome as a circadian photoreceptor in Drosophila. *Cell* 95: 681–692, 1998.

Stanewsky R. Genetic analysis of the circadian system in Drosophila melanogaster and mammals. *J. Neurobiol.* 54: 111–147, 2003.

Stewart BA, Atwood HL, Renger JJ, Wang J, Wu CF. Improved stability of Drosophila larval neuromuscular preparations in haemolymph-like physiological solutions. *J. Comp. Physiol. [A]* 175: 179–191, 1994.

Stoleru D, Peng Y, Agosto J, Rosbash M. Coupled oscillators control morning and evening locomotor behaviour of Drosophila. *Nature* 431: 862–868, 2004.

Suri V, Qian Z, Hall JC, Rosbash M. Evidence that the TIM light response is relevant to light-induced phase shifts in Drosophila melanogaster. *Neuron* 21: 225–234, 1998.

Taghert PH, Shafer OT. Mechanisms of clock output in the Drosophila circadian pacemaker system. *J. Biol. Rhythms* 21: 445–457, 2006.

Talsma AD, Christov CP, Terriente-Felix A, Linneweber GA, Perea D, Wayland M, Shafer OT, Miguel-Aliaga I. Remote control of renal physiology by the intestinal neuropeptide pigment-dispersing factor in Drosophila. *Proc. Natl. Acad. Sci. U. S. A.* 109: 12177–12182, 2012.

Tei H, Okamura H, Shigeyoshi Y, Fukuhara C, Ozawa R, Hirose M, Sakaki Y. Circadian oscillation of a mammalian homologue of the Drosophila period gene. *Nature* 389: 512–516, 1997.

Tian L, Hires SA, Mao T, Huber D, Chiappe ME, Chalasani SH, Petreanu L, Akerboom J, McKinney SA, Schreiter ER, Bargmann CI, Jayaraman V, Svoboda

K, Looger LL. Imaging neural activity in worms, flies and mice with improved GCaMP calcium indicators. *Nat. Methods* 6: 875–881, 2009.

Tischkau SA, Barnes JA, Lin FJ, Myers EM, Barnes JW, Meyer-Bernstein EL, Hurst WJ, Burgoon PW, Chen D, Sehgal A, Gillette MU. Oscillation and light induction of timeless mRNA in the mammalian circadian clock. *J. Neurosci.* 19: RC15, 1999.

Tischkau SA, Mitchell JW, Tyan S-H, Buchanan GF, Gillette MU. Ca2+/cAMP response element-binding protein (CREB)-dependent activation of Per1 is required for light-induced signaling in the suprachiasmatic nucleus circadian clock. *J. Biol. Chem.* 278: 718–723, 2003.

Tomchik SM, Davis RL. Dynamics of learning-related cAMP signaling and stimulus integration in the Drosophila olfactory pathway. *Neuron* 64: 510–521, 2009.

Ultsch A, Schuster CM, Laube B, Schloss P, Schmitt B, Betz H. Glutamate receptors of Drosophila melanogaster: cloning of a kainate-selective subunit expressed in the central nervous system. *Proc. Natl. Acad. Sci. U. S. A.* 89: 10484–10488, 1992.

Veleri S, Brandes C, Helfrich-Förster C, Hall JC, Stanewsky R. A self-sustaining, light-entrainable circadian oscillator in the Drosophila brain. *Curr. Biol. CB* 13: 1758–1767, 2003.

Veleri S, Rieger D, Helfrich-Förster C, Stanewsky R. Hofbauer-Buchner eyelet affects circadian photosensitivity and coordinates TIM and PER expression in Drosophila clock neurons. *J. Biol. Rhythms* 22: 29–42, 2007.

Vincent P, Gervasi N, Zhang J. Real-time monitoring of cyclic nucleotide signaling in neurons using genetically encoded FRET probes. *Brain Cell Biol.* 36: 3–17, 2008.

Viswanath V, Story GM, Peier AM, Petrus MJ, Lee VM, Hwang SW, Patapoutian A, Jegla T. Opposite thermosensor in fruitfly and mouse. *Nature* 423: 822–823, 2003.

Völkner M, Lenz-Böhme B, Betz H, Schmitt B. Novel CNS glutamate receptor subunit genes of Drosophila melanogaster. *J. Neurochem.* 75: 1791–1799, 2000.

Wang JW, Wong AM, Flores J, Vosshall LB, Axel R. Two-photon calcium imaging reveals an odor-evoked map of activity in the fly brain. *Cell* 112: 271–282, 2003.

Waseem T, Mukhtarov M, Buldakova S, Medina I, Bregestovski P. Genetically encoded Cl-Sensor as a tool for monitoring of Cl-dependent processes in small neuronal compartments. *J. Neurosci. Methods* 193: 14–23, 2010.

Wegener C, Hamasaka Y, Nässel DR. Acetylcholine increases intracellular Ca2+ via nicotinic receptors in cultured PDF-containing clock neurons of Drosophila. *J. Neurophysiol.* 91: 912–923, 2004.

Weiner J. Time, love, memory: a great biologist and his quest for the origins of behavior. New York: Vintage Books, 2000.

Wheeler DA, Hamblen-Coyle MJ, Dushay MS, Hall JC. Behavior in light-dark cycles of Drosophila mutants that are arrhythmic, blind, or both. *J. Biol. Rhythms* 8: 67–94, 1993.

Willoughby D, Cooper DMF. Live-cell imaging of cAMP dynamics. *Nat. Methods* 5: 29–36, 2008.

Wu JS, Luo L. A protocol for dissecting Drosophila melanogaster brains for live imaging or immunostaining. *Nat. Protoc.* 1: 2110–2115, 2006.

Wu MN, Ho K, Crocker A, Yue Z, Koh K, Sehgal A. The effects of caffeine on sleep in Drosophila require PKA activity, but not the adenosine receptor. *J. Neurosci.* 29: 11029–11037, 2009.

Xia Z, Liu Y. Reliable and global measurement of fluorescence resonance energy transfer using fluorescence microscopes. *Biophys. J.* 81: 2395–2402, 2001.

Yao Z, Macara AM, Lelito KR, Minosyan TY, Shafer OT. Analysis of functional neuronal connectivity in the Drosophila brain. *J. Neurophysiol.* 108: 684–696, 2012.

Yao Z, Shafer OT. The Drosophila circadian clock is a variably coupled network of multiple peptidergic units. *Science* 343: 1516–1520, 2014.

Yasuyama K, Kitamoto T, Salvaterra PM. Immunocytochemical study of choline acetyltransferase in Drosophila melanogaster: an analysis of cis-regulatory regions controlling expression in the brain of cDNA-transformed flies. *J. Comp. Neurol.* 361: 25–37, 1995.

Yasuyama K, Meinertzhagen IA. Extraretinal photoreceptors at the compound eye's posterior margin in Drosophila melanogaster. *J. Comp. Neurol.* 412: 193–202, 1999.

Yasuyama K, Salvaterra PM. Localization of choline acetyltransferase-expressing neurons in Drosophila nervous system. *Microsc. Res. Tech.* 45: 65–79, 1999.

Yin JC, Tully T. CREB and the formation of long-term memory. *Curr. Opin. Neurobiol.* 6: 264–268, 1996.

Yoshii T, Hermann C, Helfrich-Förster C. Cryptochrome-positive and -negative clock neurons in Drosophila entrain differentially to light and temperature. *J. Biol. Rhythms* 25: 387–398, 2010.

Yoshii T, Heshiki Y, Ibuki-Ishibashi T, Matsumoto A, Tanimura T, Tomioka K. Temperature cycles drive Drosophila circadian oscillation in constant light that otherwise induces behavioural arrhythmicity. *Eur. J. Neurosci.* 22: 1176–1184, 2005.

Yoshii T, Todo T, Wülbeck C, Stanewsky R, Helfrich-Förster C. Cryptochrome is present in the compound eyes and a subset of Drosophila's clock neurons. *J. Comp. Neurol.* 508: 952–966, 2008.

Yu W, Zheng H, Houl JH, Dauwalder B, Hardin PE. PER-dependent rhythms in CLK phosphorylation and E-box binding regulate circadian transcription. *Genes Dev.* 20: 723–733, 2006.

Yuan Q, Lin F, Zheng X, Sehgal A. Serotonin modulates circadian entrainment in Drosophila. *Neuron* 47: 115–127, 2005.

Zheng X, Sehgal A. Speed control: cogs and gears that drive the circadian clock. *Trends Neurosci.* 35: 574–585, 2012.

Zylka MJ, Shearman LP, Weaver DR, Reppert SM. Three period homologs in mammals: differential light responses in the suprachiasmatic circadian clock and oscillating transcripts outside of brain. *Neuron* 20: 1103–1110, 1998.

CHAPTER 3

RECIPROCAL CHOLINERGIC AND GABAERGIC MODULATION OF THE SMALL VENTROLATERAL PACEMAKER NEURONS OF *DROSOPHILA*'S CIRCADIAN CLOCK NEURON NETWORK

3.1 ABSTRACT

The relatively simple clock neuron network of *Drosophila* is a valuable model system for the neuronal basis of circadian timekeeping. Unfortunately, many key neuronal classes of this network are inaccessible to electrophysiological analysis. We have therefore adopted the use of genetically encoded sensors to address the physiology of the fly's circadian clock network. Using genetically encoded $Ca^{2+}$and cAMP sensors, we have investigated the physiological responses of two specific classes of clock neuron, the large and small ventrolateral neurons (l- and s-LN_vs), to two neurotransmitters implicated in their modulation: acetylcholine (ACh) and γ-aminobutyric acid (GABA). Live imaging of l-LN_v cAMP and Ca^{2+} dynamics in response to cholinergic agonist and GABA application were well aligned with published electrophysiological data, indicating that our sensors were capable of faithfully reporting acute physiological responses to these transmitters within single adult clock neuron soma. We extended these live imaging methods to s-LN_vs, critical neuronal pacemakers whose physiological properties in the adult brain are largely unknown. Our s-LN_v experiments revealed the predicted excitatory responses to bath-applied cholinergic agonists and the predicted inhibitory effects of GABA and established that the antagonism of ACh and GABA extends to their effects on cAMP signaling. These data support recently published but physiologically untested models of s-LN_v modulation and lead to the prediction that cholinergic and

GABAergic inputs to s-LN_vs will have opposing effects on the phase and/or period of the molecular clock within these critical pacemaker neurons.

3.2 INTRODUCTION

The circadian clock is an innate temporal program that rhythmically orchestrates most aspects of animal behavior and physiology (Aschoff 1981). Circadian clocks are a ubiquitous adaptation to the predictable and often severe daily and seasonal fluctuations that characterize much of the Earth's surface. The proper entrainment of these endogenous clocks to local time is a prerequisite for the optimal orchestration of clock-controlled behavioral and physiological outputs with an everchanging environment. In animals, the master circadian clock comprises a network of central brain neurons, each of which expresses a highly conserved molecular clockwork (Herzog 2007), and the proper entrainment of this network to the 24-h rhythm of the environment is critical for human health and psychological well-being (Foster 2010; Schwartz and Roth 2006). Clock neuron networks are closely associated with input from the visual system in animals, and environmental light-dark cycles are thought to be the network's most salient entrainment cue (Golombek and Rosenstein 2009; Helfrich- Förster 2004). However, the clock neuron network is sensitive to many environmental, physiological, and social cues and likely responds to a diverse set of modulatory inputs to maintain entrainment to the external world (Challet 2007). The disruption of the normal timing of these inputs is thought to be the cause of circadian misalignment in humans (Arble et al. 2010). Understanding how the brain's clock integrates various modulatory inputs is therefore critical for understanding circadian timekeeping and its misalignment.

Compared to the mammalian clock center in the hypothalamic suprachiasmatic nuclei, the circadian clock neuron network of the fly *Drosophila melanogaster* is simple, consisting of fewer than 200 neurons (Kaneko and Hall 2000; Shafer et al. 2006). Subsets of these neurons, the large and small ventrolateral neurons (l-LN_vs and s-LN_vs), are critical for the control of sleep and arousal and for several aspects of circadian timekeeping (Chung et al. 2009; Parisky et al. 2008;

Renn et al. 1999; Shang et al. 2008; Sheeba et al. 2008a; Yoshii et al. 2009). The s-LN_vs are thought to be the dominant neuronal pacemaker of the circadian clock neuron network under light-dark cycles and under constant darkness and temperature (Grima et al. 2004; Rieger et al. 2006; Stoleru et al. 2004, 2005). Given the important roles that these neurons serve in timekeeping, an understanding of the physiological basis of their circadian function is critical to our understanding of the clock network in *Drosophila*. The l-LN_vs —probably because of their large cell body diameters and superficial locations— have been the focus of detailed electrophysiological analysis within the intact adult clock neuron network (Fogle et al. 2011; McCarthy et al. 2011; Park and Griffith 2006; Sheeba et al. 2008b). In contrast, the electrophysiological analysis of s-LN_vs is challenging, and, to our knowledge, only one electrophysiological experiment, which described the resting membrane potential of s-LN_vs across the diurnal cycle, has been reported for this neuron type (Cao and Nitabach 2008). Thus the physiological properties of the critical adult s-LN_vs remain largely unknown. Likewise, the physiology of the majority of clock neuron classes has not been addressed through electrophysiological observations, likely owing to inaccessibility. For this reason we have sought to employ live imaging methods for the measurement of Ca^{2+} and cAMP signaling to extend the physiological analysis of the adult clock neuron network beyond the l-LN_vs.

Acetylcholine (ACh) and γ-aminobutyric acid (GABA) have both been proposed as important neurochemical modulators of the clock neuron networks of both insects and mammals (Albus et al. 2005; Dahdal et al. 2010; Hamasaka et al. 2005; Liu and Reppert 2000). Electrophysiological studies of l-LN_vs have established that these neurons are excited by ACh through nicotinic acetylcholine receptors (McCarthy et al. 2011) and are inhibited by GABA, likely via ionotropic $GABA_A$ receptors (Chung et al. 2009; McCarthy et al. 2011; Parisky et al. 2008). A growing body of work indicates that the l-LN_vs are important GABA-modulated regulators of sleep and arousal in the adult fly (Chung et al. 2009; Parisky et al. 2008; Shang et al. 2008; Sheeba et al. 2008a). Several lines of evidence suggest that, like l-LN_vs, s-LN_vs are reciprocally modulated by ACh and GABA (Chung et al. 2009; Dahdal et al. 2010;

Hamasaka et al. 2005; Parisky et al. 2008; Wegener et al. 2004). Nevertheless, the predicted physiological effects of these transmitters on adult s-LN_vs have not yet been directly tested in the adult brain.

Although live cAMP imaging has been previously conducted on adult s-LN_vs (Shafer et al. 2008; Shang et al. 2011), previous attempts to address the acute Ca^{2+} responses of the s-LN_vs to neurotransmitters have focused on dissociated and cultured LN_vs of the larval brain (Dahdal et al. 2010; Hamasaka et al. 2005; Wegener et al. 2004). These neurons persist through metamorphosis to become the adult s-LN_vs (Helfrich-Förster 1997) and may maintain many aspects of their larval physiology. Nevertheless, the circadian clock network of the adult brain is radically different from the relatively simple larval clock network, and the s-LN_v neurons of the adult likely acquire a large number of new synaptic inputs and neuronal targets during metamorphosis (Helfrich-Förster et al. 2007; Kaneko and Hall 2000; Kaneko et al. 1997). Thus it is likely that some aspects of s-LN_v physiology will differ between the larval and adult stages of *Drosophila*. For this reason it is critical that models of connectivity and modulation be tested in the intact adult clock neuron network. Here we test the efficacy and limitations of genetically encoded Ca^{2+} and cAMP sensors for measuring the physiological responses of deeply situated neurons of the adult circadian clock neuron network and use these tools to investigate the physiological effects of ACh and GABA on the critical s-LN_v pacemakers of the adult Drosophila brain.

3.3 METHODS

Fly strains

Expression of the GCaMP3.0 and Epac1-camps sensors was achieved with the previously described; UAS-GCaMP3.0; (Tian et al. 2009) and ;UAS-Epac1-camps(50A); elements (Shafer et al. 2008). We created stable lines expressing these sensors in l- and s-LN_vs, by combining each of these second chromosome UAS elements with the X-chromosome PDF driver Pdf(M)-GAL4 (Renn et al. 1999). These Pdf-GAL4; UAS-GCaMP3.0; and Pdf-GAL4;UAS-Epac1-camps flies were reared under a 12:12-h light-dark cycle at 25°C on cornmeal-yeast-sucrose media. Male flies were

used for all live imaging experiments and were dissected and imaged 2–4 days after adult emergence. Only flies dissected during the day were used for our experiments.

Dissection and solutions

Flies were anesthetized on ice, and the brains were dissected directly into ice-cold Tübingen and Düsseldorf *Drosophila* Ringer solution consisting of (in mM) 46 NaCl, 182 KCl, 3 $CaCl_2$, and 10 Tris, pH 7.2 (Sullivan et al. 2000). All cuticle, compound eye tissue, and large trachea were removed from the dissected brains. Brains were mounted anterior surface up in drop of hemolymph-like saline (HL3) consisting of (in mM) 70 NaCl, 5 KCl, 1.5 $CaCl_2$, 20 $MgCl_2$, 10 $NaHCO_3$, 5 trehalose, 115 sucrose, and 5 HEPES, pH 7.1 (Stewart et al. 1994) placed on the center of a 35-mm Falcon dish (Becton Dickenson Labware, Franklin Lakes, NJ). A petri dish insert for a PS-8H perfusion system (Bioscience Tools, San Diego, CA) was lowered around the brain. Brains were allowed to recover for 5–10 min before the start of imaging experiments. HL3 flow was established across the brain at the beginning of each experiment with the gravity-fed PS-8H perfusion system. Test compounds were applied by switching perfusion flow from the main HL3 line to a second line containing test compound for 30 s, followed by a return to HL3 flow. For vehicle controls, we switched to a second HL3 perfusion line for 30 s, followed by a return to the main HL3 line. All test compounds were purchased from Sigma-Aldrich (St. Louis, MO) and were dissolved in HL3.

For both GCaMP3.0 and Epac1-camps imaging experiments, single brains were treated with multiple doses of agonist and with vehicle controls unless otherwise noted. A typical brain received two to five agonist stimulations of differing concentrations and was allowed to recover for 5–10 min between stimulations with continuous washout with HL3 saline. Thus, for dose-response experiments, multiple concentrations of agonist and a control perfusion were delivered to each brain. Although this approach revealed dose-dependent effects of agonist treatments, the magnitudes of the individual responses were likely affected somewhat by previous treatments. We therefore used only single-agonist perfusions when comparing neuronal responses in the presence or absence of tetrodotoxin

(TTX). We performed TTX treatments by diluting TTX in both the HL3 perfusion flow and in each solution of diluted agonist. To ensure that TTX had time to penetrate our intact brain preparation, brains were incubated in 2 μM TTX for 20 min before imaging and experienced 60–90 s of 2 μM TTX flow before being treated with agonist solutions containing 2 μM TTX.

Live imaging and analysis

Live imaging of the GCaMP3.0 and Epac1-camps sensors was conducted on an Olympus FV1000 laser scanning confocal microscope (Olympus, Center Valley, PA). LN_vs were first located based on their basal sensor expression under epifluorescent illumination using green fluorescent protein (GFP) optics. The l- and s-LN_vs were differentiated based on their cell body sizes and locations. We used a 60 X 1.10 N/A W, FUMFL N objective with a dipping cone and correction collar for all live imaging experiments (Olympus). For GCaMP3.0 imaging experiments, frames were scanned with a 488-nm laser at 10 Hz for a recording duration of 5 min and GFP emission was directed to a photomultiplier tube using standard GFP optics. Epac1-camps FRET imaging was performed by scanning frames with a 440-nm laser at a frequency of 1 Hz for 5 min. Cyan fluorescent protein (CFP) and yellow fluorescent protein (YFP) emission were separated by means of a SDM510 dichroic mirror. In the l-LN_vs, some cAMP responses to GABA were observed to have relatively long latencies; Epac1-camps time courses for GABA treatments were therefore extended to a recording duration of 10 min. For both GCaMP3.0 and Epac1-camps experiments, regions of interest (ROIs) were selected over single cell bodies of l- and s-LN_vs within a single focal plane. To reduce movement artifacts for GCaMP3.0 experiments, the confocal aperture was increased to a diameter of 564 μm to increase the thickness of the optical section, and focal planes were focused on center of somata of interest. The ratiometric nature of Epac1-camps made these precautions unnecessary for our cAMP imaging experiments. Mean ROI pixel intensities for GCaMP3.0 fluorescence or Epac1-camps CFP and YFP fluorescence (value range: 0 – 4,095) were collected for each time point with Olympus Fluoview software (v. 10).

Raw GCaMP3.0 fluorescence traces were processed with custom analysis software written in MATLAB (MathWorks, Natick MA). GCaMP3.0 traces were first filtered with a 10-point moving average to remove high-frequency noise. Each filtered intensity trace was then transformed to a percent fluorescence change (ΔF/F0) trace with the following equation: $[(F_n - F_0)/F_0] \times 100$, where F_n is the intensity value at each point in time and F_0 is the baseline fluorescence calculated as the average fluorescence intensity recorded during the first 10 s of imaging. Mean ± SE traces were created based on all filtered and normalized GCaMP3.0 fluorescence traces for each neuronal class and treatment. The maximum increase in GCaMP3.0 fluorescence was determined for each filtered and normalized trace based on the entire 5-min duration of the recording. These values were then used to determine the mean maximum GCaMP3.0 fluorescence change for each treatment and neuron type. Rarely, individual neurons displayed rather large monotonic increases in GCaMP3.0 fluorescence over the course of an experiment. We defined outlier plots as monotonic plots with maximal changes that were two standard deviations or more from the mean maximal change for the vehicle treatment group. These plots were removed from the data set prior to the application of statistical tests.

Time course data collected for Epac1-camps experiments consisted of raw CFP and YFP values for each time point. The YFP channel was corrected to subtract CFP spillover into the YFP channel with the following equation: $YFP_{soc} = YFP - (CFP \times 0.444)$, where YFP_{soc} is the spillover-corrected YFP intensity, YFP and CFP are the raw intensity values, and 0.444 is the proportion of CFP emission that spills over into the YFP channel on our imaging system. The inverse FRET ratio, which is proportional to changes in cAMP, was calculated by taking the ratio CFP/YFP_{soc}. Raw inverse FRET traces were filtered with a 10-point moving average to remove high-frequency noise, and the initial time point for each trace was normalized to "1.0." Filtered and normalized inverse FRET ratio traces were averaged to create average traces for each treatment and neuron type and were expressed as percent changes in inverse Epac1-camps FRET. The maximum increase or decrease in inverse Epac1-camps FRET was determined for each individual trace from the entire 5- or 10-min duration of the recording. These values were used to generate the mean maximum

changes in inverse Epac1-camps FRET for each treatment and neuron type. For our nicotine experiments, the maximum change in inverse Epac1-camps FRET was determined for the first 3 min of the time course to compensate for the steadily increasing baseline observed for all vehicle control plots in this experiment.

For all comparisons of mean maximum change in GCaMP3.0 fluorescence or Epac1-camps inverse FRET ratio, a Kruskal-Wallis one-way ANOVA was performed on the maximum response magnitudes for each set of experimental compounds and neuron type and a Dunn's multiple comparison test was performed to determine which treatments within the group of compounds tested produced responses significantly different from vehicle controls. Statistical significance was set at $P < 0.05$ for the ANOVA and multiple comparisons test. For pairwise comparisons of maximum changes in GCaMP3.0 fluorescence or inverse Epac1-camps FRET, we employed the Mann Whitney U-test. All data were statistically analyzed and plotted with Prism 5 (GraphPad, San Diego, CA). For all data, sample sizes are reported as two numbers, separated by a comma, representing the number of neurons and number of brains sampled, respectively.

3.4 RESULTS

s-LN$_v$s retain their receptivity to cholinergic agonists in the adult brain

We first investigated the Ca^{2+} responses of l- LN$_v$s, which have been previously shown by electrophysiology to be responsive to ACh (McCarthy et al. 2011), to cholinergic agonists. For vehicle-treated l-LN$_v$s, a gradual, steady, and relatively small decline in GCaMP3.0 fluorescence was typically observed (Fig. 3.1A). We found no evidence for spontaneous increases in GCaMP3.0 fluorescence in vehicle-treated or untreated l-LN$_v$s, despite the fact that these neurons have been shown to fire spontaneous streams of action potentials, sometimes organized as low-frequency bursts (McCarthy et al. 2011; Sheeba et al. 2008b). However, given the relatively slow nature of the return to basal Ca^{2+} levels following bursts of action potentials in neurons (e.g., Irwin and Allen 2009) and the well-described kinetics of GCaMP3.0 responses to neuronal firing (Tian et al. 2009), we would not expect this sensor to detect such spontaneous activity. We first tested the responses of single l-

LN_vs to 30-s perfusions of 10^{-5}, 10^{-4}, 10^{-3}, and 10^{-2} M ACh and vehicle. Only ACh delivered at 10^{-2} M resulted in a significant increase in GCaMP3.0 fluorescence compared with vehicle controls (Fig. 3.1B). Given the fact that electrophysiological analysis of l-LN_vs has established that l-LN_vs are directly receptive to ACh (McCarthy et al. 2011), we wondered whether the apparent low sensitivity of these neurons to bath-applied ACh might be due to degradation or uptake of the transmitter within our largely intact brain preparation. We therefore tested the responses of single l-LN_vs to 30-s perfusions of the cholinergic agonist carbamoylcholine (CCh) (Fig. 3.1, A and B). Perfusion of 10^{-5} M CCh did not result in significant Ca^{2+} responses compared with vehicle controls in l-LN_vs, but CCh concentrations of 10^{-4} M and greater produced significant increases in GCaMP3.0 fluorescence [Fig. 3.1, A and B; $P < 0.05$ by Kruskal-Wallis 1-way ANOVA with Dunn's multiple comparisons test; for CCh: $n_{veh} = 21$ neurons from 10 brains (21,10), $n_{10\text{-}5} = 17,7$; $n_{10\text{-}4} = 27,11$; $n_{10\text{-}3} = 16,7$; $n_{10\text{-}2} = 10,5$; for ACh: $n_{veh} = 29,9$; $n_{10\text{-}5} = 21,7$; $n_{10\text{-}4} = 21,7$; $n_{10\text{-}3} = 24,8$; $n_{10\text{-}2} = 32,11$]. Thus the l-LN_vs displayed Ca^{2+} increases consistent with neuronal excitation in response to bath-applied cholinergic agonists, with CCh eliciting much larger responses than ACh (Fig. 3.1B). These results indicated that GCaMP3.0 is suitable for the measurement of excitatory Ca^{2+} responses within single clock neuron somata of the explanted adult brain.

We next asked whether the s-LN_vs of the adult brain also respond to cholinergic agonists. Figure 3.1C shows the mean GCaMP3.0 traces of s-LN_vs to 30-s perfusions of 10^{-5}, 10^{-4}, 10^{-3}, and 10^{-2} M CCh and vehicle. The s-LN_vs displayed significant increases in GCaMP3.0 fluorescence in response to CCh concentrations of 10^{-4} M and higher (Fig. 3.1D; $P < 0.05$ by Kruskal-Wallis 1-way ANOVA with Dunn's multiple comparisons test; for CCh: $n_{veh} = 24,9$; $n_{10\text{-}5} = 15,5$; $n_{10\text{-}4} = 15,5$; $n_{10\text{-}3} = 15,5$; $n_{10\text{-}2} = 13,6$). The response of s-LN s to 10^{-4} M CCh was markedly bimodal, with a large peak v preceded by a smaller peak (Fig. 3.1C). This bimodality was evident in individual plots and was not due to differing latencies among individual neurons (data not shown). Higher doses of CCh caused responses that were less bimodal and dominated by a single large peak of GCaMP3.0 fluorescence. Like l-LN_vs, the s-LN_vs

displayed stronger responses to CCh than to ACh (Fig. 3.1D; for ACh: n_{veh} = 20,7; $n_{10\text{-}5}$ = 18,7; $n_{10\text{-}4}$ = 18,7; $n_{10\text{-}3}$ = 21,8; $n_{10\text{-}2}$ = 29,11).

Given the largely intact nature of our explanted brain preparation and the widespread use of ACh as an excitatory neurotransmitter in the fly brain, it is possible that some or even all of the responses of the s-LN_vs to cholinergic agonists were indirect responses mediated by neuronal intermediaries. A widely used approach to determining whether a neurophysiological response is due to direct excitation employs the voltage-gated Na^+ channel blocker TTX (Soderlund 2005). We therefore asked whether the Ca^{2+} response of s-LN_vs to 10^{-4} M CCh persisted in the presence of 2 μM TTX, which has been used previously for electrophysiological and live imaging experiments on the explanted fly brain (McCarthy et al. 2011; Shang et al. 2011; Sheeba et al. 2008b). In the presence of TTX, s-LN_vs displayed bimodal GCaMP3.0 fluorescence increases in response to 10^{-4} M CCh that were highly similar to those of -TTX controls (Fig. 3.1E). In fact, there was no significant difference in the magnitudes of the CCh-induced GCaMP3.0 fluorescence increases displayed by s-LN_vs in the presence and absence of TTX, although the +TTX responses trended toward lower magnitudes (Fig. 3.1F; P = 0.2775 by Mann-Whitney U-test; n = 10,5 for -TTX and n = 9,5 for +TTX). Our results indicate that, like l-LN_vs, s-LN_vs are directly excited by cholinergic agonists in the adult brain.

Nicotinic ACh receptors mediate Ca2+ responses of s-LN_vs to cholinergic agonists

Previous studies have shown that nicotinic receptors mediate the cholinergic response of adult l-LN_vs (McCarthy et al. 2011). Furthermore, work in the dissociated larval central nervous system (CNS) indicates that larval s-LN_vs express nicotinic ACh receptors (Dahdal et al. 2010; Wegener et al. 2004), suggesting that adult s-LN_vs will likewise express nicotinic receptors. We therefore measured the effects of bath-applied nicotine on Ca^{2+} dynamics within single LN_vs. Thirty-second perfusions of nicotine evoked clear increases in GCaMP3.0 fluorescence in both l- and s-LN_vs (Fig.3.2 A, B, E, and F; $P<0.05$ for 10^{-4} M CCh in l-LN_vs and for 10^{-5} and 10^{-4} M CCh in s-LN_vs by Kruskal-Wallis 1-way ANOVA and Dunn's multiple comparisons

test; for l-LN$_v$s, n_{veh} = 12,5; $n_{10\text{-}5}$ = 12,5; $n_{10\text{-}4}$ = 12,5; $n_{10\text{-}3}$ =12,5; for s-LN$_v$s, n_{veh} = 12,5; $n_{10\text{-}5}$ = 12,5; $n_{10\text{-}4}$ = 13,5; $n_{10\text{-}3}$ = 12,5). Thus both l- and s-LN$_v$s displayed excitatory Ca^{2+} increases in response to nicotine.

We wondered whether the activation of muscarinic ACh receptors might also have contributed to the LNv Ca^{2+} responses to CCh. We therefore asked whether bath application of the muscarinic agonist pilocarpine had measurable effects on Ca^{2+} dynamics in l- and s-LN$_v$s. Thirty-second perfusions of 10^{-5} to 10^{-3} M pilocarpine had no significant effects on GCaMP3.0 fluorescence in either l- or s-LN$_v$s (Fig. 3.2, C–F; P > 0.05 for all pairwise comparisons of pilocarpine treatments with vehicle control by Kruskal- Wallis 1-way ANOV A with Dunn' s multiple comparisons test; for l-LN$_v$s, n_{veh} = 12,5; $n_{10\text{-}5}$ = 12,5; $n_{10\text{-}4}$ = 12,5; $n_{10\text{-}3}$ = 12,5; for s-LN$_v$s, n_{veh} = 12,5; $n_{10\text{-}5}$ = 12,5; $n_{10\text{-}4}$ = 12,5; $n_{10\text{-}3}$ = 12,5). Thus the muscarinic agonist had no measurable effects on the Ca^{2+} dynamics of l- and s-LN$_v$s, consistent with previous work on dissociated larval LN$_v$s indicating that these neurons are not sensitive to pilocarpine (Wegener et al. 2004).

We next confirmed that the effects of nicotine on Ca^{2+} in the s-LN$_v$s were direct by comparing the GCaMP3.0 responses of s-LN$_v$s treated with 10^{-4} M nicotine in the presence or absence of 2 μM TTX. Under both conditions, 30-s perfusions of nicotine caused clear increases in GCaMP3.0 fluorescence whose maximum changes were not significantly different (Fig.3.2, G and H; for -TTX, n=25, 8; for +TTX n=27, 10; P = 0.3793 by Mann-Whitney U-test). Thus s-LN$_v$s are directly receptive to nicotine, further supporting the conclusion that these critical pacemaker neurons express nicotinic ACh receptors in the adult brain.

Carbamoylcholine causes acute cAMP increases in ventrolateral neurons

G protein and cAMP signaling is critical for the maintenance of normally paced circadian rhythms in animals (Dahdal et al. 2010; O'Neill et al. 2008). We therefore wondered whether cholinergic excitation of adult LN$_v$s had acute effects on cAMP signaling. To further characterize the nature of the cholinergic responses in these neurons, we used the genetically encoded cAMP sensor Epac1-camps to measure the effects of bath-applied cholinergic agonists on cAMP signaling. Figure

3.3A shows the mean inverse Epac1-camps FRET traces for single l-LN_vs treated with 30-s perfusions of 10^{-5}, 10^{-4}, 10^{-3}, and 10^{-2} M CCh and vehicle. Concentrations of 10^{-4} and 10^{-3} M CCh evoked significant increases in Epac1-camps FRET ratio in l-LN_vs compared with vehicle controls (Fig. 3.3C; $P < 0.05$ by Kruskal-Wallis 1-way ANOVA with Dunn's multiple comparisons test; $n_{veh} = 15,6$; $n_{10\text{-}5} = 17,7$; $n_{10\text{-}4} = 17,7$; $n_{10\text{-}3} = 17,7$; $n_{10\text{-}2} = 17,7$). The Epac1-camps responses to CCh appeared to be biphasic, with a small and brief decrease in inverse FRET followed by a large increase in the inverse FRET ratio (Fig. 3.3A). However, this initial loss of inverse FRET may simply have been a reflection of a steady loss of inverse FRET, which was apparent in the vehicle controls, preceding the large CCh-induced cAMP increase (Fig. 3.3A). The 10^{-2} M CCh treatment did not result in significant cAMP increases compared with vehicle controls, consistent with previous work in dissociated larval neurons, which revealed decreased Ca^{2+} responses at very high ACh doses (Wegener et al. 2004) (Fig. 3.3, A and C).

The s-LN_vs displayed a highly similar pattern of Epac1- camps responses to perfusions of 10^{-5}, 10^{-4}, 10^{-3}, and 10^{-2} M CCh (Fig. 3.3B). Concentrations of 10^{-4} and 10^{-3} M CCh evoked significant increases in Epac1-camps FRET ratio in s-LN_vs compared with vehicle controls (Fig. 3.3C; $P < 0.05$ by Kruskal-Wallis 1-way ANOVA with Dunn's multiple comparisons test; $n_{veh} = 12,5$; $n_{10\text{-}5} = 15,6$; $n_{10\text{-}4} = 15,6$; $n_{10\text{-}3} = 15,6$; $n_{10\text{-}2} = 15,6$). Like l-LN_vs, the s-LN_vs displayed biphasic responses to 10^{-4} and 10^{-3} M CCh and failed to display significant responses to the 10^{-2} M treatment relative to vehicle controls (Fig. 3.3B; $P > 0.05$ by Kruskal-Wallis with Dunn's multiple comparisons test). For s-LN_vs the bimodality of the cAMP response was less equivocal than that of l-LN_vs, as the vehicle controls displayed no obvious loss of inverse FRET immediately following perfusion. We do not know the cellular basis for this bimodality or how it might relate to the bimodality observed in the s-LN_v Ca^{2+} response to 10^{-4} M CCh (Fig. 3.1C), but it might reflect the nature of the coupling of acute ionotropic excitation to cAMP increases in these neurons. Nevertheless, these results suggest that cholinergic excitation is coupled to cAMP increases in the l- and s-LN_vs of the adult brain.

To confirm that the cAMP responses of the critical s-LN_v pacemakers were in fact a direct response to CCh and not an indirect modulatory effect of other CCh-stimulated pathways, we asked whether CCh-induced cAMP increases in s-LN_vs persisted in the presence of TTX. Indeed, the cAMP responses of s-LN_vs to CCh was direct, as the increase in inverse Epac1-camps FRET caused by 10^{-4} M CCh persisted in the presence of 2 μM TTX (Fig. 3.3, D and E). There was no significant difference in the maximum increases in inverse Epac1-camps FRET between the -TTX and -TTX conditions (Fig. 3.3E; P = 0.4074 by Mann-Whitney U-test; n = 25,10 for -TTX and n = 34,10 for +TTX). These results indicate that direct cholinergic excitation is coupled to cAMP increases in the critical s-LN_v pacemakers of the adult brain.

Nicotinic ACh receptors mediate cAMP responses of s-LN_vs to cholinergic agonists

The finding that cholinergic excitation is coupled to cAMP increases in the LN_vs has important implications for how the molecular clock within these neurons might be affected by synaptic inputs, as cAMP signaling is thought to be a central component of circadian timekeeping in animals (Levine et al. 1994; O'Neill et al. 2008). We therefore sought to characterize the cholinergic stimulation of cAMP in the LN_vs by pharmacologically addressing the nature of the ACh receptors that underlie it. Bath-applied 10^{-4} and 10^{-5} M nicotine, doses that caused consistent Ca^{2+} responses in LN_vs (Fig. 3.2, A and B), also caused inverse Epac1-camps FRET increases in both l- and s-LN_vs (Fig. 3.4, A and B). The l-LN_vs also responded to 10^{-5} M nicotine (Fig. 3.4A). Because of constantly increasing inverse FRET levels in vehicle-treated and nonresponding neurons, our conservative statistical analysis indicated significant cAMP responses only at the 10^{-4} M dose for l-LN_vs and at the 10^{-5} M dose for s-LN_vs (Fig. 3.4, E and F; $P < 0.05$ for these 2 treatments vs. vehicle controls by Kruskal-Wallis 1-way ANOVA and Dunn's multiple comparisons test, $P > 0.05$ for all remaining doses of nicotine vs. vehicle perfusion; for l-LN_vs, $n_{veh} = 18,5$; $n_{10\text{-}5} = 18,5$; $n_{10\text{-}4} = 18,5$; $n_{10\text{-}3} = 17,5$; for s-LN_vs, $n_{veh} = 14,5$; $n_{10\text{-}5} = 14,5$; $n_{10\text{-}4} = 14,5$; $n_{10\text{-}3} = 14,5$). The steady increase in the inverse Epac1-camps FRET observed for vehicle controls was due to an uneven photobleaching of YFP and CFP, with greater

bleaching for the former fluorophore, as has been reported in previous studies using Epac1-camps (Börner et al. 2011). It was not clear why this occurred in some experiments but not others. Nevertheless, these results indicate that bath-applied nicotine causes increases in cAMP in l- and s-LN_vs.

We wondered whether the activation of muscarinic ACh receptors might also have contributed to the LN_v cAMP responses to CCh (Fig. 3.3, A–C). We therefore tested the effects of pilocarpine perfusion on inverse Epac1-camps FRET levels in l- and s-LN_vs. Thirty-second perfusions of 10^{-5} to 10^{-3} M pilocarpine had no measurable effects on inverse Epac1-camps FRET in l- or s-LN_vs (Fig. 3.4, C–F; $P > 0.05$ for all comparisons of pilocarpine dose and vehicle control by Kruskal-Wallis 1-way ANOVA and Dunn's multiple comparisons test; for l-LN_vs, $n_{veh} = 18,5$; $n_{10\text{-}5} = 21,6$; $n_{10\text{-}4} = 18,5$; $n^{10\text{-}3} = 18,5$; for s-LN_vs, $n^{veh} = 14,5$; $n^{10\text{-}5} = 14,5$; $n^{10\text{-}4} = 14,5$; $n_{10\text{-}3} = 14,5$). These results suggest that muscarinic pathways do not significantly affect cAMP levels in adult LN_vs.

To confirm that the cAMP responses of s-LN_vs to nicotine were direct responses rather than indirect modulatory effects of other nicotine-sensitive pathways, we asked whether nicotine- induced cAMP increases in s-LN_vs persisted in the presence of TTX. Indeed, the cAMP responses of s-LN_vs to nicotine were direct, as significant increases in inverse Epac1-camps FRET in response to 30-s perfusions of 10^{-4} M nicotine persisted in the presence of 2 μM TTX (Fig. 3.4, G and H). The s-LN_vs appeared to display slightly smaller and briefer cAMP responses in the presence of toxin (Fig. 3.4G), but a statistical comparison of the maximum changes in inverse Epac1-camps FRET displayed in the -TTX and +TTX conditions revealed no significant differences in the mean maximum increases (Fig. 3.4H; $P = 0.2541$ by Mann-Whitney U-test; $n = 14,6$ for -TTX and $n = 13,6$ for +TTX). Taken together, our results indicate that the direct activation of nicotinic ACh receptors is coupled to cAMP increases in s-LN_vs of the adult brain.

GABA antagonizes cholinergic excitation in adult LN_vs

We next tested the ability of the GCamp3.0 and Epac1-camps sensors to detect inhibitory responses in single adult LN_v soma. The l-LN_vs express the $GABA_A$

receptor RDL, an inhibitory ligand-gated Cl^- channel (Chung et al. 2009; Parisky et al. 2008), and electrophysiological analysis has established that bath application of GABA inhibits l-LN_v action potentials, likely via $GABA_A$ receptors (McCarthy et al. 2011). We therefore asked whether GCaMP3.0 imaging could detect acute GABAergic inhibition in l-LN_vs. Thirty-second perfusions of GABA alone at concentrations of 10^{-4}, 10^{-3}, and 10^{-2} M had no significant effects on GCaMP3.0 fluorescence compared with vehicle controls (Fig. 3.5, *A* and *C*; $P > 0.05$ for all 3 concentrations by Kruskal-Wallis 1-way ANOVA and Dunn's multiple comparisons test; $n_{veh} = 14,5$; $n_{10\text{-}4} = 14,5$; $n_{10\text{-}3} = 14,5$; $n_{10\text{-}2} = 14,5$). It is possible that GABA alone might not alter Ca^{2+} levels significantly, particularly if Ca^{2+} was already at or near baseline levels, or that GCaMP3.0 is insufficiently sensitive to detect inhibitory effects on intracellular Ca^{2+}. We wondered whether GCaMP3.0 could detect GABAergic inhibition when GABA is coapplied with an excitatory stimulus, as has been shown previously for dissociated larval LN_vs (Dahdal et al. 2010). We therefore tested whether coapplication of GABA with CCh would reduce or abolish the direct CCh response of l-LN_vs. In the presence of 2 μM TTX, coapplication of 10^{-3} M GABA and 10^{-4} M CCh significantly reduced the Ca^{2+} response to CCh by the l-LN_v (Fig. 3.5, *D* and *F*; $P = 0.0096$ by Mann-Whitney *U*-test; $n_{CCh} = 12,5$ and $n_{CCh\&GABA} = 12,5$).

We next examined GABA's effects on s-LN_vs, whose physiological responses to GABA have not been previously addressed in the adult brain. As for l-LN_vs, perfusion of GABA alone had no significant effects on GCaMP3.0 fluorescence in s-LN_vs (Fig. 3.5, *B* and *C*; $P > 0.05$ for all 3 concentrations by Kruskal-Wallis 1-way ANOVA and Dunn's multiple comparisons test; $n_{veh} = 17,5$; $n_{10\text{-}4} = 17,5$, $n_{10\text{-}3} = 17,5$; $n_{10\text{-}2} = 17,5$) but coapplication of GABA and CCh revealed that GABA significantly reduced the s-LN_v response to CCh in the presence of 2μM TTX (Fig.3.5, *E* and *F*: $P = 0.0122$ by Mann-Whitney U-test; $n_{CCh} = 11,5$ and $n_{CCh\&GABA} = 11,5$). Thus, as predicted by studies on dissociated larval LN_vs (Dahdal et al. 2010), adult s-LN_vs were directly inhibited by bath-applied GABA.

GABA causes acute reduction in cAMP levels in adult LN_vs

There is evidence for the expression of both ionotropic $GABA_A$ receptors and metabotropic $GABA_B$ receptors by the PDF-positive l- and s-LN_vs (Chung et al. 2009; Dahdal et al. 2010; Hamasaka et al. 2007; Parisky et al. 2008). In mammals $GABA_B$ receptors are negatively coupled to adenylate cyclase through G_o signaling, and Drosophila $GABA_B$ receptors expressed in mammalian cell lines can elicit decreases in cAMP (Bettler et al. 2004; Mezler et al. 2001). If $GABA_B$ receptors signal through G_o in Drosophila and are indeed present in the LN_vs, we would predict that GABA application would result in a reduction in cAMP levels. Thirty-second perfusions of GABA alone at 10^{-4} to 10^{-2} M resulted in significant reductions in inverse Epac1-camps FRET in l-LN_vs relative to vehicle controls, consistent with a GABA-induced loss of cAMP in these neurons (Fig. 3.6, A and C; $P < 0.05$ for these concentrations compared with vehicle by Kruskal-Wallis 1-way ANOVA and Dunn's multiple comparisons test; $n_{veh} = 30,11$; $n_{10\text{-}4} = 17, 6$; $n_{10\text{-}3} = 17,6$; $n_{10\text{-}2} = 17,7$). Likewise, 30-s perfusions of 10^{-3} M GABA resulted in significant decreases in inverse Epac1-camps FRET in s-LN_vs (Fig. 3.6, B and C; $P < 0.05$ for this dose compared with vehicle by Kruskal-Wallis 1-way ANOVA and Dunn's multiple comparisons test, $P > 0.05$ for the remaining concentrations; $n_{veh} = 26,11$; $n_{10\text{-}4} = 26,11$; $n_{10\text{-}3} = 14,5$; $n_{10\text{-}2} = 11,5$). The GABA-induced loss of inverse FRET displayed by l- and s-LN_vs was due to a reciprocal increase in YFP and decreases in CFP emission (i.e., caused by bona fide FRET changes) and not due to uneven photobleaching (data not shown).

Although both classes of LN_v neurons responded to GABA with cAMP decreases, the character of their responses differed. The l-LN_v cAMP response was relatively large and long lasting, with cAMP levels remaining low for the duration of the 10-min time course experiment (Fig. 3.6A). The s-LN_v response to 10^{-3} M GABA, in contrast, was relatively small, and transient compared with the l-LN_v responses (compare Fig. 3.6, A and B). Furthermore, in contrast to l-LN_vs, s-LN_vs displayed no apparent response to 10^{-2} M GABA, whereas l-LN_vs displayed large cAMP decreases in response to this dose (compare Fig. 3.6, A and B). These results suggest that bath-applied GABA causes significant reductions of cAMP in both l- and s-LN_vs and that these two neuronal classes may differ in their transduction of GABAergic input.

Anatomical and genetic evidence suggests that the responses of s-LN_vs to GABAergic inputs are the result of the direct effects of agonist binding receptors expressed by s-LN_vs (Chung et al. 2009; Dahdal et al. 2010; Hamasaka et al. 2007; Parisky et al. 2008). We therefore asked whether GABA- induced cAMP decreases persisted in s-LN_vs in the presence of 2 μM TTX. Thirty-second perfusions of 10^{-3} M GABA produced clear decreases in inverse Epac1-camps FRET in the presence of TTX with magnitudes that were not significantly different from those displayed in the absence of toxin (Fig. 3.6, D and E; P = 0.0503 by Mann-Whitney U-test; n = 34,12 for -TTX and n = 30,11 for +TTX). We conclude that GABA's inhibitory effect on cAMP in the s-LN_vs was direct.

GABA antagonizes cholinergic cAMP increases in s-LN_vs

Our GCaMP3.0 imaging experiments indicated that GABA antagonizes CCh's effects on Ca^{2+} in l- and s-LN_vs. We next asked whether GABA also inhibits the excitatory cAMP increases caused by CCh in these neurons. Coapplication of 10^{-3} M GABA with 10^{-4} M CCh did not significantly reduce the CCh-induced increase in cAMP in the l-LN_v (Fig. 3.7, A and C; P = 0.0915 by Mann-Whitney U-test; n_{CCh} = 17,5 and $n_{CCh\&GABA}$ = 17,5), although in some single-neuron traces a residual decrease in cAMP that resembled an inhibitory cAMP response to GABA was observed following the excitatory CCh response (data not shown). In contrast, coapplication of 10^{-3} M GABA significantly reduced the cAMP response to 10^{-4} M CCh in s-LN_vs (Fig. 3.7, B and C; P = 0.0048 by Mann-Whitney U-test; n_{CCh} = 21,7 and $n_{CCh\&GABA}$ = 21,8). The inhibitory effect of GABA on CCh-induced cAMP increases was direct, as coapplication of 10^{-3} M GABA significantly reduced the magnitude of the cAMP response to CCh in the presence of 2 μM TTX (Fig. 3.7, D and E; P = 0.0173 by Mann-Whitney U-test; $n_{CCh,TTX}$ = 12,5 and $n_{CCh\&GABA,TTX}$ = 9,5). These results suggest that GABAergic input directly antagonizes the effects of cholinergic input on cAMP levels within the s-LN_vs in adult brain.

3.5 DISCUSSION

In Drosophila, circadian timekeeping appears to be distributed across multiple classes of clock neuron and is thought to depend on physiological interactions between them (Grima et al. 2004; Lin et al. 2004; Peng et al. 2003; Picot et al. 2007; Rieger et al. 2006; Stoleru et al. 2004, 2005). Likewise, the synchronization of the circadian clock neuron network to the environment is maintained, at least in part, by inputs from peripheral sensory receptors, which must ultimately modulate the physiology and molecular timekeeping of the clock neuron network (Helfrich-Förster 2002; Helfrich-Förster et al. 2001; Klarsfeld et al. 2004; Sehadova et al. 2009). However, the physiological basis of clock network timekeeping, its modulation by sensory inputs, and the neurotransmitters employed by these pathways are largely unknown in the adult fly brain. The electrophysiological inaccessibility of much of the fly's circadian clock neuron network is a fundamental barrier to understanding the neural basis of timekeeping in the fly. Recently developed genetically encoded sensors for Ca^{2+} and cAMP signaling make possible the measurement of physiological responses in electrophysiologically inaccessible neurons of the clock network. Here we have tested the performance of two of these sensors, the Ca^{2+} sensor GCaMP3.0 and the cAMP sensor Epac1-camps, within single deeply situated adult clock neurons and have used them to test the predicted effects of ACh and GABA on the critical s-LN_v pacemakers of the adult circadian clock neuron network.

Testing the sensitivity of genetically encoded sensors in single adult clock neuron somata

The l-LN_vs are the only neurons of the adult clock neuron network that have been routinely analyzed electrophysiologically in the intact adult brain (Cao and Nitabach 2008; Fogle et al. 2011; McCarthy et al. 2011; Park and Griffith 2006; Sheeba et al. 2008b). We therefore tested the performance of GCaMP3.0 and Epac1-camps within the l-LN_v in response to modulators with established excitatory and inhibitory effects on these neurons. For single l-LN_vs, we find that GCaMP3.0 readily detects acute responses to excitatory agonists but fails to detect acute ionotropic

inhibitory responses. Given the strong coupling of neuronal excitation with Ca^{2+} entry, it was not surprising that GCaMP3.0 could detect excitatory responses within single l-LN_vs. In contrast, the suitability of genetically encoded Ca^{2+} sensors for the measurement of acute inhibitory responses seems less straightforward. Nevertheless, GCaMP sensors can be used to detect inhibitory effects in the presence of excitation, as previously reported (Dahdal et al. 2010; Ignell et al. 2009).

Previous experiments on dissociated larval LN_vs found that GABA application resulted in significant decreases in Ca^{2+} as reported by fura-2 imaging (Hamasaka et al. 2005). We suspect that this might reflect the high sensitivity of the synthetic Ca^{2+} dye relative to genetically encoded sensors. Indeed, experiments using an earlier version of GCaMP in a similar dissociated larval preparation were unable to detect these inhibitory responses to GABA (Dahdal et al. 2010). We therefore suspect that the Ca^{2+} changes induced by GABA application are too low for detection by GCaMP3.0 and that coapplication of putative inhibitors with excitatory agonists is necessary to address inhibition when using this sensor. We wonder if newly developed Cl^- sensors (Markova et al. 2008; Waseem et al. 2010) might be more suitable than GCaMP3.0 for the detection of such acute inhibitory input within deep networks of the fly brain. In contrast to our results with GCaMP3.0 and Ca^{2+} signaling, we found that Epac1-camps was capable of detecting inhibitory effects on cAMP signaling. However, it is important to note that despite the fact that Epac1-camps is nearly 10 times more sensitive to cAMP than to cyclic guanosine monophosphate (cGMP) in vitro (Nikolaev et al. 2004), it appears to be sensitive to physiologically relevant cGMP levels in fly neurons (Shakiryanova and Levitan 2008).

The l-LN_v neurons displayed much stronger responses to CCh compared with ACh (Fig. 3.1). The relatively intact nature of our brain preparation may account for the relatively high efficacy of CCh in our study. ACh, a widespread excitatory neurotransmitter in the insect CNS, is tightly regulated in the intact brain via degradation by acetylcholinesterases (Treherne and Smith 1965a, 1965b). Consistent with this notion, previous studies of cholinergic responses in another

dipteran CNS have reported a relatively high efficacy of CCh relative to ACh (Brotz et al. 1995).

Testing predicted physiological responses of s-LN$_v$s to cholinergic and GABAergic stimulation

Having characterized the sensitivity of GCaMP3.0 and Epac1-camps for imaging excitatory and inhibitory responses within the physiologically well- studied l-LN$_v$s, we turned our attention to the s-LN$_v$s. Unlike l-LN$_v$s, these neurons are critical for the maintenance of circadian rhythms and are thought to play a central role in the synchronization of the various clock neuron classes (Grima et al. 2004; Rieger et al. 2006; Shafer and Taghert 2009; Stoleru et al. 2004). Understanding the physiological basis of s-LN$_v$ function is therefore critical to our understanding the clock network. The small diameters and deep brain locations of the s-LN$_v$s have made electrophysiological analysis challenging (Cao and Nitabach 2008). We therefore sought to test the predicted effects of cholinergic and GABAergic agonists on s-LN$_v$s using genetically encoded sensors.

Our results indicate that s-LN$_v$s maintain their receptivity to cholinergic agonists via nicotinic ACh receptors, as predicted by previous work on the dissociated larval CNS (Dahdal et al. 2010; Wegener et al. 2004). Ca^{2+} and cAMP responses of s-LN$_v$s to nicotine persisted in the presence of TTX, indicating that s-LN$_v$s maintain direct receptivity to cholinergic input through nicotinic receptors after metamorphosis. Furthermore, we have found no evidence for sensitivity to muscarinic agonists by l- and s-LN$_v$s. CCh- and nicotine-induced Ca^{2+} and cAMP responses displayed similar time courses, suggesting a strong coupling of excitation and cAMP production in these neurons. Given the important role that cAMP signaling plays in the maintenance of circadian rhythms (Levine et al. 1994; O'Neill et al. 2008), these results suggest that cholinergic modulation of s-LN$_v$s might contribute to the entrainment of the molecular circadian rhythms of these neurons through the modulation of cAMP levels.

ACh is a widespread excitatory neurotransmitter in the fly brain and serves as the transmitter of most sensory neurons (Buchner et al. 1986; Gorczyca and Hall

1987; Nässel 1991). Thus, there are many potential sources for the cholinergic modulation of the s-LN_vs. One prime candidate in this regard is input from the Hofbauer-Buchner eyelet (H-B eyelet), an extraretinal light input pathway that has been implicated in the entrainment of circadian rhythms to light-dark cycles (Helfrich-Förster et al. 2002; Malpel et al. 2002; Rieger et al. 2003). The axons of the H-B eyelet express choline acetyltransferase and project to the accessory medulla, where they terminate near s-LN_v arborizations (Helfrich-Förster et al. 2002; Malpel et al. 2002; Yasuyama and Meinertzhagen 1999).

Our results also support the prediction, based on anatomical and genetic studies, that GABA inhibits adult s-LN_vs (Chung et al. 2009; Dahdal et al. 2010; Hamasaka et al. 2005; Parisky et al. 2008). Furthermore, the acute GABAergic reduction of cAMP in s-LN_vs is consistent with recent work suggesting that $GABA_B$ receptors expressed by these neurons are an important component of circadian timekeeping (Dahdal et al. 2010; Hamasaka et al. 2005). A recent report has shown that G_o signaling is required for the GABAergic inhibition of dissociated larval LN_vs and that G_o signaling via phospholipase C in adult LN_vs is critical for the maintenance of normally paced locomotor rhythms (Dahdal et al. 2010). $GABA_B$ receptors and G_o signaling can also be negatively coupled to adenylate cyclase, as has been reported for *Drosophila* $GABA_B$ receptors in heterologous cell culture (Mezler et al. 2001), although some doubt has been cast upon the presence of such negative cAMP coupling in the fly brain (Dahdal et al. 2010; Ferris et al. 2006).

Like ACh, GABA is a widespread neurotransmitter in the adult fly brain (Küppers et al. 2003), and the potential sources of the GABAergic input to s-LN_vs are manifold. GABA immunoreactivity is found in the accessory medulla where projections from the s-LN_v are found (Hamasaka et al. 2005), and GABA is released by many neurons of the visual system (Nässel 1991). Interestingly, GABA is thought to modulate light input to the accessory medulla of the cockroach (Petri et al. 2002), suggesting that GABA might play a similar modulatory role in the fly through the modulation of the s-LN_v response to input from external photoreceptors. One interesting possibility is that GABA might act to modulate the response of s-LN_vs to cholinergic input coming from the H-B eyelet or other sensory inputs.

In conclusion, our results experimentally confirm the prediction—based on previously published experiments in the dissociated larval CNS and on genetic and anatomical experiments in adults—that s-LN_vs are modulated antagonistically by cholinergic and GABAergic input. Importantly, our work establishes for the first time that this antagonism extends to cAMP signaling, which is known to be a central component of molecular timekeeping in animals (Levine et al. 1994; O'Neill et al. 2008). We therefore predict that acute cholinergic and GABAergic stimulation of s-LN_vs have opposing effects on the phase and or period of the molecular clock within these critical neuronal pacemakers. Finally, the utility of the genetically encoded sensors used in this study within deeply situated adult clock neurons indicates that such physiological analysis can now be extended to the entire clock neuron network with these tools. These imaging methods, particularly when combined with the considerable genetic tools available in the fly, will be critical for advancing our understanding of circadian timekeeping in the brain.

3.6 FIGURES

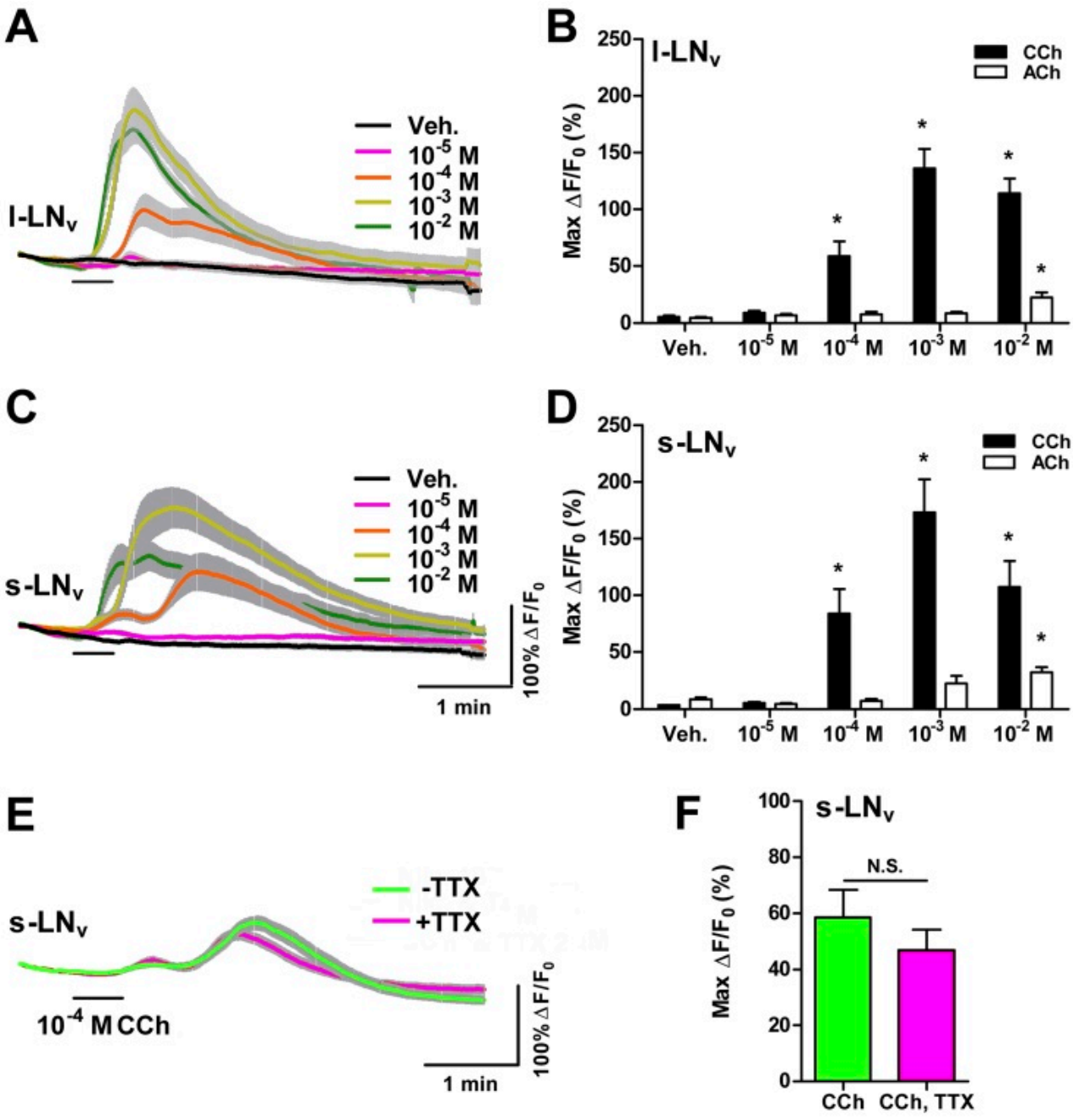

Figure 3.1 Cholinergic agonists cause Ca^{2+} increases in adult ventrolateral neurons (LN_vs). A: mean GCaMP3.0 fluorescence traces from single large (l)-LN_v somata from brains treated with 30-s (black bar) perfusions of 10^{-5}, 10^{-4}, 10^{-3}, and 10^{-2} M carbamoylcholine (CCh) and vehicle (Veh) controls. Error bars indicate SE. For CCh treatments, n_{veh} = 21 neurons from 10 brains (21,10), $n_{10^{-5}}$ = 17,7; $n_{10^{-4}}$

= 27,11; n_{10}-3 = 16,7; n_{10}-2 = 10,5. Key in A also applies to C. B: mean ± SE maximum GCaMP3.0 fluorescence increases ($\Delta F/F_0$) for l-LN_v CCh data shown in A and for an identical range of acetylcholine (ACh) treatments. Asterisks indicate a mean maximum fluorescence change that was significantly different from the change evoked by Veh perfusion ($P < 0.05$ by Kruskal-Wallis ANOVA and Dunn's multiple comparisons test). For ACh treatments, n_{veh} = 29,9; n_{10}-5 = 21,7; n_{10}-4 = 21,7; n_{10}-3 = 24,8; n_{10}-2 = 32,11. C: mean ± SE GCaMP3.0 fluorescence traces recorded from single small (s) -LN_v somata from brains treated with 30-s perfusions of various CCh concentrations and Veh. Scale bars in C also apply to A. Sample sizes were n_{veh} = 24,9; n_{10}-5 = 15,5; n_{10}-4 = 15,5; n_{10}-3 = 15,5; n_{10}-2 = 13,6. D: summary of mean maximum GCaMP3.0 fluorescence increases for s-LN_v CCh responses shown in C and for an identical range of ACh concentrations. Sample sizes for ACh treatments were n_{veh} = 20,7; n_{10}-5 = 18,7; n_{10}-4 = 18,7; n_{10}-3 = 21,8; n_{10}-2 = 29,11. Asterisks indicate a mean maximum fluorescent intensity change that was significantly different from the change evoked by Veh perfusion ($P < 0.05$ by Kruskal-Wallis ANOVA and Dunn's multiple comparisons test). E: mean traces of GCaMP3.0 fluorescence recorded from single s-LN_vs somata from brains treated with 30-s (black bar) perfusions of 10^{-4} M CCh with (magenta; n = 9,5) or without (green; n = 10,5) the presence of 2 μM tetrodotoxin (TTX). F: mean maximum GCaMP3.0 fluorescence increases for s-LN_v data shown in E. There was no significant difference in mean maximum fluorescence increases between the -TTX and +TTX conditions ($P = 0.2775$ by Mann-Whitney U-test). N.S., not significant.

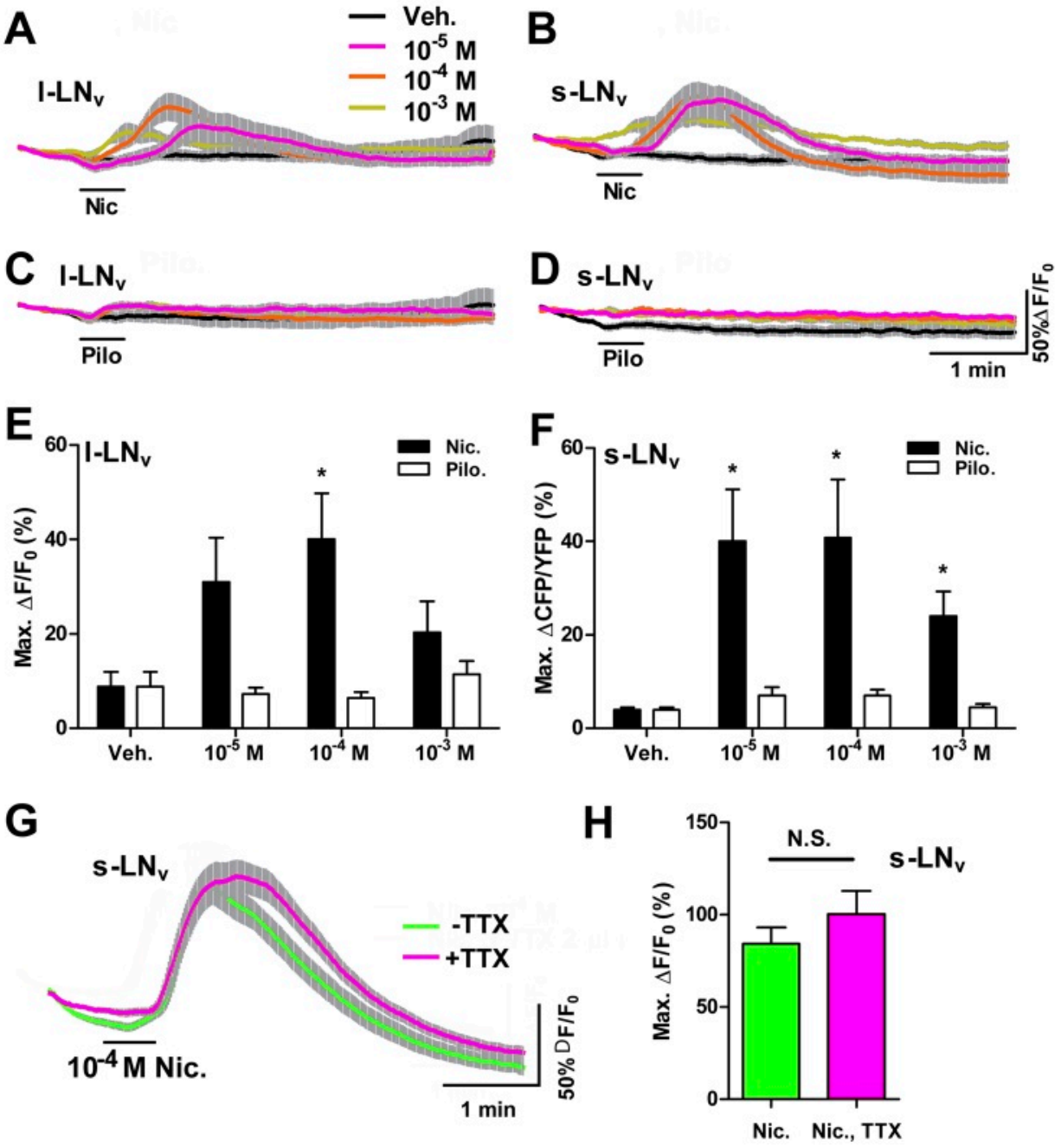

Figure 3.2 A nicotinic but not a muscarinic ACh receptor agonist causes Ca^{2+} increases in adult LN_vs. A and B: mean ± SE GCaMP3.0 fluorescence traces recorded from single l-LN_v (A) and s-LN_v (B) somata from brains treated with 30-s (black bar) perfusions of 10^{-5}, 10^{-4}, and 10^{-3} M nicotine (Nic) and vehicle (Veh). For A: n_{veh} = 12 neurons from 5 brains (12,5); $n_{10^{-5}}$ = 12,5; $n_{10^{-4}}$ = 12,5; $n_{10^{-3}}$ = 12,5. For B: n_{veh} = 12,5; $n_{10^{-5}}$ = 12,5; $n_{10^{-4}}$ = 13,5; $n_{10^{-3}}$ = 12,5. Key in A also applies to B–D. C and D: mean ± SE GCaMP3.0 fluorescence traces recorded from single l-LN_v (C) and s-LN_v (D) somata in response to 30-s (black bar) perfusions of

10^{-5}, 10^{-4}, and 10^{-3} M pilocarpine (Pilo) and Veh. For C, n_{veh} = 12; $n_{10^{-5}}$ = 12,5; $n_{10^{-4}}$ = 12,5; $n_{10^{-3}}$ = 12,5. For D, n_{veh}= 12,5; $n_{10^{-5}}$ = 12,5; $n_{10^{-4}}$ = 12,5; $n_{10^{-3}}$ = 12,5. E: summary of mean ± SE maximum GCaMP3.0 fluorescence increases displayed by l-LN_vs in response to Veh, Nic, and Pilo based on data shown in A and C. F: summary of mean ± SE maximum GCaMP3.0 fluorescence increases displayed by s-LN_vs in response to Veh, Nic, and Pilo based on data in B and D. For E and F, asterisks indicate a mean maximum fluorescence increase that was significantly different from the change evoked by Veh ($P < 0.05$, by Kruskal-Wallis ANOVA and Dunn's multiple comparisons test). G: mean ± SE GCaMP3.0 fluorescence traces recorded from single s-LN_vs somata from brains treated with 30-s (black bar) perfusions of 10^{-4} M Nic in the presence (magenta; n = 27,10) or absence (green; n = 25,8) of 2 μM TTX. H: summary of mean maximum GCaMP3.0 fluorescence increases displayed by s-LN_vs in response to 10^{-4} M Nic in the presence (magenta) or absence (green) of TTX based on data shown in G. There was no significant difference in mean maximum fluorescence increases between the -TTX and +TTX conditions ($P = 0.3793$ by Mann-Whitney U-test).

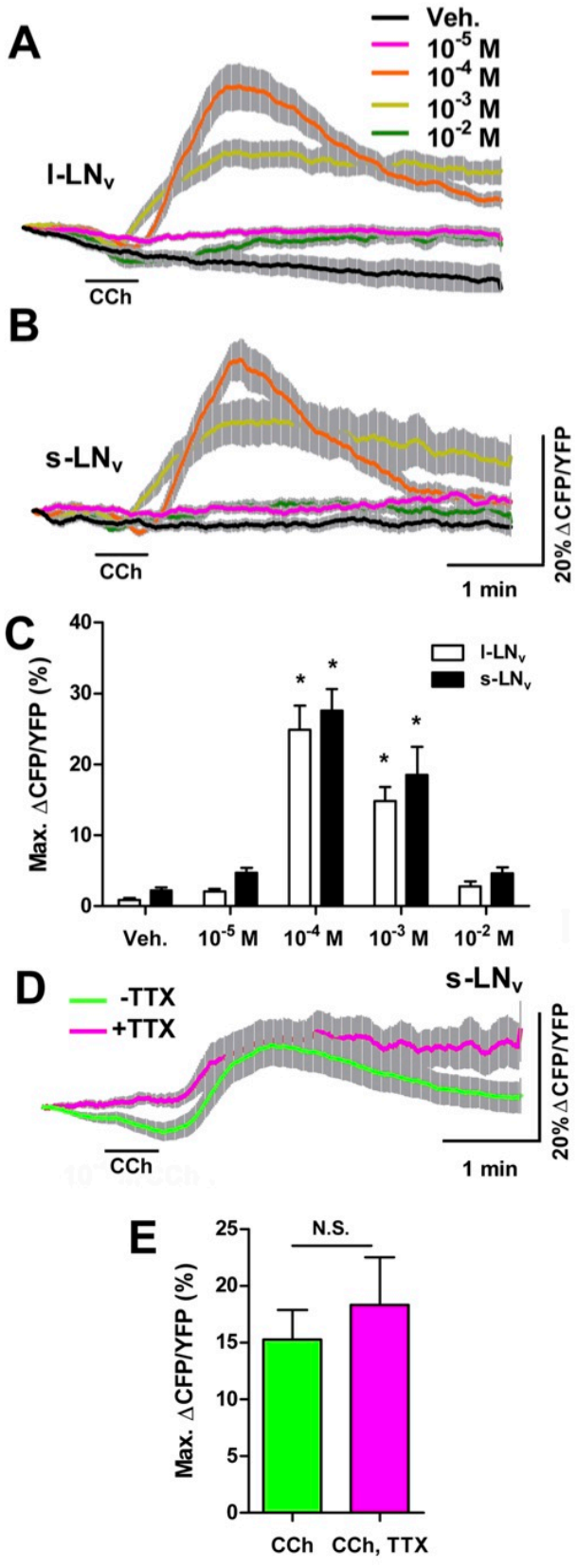

Figure 3.3. The general cholinergic agonist CCh causes cAMP increases in adult LN_vs. A and B: mean ± SE inverse Epac1-camps FRET traces recorded from single l-LN_v (A) and s-LN_v (B) somata from brains treated with 30-s perfusions of 10^{-5}, 10^{-4}, 10^{-3}, and 10^{-2} M CCh. Scale bars in B also apply to A. For A, n_{veh} = 15 neurons from 6 brains (15,6); $n_{10^{-5}}$ = 17,7; $n_{10^{-4}}$ = 17,7; $n_{10^{-3}}$ = 17,7; $n_{10^{-2}}$ =17,7. For B, n_{veh} =12,5; $n_{10^{-5}}$ = 15,6; $n_{10^{-4}}$ = 15,6; $n_{10^{-3}}$ = 15,6; $n_{10^{-2}}$ = 15,6. Key in A also applies to B. CFP, cyan fluorescent protein; YFP, yellow fluorescent protein. C: summary of mean ± SE maximum increases in inverse Epac1-camps FRET from l- and s-LN_vs data displayed in A and B. Asterisks indicate a mean maximum inverse FRET ratio change that was significantly different from the ratio change evoked by Veh ($P < 0.05$ by Kruskal-Wallis ANOVA and Dunn's multiple comparisons test). D: mean inverse Epac1-camps FRET traces for single s-LN_vs somata from brains treated with 30-s perfusions of 10^{-4} M CCh in the presence (magenta; n = 25,10) or absence (green; n = 34,10)of 2 μM TTX. E: summary of mean maximum increases in inverse Epac1-camps FRET based on s-LN_v data displayed in D. There was no significant difference in maximum inverse FRET change between the -TTX and +TTX conditions (P = 0.4074 by Mann-Whitney U-test).

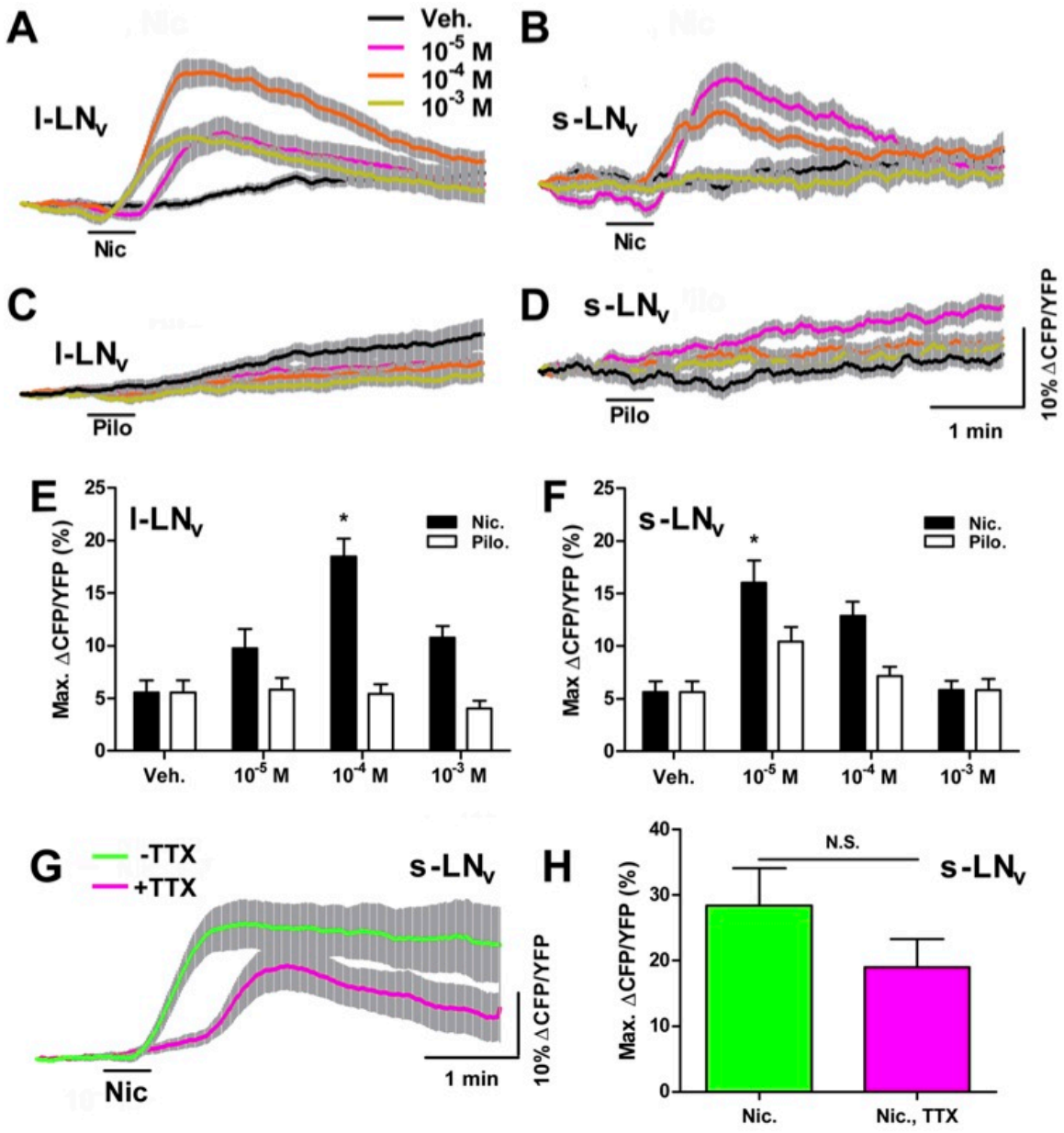

Figure 3.4. A nicotinic but not a muscarinic receptor agonist causes cAMP increases in adult LN$_v$s. A and B: mean ± SE inverse Epac1- camps FRET traces recorded from single l-LN$_v$ (A) and s-LN$_v$ (B) somata from brains treated with 30-s perfusions (black bar) of 10^{-5}, 10^{-4}, and 10^{-3} M nicotine (Nic) and vehicle (Veh). For A, n_{veh} = 18 neurons from 5 brains (18,5); $n_{10^{-5}}$ = 18,5; $n_{10^{-4}}$ = 18,5; $n_{10^{-3}}$ = 17,5. For B, n_{veh} = 14,5; $n_{10^{-5}}$ = 14,5; $n_{10^{-4}}$ = 14,5; $n_{10^{-3}}$ = 14,5. Key in A also applies to B–D. C and D: mean ± SE inverse Epac1-camps FRET traces recorded from single l-LN$_v$ (C) and s-LN$_v$ (D) somata from brains treated with 30-s perfusions of 10^{-5}, 10^{-4}, and 10^{-3} M pilocarpine (Pilo) and Veh. For C, n_{veh} = 18,5; $n_{10^{-5}}$ = 21,6;

$n_{10^{-4}}$ = 18,5; $n_{10^{-3}}$ = 18,5. For D, n_{veh} = 14,5; $n_{10^{-5}}$ = 14,5; $n_{10^{-4}}$ = 14,5; $n_{10^{-3}}$ = 14,5. Scale bars in D apply to A–D. E: summary of mean ± SE maximum increases in inverse Epac1-camps FRET for l-LN_v responses to Nic, Pilo, and Veh shown in A and C. F: summary of mean maximum increases in inverse Epac1-camps FRET for s-LN_v responses to Nic, Pilo, and Veh shown in B and D. For E and F, asterisks indicate a mean maximum change in inverse FRET that was significantly different from the change evoked by Veh ($P < 0.05$, by Kruskal-Wallis ANOVA and Dunn's multiple comparisons test). G: mean ± SE inverse Epac1- camps FRET traces recorded from single s-LN_vs somata from brains treated with 30-s perfusions of 10^{-4} M Nic in the presence (magenta; n = 14,6) or absence (green; n = 13,6) of 2 μM TTX. H: summary ± SE of mean maximum increases in inverse FRET displayed by s-LN_vs based on data in G. Mean maximum increase in inverse FRET did not differ significantly between the -TTX and +TTX conditions ($P = 0.2541$ by Mann-Whitney U-test).

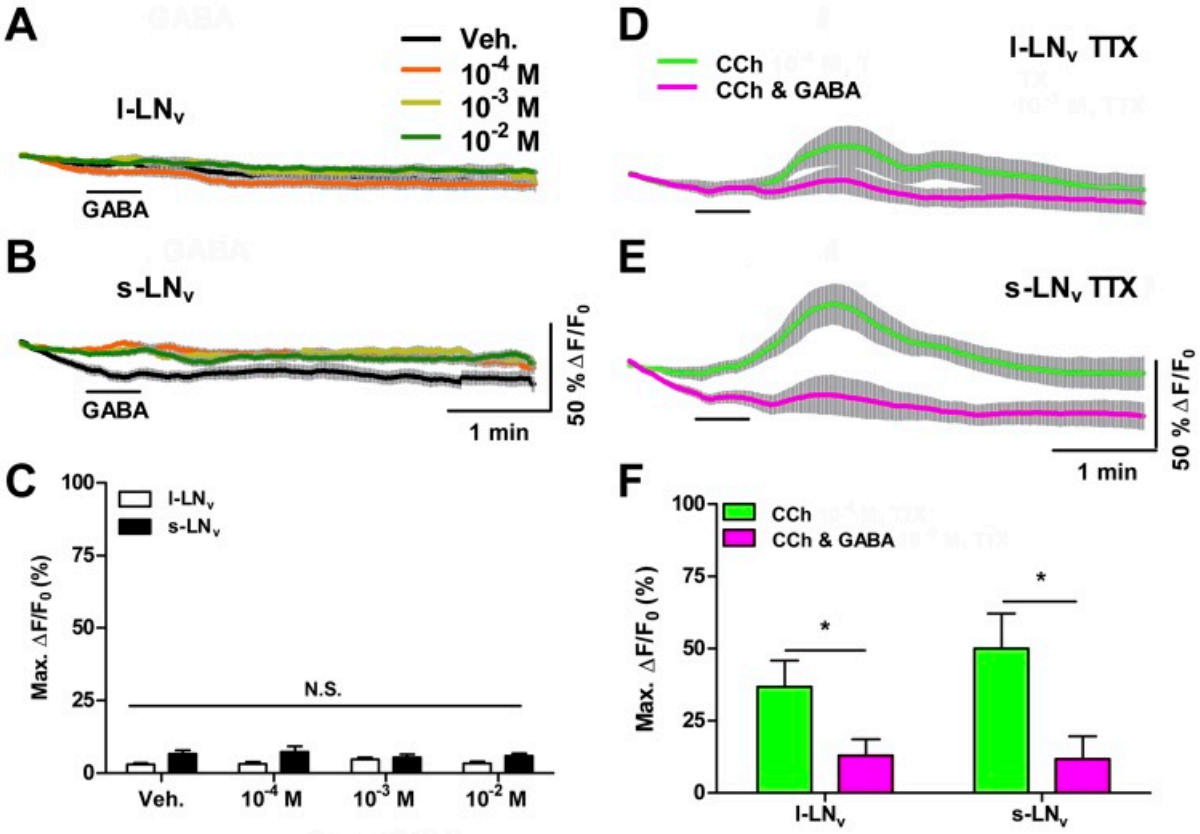

Figure 3.5. GABA alone has no acute effects on GCaMP3.0 fluorescence in adult LN$_v$s but inhibits their CCh-induced Ca^{2+} responses. A and B: mean ± SE GCaMP3.0 fluorescence traces recorded from single l-LN$_v$ (A) and s-LN$_v$ (B) somata from brains treated with 30-s (black bar) perfusions of 10^{-4}, 10^{-3}, and 10^{-2} M GABA and vehicle (Veh). Scale bars in B apply to both A and B. For A, n_{veh} = 14 neurons from 5 brains (14,5); $n_{10^{-4}}$ = 14,5; $n_{10^{-3}}$ = 14,5; $n_{10^{-2}}$ = 14,5. For B, n_{veh} = 17,5; $n_{10^{-4}}$ = 17,5; $n_{10^{-3}}$ = 17,5; $n_{10^{-2}}$ = 17,5. Key in A also applies to B. C: summary of mean maximum GCaMP3.0 fluorescence changes for l-LN$_v$ and s-LN$_v$ responses to GABA. Values are based on data shown in A and B. There was no significant difference between the effects of any concentration of GABA perfusion and Veh controls ($P > 0.05$ by Kruskal-Wallis ANOVA and Dunn's multiple comparisons test). D and E: mean ± SE GCaMP3.0 fluorescence traces recorded from single l-LN$_v$ (D) and s-LN$_v$ (E) somata from brains treated with 30-s perfusions of 10^{-4} M CCh with (magenta) and without (green) coapplication of 10^{-3} M GABA. These experiments were conducted in the presence of 2 µM TTX. Sample sizes were n_{CCh} = 12,5 and $n_{CCh\&GABA}$ = 12,5 for D and n_{CCh} = 11,5 and $n_{CCh\&GABA}$ = 11,5 for E. F: summary of mean ± SE maximum GCaMP3.0 fluorescence intensity increases recorded from l-LN$_v$ and s-LN$_v$ in response to 10^{-4} M CCh with or without coapplication of 10^{-3} M

GABA in the presence of 2 μM TTX. Values are based on data shown in D and E. Asterisks indicate a significant difference in mean maximum CCh-induced increase in GCaMP3.0 fluorescence recorded in the presence or absence of GABA ($P_{l\text{-}LNv}$ = 0.0096, $P_{S\text{-}LNv}$ = 0.0122 by Mann-Whitney U-test).

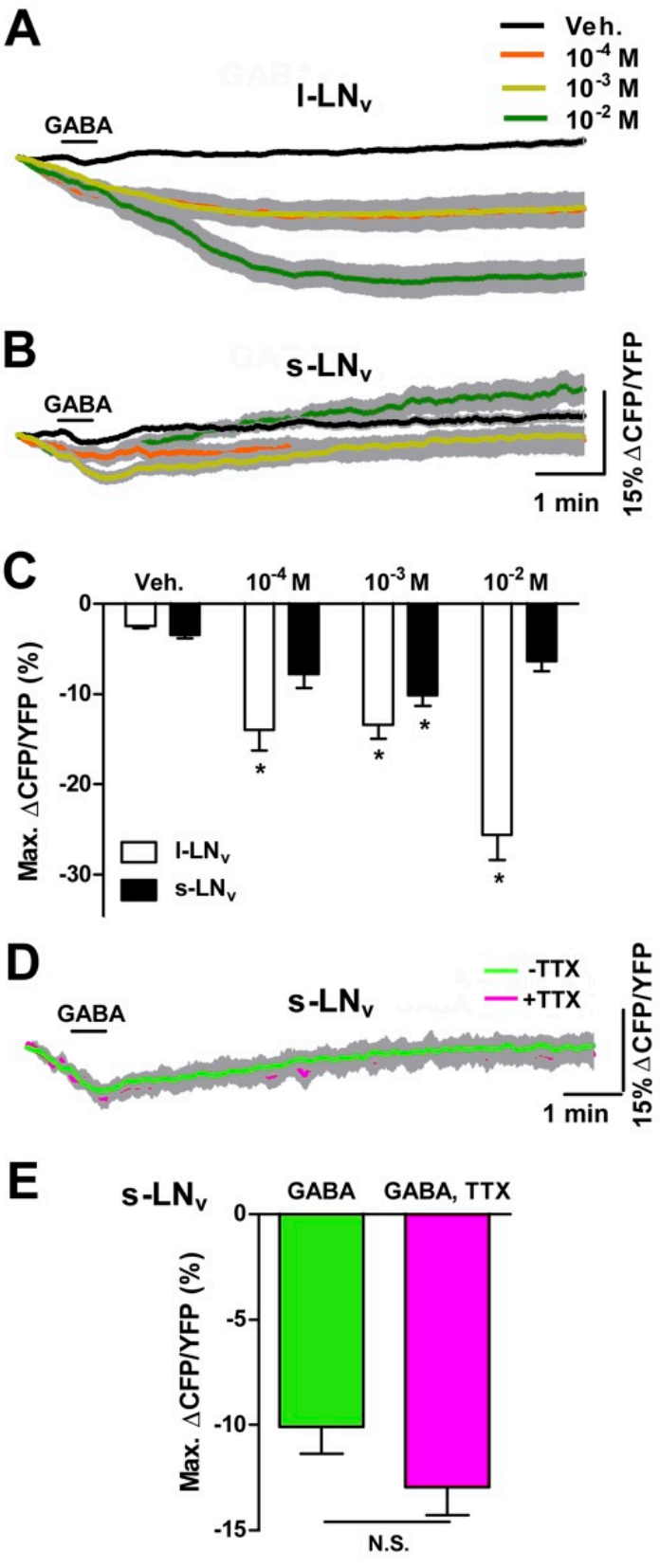

Figure 3.6. GABA causes cAMP decreases in adult LN$_v$s. A and B: mean ± SE inverse Epac1-camps FRET traces recorded from single l-LN$_v$ (A) and s-LN$_v$ (B) somata from brains treated with 30-s perfusions (black bar) of 10^{-4}, 10^{-3}, and 10^{-2} M GABA. Scale bars in B also apply to A. For A, n_{veh} = 30 neurons from 11 brains (30,11); $n_{10^{-4}}$ = 17,6; $n_{10^{-3}}$ = 17,6; $n_{10^{-2}}$ = 17,7. For B, n_{veh} =26,11; $n_{10^{-4}}$ = 26,11; $n_{10^{-3}}$ = 14,5; $n_{10^{-2}}$ = 11,5. Key in A also applies to B. C: summary of mean ± SE maximum decreases in inverse Epac1-camps FRET recorded from l- and s-LN$_v$s in response to GABA perfusion. Values are based on data shown in A and B. Asterisks indicate a maximum decrease in inverse Epac1-camps FRET that was significantly different from the maximum decrease evoked by Veh ($P < 0.05$ by Kruskal-Wallis ANOVA and Dunn's multiple comparisons test). D: mean ± SE inverse Epac1-camps FRET traces recorded from single s-LN$_v$s somata from brains treated with 30-s perfusions (black bar) of 10^{-3} M GABA in the presence (magenta; n = 34,12) or absence (green; n = 30,11) of 2 μM TTX. E: summary of mean maximum decreases in inverse Epac1-camps FRET

displayed by s-LN$_v$s in response to 10^{-3} M GABA in the presence or absence of 2 μM TTX. Values are based on data displayed in D. There was no significant difference in mean maximum loss of inverse Epac1-camps FRET between the -TTX and +TTX conditions (P = 0.0503 by Mann-Whitney U-test).

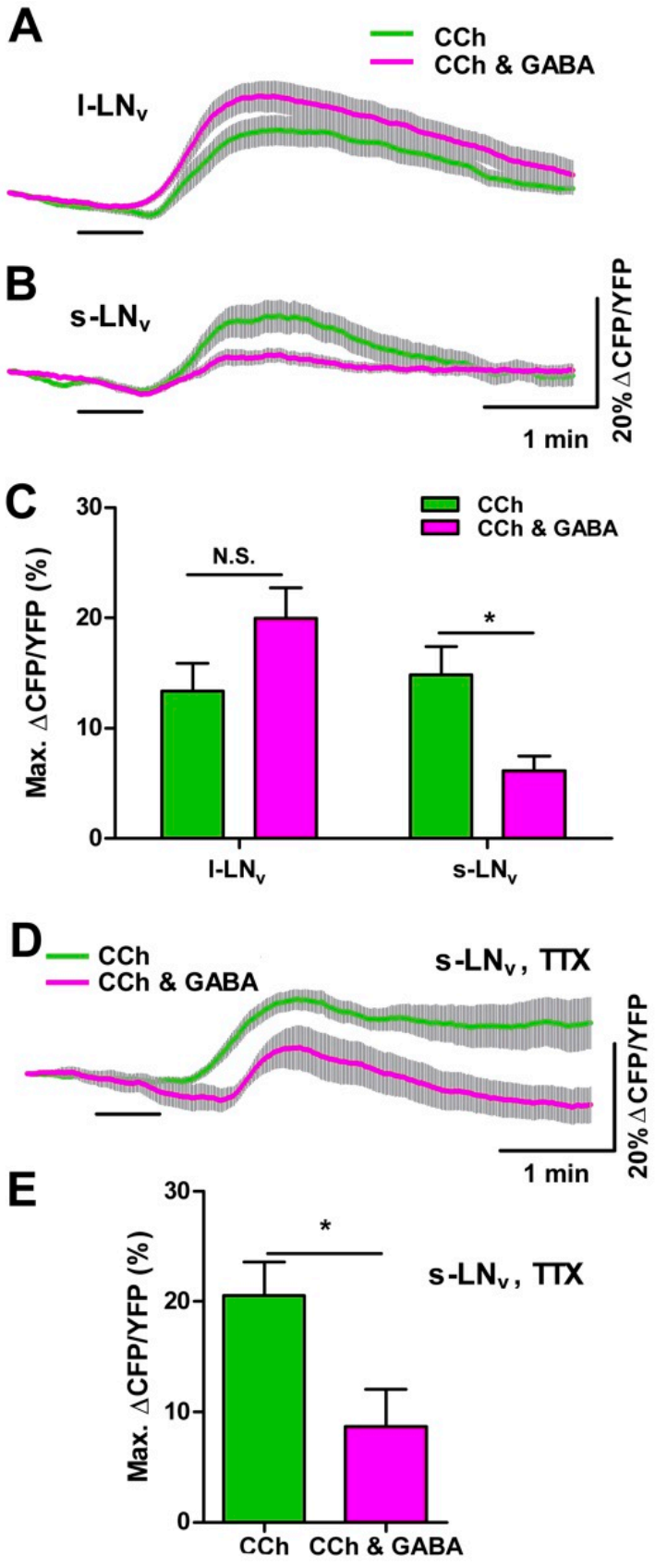

Figure 3.7. GABA inhibits CCh-induced cAMP increases in s-LN$_v$s but not in l-LN$_v$s. A and B: mean ± SE inverse Epac1-camps FRET ratio traces recorded from single l-LN$_v$ (A) and s-LN$_v$ (B) somata from brains treated with 30-s perfusions of 10^{-4} M CCh applied with (magenta) or without (green) 10^{-3} M GABA. Scale bars in B also apply to A. For A, n_{CCh} = 17 neurons from 5 brains (17,5); $n_{CCh\&GABA}$ = 17,5. For B, n_{CCh} = 21,7; $n_{CCh\&GABA}$ = 21,8. Key in A also applies to B. C: summary of mean ± SE maximum inverse Epac1-camps FRET increases recorded in l- and s-LN$_v$s in response to 10^{-4} M CCh applied alone (green) or with 10^{-3} M GABA (magenta). Values are based on data displayed in A and B. GABA did not significantly change the cAMP response to CCh in l-LN$_v$s (P = 0.0915 by Mann-Whitney U-test). GABA significantly reduced the CCh-induced the cAMP response in s-LN$_v$s (*P = 0.0048 by Mann-Whitney U-test). D: mean ± SE inverse Epac1-camps FRET traces recorded from single s-LN$_v$s somata from brains treated with 30-s perfusions of 10^{-4} M CCh applied with (magenta; n = 9,5) or without (green; n = 12,5) 10^{-3} M GABA in the presence of 2 μM

TTX. E: summary of mean ± SE maximum increases in inverse Epac1-camps FRET displayed by s-LN_vs in response to 10^{-4} M CCh applied with (magenta) or without (green) 10^{-3} M GABA in the presence of TTX. Values are based on data displayed in D. GABA significantly reduced the CCh-induced cAMP response of s-LN_vs in the presence of toxin (*P = 0.0173 by Mann-Whitney U-test).

3.7 REFERENCES

Albus H, Vansteensel MJ, Michel S, Block GD, Meijer JH. A GABAergic mechanism is necessary for coupling dissociable ventral and dorsal regional oscillators within the circadian clock. *Curr Biol* 15: 886–893, 2005.

Arble DM, Ramsey KM, Bass J, Turek FW. Circadian disruption and metabolic disease: findings from animal models. *Best Pract Res Clin Endocrinol Metab* 24: 785–800, 2010.

Aschoff J. *Biological Rhythms*. New York: Plenum, 1981. **Bettler B, Kaupmann K, Mosbacher J, Gassmann M.** Molecular structure and physiological functions of GABAB receptors. *Physiol Rev* 84: 835– 867, 2004.

Börner S, Schwede F, Schlipp A, Berisha F, Calebiro D, Lohse MJ, Nikolaev VO. FRET measurements of intracellular cAMP concentrations and cAMP analog permeability in intact cells. *Nat Protoc* 6: 427– 438, 2011.

Brotz TM, Egelhaaf M, Borst A. A preparation of the blowfly (*Calliphora erythrocephala*) brain for in vitro electrophysiological and pharmacological studies. *J Neurosci Methods* 57: 37–46, 1995.

Buchner E, Buchner S, Crawford G, Mason WT, Salvaterra PM, Sattelle DB. Choline acetyltransferase-like immunoreactivity in the brain of *Drosophila melanogaster*. *Cell Tissue Res* 246: 57–62, 1986.

Cao G, Nitabach MN. Circadian control of membrane excitability in *Drosophila melanogaster* lateral ventral clock neurons. *J Neurosci* 28: 6493– 6501, 2008. **Challet E.** Minireview: entrainment of the suprachiasmatic clockwork in diurnal and nocturnal mammals. *Endocrinology* 148: 5648–5655, 2007.

Chung BY, Kilman VL, Keath JR, Pitman JL, Allada R. The GABAA receptor RDL acts in peptidergic PDF neurons to promote sleep in *Drosophila*. *Curr Biol* 19: 386–390, 2009.

Dahdal D, Reeves DC, Ruben M, Akabas MH, Blau J. *Drosophila* pacemaker neurons require G protein signaling and GABAergic inputs to generate twenty-four hour behavioral rhythms. *Neuron* 68: 964–977, 2010.

Ferris J, Ge H, Liu L, Roman G. Go signaling is required for *Drosophila* associative learning. *Nat Neurosci* 9: 1036–1040, 2006.

Fogle KJ, Parson KG, Dahm NA, Holmes TC. CRYPTOCHROME is a blue-light sensor that regulates neuronal firing rate. *Science* 331: 1409–1413, 2011.

Foster FRG. A sense of time: body clocks, sleep and health. *Dtsch Med Wochenschr* 135: 2601–2608, 2010.

Golombek DA, Rosenstein RE. Physiology of circadian entrainment. *Physiol Rev* 90: 1063–1102, 2009.

Gorczyca M, Hall J. Immunohistochemical localization of choline acetyltransferase during development and in Chats mutants of *Drosophila melanogaster*. *J Neurosci* 7: 1361–1369, 1987.

Grima B, Chelot E, Xia R, Rouyer F. Morning and evening peaks of activity rely on different clock neurons of the *Drosophila* brain. *Nature* 431: 869–873, 2004.

Hamasaka Y, Rieger D, Parmentier ML, Grau Y, Helfrich-Förster C, Nässel DR. Glutamate and its metabotropic receptor in *Drosophila* clock neuron circuits. *J Comp Neurol* 505: 32–45, 2007.

Hamasaka Y, Wegener C, Nässel DR. GABA modulates *Drosophila* circadian clock neurons via GABAB receptors and decreases in calcium. *J Neurobiol* 65: 225–240, 2005.

Helfrich-Förster C. Development of pigment-dispersing hormone-immunoreactive neurons in the nervous system of *Drosophila melanogaster*. *J Comp Neurol* 380: 335–354, 1997.

Helfrich-Förster C. The circadian clock in the brain: a structural and functional comparison between mammals and insects. *J Comp Physiol A* 190: 601–613, 2004.

Helfrich-Förster C. The circadian system of *Drosophila melanogaster* and its light input pathways. *Zoology* 105: 297–312, 2002.

Helfrich-Förster C, Edwards T, Yasuyama K, Wisotzki B, Schneuwly S, Stanewsky R, Meinertzhagen IA, Hofbauer A. The extraretinal eyelet of *Drosophila*: development, ultrastructure, and putative circadian function. *J Neurosci* 22: 9255–9266, 2002.

Helfrich-Förster C, Shafer OT, Wülbeck C, Grieshaber E, Rieger D, Taghert P. Development and morphology of the clock-gene-expressing lateral neurons of *Drosophila melanogaster*. *J Comp Neurol* 500: 47–70, 2007.

Helfrich-Förster C, Winter C, Hofbauer A, Hall JC, Stanewsky R. The circadian clock of fruit flies is blind after elimination of all known photoreceptors. *Neuron* 30: 249–261, 2001.

Herzog ED. Neurons and networks in daily rhythms. *Nat Rev Neurosci* 8: 790–802, 2007.

Ignell R, Root CM, Birse RT, Wang JW, Nässel DR, Winther ÅME. Presynaptic peptidergic modulation of olfactory receptor neurons in *Drosophila*. *Proc Natl Acad Sci USA* 106: 13070–13075, 2009.

Irwin RP, Allen CN. GABAergic signaling induces divergent neuronal Ca2 responses in the suprachiasmatic nucleus network. *Eur J Neurosci* 30: 1462–1475, 2009.

Kaneko M, Hall JC. Neuroanatomy of cells expressing clock genes in *Drosophila*: transgenic manipulation of the period and timeless genes to mark the perikarya of circadian pacemaker neurons and their projections. *J Comp Neurol* 422: 66–94, 2000.

Kaneko M, Helfrich-Förster C, Hall JC. Spatial and temporal expression of the period and timeless genes in the developing nervous system of *Drosophila*: newly identified pacemaker candidates and novel features of clock gene product cycling. *J Neurosci* 17: 6745–6760, 1997.

Klarsfeld A, Malpel S, Michard-Vanhée C, Picot M, Chélot E, Rouyer F. Novel features of cryptochrome-mediated photoreception in the brain circadian clock of *Drosophila*. *J Neurosci* 24: 1468–1477, 2004.

Küppers B, Sánchez-Soriano N, Letzkus J, Technau GM, Prokop A. In developing *Drosophila* neurones the production of -amino butyric acid is tightly regulated downstream of glutamate decarboxylase translation and can be influenced by calcium. *J Neurochem* 84: 939–951, 2003.

Levine JD, Casey CI, Kalderon DD, Jackson FR. Altered circadian pacemaker functions and cyclic AMP rhythms in the *Drosophila* learning mutant dunce. *Neuron* 13: 967–974, 1994.

Lin Y, Stormo GD, Taghert PH. The neuropeptide pigment-dispersing factor coordinates pacemaker interactions in the *Drosophila* circadian system. *J Neurosci* 24: 7951–7957, 2004.

Liu C, Reppert SM. GABA synchronizes clock cells within the suprachiasmatic circadian clock. *Neuron* 25: 123–128, 2000.

Malpel S, Klarsfeld A, Rouyer F. Larval optic nerve and adult extra-retinal photoreceptors sequentially associate with clock neurons during *Drosophila* brain development. *Development* 129: 1443–1453, 2002.

Markova O, Mukhtarov M, Real E, Jacob Y, Bregestovski P. Genetically encoded chloride indicator with improved sensitivity. *J Neurosci Methods* 170: 67–76, 2008.

McCarthy EV, Wu Y, deCarvalho T, Brandt C, Cao G, Nitabach MN. Synchronized bilateral synaptic inputs to *Drosophila melanogaster* neuropeptidergic rest/arousal neurons. *J Neurosci* 31: 8181–8193, 2011.

Mezler M, Müller T, Raming K. Cloning and functional expression of GABAB receptors from *Drosophila*. *Eur J Neurosci* 13: 477–486, 2001.

Nässel DR. Neurotransmitters and neuromodulators in the insect visual system. *Prog Neurobiol* 37: 179–254, 1991.

Nikolaev VO, Bünemann M, Hein L, Hannawacker A, Lohse MJ. Novel single chain cAMP sensors for receptor-induced signal propagation. *J Biol Chem* 279: 37215–37218, 2004.

O'Neill JS, Maywood ES, Chesham JE, Takahashi JS, Hastings MH. cAMP-dependent signaling as a core component of the mammalian circadian pacemaker. *Science* 320: 949–953, 2008.

Parisky KM, Agosto J, Pulver SR, Shang Y, Kuklin E, Hodge JJL, Kang K, Liu X, Garrity PA, Rosbash M, Griffith LC. PDF cells are a GABA-responsive wake-promoting component of the *Drosophila* sleep circuit. *Neuron* 60: 672–682, 2008.

Park D, Griffith LC. Electrophysiological and anatomical characterization of PDF-positive clock neurons in the intact adult *Drosophila* brain. *J Neurophysiol* 95: 3955–3960, 2006.

Peng Y, Stoleru D, Levine JD, Hall JC, Rosbash M. *Drosophila* free-running rhythms require intercellular communication. *PLoS Biol* 1: e13, 2003.

Petri B, Homberg U, Loesel R, Stengl M. Evidence for a role of GABA and Mas-allatotropin in photic entrainment of the circadian clock of the cockroach *Leucophaea maderae*. *J Exp Biol* 205: 1459–1469, 2002.

Picot M, Cusumano P, Klarsfeld A, Ueda R, Rouyer F. Light activates output from evening neurons and inhibits output from morning neurons in the *Drosophila* circadian clock. *PLoS Biol* 5: e315, 2007.

Renn SCP, Park JH, Rosbash M, Hall JC, Taghert PH. A pdf neuropeptide gene mutation and ablation of PDF neurons each cause severe abnormalities of behavioral circadian rhythms in *Drosophila*. *Cell* 99: 791–802, 1999.

Rieger D, Shafer OT, Tomioka K, Helfrich-Forster C. Functional analysis of circadian pacemaker neurons in *Drosophila melanogaster*. *J Neurosci* 26: 2531–2543, 2006.

Rieger D, Stanewsky R, Helfrich-Förster C. Cryptochrome, compound eyes, Hofbauer-Buchner eyelets, and ocelli play different roles in the entrainment and masking pathway of the locomotor activity rhythm in the fruit fly *Drosophila melanogaster*. *J Biol Rhythms* 18: 377–391, 2003.

Schwartz JRL, Roth T. Shift work sleep disorder: burden of illness and approaches to management. *Drugs* 66: 2357–2370, 2006.

Sehadova H, Glaser FT, Gentile C, Simoni A, Giesecke A, Albert JT, Stanewsky R. Temperature entrainment of *Drosophila*'s circadian clock involves the gene nocte and signaling from peripheral sensory tissues to the brain. *Neuron* 64: 251–266, 2009.

Shafer OT, Helfrich-Förster C, Renn SCP, Taghert PH. Reevaluation of *Drosophila melanogaster*'s neuronal circadian pacemakers reveals new neuronal classes. *J Comp Neurol* 498: 180–193, 2006.

Shafer OT, Kim DJ, Dunbar-Yaffe R, Nikolaev VO, Lohse MJ, Taghert PH. Widespread receptivity to neuropeptide PDF throughout the neuronal circadian clock network of *Drosophila* revealed by real-time cyclic AMP imaging. *Neuron* 58: 223–237, 2008.

Shafer OT, Taghert PH. RNA-interference knockdown of *Drosophila* pigment dispersing factor in neuronal subsets: the anatomical basis of a neuropeptide's circadian functions. *PLoS One* 4: e8298, 2009.

Shakiryanova D, Levitan ES. Prolonged presynaptic posttetanic cyclic GMP signaling in *Drosophila* motoneurons. *Proc Natl Acad Sci USA* 105: 13610 – 13613, 2008.

Shang Y, Griffith L, Rosbash M. Light-arousal and circadian photoreception circuits intersect at the large PDF cells of the *Drosophila* brain. *Proc Natl Acad Sci USA* 105: 19587–19594, 2008.

Shang Y, Haynes P, Pirez N, Harrington KI, Guo F, Pollack J, Hong P, Griffith LC, Rosbash M. Imaging analysis of clock neurons reveals light buffers the wake-promoting effect of dopamine. *Nat Neurosci* 14: 889 – 895, 2011.

Sheeba V, Fogle KJ, Kaneko M, Rashid S, Chou YT, Sharma VK, Holmes TC. Large ventral lateral neurons modulate arousal and sleep in *Drosophila*. *Curr Biol* 18: 1537–1545, 2008a.

Sheeba V, Gu H, Sharma VK, O'Dowd DK, Holmes TC. Circadian- and light-dependent regulation of resting membrane potential and spontaneous action potential firing of *Drosophila* circadian pacemaker neurons. *J Neurophysiol* 99: 976–988, 2008b.

Soderlund DM. Sodium channels. In: *Comprehensive Molecular Insect Science*, edited by Gilbert LI, Latrou K, Gill SS. Amsterdam: Elsevier, 2005.

Stewart BA, Atwood HL, Renger JJ, Wang J, Wu CF. Improved stability of *Drosophila* larval neuromuscular preparations in haemolymph-like physiological solutions. *J Comp Physiol A* 175: 179–191, 1994.

Stoleru D, Peng Y, Agosto J, Rosbash M. Coupled oscillators control morning and evening locomotor behaviour of *Drosophila*. *Nature* 431: 862–868, 2004.

Stoleru D, Peng Y, Nawathean P, Rosbash M. A resetting signal between *Drosophila* pacemakers synchronizes morning and evening activity. *Nature* 438: 238–242, 2005.

Sullivan W, Ashburner M, Hawley RS. *Drosophila Protocols*. Cold Spring Harbor, NY: Cold Spring Harbor Laboratory Press, 2000, p. xiv.

Tian L, Hires SA, Mao T, Huber D, Chiappe ME, Chalasani SH, Petreanu L, Akerboom J, McKinney SA, Schreiter ER, Bargmann CI, Jayaraman V, Svoboda K, Looger LL. Imaging neural activity in worms, flies and mice with improved GCaMP calcium indicators. *Nat Methods* 6: 875–881, 2009.

Treherne JE, Smith DS. The metabolism of acetylcholine in the intact central nervous system of an insect (*Periplaneta americana* L.). *J Exp Biol* 43: 441–454, 1965a.

Treherne JE, Smith DS. The penetration of acetylcholine into the central nervous tissues of an insect (*Periplaneta americana* L.). *J Exp Biol* 43: 13–21, 1965b.

Waseem T, Mukhtarov M, Buldakova S, Medina I, Bregestovski P. Genetically encoded Cl-Sensor as a tool for monitoring of Cl-dependent processes in small neuronal compartments. *J Neurosci Methods* 193: 14 –23, 2010.

Wegener C, Hamasaka Y, Nässel DR. Acetylcholine increases intracellular Ca2 via nicotinic receptors in cultured PDF-containing clock neurons of *Drosophila*. *J Neurophysiol* 91: 912–923, 2004.

Yasuyama K, Meinertzhagen IA. Extraretinal photoreceptors at the compound eye's posterior margin in *Drosophila melanogaster*. *J Comp Neurol* 412: 193–202, 1999.

Yoshii T, Wülbeck C, Sehadova H, Veleri S, Bichler D, Stanewsky R, Helfrich-Förster C. The neuropeptide pigment-dispersing factor adjusts period and phase of *Drosophila*'s clock. *J Neurosci* 29: 2597–2610, 2009.

CHAPTER 4
ANALYSIS OF FUNCTIONAL NEURONAL CONNECTIVITY IN THE *DROSOPHILA* BRAIN

4.1 ABSTRACT

Drosophila melanogaster is a valuable model system for the neural basis of complex behavior, but an inability to routinely interrogate physiologic connections within central neural networks of the fly brain remains a fundamental barrier to progress in the field. To address this problem, we have introduced a simple method of measuring functional connectivity based on the independent expression of the mammalian P2X2 purinoreceptor and genetically encoded Ca^{2+} and cAMP sensors within separate genetically defined subsets of neurons in the adult brain. We show that such independent expression is capable of specifically rendering defined sets of neurons excitable by pulses of bath-applied ATP in a manner compatible with high-resolution Ca^{2+} and cAMP imaging in putative follower neurons. Furthermore, we establish that this approach is sufficiently sensitive for the detection of excitatory and modulatory connections deep within larval and adult brains. This technically facile approach can now be used in wild-type and mutant genetic backgrounds to address functional connectivity within neuronal networks governing a wide range of complex behaviors in the fly. Furthermore, the effectiveness of this approach in the fly brain suggests that similar methods using appropriate heterologous receptors might be adopted for other widely used model systems.

4.2 INTRODUCTION

Despite it's relative simplicity, the nervous system of *Drosophila melanogaster* is capable of producing a remarkable repertoire of complex behaviors (Weiner 1999). Work on *Drosophila* has identified discrete networks of neurons that govern circadian timekeeping (Nitabach and Taghert 2008), courtship (Villella et al. 2008), memory (McGuire et al. 2005), sleep (Crocker and Sehgal 2010), feeding (Melcher et al. 2007), and decision-making (e.g., Dickson 2008; Peabody et al. 2009). The study of these and other neural networks in the fly continues to enrich and inform our understanding of the neural control of animal behavior. For many of these central brain networks the pattern and physiologic basis of their constituent connections have been proposed; however, due to the electrophysiologic inaccessibility of much of the fly CNS, many aspects of these network models remain unchallenged experimentally. The development of technically feasible methods to test for the presence and physiologic nature of connections between defined neuronal classes of the fly CNS will therefore be critical for progress in the field. The ability to address the nature of connections between pairs of identified neurons has been one of the great strengths of large invertebrate model systems (Kandel 1976). The stereotyped and large neurons of these organisms are accessible to multiple recording and stimulating electrodes, making it possible to stimulate activity in a neuron of interest while measuring electrophysiologic responses in putative follower neurons (e.g., Kandel et al. 1967; Willows and Hoyle 1969; Fig. 4.1). Unfortunately, such multielectrode experiments are not feasible for most central neural networks of the *Drosophila* brain. The electrophysiologic inaccessibility of many central fly neurons has been surmounted somewhat by the use of genetically encoded sensors for neuronal excitation and second-messenger signaling (e.g., Lissandron 2007; Ruta 2010; Shafer 2008; Tian 2009; Tomchik 2009; Wang 2003; Yu 2003) and the physiologic responses of single deeply situated neurons can now be routinely observed in the fly brain using live imaging techniques. Combining these techniques with an ability to acutely activate subsets of neurons would allow for existing models of neural connectivity to be tested and the downstream targets of neurons of interest to be identified physiologically.

Several genetically encoded triggers of neural excitation have been successfully used in *Drosophila* in conjunction with various chemical or physical triggering methods (reviewed in Venken et al. 2011). The first instance of such triggering in the fly used the photochemical excitation of neurons expressing transgenic P2X2 receptor, a mammalian ATP receptor that is not encoded by the *Drosophila* genome (Lima and Miesenböck 2005; Littleton and Ganetzky 2000). The mammalian thermosensitive TRPV1 channel has been used to excite fly sensory neurons using its ligand capsaicin (Marella et al. 2006) and ectopic expression of the *Drosophila* thermosensitive TRPA1 channel has also been used to activate multiple neuron types with pulses of high temperature (e.g., Parisky et al. 2008).

Furthermore, the mammalian cold-sensitive TRPM8 channel has been used with both low-temperature pulses and menthol vapor as exogenous excitation triggers in the fly (Peabody et al. 2009). Finally, several groups have used the bacterial opsin Channelrhodopsin-2 (ChR2) to trigger neuronal excitation in *Drosophila* with blue light (e.g., Pulver et al. 2009; Schroll et al. 2006; Zimmermann et al. 2009). The fact that ChR2 is maximally activated by blue wavelengths makes it problematic for use in live imaging experiments, since GFP-based sensors must be excited with the same wavelengths that activate opsin conductance (Guo et al. 2009). The recent development of red-shifted optogenetic controls (Yizhar et al. 2011) and Ca^{2+} sensors (Zhao et al. 2011) may ultimately circumvent this problem, but these newly developed tools have not yet been successfully introduced to *Drosophila*. The use of temperature pulses to trigger the opening of TRPA1 or TRPM8 channels during live imaging experiments is also problematic, because acute shifts in temperature can cause significant movement of imaging targets within the explanted brain during high-resolution imaging, which makes the analysis of single-neuron somata difficult (Q. Zhang and O. Shafer, unpublished observations). For these reasons we have opted for ligand-gated triggering of transgenic receptors as a means for acute neuronal excitation. The feasibility of combining ATP excitation of P2X2-expressing fly neurons to attain biologically relevant neural excitation during behavioral and physiologic experiments has already been established for both larval

and adult nervous systems (e.g., Hu et al. 2010; Lima and Miesenböck 2005). We have therefore chosen ATP/P2X2 excitation for use in our live imaging experiments.

In *Drosophila* the Gal4/UAS system is a powerful and versatile method of transgene expression that has been the tool of choice for directing sensor expression in specific neuronal classes within the fly brain (Brand and Perrimon 1993; Venken et al. 2011). The recent development of alternative binary expression systems, the LexA and Q systems (Lai and Lee 2006; Potter et al. 2010), now makes it possible to independently direct P2X2 and sensor expression within different neuronal classes. Here we have used the simultaneous use of the Gal4 and LexA systems for the independent dual binary expression of P2X2 and genetically encoded sensors of Ca^{2+} or cAMP, thereby allowing for the acute excitation of defined neuronal populations during the simultaneous live imaging of Ca^{2+} and cAMP dynamics within putative neuronal targets (Fig. 4.1).

Here we establish the feasibility of the simultaneous use of the GAL4 and LexA systems to render defined groups of neurons excitable by pulses of bath-applied ATP while simultaneously and independently expressing the Ca^{2+} sensor GCaMP3.0 or the cAMP sensor Epac1-camps in putative follower neurons. We present proof of principle experiments that establish the efficacy of this method for detecting established and/or predicted excitatory and modulatory connections within larval and adult brains, concentrating on the well-characterized circadian clock neuron network of the fly (Nitabach and Taghert 2008), the constituent physiologic connections of which have remained largely unexamined. The *LexAop-P2X2*, *LexAop-GCaMP3.0*, and *LexAop-Epac1-camps* lines we have used for these studies, along with large and growing number of existing GAL4, UAS, and LexA lines, constitute a useful and technically facile toolkit for the interrogation of central neuronal networks in the *Drosophila* brain.

4.3 METHODS

Fly stocks and rearing

Flies were reared on cornmeal-yeast-sucrose media at 25°C under a 12:12 light:dark cycle or under the diurnal conditions of the lab. All Gal4 and UAS lines used in this study have been previously described: *Pdf(M)-Gal4;; and ;Pdf(bmrj)-Gal4;* (Renn et al. 1999), *;UAS-GCaMP3.0;* (Tian et al. 2009), *;;UAS-P2X2* (Lima and Miesenböck 2005), ;;*Clock(4.1M)-Gal4* (Zhang et al. 2010a,b), ;*Clock (-856[8.2/2])-Gal4;* (Gummadova et al. 2009), *;c929-Gal4;* (Hewes et al. 2000), *;Rh6-Gal4;* (Pichaud and Desplan 2001), *;UAS-Epac1- camps(50A);* (Shafer and Taghert 2009), and *;Cha(7.4)-Gal4/CyO*; (Salvaterra and Kitamoto 2001). The *;Pdf-LexA;* line has also been described previously (Shang et al. 2008). The creation of the *LexAop-P2X2*, *Lex Aop-GCaMP3.0*, and *LexAop-Epac1-camps* lines is described in the following text. Stable lines carrying combinations of these elements were created using standard *Drosophila* genetic techniques.

Creation of LexAop P2X2 and sensor lines

We used the LexA- response element containing pLOT vector (Lai and Lee 2006) for the creation of *LexAop-GCaM3.0*, *LexAop-Epac1-camps*, and *LexAop- P2X2* plasmids. GCaMP3.0 (Tian et al. 2009) was obtained in a pEGFP-N1 vector from Addgene (Cambridge, MA; plasmid #22692) and digested with *Eag*I. The resulting GCaMP3.0-containing fragment was gel purified, digested with *Bgl*II, and subsequently PCR purified using a QIAquick PCR Purification Kit (Qiagen, Valencia, CA). In parallel, pLOT vector was digested with *Eag*I and *Bgl*II, and treated with CIP alkaline phosphatase (New England Biolabs, Ipswich, MA) following manufacturer's instructions. The GCaMP3.0 fragment was ligated with the linearized pLOT vector with a Quick Ligation Kit from New England Biolabs. Epac1-camps (Nikolaev et al. 2004) was sequentially digested from the pUAST-Epac1-camps plasmid (Shafer et al. 2008) using *Xho*I and *Bgl*II, and PCR purified. This Epac1-camps fragment was cloned into pLOT as above using sequential *Xho*I and *Bgl*II restriction digests of pLOT. The P2X2 trimer (Lima and Miesenböck 2005) was obtained as the Gateway entry clone pENTRA1_P2X2 from G. Miesenböck (Oxford University). We created a

pLOT Gateway vector by cutting pLOT with KPN1, generating blunt ends using T4 DNA Polymerase (Invitrogen), and inserting the chloramphenicol/ccdB-resistant Gateway cassette A using T4 DNA Ligase following manufacturer's instructions (Invitrogen). We transformed OmniMAX 2T1R cells (Invitrogen) with the resulting pLOT-Gateway vector, selected ampicillin- and chloramphenicol-resistant clones for vector propagation, and purified the pLOT-Gateway vector using a Qiagen Mini Prep kit (Qiagen). The transfer of the P2X2 trimer from pENTRA1_P2X2 to the pLOT-Gateway vector was accomplished via LR recombination reaction according to manufacturer's instructions (Invitrogen) using LR II clonase (Invitrogen).

All three LexAop plasmids were extracted and purified using a Qiagen Mini Prep kit. Purified plasmids were sent to Genetic Services, Inc. (Cambridge, MA), where they were injected into *w1118* embryos. We isolated and mapped several independent transgenic lines for each LexAop element using standard fly genetic techniques. The specific lines used here were: *w;LexAop-GCaMP3.0(4B)*;, *w;LexAop-Epac1- camps(1A);*, *w;LexAop-P2X2(7);*, and *w;;LexAop-P2X2(1)*.

Dissections, solutions, and test compound delivery

Flies were anesthetized on CO_2 and brains were dissected into room temperature hemolymph-like saline (HL3) consisting of (in mM): 70 NaCl, 5 KCl, 1.5 CaCl2, 20 MgCl2, 10 NaHCO3, 5 trehalose, 115 sucrose, 5 HEPES; pH 7.1 (Stewart et al. 1994). For larval brain dissections, third instar (nonwandering) larvae were removed from the food and brains were dissected directly into HL3, keeping the eye disks and ventral nerve cord intact. Mouth hooks continued to move after dissections and were therefore removed to prevent brain movement during imaging experiments. All brains were allowed to adhere to the bottom of 35-mm FALCON culture dishes (Becton Dickenson Labware, Franklin Lakes, NJ) under a drop of HL3 contained within a petri dish insert (Bioscience Tools, San Diego, CA) for directing perfusion flow. Brains were imaged 5 to 10 min after dissection to allow for optimum baseline stabilization and settling of the brain to the dish. Perfusion flow was established over the brain with a gravity-fed PS-8H perfusion system (Bioscience Tools). Test compounds were delivered to mounted brains by switching

perfusion flow from the main HL3 line to another channel containing diluted compound for desired durations followed by a return to HL3 flow. All test compounds were dissolved in HL3. To control for the effects of switching channels, we perfused HL3 for 30 s from a second vehicle channel as a vehicle control. Adenosine 5[prime]-triphosphate disodium salt hydrate (ATP), guanosine 5[prime]-triphosphate disodium salt hydrate (GTP), and carbamoylcholine chloride (carbachol) were purchased from Sigma-Aldrich (St. Louis, MO).

Live imaging and analysis

Live imaging was performed using an Olympus FV1000 laser-scanning microscope (Olympus, Center Valley, PA) under a 20 X (0.50 N/A W, UMPlan FL N) or 60 X (1.10 N/A W, FUMFL N) objective (Olympus, Center Valley, PA). Regions of interest (ROIs) were selected over single neuronal somata or, in the case of Bolwig's nerve, over the length of a nerve. For GCaMP3.0 imaging experiments, frames were scanned with a 488-nm laser at 1—10 Hz for 5 min and GCaMP emission was directed to a photomultiplier tube by means of a DM405/488 dichroic mirror. Scanning frequencies for GCaMP3.0 imaging were kept constant within experiments, but varied between experiments. Experiments involving multiple neuronal classes demanded larger scanning areas and therefore lower scan rates. Epac1-camps FRET imaging was performed by scanning frames with a 440-nm laser at a frequency of 1 Hz for 5 min. CFP and YFP emission was separated by means of a SDM510 dichroic mirror.

For each neuron within an optical section, ROIs were drawn over somata using Fluoview software (Olympus). Raw intensity values for GCaMP3.0 emission or Epac1-camps CFP and YFP emission were recorded as mean pixel intensities (value range: 0—4,095) for each ROI at each time point and exported from Fluoview. Data transformations (see details in the following text) were conducted using custom software developed in Matlab (The MathWorks, Natick MA). For GCaMP3.0 experiments, raw intensity traces were filtered with a 10-point moving average to remove high-frequency noise and then normalized to percentage fluorescence

changes ($\Delta F/F_0$) using the following equation:

$$((F_n \times F_0)/F_0) \times 100\%$$

where F_n is a raw intensity value recorded at each point in time and F_0 is the baseline fluorescence value, calculated from the average of the raw intensity values in the first 10 s of recording from each trace. Maximum GCaMP3.0 fluorescence change values (max $\Delta F/F_0$) were determined as the maximum percentage change observed for each trace over the entire duration of each imaging experiment. Maximum values for each treatment and genotype were averaged to calculate the mean maximum change from baseline. To remove the direct excitatory effects of 488-nm light on Bolwig's Nerve (BN) (Yuan et al. 2011) from our analysis, which we observed during the start of a subset of our 488-nm scans, the F_0 for all larval BN experiments was calculated from the average fluorescent intensities observed during the 15 s preceding the stimulus onset, by which time the baseline GCaMP3.0 fluorescence had stabilized following the light-induced excitation of the nerve.

For Epac1-camps data processing, we corrected YPF intensity values for spillover from the CFP channel by the following equation:

$$YFP_{SOC} = YFP - (CFP \times 0.444)$$

where YFP_{soc} is the spillover—corrected YFP intensity, YFP and CFP are the raw intensity values, and 0.444 is the proportion of CFP emission that spills over into the YFP channel on our imaging system. The inverse FRET ratio, which is proportional to increases in cAMP, was calculated by taking the ratio of CFP/YFP_{SOC} at all time points for each ROI. Each ratio trace was filtered with a 10-point moving average. All spillover-corrected and filtered Epac1-camps inverse FRET traces were normalized to the first time point to an initial value of "1.0." Filtered, corrected, and normalized inverse FRET traces were expressed as percentage inverse FRET changes and averaged for each treatment and neuron type to create mean inverse FRET traces. The maximum percentage inverse FRET change was determined for every neuron based on the entire duration of the experiment. Such maximum inverse FRET changes were averaged for each treatment and neuron type to determine the mean maximum inverse FRET change. For most Epac1-camps inverse FRET traces, a

spontaneous and gradual increase in inverse FRET was observed due to a slow photobleaching of YFP, as has been described previously for this sensor (Börner et al. 2011; Shafer et al. 2008). To correct for these spontaneous changes, we determined the mean inverse FRET increase for 10—20 untreated or vehicle treated neurons of a particular genotype, depending on the nature of the experiment. This mean trace was then subtracted from each individual experimental trace to generate corrected inverse FRET traces.

To statistically compare maximum changes in GCaMP3.0 fluorescence or Epac1-camps inverse FRET ratio between the vehicle and test compounds, we used a Kruskal—Wallis one-way ANOVA with a Dunn's multiple comparison test. Pairwise comparisons of maximum changes in GCaMP3.0 fluorescence or inverse Epac1-camps FRET in response to test compound or vehicle perfusion were made using the Mann—Whitney *U* test. All plots and statistical tests were generated and performed using Prism 5 (GraphPad, San Diego CA). Figures were constructed in Adobe Illustrator and Photoshop (Adobe Systems, San Jose, CA). To obtain intensity-mapped images representing select time points before, during, and after ATP/P2X2 stimulation, single frames were captured from intensity-mapped still images using Fluoview. These images were imported to Photoshop (Adobe Systems, San Diego CA), and trimmed to size.

4.4 RESULTS

Controlled excitation of P2X2-expressing deep brain neurons with perfused ATP is compatible with high-resolution live imaging

Previous work has established that neurons expressing transgenic P2X2 receptor in *Drosophila* can be excited at biologically relevant levels through the global uncaging of ATP in freely moving flies (Lima and Miesenböck 2005) or through the puffing of ATP on explanted brains during electrophysiologic recordings of superficial brain neurons (Hu et al. 2010). We wondered if the simple perfusion of ATP across the explanted brain could provide a reliable and technically facile means of exciting deeply situated adult neurons in a manner compatible with high-resolution live imaging. We therefore used a *Pdf-Gal4* driver to coexpress *UAS-*

GCaMP3.0 (Tian et al. 2009) and *UAS-P2X2* (Lima and Miesenböck 2005) in the small ventral lateral neurons (s-LN_vs). These cells are critical circadian pacemaker neurons whose small somata and deep position within the central brain make them difficult neurons to investigate electrophysiologically (Cao and Nitabach 2008). Compared with vehicle controls (Fig. 4.2*A*), 30-s perfusions of 1 or 2.5 mM ATP resulted in significant GCaMP3.0 fluorescence increases, thereby revealing acute excitation of the s-LN_vs (Fig. 4.2, *B, C*, *E, F*). In contrast, 30-s perfusions of 2.5 mM GTP did not result in significant increases in on GCaMP3.0 fluorescence, instead causing very small decreases in fluorescence during perfusion (Fig. 4.2, *D* and *E*). The latencies of the s-LN_v responses to 1 mM ATP were less consistent compared with the responses to 2.5 mM, although a few s-LN_vs did display relatively late responses to the higher dose (Fig. 4.2, *B* and *C*). Many of the GCaMP3.0 fluorescence increases displayed by the s-LN_vs following 1 mM ATP perfusion were markedly bimodal, unlike the majority of responses to 2.5 mM (Fig. 4.2, *B* and *C*). This was reminiscent of s-LN_v GCaMP3.0 responses to nicotinic acetylcholine receptor activation. Carbachol (CCh) excitation of s-LN_v nicotinic acetylcholine receptors (nAChRs), which like P2X2 are expected to gate both Na^+ and Ca^{2+} upon ligand binding, results in bimodal GCaMP3.0 responses at low CCh concentrations but in single fluorescence peaks at high concentrations (Lelito and Shafer 2012). It is possible that, in the case of bimodal responses, the first peak reflects the direct gating of Ca^{2+} through P2X2, whereas the second peak represents Ca^{2+} entry through voltage-gated Ca^{2+} channels or the release of intracellular Ca^{2+}.

The *Drosophila* genome does not encode a P2X2 receptor homolog and previous studies suggest that there are no acute behavioral or physiologic effects of ATP in the absence of transgenic P2X2 (Lima and Miesenböck 2005; Littleton and Ganetzky 2000). Nevertheless, it is still possible that bath- applied ATP might have previously uncharacterized effects on the physiology of fly neurons, possibly through effects on the conserved ATP sensitive K^+ channel (Kim and Rulifson 2004), or might have effects on properties of the genetically encoded sensors themselves (Willemse et al. 2007). We therefore treated brains expressing *UAS-GCaMP3.0* or

UAS-Epac1- camps in the absence of transgenic P2X2 expression with 30-s perfusions of 2.5 mM ATP to determine if ATP had measurable effects on GCaMP3.0 fluorescence or the inverse Epac1- camps FRET ratio (CFP/YFP), which are directly proportional to Ca^{2+} and cAMP levels, respectively. The 30-s perfusions of 2.5 mM ATP resulted in very small but consistent transient decreases in GCaMP3.0 fluorescence relative to vehicle controls (Fig. 4.2, *G* and *H*). Bath-applied ATP also caused a consistent increase in Epac1-camps inverse FRET values relative to vehicle controls (Fig. 4.2, *I* and *J*). However, the evaluation of raw CFP and YFP traces revealed that this change was not due to bona fide FRET changes, but rather to decreases in YFP fluorescence, reminiscent of GCaMP3.0 fluorescence loss (Fig. 4.2*J* and data not shown). We therefore conclude that bath-applied ATP has only small and easily accounted for effects on GCaMP3.0 fluorescence and Epac1- camps inverse FRET.

LexA operator-driven sensors and P2X2 for dual binary expression experiments

Our proposed method of circuit interrogation requires the independent expression of the P2X2 receptor and genetically encoded sensors in neurons of interest and their putative follower neurons (Fig. 4.1). To complement existing *UAS-Sensor* and *UAS-P2X2* lines and the large number of existing GAL4 and LexA drivers, we have created a series of transgenic flies containing GCaMP3.0, Epac1-camps, and P2X2 elements under the control of the LexA operator (LexAop) (Lai and Lee 2006). We tested the functionality of our *LexAop-GCaMP3.0* and *LexAop-Epac1-camps* elements within s-LN_vs using the previously described *Pdf-LexA* element (Shang et al. 2008). The adult s-LN_vs respond to the general cholinergic agonist carbachol (CCh) with rapid Ca^{2+} and cAMP increases (Lelito and Shafer 2012). LexAop-driven GCaMP3.0 and Epac1-camps were indeed capable of detecting significant increases in Ca^{2+} and cAMP in response to 30-s perfusions of 10^{-4} M CCh (Fig. 4.3, *A*—*D*). Along with evidence presented below, these results indicate that our *LexAop-GCaMP3.0* and *LexAop-Epac1-camps* elements are suitable for the observation of

Ca^{2+} and cAMP dynamics within single somata of deeply situated neurons of the adult brain.

We tested the functionality of our *LexAop-P2X2* element by coexpressing it with *LexAop-GCaMP3.0* in the s-LN_vs using *Pdf-LexA*. The s-LN_vs of *Pdf-LexA,LexAop-GCaMP3.0/+; Lex- Aop-P2X2/+* brains displayed clear increases in GCaMP3.0 fluorescence in response to 30-s perfusions of 1 mM ATP, indicating that the LexAop-driven P2X2 element had rendered the s-LN_vs sensitive to bath-applied ATP (Fig. 4.3, *E* and *F*). Importantly, the *LexAop-P2X2* element rendered the s-LN_vs sensitive to ATP only when driven by the *Pdf-LexA* driver: when *UAS-GCaMP3.0* was driven in the s-LN_vs with *Pdf- GAL4* in flies carrying the *LexAop-P2X2* element, ATP had no significant effects on GCaMP3.0 fluorescence (Fig. 4.3, *E* and *F*). This observation, along with work presented in the following text, indicates that the presence of the *LexAop-P2X2* element does not cause significant P2X2 expression in the absence of LexA drivers. The same was true for the previously described *UAS-P2X2* element (Fig. 4.3, *E* and *F*; Lima and Miesenböck 2005). We conclude that, like its UAS counterpart, our *LexAop-P2X2* element is capable of specifically rendering deeply situated adult neurons excitable by bath- applied ATP.

Bath-applied ATP reliably and repeatedly activates P2X2- expressing neurons of the adult brain

Having acquired the genetic elements necessary for dual binary control of P2X2 and sensor expression, we sought to determine the most reliable means of exciting deep brain neurons expressing *UAS-P2X2* and *LexAop-P2X2* elements using bath-applied ATP. We first imaged the somata of three different classes of neuron coexpressing P2X2 and GCaMP3.0: the s-LN_vs and $DN1_p$ clock neurons [using *Pdf(bmrj)-GAL4* and *Clock(4.1M)-Gal4*, respectively] and the olfactory projection neurons [PNs; using *Cha(7.4)-Gal4*] and compared the effects of 30-s perfusions of a range of ATP concentrations on GCaMP3.0 fluorescence (Fig. 4.4*A*). For all three neuron types, 30-s perfusions of 0.1 mM ATP had no significant effects on GCaMP3.0 fluorescence. Higher concentrations resulted in dose-dependent increases in Ca^{2+}

responses, with the s-LN_vs and $DN1_p$s displaying sigmoidal response curves and the PNs (the most superficial of the neurons tested) displaying a biphasic response curve with diminished response magnitudes at doses >5 mM (Fig. 4.4*A*). We also compared the effects of these ATP concentrations between s-LN_vs expressing GCaMP3.0 and P2X2 using either the GAL4 or LexA expression system. The LexA-expressing s-LN_vs displayed significant GCaMP3.0 responses over the same range of ATP concentrations as their GAL4-expressing counterparts, but did so with lower response amplitudes, most likely due to lower levels of transgene expression (Fig. 4.4*E*). Nevertheless, the LexA-expressing s-LN_vs displayed maximum fluorescence changes ($\Delta F/F_0$) approaching 100%, amplitudes on par with the GCaMP3.0 responses displayed by fly sensory neurons subjected to acute sensory excitation (Tian et al. 2009). As shown in Fig. 4.4, *C* and *D*, the excitatory responses of single P2X2-expressing neurons to a series of increasing ATP doses were proportional to the concentration of perfused ATP. Thus, the excitatory responses of single neurons can be controlled through the manipulation of ATP dose, thereby making it possible to excite neurons at a range of intensities.

Our results suggest that 30-s perfusions of 1—5 mM ATP result in significant neuronal excitation for all three neuron types we tested. To gauge the reliability of such ATP/P2X2 excitation we analyzed how often each of these 30-s ATP treatments failed to excite the P2X2-expressing s-LN_vs, $DN1_p$s, and PNs. We defined a failure conservatively as any ATP-treated neuron displaying less than a 25% maximal increase in GCaMP3.0 fluorescence. For all three neuron types, failure rates were <50% for 1 mM ATP perfusions and approached zero at higher concentrations (Fig. 4.4*B*). Our choice of 30-s perfusions was based on previous experiments involving the bath application of neurotransmitters and receptor agonists (Lelito and Shafer 2012). We wondered if shorter applications of ATP might still yield sufficient excitation of the s-LN_vs, the most deeply situated of the neurons tested, using both the LexA and Gal4 expression systems. We therefore determined the failure rates for various durations of 2.5 mM ATP for s-LN_vs coexpressing GCaMP3.0 and P2X2 with either LexA or Gal4 drivers. For perfusion durations of 10 to 20 s, failure rates for

both genotypes were all near 30%. Failure rates reached zero at perfusion durations of 25 s for LexA s-LN_vs and at 30 s for GAL4 s-LN_vs (Fig. 4.4*F*).

The ability to excite the same set of P2X2-expressing neurons repeatedly would allow for multiple sets of putative follower neurons residing in different focal planes to be investigated in the same brain preparation. We therefore asked if P2X2-mediated excitation by bath-applied ATP could be used to repeatedly stimulate deep brain neurons. Indeed, repeated 30-s perfusions of 2.5 mM ATP resulted in reliable repeated excitation of s-LN_vs expressing either GAL4- or LexA-driven P2X2 (Fig. 4.4, *G* and *H*). Although the baseline fluorescence of these neurons displayed a slow and steady drop in intensity, there was no significant difference in the mean maximum GCaMP3.0 fluorescence increases displayed in response to the first and last (fifth) 30-s perfusion of ATP, when compared with the baseline fluorescence preceding each ATP pulse. For repeated excitation using the GAL4 system to coexpress GCaMP3.0 and P2X2 expression (Fig. 4.4*G*), the first ATP perfusion caused a mean maximum GCaMP3.0 increase of 126.6 ± 32.9% and the fifth and final pulse caused a mean increase of 114.5 ± 21.9% ($P = 0.8438$ by Mann—Whitney *U* test). For repeated excitation using the LexA system (Fig. 4.4*H*) the first ATP perfusion caused a mean maximum GCaMP3.0 increase of 145.3 ± 19.1% and final pulse caused a mean increase of 94.1 ± 18.8% ($P = 0.0524$ by Mann—Whitney *U* test). Thus, P2X2-expressing neurons can be repeatedly activated in the same dissected brain without a significant rundown in excitation.

Based on these results, we conclude that 30-s perfusions of 1—5 mM ATP result in robust, reliable, and repeatable excitation of deep brain P2X2-expressing neurons, using either the GAL4 or LexA expression system to drive the expression of P2X2. However, we note that different neuronal types display differing profiles of excitation, indicating that specific excitation parameters should be determined empirically for every neuron class and genotype to be excited.

Dual binary expression of P2X2 and genetically encoded sensors allow for the specific excitation of neuronal subsets during live imaging experiments

Having confirmed the efficacy of our LexAop-driven sensor and P2X2

elements, we next sought to confirm that the simultaneous use of the GAL4 and LexA systems could render specific neuron classes excitable by ATP during high-resolution imaging experiments. We therefore used the *Pdf-LexA* element to drive *LexAop-GCaMP3.0* expression in both the s-LN_vs and the large ventrolateral neurons (l-LN_vs) of the circadian clock network, while simultaneously using the *c929-GAL4* element, which is expressed by the l-LN_vs but not the s-LN_vs, to drive P2X2 in the l-LN_vs and in the many other peptidergic neurons expressing this GAL4 driver (Fig 5*A*; Hewes et al. 2000). Thus, the l-LN_vs of ;*Pdf-LexA,Lex- Aop-GCaMP3.0/c929-GAL4;UAS-P2X2/*□ brains will express P2X2, whereas the s-LN_vs will not. If the specific dual binary expression of P2X2 and GCaMP3.0 were successful, the l- LN_vs would be expected to display acute GCaMP3.0 responses to bath-applied ATP, whereas the s-LN_vs would not. As predicted, 30-s perfusions of 1 mM ATP resulted in the excitation of the l-LN_vs, but did not excite the s-LN_vs imaged within the same focal planes (Fig. 4.5, *B*–*D*). This result, along with the experiments presented in the following text, indicate that the simultaneous use of the GAL4 and LexA systems for the independent expression of P2X2 and genetically encoded sensors, makes possible the specific excitation of neuronal subsets in a manner compatible with high-resolution live imaging experiments. This result also suggests that the excitation of the l-LN_vs, neurons important for the control of arousal, sleep, and the integration of circadian light input (Parisky et al. 2008; Shang et al. 2008; Sheeba et al. 2008), does not result in large acute Ca^{2+} increases in the critical s-LN_v pacemaker neurons.

Gal4-based excitation and LexA-based live imaging for an established excitatory connection in the larval brain

We next sought to determine if our proposed method of addressing functional connectivity was sufficiently sensitive to detect an established neuronal connection in *Drosophila*. We were motivated to propose the present approach to circuit analysis because there are few well-established synaptic connections in our circuitry of interest, the circadian clock neuron network. One of the only fully

confirmed synaptic connections in the *Drosophila* clock network is the excitatory connection between Bolwig's organ (BO), the maggot eye, and the LN_v clock neurons, which persist through metamorphosis to become the adult s-LN_vs (Fig. 4.6*A*; Helfrich-Förster et al. 2007). BO projects directly to the larval optic neuropil via Bolwig's nerve (BN), where its terminals reside in close apposition to LN_v arbors (Helfrich-Förster et al. 2002; Malpel et al. 2002). BN expresses ChAT, an enzyme required for acetylcholine (ACh) synthesis (Yasuyama and Salvaterra 1999) and ChAT is required in BN for photic resetting of larval clock neurons (Keene et al. 2011). Dissociated and cultured larval LN_vs are directly excited by bath-applied ACh and nicotine (Wegener et al. 2004). Finally, Yuan and colleagues (2011) have recently shown that blue-light stimulation of BO causes acute Ca^{2+} increases in the larval LN_vs clock neurons. Thus, the BN to LN_v connection in the larval brain offers a well-established excitatory connection in the clock network on which to test our method for addressing connectivity.

Under our experimental conditions, we found it necessary to remove the larval mouth hooks to prevent brain movement during imaging. Mouth hook removal was associated with the loss of BO, leaving only the afferent BNs associated with the eye disks and central brain (Fig. 4.6, *A* and *B*). We therefore first confirmed that excitation of BN was possible in the absence of BO by coexpressing P2X2 and GCaMP3.0 in BN using the *Rh6-Gal4* driver, which is expressed in a subset of BN axons (Fig. 4.6*A*; Keene et al. 2011). We found that 30-s perfusions of 5 mM ATP caused reliable Ca^{2+} responses in BNs of ;*Rh6- GAL4/UAS-GCaMP3.0;UAS-P2X2/*+ brains, indicating the successful excitation of BNs (Fig. 4.6, *B*, *D*, and *G*).

Having confirmed successful ATP/P2X2 excitation of BN in our preparation, we asked if the predicted excitatory responses could be detected in larval LN_vs in response to BN excitation. We therefore created *;Rh6-Gal4/Pdf-lexA, LexAop-GCaMP3.0; UAS- P2X2/*+ larvae to independently express P2X2 in BN and GCaMP3.0 in the LN_vs (Fig. 4.6*A*). Consistent with previous reports, we observed no *Rh6-GAL4* driver expression in the LN_vs or in any other central neurons of the larval brain (e.g., Keene et al. 2011 and data not shown). All 30-s perfusions of 5 mM ATP caused

significant GCaMP3.0 fluorescence increases in the LN_vs of *Rh6-Gal4/Pdf-lexA, LexAop-GCaMP3.0; UAS-P2X2/+* brains (Fig. 4.6, *C*, *E*, and *H*). To confirm that the LN_v responses to ATP perfusion were due to the specific excitation of the BN and not to the leaky expression of *UAS-P2X2* in non-BN cell types or native responses of larval LN_vs to ATP, we repeated the experiment on brains dissected from *;Pdf-lexA, LexAop-GCaMP3.0/+; UAS- P2X2/+* larvae, which lacked the *Rh6-GAL4* element and therefore would not have driven P2X2 expression specifically in BN. The LN_vs of these flies did not display significant changes in GCaMP3.0 fluorescence following 30-s perfusions of 5 mM ATP (Fig. 4.6, *F* and *I*), indicating that nonspecific *UAS-P2X2* expression or native ATP responses had not caused the Ca^{2+} responses displayed by the LN_vs following the ATP/P2X2 excitation of BN. We conclude that our method of addressing connectivity was sufficiently sensitive to detect an established excitatory connection deep within the larval brain.

LexA-based excitation and GAL4-based live imaging to test a predicted peptidergic connection in the adult central brain

The circadian clock neuron network of the adult fly consists of approximately 150 neurons that express conserved molecular clockwork (Nitabach and Taghert 2008). Understanding the connective properties of this network was our motivation for developing a means for interrogating the physiologic connections between neuronal classes deep within the fly brain. The s-LN_vs are critical neuronal pacemakers required for the maintenance of robust rhythms in sleep and activity in the fly under constant darkness and temperature (Grima et al. 2004; Renn et al. 1999; Shafer and Taghert 2009; Stoleru et al. 2004). A large and growing body of anatomic, genetic, and physiologic evidence suggests that the clock neuron network is coordinated through modulatory connections between the s-LN_vs and the various classes of dorsal clock neurons. The s-LN_vs project to the dorsal brain, where their terminals comingle with terminals from the dorsal clock neuron classes (Helfrich-Förster et al. 2007; Kaneko and Hall 2000). The s-LN_vs express the neuropeptide pigment-dispersing factor (PDF), the genetic loss of which causes a weakening or

loss of free-running behavioral rhythms (Helfrich-Förster 1995; Renn et al. 1999; Shafer and Taghert 2009) and a loss of synchronization among various clock neuron classes (Lin et al. 2004). PDF signals through PDFR, a G-protein—coupled receptor (GPCR) that signals through cAMP increases (Hyun et al. 2005; Lear et al. 2005; Mertens et al. 2005) and is expressed by dorsal clock neurons (Im and Taghert 2010). Finally, the dorsal neuron classes respond to bath-applied PDF peptide with cAMP increases (Shafer et al. 2008). Taken together, these findings provide strong evidence for a neuromodulatory connection between the s-LN_vs and dorsal clock neurons in the adult fly brain. Thus, the current prevailing model predicts that the excitation of the s-LN_vs will result in acute cAMP increases within dorsal clock neurons.

Nevertheless, the physiologic nature of this proposed connection has not been confirmed experimentally. Indeed, recent work has shown that the s-LN_vs also express *short neuropeptide F* (*sNPF*) (Johard et al. 2009), which encodes four peptides whose GPCR would likely antagonize PDFR signaling (Garczynski et al. 2007; Mertens et al. 2002; Reale et al. 2004). The coexpression of potentially antagonistic peptides in the s-LN_vs suggests that the excitation of these neurons might in fact cause cAMP decreases in dorsal clock neuron classes. Determining the functional nature of this proposed connection therefore requires the ability to experimentally interrogate its physiology. We therefore set out to determine the nature of the predicted connection between the s-LN_v pacemakers and the LN_ds, which are among the predicted neuronal targets of the s-LN_vs (Im and Taghert 2010; Shafer et al. 2008) and are thought to play a critical role in the control of the fly's evening bout of daily activity (Grima et al. 2004; Stoleru et al. 2004).

To investigate the proposed connection between the s-LN_vs and the LN_d clock neurons, we drove P2X2 expression specifically in the l-LN_vs and s-LN_vs using *Pdf-LexA*, while driving GCaMP3.0 or Epac1-camps expression with *Clock(856)-GAL4*, which is expressed throughout most of clock neuron network (Fig. 4.7*A*; Gummadova et al. 2009). Note that although *Pdf-LexA* drives *LexAop- P2X2* in both the l-LN_vs and s-LN_vs, only the s-LN_vs send projections to the dorsal brain, whereas

the l-LN_vs project to both optic lobes (Fig. 4.7*A*; Helfrich-Förster et al. 2007). For brains dissected from *;Clock(856)-GAL4,UAS-GCaMP3.0/+;Pdf- LexA,LexAop-P2X2/+* flies, excitation of the l-LN_vs and s-LN_vs with 30-s perfusions of 1 mM ATP caused clear increases in GCaMP3.0 fluorescence in the LN_vs, but had no measurable effects on the LN_ds residing in the same optical sections, suggesting that LN_v excitation does not cause large acute Ca^{2+} increases or acute excitation in the LN_ds (Fig. 4.7*B*). In contrast, 30-s perfusions of 1 mM ATP across *;Clock(856)-GAL4,UAS-Epac1-camps/+;Pdf-LexA,LexAop-P2X2/+* brains resulted in significant increases in Epac1-camps inverse FRET within the LN_ds, consistent with cAMP increases in response to LN_v excitation (Fig. 4.7, *C* and *D*). Direct ATP/P2X2 excitation of the l-LN_vs and s-LN_vs caused significant increases in Epac1-camps inverse FRET (Fig. 4.7, *E* and *F*, and data not shown), indicating a strong coupling of neuronal excitation and cAMP production in these neurons. The large increase in LN_d inverse Epac1-camps FRET was preceded by a small and transient decrease in inverse FRET (Fig. 4.7*C*). However, this decrease was not caused by LN_v excitation, because we observed a similar initial decrease in mean inverse FRET in control brains lacking the *Pdf-LexA* element for driving *LexAop-P2X2* expression in the LN_vs (Fig. 4.7*C*).

The LN_d cAMP response to bath-applied ATP required P2X2 expression in the LN_vs, because brains carrying the *LexAop-P2X2* element but lacking the *Pdf-LexA* driver failed to show cAMP increases in either the LN_ds or LN_vs (Fig. 4.7, *C*–*F*; "—P2X2"). Furthermore, the LN_d cAMP response to LN_v excitation required functional PDF receptor, because ATP perfusion over brains from *$PdfR^{5304}$;Clock(856-GAL4,UAS- Epac1-camps/+;Pdf-LexA,LexAop-$P2X_2$/+* flies failed to produce significant changes in LN_d Epac1-camps inverse FRET levels (Fig. 4.7, *C* and *D*; "—PDFR"), despite clear excitation of LN_vs within the same optical sections (Fig. 4.7, *E* and *F*; "—PDFR").

Our results indicate that the excitation of the l-LN_vs and s-LN_vs results in acute cAMP increases in the LN_ds and that this response requires functional PDF receptor signaling (Fig. 4.7, *C* and *D*). Thus, our method of connectivity analysis was

sufficiently sensitive to experimentally confirm a predicted modulatory connection deep within the adult brain. Given the thorough vetting of GCaMP3.0 and Epac1-camps sensors in the fly CNS by previous studies (e.g., Shafer et al. 2008; Tian et al. 2009), the lack of GCaMP3.0 responses in the face of clear Epac1-camps responses in the LN_ds following LN_v excitation suggests that the LN_ds are not strongly excited by the LN_vs and that the LN_v-to-LN_d connection acts predominantly as a modulator of LN_d cAMP signaling. Thus, the connection between these neuronal classes could not have been detected with Ca^{2+} imaging alone, which argues for the use of diverse sensor types in the investigation of functional connectivity. The efficacy of this approach to circuit interrogation now makes possible a wider analysis of the patterns of clock network connections, and an investigation of how these connections might change over the course of the circadian cycle or in response to changing environmental conditions such as photoperiod and temperature. Furthermore, these experiments establish the feasibility of conducting such experiments in mutant backgrounds of choice.

4.5 DISCUSSION

Animal behavior is an emergent property of neural networks and is shaped by the pattern and nature of the connections between their constituent neurons. Connectivity is therefore an abiding problem in neuroscience, and understanding how it governs complex behavior is a fundamental goal of the field (Lichtman and Sanes 2008). Here we have introduced a method for addressing the physiologic connections between discrete neuronal classes in *Drosophila*. We have shown that the independent dual binary expression of the vertebrate purinergic P2X2 receptor and genetically encoded sensors makes possible the specific excitation of neuronal classes of interest while simultaneously imaging Ca^{2+} and cAMP dynamics within putative follower neurons. Our proof of principle experiments establish this "physiogenetic" approach as a technically facile method of investigating physiologic connections between electrophysiologically inaccessible neuronal classes of the *Drosophila* CNS.

Although the method we introduce here makes possible the detection of neural connections in regions of the brain where multielectrode electrophysiologic experiments are not possible, it is important to note its limitations relative to electrophysiologic techniques. For example, the use of bath-applied ATP to excite P2X2-expressing neurons does not offer the fine temporal control associated with the depolarization of neurons by brief current injections (Fig. 4.1). Likewise, genetically encoded sensors of neural signaling have not yet attained the sensitivity and temporal resolution of electrodes for detecting small changes in membrane voltage or modest excitatory/inhibitory responses. Thus, connections producing subthreshold excitatory input or only very weak excitation in follower neurons might be missed using the approach we have described. Furthermore, some inhibitory connections may not be detectable using existing genetically encoded sensors (e.g., Lelito and Shafer 2012). Thus, for any pair of neuronal classes, the absence of both cAMP and Ca^{2+} responses in a putative follower neuron is not in itself compelling evidence for a complete lack of connection. Despite these limitations, the work presented here establishes that our method of addressing functional connectivity is sufficiently sensitive to detect both excitatory and modulatory connections between electrophysiologically inaccessible neuronal classes within the adult fly brain, thereby allowing for the analysis of functional connectivity in regions of the brain where electrodes cannot be used. We therefore believe that this method will be immediately useful for the investigation of connectivity within a variety of electrophysiologically inaccessible networks in the fly brain.

The ultimate cellular resolution afforded by this approach is currently limited by the number of available highly specific LexA and Gal4 drivers for directed P2X2 expression. This is no less true for the widespread use of these same drivers for the experimental manipulation of neuronal function and behavior, a limitation that has not prevented the field from learning a great deal about the neuronal classes underlying a wide range of behaviors (Simpson and Stephen 2009). Nevertheless, the current supply of specific drivers allows for many hypothesized

connections between neuronal classes to be experimentally tested using the approach we have described, and the production of highly specific genetic drivers continues apace (e.g., Bohm et al. 2010; Luan and White 2007; Pfeiffer et al. 2008, 2010). Furthermore, in instances when sufficiently specific drivers prove unattainable, increased specificity of ATP/P2X2 excitation can be realized through localized puffing of ATP (Hu et al. 2010; Huang et al. 2010) or through the focal liberation of caged ATP using focused laser light (Z. Yao and O.T. Shafer, unpublished observations).

Although the methods described here allow for connections between discrete neuronal classes to be detected and characterized, they do not currently allow for a differentiation between monosynaptic (direct) and polysynaptic (indirect) connections. This limitation does not preclude the usefulness of the technique, which can nevertheless reveal the presence and physiologic nature of connections between defined neuronal classes, whether monosynaptic or polysynaptic. Furthermore, it may be possible in the future to adapt established pharmacologic methods for determining if a given downstream response to ATP/P2X2 excitation is monosynaptic or polysynaptic. For example, the use of bathing saline containing high concentrations of divalent cations (e.g., Kandel et al. 1967) or tetrodotoxin (e.g., Mizunami 1990) to block the synaptic release from or the firing of interposed neurons could be compatible with this technique if P2X2, a nonselective cation channel, can drive sufficiently high Ca^{2+} in the presynaptic terminals of P2X2-expressing neurons in the presence of these manipulations. We are currently investigating these possibilities in multiple neuronal types.

Although other methods to detect physiologic connectivity have recently been used in the fly brain (e.g., Hu et al. 2010; Ruta et al. 2010), we feel that the approach outlined here has the virtue of a relative technical simplicity, requiring only standard confocal or epifluorescent microscopy and a means of delivering controlled perfusions of ATP solutions. Thus, the LexAop-driven P2X2, GCaMP3.0, and Epac1-camps elements we describe here, in combination with the large number of available Gal4, UAS, and LexA elements, constitute a flexible and technically facile

toolkit for the interrogation of central neuronal networks in the fly. These tools can now be used to address functional connectivity within neuronal networks governing a wide range of behaviors in *Drosophila*. Furthermore, *Drosophila* photoreceptors and ligand-gated receptors have been successfully introduced into mammalian neurons (Morita et al. 2006; Zemelman et al. 2002), suggesting that an approach similar to the one described here using appropriate heterologous receptors could be used to investigate the physiologic connections between neuronal ensembles within other model systems.

4.6 FIGURES

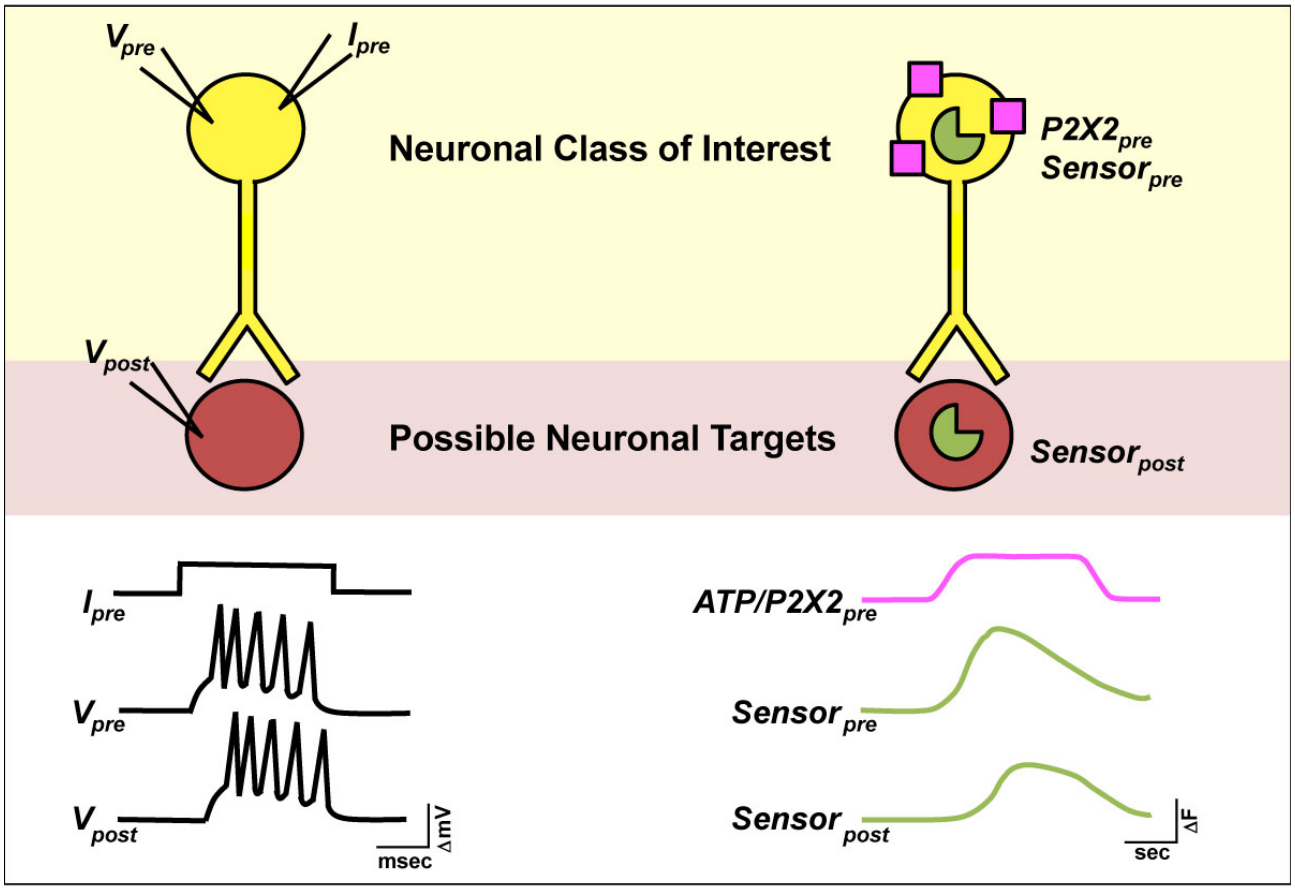

Figure 4.1. Schematic of dual binary, ATP/P2X2 excitation approach to network interrogation. *Left*: an electrophysiologic approach to connectivity in invertebrate nervous systems. The investigator stimulates a neuron of interest with depolarizing current while simultaneously recording membrane voltage in putative follower neurons (e.g., Kandel et al. 1967). *Right*: a physiogenetic approach to connectivity in the *Drosophila* nervous system. Depolarizing current is induced in neuronal classes of interest through ATP gating of transgenic P2X2 receptors (shown in purple), whereas Ca^{2+} or cAMP levels are simultaneously monitored in putative follower neurons using genetically encoded sensors (shown in green). Note the differing time scales between methods.

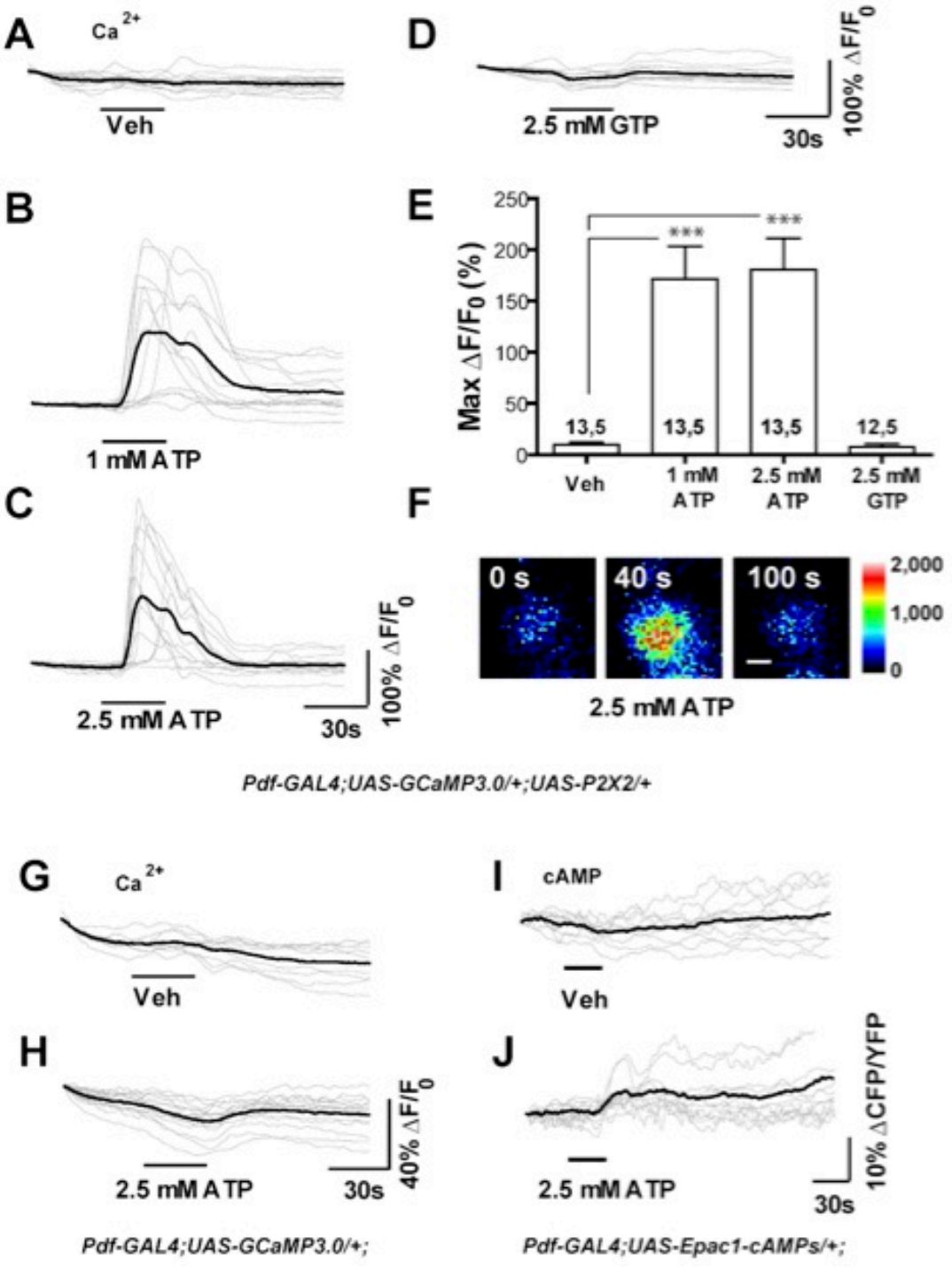

Figure 4.2. Bath application of ATP results in the excitation of P2X2-expressing deep brain neurons during live imaging experiments. *A–D*: individual (*gray*) and mean (*black*) traces of *Pdf(M)-Gal4;UAS-GCaMP3.0/+;UAS-P2X2/+* s-LN_v responses to 30-s perfusion of (*A*) vehicle (*N* = 13 neurons from 5 brains [13,5]), (*B*) 1 mM ATP (*N* = 13,5) (*C*) 2.5 mM ATP (*N* = 13,5), and (*D*) 2.5 mM GTP (*N* = 12,5). Test compounds were perfused after a 35-s baseline interval and

responses were recorded for a total of 150 s. *E*: histogram summarizing the mean maximum percentage increase in GCaMP3.0 fluorescence displayed by the neurons plotted in *A*–*D*. Perfusion of 1 and 2.5 mM ATP caused fluorescence increases that were significantly greater than vehicle control ($P < 0.0001$, by Mann—Whitney *U* test). The perfusion of 2.5 mM GTP did not cause significant fluorescence increases relative to the vehicle control ($P = 0.6302$ by Mann—Whitney *U* test). The two numbers displayed within or above each bar of the histogram indicate the number of neurons and the number of brains examined, respectively. *F*: representative intensity mapped micrographs of a single *Pdf(M)-Gal4;UAS-GCaMP3.0/+;UAS-P2X2/+* s-LN_v before (0 s), during (40 s), and after (100 s) its response to bath-applied 2.5 mM ATP. The scale bar in *F* = 2.5 μm. *G* and *H*: characterization of ATP's P2X2-independent effects on GCaMP3.0 fluorescence: unlike vehicle perfusion (*G*), 30-s 2.5 mM ATP perfusion (*H*) caused a slight but consistent decrease in GCaMP3.0 fluorescence. *I* and *J*: characterization of ATP's P2X2-independent effects on Epac1-camps inverse FRET levels. Unlike vehicle perfusion (*I*), 30-s 2.5 mM ATP perfusion caused a slight increase in inverse FRET (*J*), due to a decrease in YFP emission.

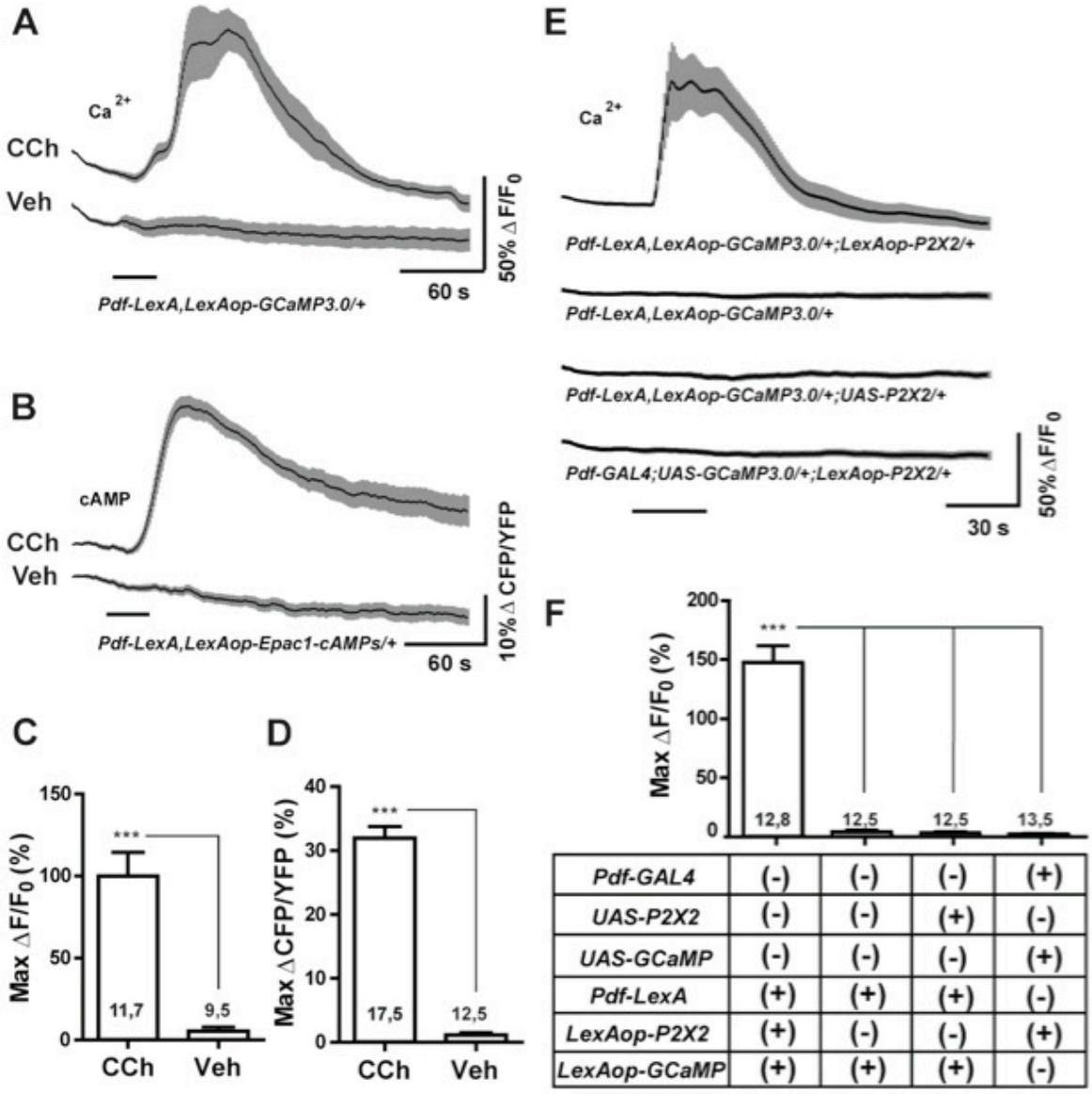

Figure 4.3. LexA operator-driven P2X2 and genetically encoded sensors for excitation and live imaging. *A*: mean GCaMP3.0 traces for *Pdf- LexA(7M),LexAop-GCaMP3.0(4A)/CyO* s- LN_vs to 30-s perfusions of 10^{-4} M carbachol (CCh) or vehicle (Veh). *B*: mean Epac1-camps inverse FRET traces for *Pdf-LexA(7M), LexAop-Epac1-camps(1A)/CyO* s-LN_vs to 30-s perfusions of 10^{-4} M CCh or Veh. *C* and *D*: maximum changes in GCaMP3.0 fluorescence (*C*) or Epac1-camps inverse FRET increases (*D*) of s-LN_v corresponding to the data in *A* and *B*, respectively. Numbers on the histograms indicate the number of neurons and brains sampled. Both LexAop-driven sensors displayed significant responses to CCh relative to Veh controls (P = 0.0004 for GCaMP3.0 fluorescence and $P < 0.0001$ for Epac1-camps inverse FRET by Mann—Whitney *U* test). *E*: mean GCaMP3.0 traces for the s-LN_vs of the genotypes

indicated below the plots to 30-s perfusions of 10^{-3} M ATP. *Pdf-LexA*—driven expression of *LexAop-P2X2* rendered s-LN_vs sensitive to bath-applied ATP. *UAS-P2X2* and *LexAop-P2X2* elements did not render neurons sensitive to ATP in the absence of their appropriate Gal4 or LexA drivers. *F*: summary of maximum Ca^{2+} responses of s-LN_v in *E*. *** indicates $P < 0.001$ by Kruskal—Wallis one- way ANOVA and a Dunn's multiple comparison test. Numbers on the histogram is in *C*, *D*, and *F* indicate the number of neurons and brains sampled. For *A*, *B*, and *E,* the time of perfusion is indicated by the bars under the plots and the *gray-shaded* regions surrounding the mean plots indicate SE, as do the error bars in *C*, *D*, and *F.*

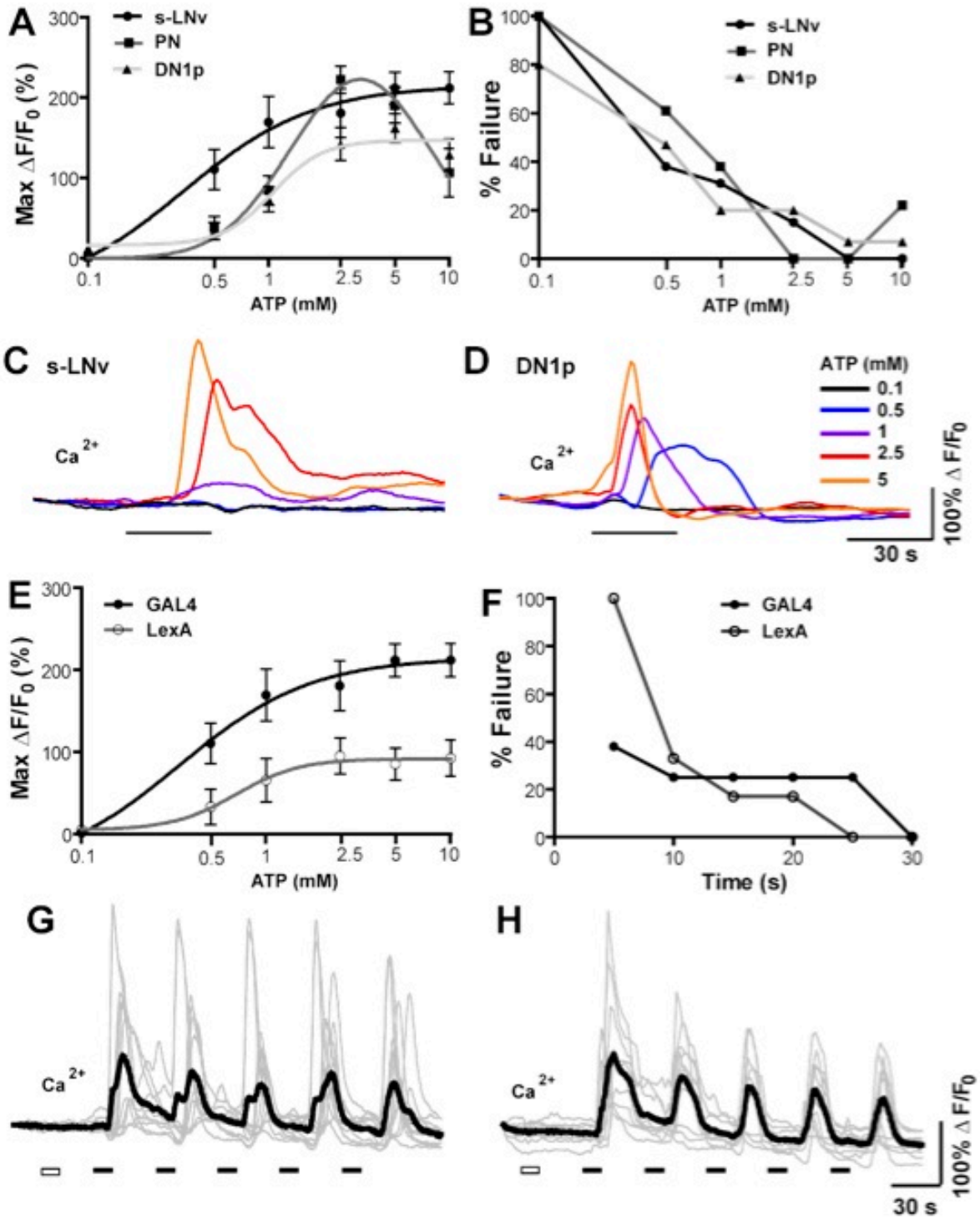

Figure 4.4. Bath-applied ATP reliably and repeatedly activates deeply situated P2X2-expressing neurons in the explanted adult brain. *A*: dose-response curves for the excitation of P2X2-expressing s-LN$_v$s (N = 13,5), DN1$_p$s (N = 15,5), and olfactory projection neurons (PN, N = 18,5)) by 30-s perfusions of ATP. The

genotypes used for each neuronal class where *Pdf- Gal4;UAS-GCaMP3.0/+;UAS-P2X2/+* for s-LN_vs, ;UAS-GCaMP3.0/+; *Clock(4.1M)-Gal4/UAS-P2X2* for $DN1_p$s, and *;Cha(7.4)-Gal4/UAS-GCaMP3.0; UAS-P2X2/+* for PNs. Values represent the mean maximum increase in GCaMP3.0 fluorescence ($\Delta F/ F_0$) detected during the 150 s following ATP perfusion. *B*: failure rate curves for 30-s ATP perfusions over a range of concentrations for s-LN_vs, $DN1_p$s, and PNs based on the data shown in *A*. A maximum GCaMP3.0 fluorescence increase of <25% was considered a failure to excite. *C* and *D*: GCaMP3.0 responses of a single s-LN_v (*C*) and $DN1_p$ (*D*) cell body to increasing ATP concentrations (0.1–5 mM), each delivered for 30 s. Single neurons displayed graded responses to increasing ATP doses. *E*: dose—response curves for s-LN_v excitation in response to 30-s ATP perfusions comparing s-LN_vs from *Pdf-Gal4;UAS-GCaMP3.0/+; UAS-P2X2/+* (*N* = 13,5) and ;*Pdf-LexA,LexAop-GCaMP3.0/LexAop-P2X2;* (*N* = 10,5) brains. *F*: failure rates of s-LN_v excitation by various durations of 2.5 mM ATP perfusions comparing s-LN_vs excited using the GAL4 (*N* = 8,5) and LexA (*N* = 10,5) systems. Genotypes were identical to those used in *E*. *G*: individual (*gray*) and mean (*black*) GCaMP3.0 traces for repeatedly activated s-LN_vs from *Pdf-Gal4; UAS-GCaMP3.0/+;UAS-P2X2* brains (N=11,5). *H*: individual (*gray*) and mean (*black*) GCaMP3.0 traces for repeatedly activated s-LN_vs from *Pdf-LexA,LexAop-GCaMP3.0/LexAopP2X2* brains (*N* = 10,5). For *G* and *H* the *white rectangles* indicate 30 s of vehicle perfusion and *black rectangles* indicate 30 s of 2.5 mM ATP perfusion, with 90-s intervals between ATP perfusions.

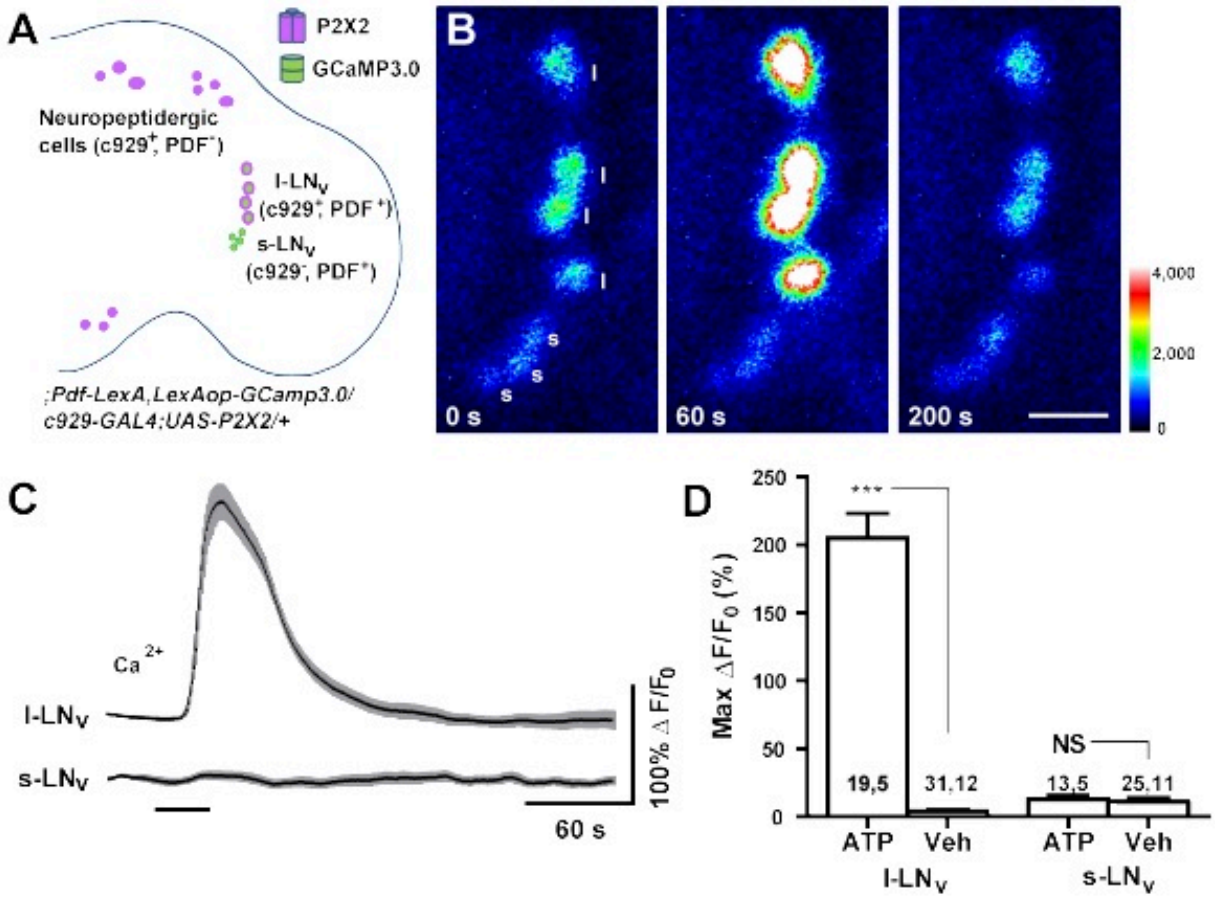

Figure 4.5. Independent expression of P2X2 and genetically encoded sensor in the fly brain by dual binary systems supports the excitation of specific neuronal subsets. *A*: schematic diagram showing the expression patterns of P2X2 (magenta) and GCaMP3.0 sensor (green) in the experimental fly brain, whose full genotype is shown. *B*: intensity-mapped stills of l-LN$_v$ and s-LN$_v$ GCaMP3.0 fluorescence before (T = 0 s), during (T = 60 s), and after (T = 200 s) perfusion of 1 mM ATP. The l-LN$_v$s but not the s-LN$_v$s responded to ATP. The colors of the legend indicate pixel intensity values. Each "l" indicates a l-LN$_v$ and each "s" indicates a s-LN$_v$. *C*: mean GCaMP3.0 fluorescence traces of l-LN$_v$s and s-LN$_v$s to 30-s perfusions of 1 mM ATP (indicated by the bar under the plots). Sample sizes for these plots are shown in *D*. The *gray- shaded* regions surrounding the mean plots indicate SE. *D*: summary of maximum GCaMP3.0 fluorescence increases displayed by the l-LN$_v$ and s-LN$_v$ to bath-applied ATP and vehicle (Veh). *** indicates a significant difference between ATP and Veh ($P < 0.001$) and NS indicates nonsignificance by Mann—Whitney *U* test. The two numbers displayed within or above each bar of the histogram indicate the number of neurons and the number of brains examined, respectively.

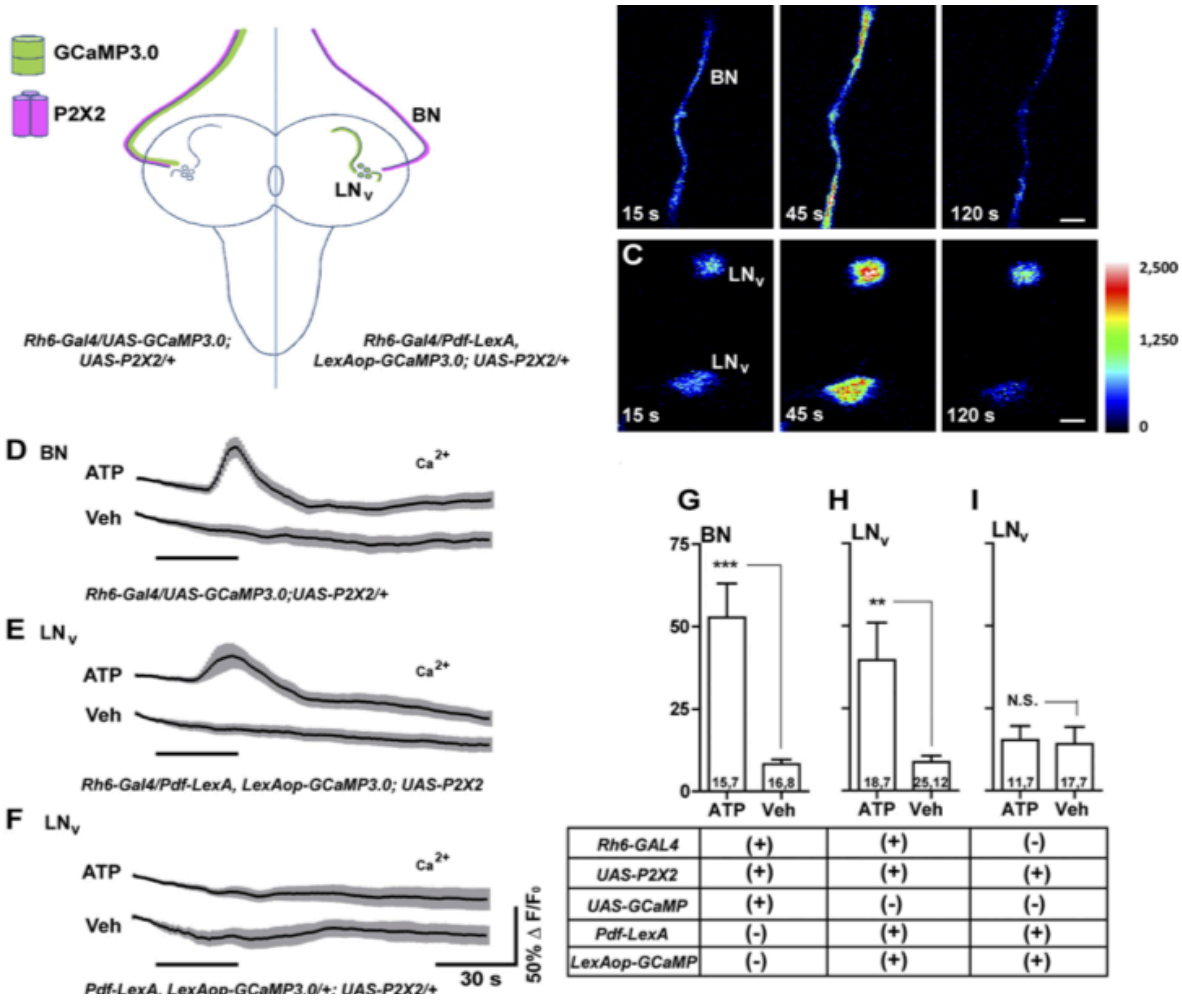

Figure 4.6. Gal4-based excitation and LexA-based live imaging for an established excitatory connection in the larval brain. *A*: schematic diagram of Bolwig's Nerve (BN) and larval LN_v anatomy. The expression of GCaMP3.0 (green) and P2X2 (magenta) are indicated for two experimental genotypes. *B*: ATP/P2X2 excitation of BN. Single-plane intensity mapped confocal images of GCaMP3.0 fluorescence in the BN of an *Rh6-Gal4/UAS-GCaMP3.0;UAS-P2X2/+* larva before (15 s), during (45 s), and after (120 s) the start of 30-s 5 mM ATP perfusion. *C*: single-plane intensity mapped confocal images of GCaMP3.0 fluorescence in two larval LN_vs of a *Pdf-LexA,LexAop-GCaMP3.0/Rh6-Gal4;UAS-P2X2/+* larva before (15 s), during (45 s), and after (120 s) their response to BN excitation. The look-up table represents pixel intensity values for both *B* and *C*. *D*: mean GCaMP3.0 fluorescence traces for BNs of ;*Rh6-gal4/UAS-GCaMP3.0;UAS-P2X2/+* larval brains treated with 30-s perfusions (black bar) of 5 mM ATP or vehicle (Veh). *E*: mean GCaMP3.0 fluorescence traces recorded from the LN_vs of *Pdf-LexA,LexAop-GCaMP3.0/Rh6-Gal4;UAS-P2X2/+* larval brains in response to 30-s perfusions of 5 mM ATP or Veh.

F: mean GCaMP3.0 fluorescence traces recorded from the LN_vs of *Pdf-LexA,LexAop-GCaMP3.0/+;UAS-P2X2/+* larval brains in response to 30-s perfusions of 5 mM ATP or Veh. For *D–F,* error bars indicate SE. *G–I*: summary histograms of the maximum GCaMP3.0 fluorescence increases displayed by the BNs (*G*) and s-LN_vs (*H* and *I*) of the genotypes shown in *D–F*. The two numbers displayed within each bar of the histogram indicate the number of neurons and the number of brains examined, respectively. Asterisks indicate a significant difference in maximum fluorescence increase between ATP and Veh treatments and "N.S." indicates no significant difference by Mann—Whitney *U* test (***$P < 0.001$ and **$P < 0.01$). The error bars in *G* represent the SE.

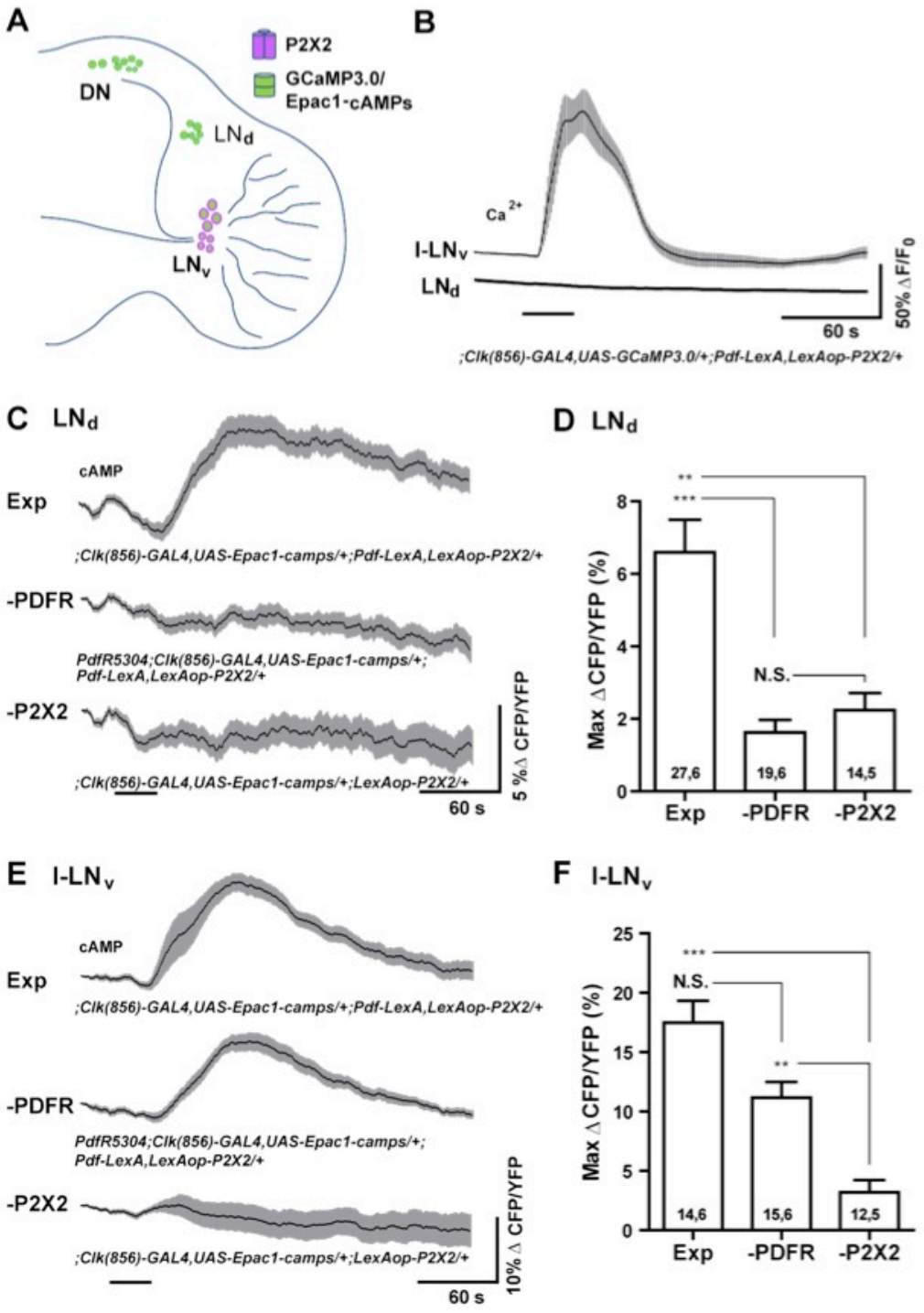

Figure 4.7. LexA-based excitation and GAL4-based live imaging to test a predicted peptidergic connection deep within the adult brain. *A*: schematic diagram showing the expression of P2X2 and genetically encoded sensors in the experimental brain for testing the predicted physiologic connection between the LN_v and the LN_d clock neurons. *B*: mean GCaMP3.0 fluorescence traces of the l-LN_vs and LN_ds during their responses to a 30-s bath application of 1 mM ATP (indicated

by the bar under the plots). l-LN_v and LN_d plots were recorded simultaneously from the same optical sections of a *;Clock(856)-GAL4,UAS-GCaMP3.0/+;Pdf-LexA,LexAop-P2X2/+* brain. Shaded regions surrounding the mean plots indicate SE. Excitation of the LN_vs had no measurable effects on GCaMP3.0 fluorescence in the LN_ds. For l-LN_vs, *N* = 14 neurons from 6 brains (14,6). For s-LN_vs, *N* = 17,6. *C*: mean Epac1-camps inverse FRET traces of the LN_ds during excitation of the LN_vs in *;Clock(856)-GAL4,UAS-Epac1-camps/+;Pdf-LexA,LexAop-P2X2/+* brains ("Exp"). LN_v excitation resulted in increases in cAMP in the LN_ds. This response was absent in *$PdfR^{5304}$;Clock(856)-GAL4,UAS-Epac1-camps/+;Pdf-LexA,LexAop-P2X2/+* brains ("—PDFR"), which lacked PDF receptor function, and in *;Clock(856)- GAL4,UAS-Epac1-camps/+; LexAop-P2X2/+* brains, which lacked a LexA driver for the P2X2 element ("—P2X2"). *D*: summary histogram of the mean maximum increases in Epac1-camps inverse FRET for the LN_d data shown in *C*. *E*: mean Epac1-camps inverse FRET traces for l-LN_vs imaged simultaneously with the LN_ds shown in *C*. Plots displayed as for *C*. ATP/P2X2 excitation of the LN_vs resulted in cAMP increases in both wild type ("Exp") and *$PdfR^{5304}$* ("—PDF") backgrounds. The l-LN_vs showed no cAMP increases in response to ATP in the absence of a LexA driver for the P2X2 element ("—P2X2"). *F*: summary histogram of maximum increases in Epac1-camps inverse FRET for the l-LN_v data shown in *E*. For *D* and *F*, the two numbers within or above each bar of the histogram indicate the number of neurons and the number of brains examined respectively. ***$P < 0.001$; **$P < 0.01$; NS, nonsignificance by Kruskal—Wallis one-way ANOVA and Dunn's multiple comparisons test. The mean plots in *C* and *E* were corrected for spontaneous FRET drift by subtracting the mean inverse FRET traces of l-LN_v and LN_d neurons from vehicle treated *;Clock(856)-GAL4,UAS-Epac1-camps/+;Pdf-LexA,LexAop-P2X2/+* ("Exp") brains (see methods for details).

4.7 REFERENCES

Bohm RA, Welch WP, Goodnight LK, Cox LW, Henry LG, Gunter TC, Bao H, Zhang B. A genetic mosaic approach for neural circuit mapping in *Drosophila*. *Proc Natl Acad Sci USA* 107: 16378–16383, 2010.

Börner S, Schwede F, Schlipp A, Berisha F, Calebiro D, Lohse MJ, Nikolaev VO. FRET measurements of intracellular cAMP concentrations and cAMP analog permeability in intact cells. *Nat Protocols* 6: 427–438, 2011.

Brand A, Perrimon N. Targeted gene expression as a means of altering cell fates and generating dominant phenotypes. *Development* 118: 401–415, 1993.

Cao G, Nitabach MN. Circadian control of membrane excitability in *Drosophila melanogaster* lateral ventral clock neurons. *J Neurosci* 28: 6493– 6501, 2008.

Crocker A, Sehgal A. Genetic analysis of sleep. *Genes Dev* 24: 1220–1235, 2010.

Dickson BJ. Wired for sex: the neurobiology of Drosophila mating decisions. *Science* 322: 904–909, 2008.

Garczynski SF, Crim JW, Brown MR. Characterization and expression of the short neuropeptide F receptor in the African malaria mosquito, *Anopheles gambiae*. *Peptides* 28: 109–118, 2007.

Grima B, Chelot E, Xia R, Rouyer F. Morning and evening peaks of activity rely on different clock neurons of the *Drosophila* brain. *Nature* 431: 869–873, 2004.

Gummadova JO, Coutts GA, Glossop NRJ. Analysis of the *Drosophila* clock promoter reveals heterogeneity in expression between subgroups of central oscillator cells and identifies a novel enhancer region. *J Biol Rhythms* 24: 353–367, 2009.

Guo ZV, Hart AC, Ramanathan S. Optical interrogation of neural circuits in *Caenorhabditis elegans*. *Nat Methods* 6: 891–896, 2009.

Helfrich-Förster C. The period clock gene is expressed in central nervous system neurons which also produce a neuropeptide that reveals the projections of circadian pacemaker cells within the brain of *Drosophila melanogaster*. *Proc Natl Acad Sci USA* 92: 612–616, 1995.

Helfrich-Förster C, Edwards T, Yasuyama K, Wisotzki B, Schneuwly S, Stanewsky R, Meinertzhagen IA, Hofbauer A. The extraretinal eyelet of *Drosophila*: development, ultrastructure, and putative circadian function. *J Neurosci* 22: 9255–9266, 2002.

Helfrich-Förster C, Shafer OT, Wulbeck C, Grieshaber E, Rieger D, Taghert P. Development and morphology of the clock-gene-expressing lateral neurons of *Drosophila melanogaster*. *J Comp Neurol* 500: 47–70, 2007.

Hewes RS, Schaefer AM, Taghert PH. The cryptocephal gene (ATF4) encodes multiple basic-leucine zipper proteins controlling molting and metamorphosis in *Drosophila*. *Genetics* 155: 1711–1723, 2000.

Hu A, Zhang W, Wang Z. Functional feedback from mushroom bodies to antennal lobes in the *Drosophila* olfactory pathway. *Proc Natl Acad Sci USA* 107: 10262–10267, 2010.

Huang J, Zhang W, Qiao W, Hu A, Wang Z. Functional connectivity and selective odor responses of excitatory local interneurons in *Drosophila* antennal lobe. *Neuron* 67: 1021–1033, 2010.

Hyun S, Lee Y, Hong ST, Bang S, Paik D, Kang J, Shin J, Lee J, Jeon K, Hwang S, Bae E, Kim J. Drosophila GPCR Han is a receptor for the circadian clock neuropeptide PDF. *Neuron* 48: 267–278, 2005.

Im SH, Taghert PH. PDF receptor expression reveals direct interactions between circadian oscillators in *Drosophila*. *J Comp Neurol* 518: 1925– 1945, 2010.

Johard HAD, Yoishii T, Dircksen H, Cusumano P, Rouyer F, Helfrich- Förster C, Nässel DR. Peptidergic clock neurons in *Drosophila*: ion transport peptide and short neuropeptide F in subsets of dorsal and ventral lateral neurons. *J Comp Neurol* 516: 59–73, 2009.

Kandel ER. *Cellular Basis of Behavior: An Introduction to Behavioral Neurobiology*. San Francisco: Freeman, 1976, p. 727.

Kandel ER, Frazier WT, Waziri R, Coggeshall RE. Direct and common connections among identified neurons in *Aplysia*. *J Neurophysiol* 30: 1352– 1376, 1967.

Kaneko M, Hall JC. Neuroanatomy of cells expressing clock genes in *Drosophila*: transgenic manipulation of the period and timeless genes to mark the perikarya of circadian pacemaker neurons and their projections. *J Comp Neurol* 422: 66–94, 2000.

Keene AC, Mazzoni EO, Zhen J, Younger MA, Yamaguchi S, Blau J, Desplan C, Sprecher SG. Distinct visual pathways mediate *Drosophila* larval light avoidance and circadian clock entrainment. *J Neurosci* 31: 6527–6534, 2011.

Kim SK, Rulifson EJ. Conserved mechanisms of glucose sensing and regulation by Drosophila corpora cardiaca cells. *Nature* 431: 316–320, 2004.

Lai SL, Lee T. Genetic mosaic with dual binary transcriptional systems in *Drosophila*. *Nat Neurosci* 9: 703–709, 2006.

Lear BC, Merrill CE, Lin JM, Schroeder A, Zhang L, Allada R. A G protein-coupled receptor, groom-of-PDF, is required for PDF neuron action in circadian behavior. *Neuron* 48: 221–227, 2005.

Lelito KR, Shafer OT 3rd. Reciprocal cholinergic and GABAergic modulation of the small ventrolateral pacemaker neurons of *Drosophila*'s circadian clock neuron network. *J Neurophysiol* 107: 2096–2108, 2012.

Lichtman JW, Sanes JR. Ome sweet ome: what can the genome tell us about the connectome? *Curr Opin Neurobiol* 18: 346–353, 2008.

Lima SQ, Miesenböck G. Remote control of behavior through genetically targeted photostimulation of neurons. *Cell* 121: 141–152, 2005.

Lin Y, Stormo GD, Taghert PH. The neuropeptide pigment-dispersing factor coordinates pacemaker interactions in the *Drosophila* circadian system. *J Neurosci* 24: 7951–7957, 2004.

Littleton JT, Ganetzky B. Ion channels and synaptic organization: analysis of the Drosophila genome. *Neuron* 26: 35–43, 2000.

Luan H, White BH. Combinatorial methods for refined neuronal gene targeting. *Curr Opin Neurobiol* 17: 572–580, 2007.

Malpel S, Klarsfeld A, Rouyer F. Larval optic nerve and adult extra-retinal photoreceptors sequentially associate with clock neurons during *Drosophila* brain development. *Development* 129: 1443–1453, 2002.

Marella S, Fischler W, Kong P, Asgarian S, Rueckert E, Scott K. Imaging taste responses in the fly brain reveals a functional map of taste category and behavior. *Neuron* 49: 285–295, 2006.

McGuire SE, Deshazer M, Davis RL. Thirty years of olfactory learning and memory research in *Drosophila melanogaster*. *Prog Neurobiol* 76: 328–347, 2005.

Melcher C, Bader R, Pankratz MJ. Amino acids, taste circuits, and feeding behavior in *Drosophila*: towards understanding the psychology of feeding in flies and man. *J Endocrinol* 192: 467–472, 2007.

Mertens I, Meeusen T, Huybrechts R, De Loof A, Schoofs L. Characterization of the short neuropeptide F receptor from *Drosophila melanogaster*. *Biochem Biophys Res Commun* 297: 1140–1148, 2002.

Mertens I, Vandingenen A, Johnson EC, Shafer OT, Li W, Trigg JS, De Loof A, Schoofs L, Taghert PH. PDF receptor signaling in *Drosophila* contributes to both circadian and geotactic behaviors. *Neuron* 48: 213–219, 2005.

Mizunami M. Nonlinear signal transmission between second- and third-order neurons of cockroach ocelli. *J Gen Physiol* 95: 297–317, 1990.

Morita M, Susuki J, Amino H, Yoshiki F, Moizumi S, Kudo Y. Use of the exogenous *Drosophila* octopamine receptor gene to study Gq-coupled receptor-mediated responses in mammalian neurons. *Neuroscience* 137: 545–553, 2006.

Nikolaev VO, Bünemann M, Hein L, Hannawacker A, Lohse MJ. Novel single chain cAMP sensors for receptor-induced signal propagation. *J Biol Chem* 279: 37215–37218, 2004.

Nitabach MN, Taghert PH. Organization of the *Drosophila* circadian control circuit. *Curr Biol* 18: R84—37215–R93, 2008.

Parisky KM, Agosto J, Pulver SR, Shang Y, Kuklin E, Hodge JJL, Kang K, Liu X, Garrity PA, Rosbash M, Griffith LC. PDF cells are a GABA-responsive wake-promoting component of the Drosophila sleep circuit. *Neuron* 60: 672–682, 2008.

Peabody NC, Pohl JB, Diao F, Vreede AP, Sandstrom DJ, Wang H, Zelensky PK, White BH. Characterization of the decision network for wing expansion in *Drosophila* using targeted expression of the TRPM8 channel. *J Neurosci* 29: 3343–3353, 2009.

Pfeiffer BD, Jenett A, Hammonds AS, Ngo TTB, Misra S, Murphy C, Scully A, Carlson JW, Wan KH, Laverty TR, Mungall C, Svirskas R, Kadonaga JT, Doe CQ, Eisen MB, Celniker SE, Rubin GM. Tools for neuroanatomy and neurogenetics in *Drosophila*. *Proc Natl Acad Sci USA* 105: 9715–9720, 2008.

Pfeiffer BD, Ngo TTB, Hibbard KL, Murphy C, Jenett A, Truman JW, Rubin GM. Refinement of tools for targeted gene expression in *Drosophila*. *Genetics* 186: 735–755, 2010.

Pichaud F, Desplan C. A new visualization approach for identifying mutations that affect differentiation and organization of the Drosophila ommatidia. *Development* 128: 815–826, 2001.

Potter CJ, Tasic B, Russler EV, Liang L, Luo L. The Q system: a repressible binary system for transgene expression, lineage tracing, and mosaic analysis. *Cell* 141: 536–548, 2010.

Pulver SR, Pashkovski SL, Hornstein NJ, Garrity PA, Griffith LC.

Temporal dynamics of neuronal activation by channelrhodopsin-2 and TRPA1 determine behavioral output in Drosophila larvae. *J Neurophysiol* 101: 3075–3088, 2009.

Reale V, Chatwin HM, Evans PD. The activation of G-protein gated inwardly rectifying K channels by a cloned *Drosophila melanogaster* neuropeptide F-like receptor. *Eur J Neurosci* 19: 570–576, 2004.

Renn SCP, Park JH, Rosbash M, Hall JC, Taghert PH. A PDF neuropeptide gene mutation and ablation of PDF neurons each cause severe abnormalities of behavioral circadian rhythms in *Drosophila*. *Cell* 99: 791–802, 1999.

Ruta V, Datta SR, Vasconcelos ML, Freeland J, Looger LL, Axel R. A dimorphic pheromone circuit in *Drosophila* from sensory input to descending output. *Nature* 468: 686–690, 2010.

Salvaterra PM, Kitamoto T. *Drosophila* cholinergic neurons and processes visualized with Gal4/UAS-GFP. *Gene Expr Patterns* 1: 73–82, 2001.

Schroll C, Riemensperger T, Bucher D, Ehmer J, Vˆller T, Erbguth K, Gerber B, Hendel T, Nagel G, Buchner E, Fiala A. Light-induced activation of distinct modulatory neurons triggers appetitive or aversive learning in *Drosophila* larvae. *Curr Biol* 16: 1741–1747, 2006.

Shafer OT, Kim DJ, Dunbar-Yaffe R, Nikolaev VO, Lohse MJ, Taghert PH. Widespread receptivity to neuropeptide PDF throughout the neuronal circadian clock network of *Drosophila* revealed by real-time cyclic AMP imaging. *Neuron* 58: 223–237, 2008.

Shafer OT, Taghert PH. RNA-interference knockdown of *Drosophila* pigment dispersing factor in neuronal subsets: the anatomical basis of a neuropeptide's circadian functions. *PLoS ONE* 4: e8298, 2009.

Shang Y, Griffith L, Rosbash M. Light-arousal and circadian photoreception circuits intersect at the large PDF cells of the *Drosophila* brain. *Proc Natl Acad Sci USA* 105: 19587–19594, 2008.

Sheeba V, Fogle KJ, Kaneko M, Rashid S, Chou YT, Sharma VK, Holmes TC. Large ventral lateral neurons modulate arousal and sleep in *Drosophila*. *Curr Biol* 18: 1537–1545, 2008.

Simpson JH, Stephen FG. Mapping and manipulating neural circuits in the fly brain. In: *Advances in Genetics.* Waltham, MA: Elsevier/Academic Press, 2009, p. 79–143.

Stoleru D, Peng Y, Agosto J, Rosbash M. Coupled oscillators control

morning and evening locomotor behaviour of *Drosophila*. *Nature* 431: 862–868, 2004.

Tian L, Hires SA, Mao T, Huber D, Chiappe ME, Chalasani SH, Petreanu L, Akerboom J, McKinney SA, Schreiter ER, Bargmann CI, Jayaraman V, Svoboda K, Looger LL. Imaging neural activity in worms, flies and mice with improved GCaMP calcium indicators. *Nat Methods* 6: 875–881, 2009.

Venken KJT, Simpson JH, Bellen HJ. Genetic manipulation of genes and cells in the nervous system of the fruit fly. *Neuron* 72: 202–230, 2011.

Villella A, Hall JC, Jeffrey CH. Neurogenetics of courtship and mating in *Drosophila*. In: *Advances in Genetics.* Waltham, MA: Elsevier/Academic Press, 2008, p. 67–184.

Wegener C, Hamasaka Y, Nässel DR. Acetylcholine increases intracellular Ca2 via nicotinic receptors in cultured PDF-containing clock neurons of *Drosophila*. *J Neurophysiol* 91: 912–923, 2004. **Weiner J.** *Time, Love, Memory*. New York: Vintage Books, 1999.

Willemse M, Janssen E, Lange FD, Wieringa B, Fransen J. ATP and FRET: a cautionary note. *Nat Biotech* 25: 170–172, 2007. **Willows AOD, Hoyle G.** Neuronal network triggering a fixed action pattern. *Science* 166: 1549–1551, 1969.

Yasuyama K, Salvaterra PM. Localization of choline acetyltransferase-expressing neurons in *Drosophila* nervous system. *Microsc Res Tech* 45: 65–79, 1999.

Yizhar O, Fenno LE, Davidson TJ, Mogri M, Deisseroth K. Optogenetics in neural systems. *Neuron* 71: 9–34, 2011.

Yuan Q, Xiang Y, Yan Z, Han C, Jan LY, Jan YN. Light-induced structural and functional plasticity in *Drosophila* larval visual system. *Science* 333: 1458–1462, 2011.

Zemelman BV, Lee GA, Ng M, Miesenböck G. Selective photostimulation of genetically charged neurons. *Neuron* 33: 15–22, 2002.

Zhang L, Chung BY, Lear BC, Kilman VL, Liu Y, Mahesh G, Meissner RA, Hardin PE, Allada R. DN1p circadian neurons coordinate acute light and PDF inputs to produce robust daily behavior in *Drosophila*. *Curr Biol* 20: 591–599, 2010a.

Zhang Y, Liu Y, Bilodeau-Wentworth D, Hardin PE, Emery P. Light and temperature control the contribution of specific DN1 neurons to *Drosophila*

circadian behavior. *Curr Biol* 20: 600–605, 2010b.

Zhao Y, Araki S, Wu J, Teramoto T, Chang YF, Nakano M, Abdelfattah AS, Fujiwara M, Ishihara T, Nagai T, Campbell RE. An expanded palette of genetically encoded Ca2 indicators. *Science* 333: 1888–1891, 2011.

Zimmermann G, Wang Lp Vaughan AG, Manoli DS, Zhang F, Deisseroth K, Baker BS, Scott MP. Manipulation of an innate escape response in *Drosophila*: photoexcitation of acj6 neurons induces the escape response. *PLoS ONE* 4: e5100, 2009.

CHAPTER 5
THE HB-EYELET IS A CIRCADIAN PHOTORECEPTOR THAT EXCITES THE SMALL AND NOT THE LARGE VENTROLATERAL NEURONS

5.1 ABSTRACT

The Fruit Fly, *Drosophila Melanogaster*, possesses multiple photoreceptive neurons that collectively can mediate entrainment and phase-shifts to circadian locomotor rhythms; however, it is unclear which specific subsets communicate to the clock network and the mechanism by which communication elicits changes in molecular timekeeping. Here, we examine the functional connectivity between Rhodopsin-6 (Rh6) expressing photoreceptors and the circadian clock neurons. The two types of Rh6-cells are 1) the histaminergic retinal photoreceptors that terminate in the distal medulla of the optic lobe and 2) the cholinergic and histaminergic Hofbauer-Buchner extra retinal eyelet (HB-eyelet) that terminates in the accessory medulla (aMe). Anatomically, the most likely candidates of the clock neuron network for reception of this light input signaling are the large and small ventrolateral clock neurons (l-LN_v and s-LN_v), where the l-LN_v project to the distal medulla and aMe, and the s-LN_v project in the aMe and the dorsal brain. We found no responsivity of either of these neuronal subsets to application of histamine, or the ability of histamine to block excitatory stimulation. However, excitation of the $Rh6^+$-cells did result in increases in Ca^{2+} and cAMP from the s-LN_v, similar to excitatory responses we previously observed when these neurons were exposed to cholinergic agonists. Acute excitation of $Rh6^+$-cells in late evening results in a phase-delaying trend in circadian locomotor rhythms that mimics time dependent stimulation the LN_v directly or exposing flies to light. Although we did not find that $Rh6^+$-cell excitation was sufficient to measurably shift cycling of the molecular clock

protein, PERIOD, Rh6^{+} photoreceptor input may target other components of the clock that were not examined in this study. Together, our results suggest that the cholinergic terminals of the HB-eyelet elicit Ca^{2+} and cAMP signaling in the dorsally projecting s-LN_v clock neurons. These important signaling events may initiate changes in the s-LN_v molecular clocks that are required for phase shifting overt behavioral rhythms and synchronizing circadian outputs with environmental light cycles.

5.2 INTRODUCTION

The clock neuron network integrates environmental input in order to synchronize endogenous circadian rhythms with the 24-hour fluctuations of the earth. In *Drosophila*, the clock neuron network consists of 150 neurons where each expresses a conserved molecular clock (Helfrich-Förster, 2003; Shafer et al., 2006b). Of these neurons, the 16 Pigment Dispersing Factor positive (PDF^{+}) ventrolateral clock neurons (LN_v) are uniquely associated neuronal sources of light input (reviewed in Helfrich-Förster, 2002). Cryptochrome (CRY), a molecular light sensor, is also expressed in the LN_v (Yoshii et al., 2010), but circadian behavioral rhythms of flies mutant for CRY can entrain to 24-hour light cycles (Helfrich-Förster et al., 2001). Therefore, external, non-CRY mediated photoreceptor signaling can entrain molecular clocks and circadian rhythms to daily light cycles. The anatomy of rhodopsin six (Rh6) expressing photoreceptors suggests their potential communication of light information to one or both of types of PDF^{+} LNv: the small (s-LN_v) and large LN_v (l-LN_v). In this study, we examine whether a functional connection exists between the Rh6-expressing photoreceptors and the LN_v clock neurons.

Here we investigate the role of Rh6-expressing photoreceptor cells in communicating to light information to the clock network by exploiting a specific Gal4 driver for these neurons (Pichaud and Desplan, 2001). The Rh6-photoreceptors consist of two cell types: 1) R8-retinal photoreceptors and 2) the extra retinal Hofbauer-Buchner (HB) eyelet. The Rh6^{+} retinal photoreceptors terminate in the distal medulla of the optic lobe (Huber et al., 1997; Chou et al., 1999). Retinal

photoreceptors release histamine in response to light excitation and the response measured electrophysiologically in post-synaptic neurons is inhibitory (Hardie, 1987, 1989b). These photoreceptors are likely candidates for modulation of the l-LN_v, which project to the distal medulla, and are immunoreactive to antibodies raised against histamine receptor expression (HisCl2) (Hong et al., 2006). Retinal photoreceptors have been implicated in imparting circadian entrainment sensitivity, but a specific role of the R8-cells in entrainment is not established (Rieger et al., 2003).

The Rh6-expressing HB-eyelet consists of 4 of neurons with cell bodies residing beneath the retina, and projections terminating near the LN_v clock neurons in the accessory medulla (aMe) (Helfrich-Förster et al., 2002). A series of experiments testing entrainment ability of multiple visual system mutants implicates the HB-eyelet in imparting spectral sensitivity at 480 nm light (blue/green) and enhancing entrainment sensitivity in extreme entrainment conditions (Helfrich-Förster et al., 2002; Veleri et al., 2007). The HB- eyelet originates from the larval photoreceptive organ, Bolwig's nerve and is immunoreactive to antibodies raised against choline acetyl transferase (ChAT) (Yasuyama et al., 1995). Our previous work showed that excitation of Bolwig's nerve elicited cholinergic-like increases in Ca^{2+} in the LN_v (Yao et al., 2012). In the adult, the eyelet maintains ChAT staining but also becomes immunoreactive to antibodies raised against histamine (Pollack and Hofbauer, 1991; Yasuyama and Meinertzhagen, 1999). Whether the eyelet employs one or both neurotransmitters and whether either neurotransmitter is used to relay light information to the clock neurons in the aMe, has not been established.

Here, we show that excitation of the Rh6-expressing photoreceptors leads to a specific excitatory response in the s-LN_v. We observe no inhibitory responses in the LN_v to histamine application and we do not observe inhibitory effects after $Rh6^+$-cell excitation. Our data suggests that of these Rh6-expressing cells, the cholinergic cells of the HB-eyelet relay light information to the clock through excitation of the s-LN_v. Further, excitation of $Rh6^+$-cells during a time of day when light has a delaying effect to circadian behavioral rhythms, also mediates a similar effect. Although we

found a delaying trend in behavioral rhythms by activating the Rh6 cells at a delay zone, we did not observe delaying effects to the cycling of a core molecular clock protein, PERIOD. This suggests an alternative molecular target of $Rh6^{+}$-cell input. Collectively, our results suggest that of the $Rh6^{+}$-cells, only HB-eyelet transmits light information specifically to the s-LN_v, and not the l-LN_v, via cholinergic increases in Ca^{2+} and cAMP signaling to align circadian rhythms with environmental light cycles.

5.3 METHODS

Fly stocks and rearing

Flies were reared on cornmeal-yeast-sucrose diet under a 12:12 light:dark cycle. For live-imaging, flies were reared at 25˚C or 28˚C. For TRP experiments, flies were reared at 22°C to prevent the activation of TRP during development. All Gal4 and UAS lines used in this study have previously been described: *Pdf(M)-Gal4;;* (Renn et al., 1999), *;UAS-GCaMP3.0;* (Tian et al., 2009), *;;UAS-P2X2* (Lima and Miesenböck, 2005), *;Rh6-Gal4;* (Pichaud and Desplan, 2001), ;;Rh6-gal4 (Ratnakumar and Desplan, 2003), *;UAS-Epac1-camps(50A);* (Shafer & Taghert 2009), and *;Cha(7.4)-Gal4/CyO*; (Salvaterra and Kitamoto, 2001), *;Pdf-LexA;* (Shang et al., 2008), *Lex- Aop-GCaMP3.0*, and *LexAop-Epac1-camps* (Yao et al., 2012),;*LexAop-GFP-11;UAS-GFP1-10* (Gordon and Scott, 2009), ;UAS-GFP^{NLS}; (Shiga et al. 1996)(Shiga et al., 1996), ;UAS-TRPA1; (Hamada et al. 2008). Stable fly strains carrying combinations of these elements were created using standard *Drosophila* genetics techniques.

Live-imaging

Live imaging was performed according to Lelito & Shafer (2012), and Yao et al. (2012). Flies were anesthetized on $C0_2$ and dissected in HL3 saline (Stewart et al. 1994). Explanted brains were mounted to the base of a 35-mm FALCON culture dish (Becton Dickenson Labware, Franklin Lakes, NJ) within HL3 saline in a Petri Dish Insert (PDI, Bioscience tools). After dissection and mounting, the brains were allowed to settle for 5-10 minutes before imaging to reduce movement and detection of signal changes associated with dissection. Continuous perfusion flow of

HL3 saline was established over the brain while the ROIs were selected. Cells were visualized under an epifluorescent lamp using basal fluorescence from the GCaMP or Epac-1cAMPS sensors. Live imaging was performed using an Olympus FV 1000 laser-scanning microscope (Olympus, Center Valley, PA) under a 60X 1.1N/A W, FUMFL N objective (Olympus, Center Valley, PA). The GCaMP3.0-expressing neurons were scanned with a 488 nm laser at 1 Hz and emission was collected via a photomultiplier tube directed from a DM405/488 dichroic mirror. The Epac-1cAMPS-expressing neurons were scanned with a 440 nm laser at 1 Hz. CFP and YFP emissions were separated using a SDM510 dichroic mirror.

Images were acquired and ROIs were selected using the Olympus Fluoview software (Olympus, Center Valley, PA). ROIs were drawn around the somata of each ventrolateral neuron. To record from the HB-eyelet, a single ROI was drawn for each brain over a portion of the HB-eyelet nerve cluster at the optic lobe. To allow for maximum stabilization of the baseline recording from the sensor, the cells were imaged until the baseline stabilized (roughly 1 minute). Each recording started with acquisition of 30 seconds of signal from each ROI during constant perfusion of saline. At 30s, the perfusion channel was switched to induce flow from another channel for the next 30s, and perfusion flow was returned to HL3 saline for the rest of the 5 minute recording. Stimuli were introduced for 30s by switching perfusion channels from saline to a stimulus dissolved in saline. As a control for the movement associated with switching perfusion channels, a vehicle stimulus is given which consists of switching channels from HL3 saline to another channel with HL3 saline. All chemical for saline and stimuli were purchased from Sigma-Aldrich (St. Louis, MO) and Fisher Scientific (Waltham, MA).

Raw fluorescence intensity values were recorded from GCaMP3.0 or Epac-1Camps CFP and YFP as mean pixel intensities from each ROI for each timepoint scan. Mean pixel intensity (value range 0-4,095) traces for each recording were exported and transformed using a custom Graphical User Interface (GUI) developed in MatLab (The MathWorks, Natick, MA). Traces from GCaMP3.0 recordings were filtered with a 10-point moving average filter to remove high frequency noise.

Traces were normalized to percent fluorescent change from baseline using the equation:

$$((F_n-F_0)/F_0)*100$$

Where F_n is the average fluorescent intensity value from an ROI at a given timepoint (n); F_0 is the baseline calculated as the fluorescent intensity from one ROI averaged over the first 10 s of each recording. The maximum GCaMP fluorescent change (Max. $\Delta F/F_0$) was determined at the maximum change in fluorescence from baseline over the duration of the 5-minute recording. GCaMP traces from each genotype and treatment were averaged to display the average response to a given stimulus. Maximum values for each genotype and treatment were averaged to calculate the mean maximum change from baseline.

Epac1-CaMPs traces were first corrected for spillover from the CFP channel using the equation:

$$YFP_{soc}= YFP-(CFP*0.444)$$

YPF_{soc} is the spillover-corrected YFP intensity value; CFP is the raw CFP fluorescence recorded from the same timepoint, and 0.444 is the proportion of the CFP emission that is collected in the YFP channel specific to our imaging system. We calculated the inverse FRET ratio, proportional to increases in cAMP, by taking the ratio of CFP/YFP_{soc} for each timepoint. Each single ratio trace was filtered with a 10-point moving average and normalized to the first timpoint for an initial CFP/YFP value of "1.0". The spillover corrected, filtered and normalized traces are expressed as percentage of change of CFP/YFP from starting value. The transformed Epac-1camps traces were averaged by genotype and treatment to display the average temporal response. The maximum percentage change in transformed CFP/YPF inverse FRET ratio trace was determined as the maximum ratio value recorded from the entire 5 minute recording. Maximum percent ratio changes were averaged by genotype and treatment to calculate the mean maximum inverse FRET change. YFP is sensitive to photobleaching (Börner et al. 2011; Shafer et al. 2008) and results in a minor but steady decrease in the inverse FRET ratio.

All statistical tests were performed using Prism 5 (GraphPad, San Diego, CA) and compared maximum changes in GCaMP fluorescence or the Epac-1caMPs inverse FRET ratio between vehicle and test compounds. We used the Mann-Whitney U test for pairwise comparisons of maximum changes, and the Kruskal-Wallis one-way ANOVA with Dunn's post-test for multiple comparisons. All plots were generated in Prism 5.

Acute neuronal excitation by TRPA1

To measure the effect of specific time-of-day neuronal activity on locomotor rhythms and molecular clock cycling, we expressed the heat activated TRPA1 channel in $Rh6^{+}$-cells or PDF neurons and activated these neurons at specific times of day with heat exposure. First, flies experienced a 12:12 light:dark (LD) cycle for 5 days. On the last night of the LD cycle, flies experienced a heat pulse of 32˚C for 3 hours centering on ZT 15 or 21. The heat pulse consisted of carefully moving the flies into an incubator set to 32˚C. The 32˚C incubator was kept dark and the transfer was also done in darkness. After 3 hours, flies were put back in the 22˚C incubator. For the locomotor rhythm experiment, a control group of each genotype was reared under the same conditions but were not moved and did not receive a heat pulse. Flies monitored for the behavioral assay were allowed to free-run in constant darkness at 22˚C for 10 days following the heat pulse (see recording circadian locomotor behavior and analysis below). For measurement of molecular clock cycling in PDF neurons, flies were allowed to free-run for 3 days and were dissected at 4 timepoints distributed over day 3 in DD (see immunocytochemistry).

Recording Circadian Locomotor Behavior and Analysis

Flies were reared on a cornmeal based diet, as described. Flies crossed for this experiment were reared at 22˚C to prevent the activation of TRP. Male flies, 2-5 days old were loaded into DAM systems (Drosophila Activity Monitors). The recorded locomotor activity was visualized and analyzed using ClockLab for MatLab (Colburn Instruments, Whitehall, PA). To measure the response of the phase of the behavioral rhythm to the heat pulse, we adapted heat pulses to the light phase-

response protocol described by Kistenpfennig et al. (2012). The offset of evening activity was used as a phase marker. For each fly, a line was fit to the evening activity offsets for the first 10 consecutive days in constant darkness. The time (in hours: minutes) at which this line crossed the x-axis on the last day of the LD cycle was marked as the phase. The phase of the evening offset was averaged for each control un-pulsed genotype of flies. The phase of the evening offset was measured in the same way for each fly that experienced a heat pulse. The phase of the evening peak of each heat pulsed fly was subtracted from the average phase of the corresponding genotype in order to calculate the change in phase or phase shift induced by the heat pulse. The phase shifts were averaged for each genotype and the shifts of the two single element controls and the experimental combination were compared statistically using one-way ANOVA and Tukey's Multiple Comparison Test.

GRASP visualization

Brains were dissected in HL3 saline and mounted on a culture dish lid, as described above for preparation in live-imaging. The freshly dissected brains were first visualized by epifluorescence and checked for GFP presence. In experimental lines, where GFP was detected in the area of the accessory medulla (aMe), the area and surrounding stacks were scanned with a 488-nm laser. In control brains, where there was no GFP fluorescence detected, a similar area at the aMe was scanned using the same settings used to acquire the experimental image.

Immunocytochemistry

For visualization of Rh6-Gal4 driven GFP expression and PDF cells (Fig. 5.2 A, C-D), brains were dissected in Ringer's solution and fixed for 1 hour in 4% Paraformaldehyde in PBS-Tx at room temperature (RT). Brains were rinsed in PBS-Tx and blocked with 3% Normal Goat Serum (NGS) for 1 hour at RT. Brains were rinsed and incubated in a primary antibody cocktail for 2 days at 4˚C on a horizontal rotator. The primary cocktail was made of 1 uL/ml Sodium Azide (NaN3), Rb-anti-GFP 1:1000, and Ms-anti-PDF (Developmental Studies Hybridoma Bank, University

of Iowa, Iowa City, Iowa, USA) 1:200, to stain for GFP and PDF simultaneously. Subsequently, the brains were rinsed and incubated in secondary antibodies overnight: Alexa 488-anti Rb 1:1000 and Alexa 568-anti Ms 1:1000 (Invitrogen, Grand Island, NY, USA). Brains were rinsed with PBS-Tx and transferred to PBS without the detergent. Brains were mounted in PBS onto a poly-lysine coated coverslip and dehydrated with serially increasing concentrations of glycerol. After dehydration, the brains were coated with VECTASHEILD Hardset mounting medium (Vector Laboratories, Burlingame, CA), and mounted onto a slide.

For visualizing the cycling of PER in PDF neurons (Fig. 5.6), living flies were removed from the experimental incubator at CT 0, 6, 12, or 18 in the 3rd day of DD conditions and transferred immediately to 4% PFA in 1 X PBS-Tx (0.1%). Whole flies were fixed for 6 hours in 1.5 mL Epindorf tubes wrapped in aluminum foil to prevent exposure to light. After fixation, the flies were rinsed and the brains were dissected in PBS. After dissection, the brains were blocked with 3% NGS for 1 hour at RT. Brains were rinsed and incubated in a primary antibody cocktail for 2 days at 4˚C on a horizontal rotator. The primary cocktail was made of 3% NGS, 1 uL/ml 0.1% NaN3, Rt-anti-PER (Michael Rosbash, Brandeis University, Waltham, MA) 1:500 and Ms-anti-PDF (Developmental Studies Hybridoma Bank, University of Iowa, Iowa City, Iowa, USA) 1:200, to stain for PER and PDF simultaneously. Subsequently, the brains were rinsed and incubated in secondary antibodies overnight: Alexa 488-anti Rt 1:1000 and Alexa 564-anti Ms (Invitrogen, Grand Island, NY, USA). Brains were rinsed with PBS-Tx and transferred to PBS without the detergent. Brains were mounted in PBS onto a poly-lysine coated coverslip. PBS was removed and the brains were coated with Fluoromount Aqueous Mounting Medium (Diagnostic Biosystems, Inc., Pleasanton, CA), and mounted onto a slide.

Confocal images of stacks were acquired using an Olympus FV 1000 laser-scanning microscope (Olympus, Center Valley, PA) under a 60X 1.1N/A W, FUMFL N objective (Olympus, Center Valley, PA). All image acquisition and laser settings were kept the same within experiments. To compare fluorescent intensity levels of PER staining between genotypes, we measured mean pixel intensity of PER in the s-LN$_v$ cell bodies with MacBiophotonics ImageJ (Tony Collins, McMaster Biophotonics

Facility, Hamilton, Ontario). PDF staining was used to draw the outline of the s-LN_v cell bodies in a plane that was centered within the depth of the cell by locating largest expanse of nucleus (PDF is cytoplasmic). The average intensity of PER staining was measured from that outline and plane.

The mean pixel intensity was averaged for each genotype within each timepoint. The averaged mean pixel intensity of PER measured from the two single element controls and the experimental genotype combination were compared statistically using one-way ANOVA and Tukey's Multiple Comparison Test. The staining was plotted by genotype and Circadian Time (CT) when fixed. Analysis and plotting was done in Prism 5.

5.4 RESULTS

The Rh6-expressing cells include the HB-eyelet and a subset of R8 retinal-photoreceptors. The HB-eyelet is putatively both cholinergic and histaminergic and projects to the accessory medulla (aMe) where s- and l-LN_v clock neuron projections are found (Pollack and Hofbauer, 1991; Yasuyama and Meinertzhagen, 1999). The R8 retinal-photoreceptors express histamine as a neurotransmitter (Pollack and Hofbauer, 1991) and terminate in the distal medulla where l-LN_v terminals project. We have shown that the s- and l-LN_v respond to cholinergic agonists with increases in Ca^{2+} and cAMP (Fig. 1; Lelito and Shafer, 2012). Here, we evaluate the receptivity of the LN_v to histamine using genetically encoded indicators of neural activity. First, the GCaMP3.0 calcium sensor was expressed in the LN_v by the PDF-gal4 driver (*Pdf-gal4;UAS-GCaMP3.0;*). There were no observable calcium changes detected with GCamp3.0 in the s- or l-LN_v in response to 10^{-2} M histamine perfusion (Fig. 5.1A&B).

To test for histamine induced cAMP responses in the s- and l-LN_v, the cAMP sensor, Epac1-camps, was also expressed in the LN_v by the PDF-gal4 driver (*Pdf-gal4;* Epac1-camps*;*). Histamine did not elicit significant changes in the FRET signal from the Epac-1caMPs sensor from either type of LN_v (Fig. 5.1 C&D). When histamine (10^{-2}M) was co-applied with nicotine (10^{-4} M), a known excitatory agonist for increasing cAMP levels in the adult LN_v (Lelito and Shafer, 2012a), there was also no significant decrease in the excitatory cAMP response in the l-LN_v or the s-LN_v

compared to nicotine perfused alone (Fig. 5.1E-H). Based on the LN_v receptivity to cholinergic agonists and not to histamine, we predicted that the cholinergic HB-eyelet cluster of Rh6-cells input on to these lateral clock neurons in the aMe.

Although we did not observe a response of the LN_v to histamine, it is possible that the histaminergic R8 retinal-photoreceptors input on to the l-LN_v projections in the distal medulla, while the HB-eyelet may target the soma or projections of one or both the s- and l-LN_v in the aMe. To evaluate the likelihood of each connection, we employed GRASP (GFP Reconstitution Across Synaptic Partners) (Feinberg et al., 2008; Gordon and Scott, 2009) to detect closely associated neurons. Flies of the genotype *;Pdf LexA; Rh6-gal4* were crossed to ; *LexAop-GFP11; UAS-GFP1-10* so that one component of the GFP molecule was expressed on the cell surface of the PDF neurons and the complimentary part of GFP was expressed in the $Rh6^+$ photoreceptors. The Rh6-gal4 driver labels R8 retinal-photoreceptors as well the HB-eyelet tract (Fig. 5.2 A) while the PDF-lexA driver labels only the 8 PDF^+ LN_v in each hemisphere of the brain (Shang et al., 2008). Based on our live-imaging results, we predicted to observe GRASP signal in the aMe but not in the distal medulla. GFP signal from freshly dissected, unfixed brains was detectable in flies that expressed both drivers and complimentary parts of the GFP protein (;*Pdf-lexA/LexAop-GFP11;Rh6-gal4/UAS-GFP1-10)*. We detected GFP signal in the aMe in a pattern that resembled a shorter HB-eyelet tract (Fig. 5.2B1). We did not detect GFP signal in the distal medulla or the dorsal protocerebrum. The GFP pattern in the area of the HB-eyelet was not detected in flies lacking the Pdf-lexA driver (;*LexAop-GFP11/+;Rh6-gal4/UAS-GFP1-10)*, although some fluorescent puncta suspected to be autofluorescence were seen (Fig.5.2B2). These results, in conjunction with the responsivity of the LN_v to cholinergic agonists, suggest that the HB-eyelet subset of Rh6-expressing cells communicates directly to one or both LN_v classes in the aMe.

To rule out overlapping expression of the Rh6-gal4 and Pdf-LexA drivers as an explanation of a positive GRASP signal, we evaluated whether the Rh6-driver was expressed in the PDF neurons. Nuclear localized GFP (UAS-NLS-GFP) was expressed in the $Rh6^+$ photoreceptors by Rh6-gal4 (*;UAS-NLS-GFP/+;Rh6-gal4/+).* Dissected brains were co-stained for PDF and GFP. Overlapping expression of the Rh6-gal4 in

the PDF neurons would result in a GFP signal in the nuclei of PDF neurons. However, GFP staining was absent in the nuclei of all PDF$^+$ s-LN$_v$ and l-LN$_v$ evaluated (Fig. 5.2C-E). The GFP construct was strongly expressed and therefore was not limited to the nuclei of Rh6-gal4 labeled cells. We detected GFP signal near the s-LN$_v$ cell bodies in many samples (Fig. 5.2E1). This staining pattern suggests that the GRASP signal observed in the aMe results from the HB-eyelet targeting the s-LN$_v$. Our driver expression analysis is in agreement with previous work that has used the Rh6-gal4 driver to evaluate the close anatomical associations of the LN$_v$ and the HB-eyelet or it's precursor, the larval Bolwig's Organ, throughout development (Malpel et al., 2002; Keene et al., 2011). From this data, we rule out overlapping expression of the drivers as the source of the GRASP signal. The staining pattern we observe suggests a close apposition of the HB-eyelet with the LNv, and even more specifically perhaps that the HB-eyelet targets only the s-LN$_v$.

Before interrogating the connection between the HB-eyelet and the LN$_v$ clock neurons, we first tested whether the Rh6-expressing cells could be excited in the explanted brain. An Rh6-gal4 driver was used to target the ATP gated cation channel, P2X2, and the GCaMP3.0 calcium sensor (*Rh6-gal4/UAS-GCaMP3.0; UAS-P2X2/+*). The P2X2 channels were activated by perfusing ATP (1mM) over explanted brains. The HB-eyelet responded to ATP with increases in Ca^{2+} that were significantly different from Ca^{2+} fluctuations evoked by perfusion of blank HL3 saline (5.3A&B). R8-retinal photoreceptors captured by the Rh6-gal4 driver also showed increases in Ca^{2+} in response to ATP and are also activated (data not shown). Although we excite both types of Rh6$^+$ photoreceptors using the Rh6-gal4 driver, expression of P2X2 and perfusion of ATP is sufficient to excite the HB-eyelet.

To test whether excitation of the HB-eyelet elicits a response from the PDF neurons, the P2X2 channel was expressed in Rh6$^+$ photoreceptors, while the GCaMP3.0 calcium sensor was expressed in the PDF neurons *(;PDF-lexA, Rh6-gal4/UAS-GCaMP3.0; UAS-P2X2/+*). Application of ATP (1 mM) elicited increases in Ca^{2+} only from the s-LN$_v$ and not from the l-LN$_v$ (Fig. 5.3C-F). Application of ATP to brains of flies that did not express P2X2 in the Rh6$^+$ cells (*;PDF-lexA/+;UAS-GCaMP3.0; UAS-P2X2/+)* actually resulted in a decrease in calcium from the s-LN$_v$

compared to vehicle (Fig. 5.3G&H) as was reported in our previous study (Yao et al., 2012). In our previous study, we were able to activate the HB-eyelet precursor, Bolwig's Organ, with P2X2/ATP and also observed increases in Ca^{2+} from the larval LN_v (Yao et al., 2012).Given the close anatomical association of the eyelet and the s-LN_vs (Fig 5.2), this excitatory response is likely a direct cholinergic input from the HB-eyelet neuron.

Our previous work showed that excitatory increases in Ca^{2+} mediated by nicotinic acetylcholine receptors in the PDF neurons are coupled with increases in cAMP (Lelito and Shafer, 2012a). We tested whether excitation of the HB-eyelet also elicited cAMP changes from the s-LN_v. The P2X2 channel was expressed in $Rh6^+$ photoreceptors, and the Epac-1cAMPs cAMP sensor was expressed in the PDF neurons *(;PDF-lexA, Rh6-gal4/UAS- Epac1-cAMPs; UAS-P2X2/+*). In agreement with the Ca^{2+} imaging above, application of ATP (1 mM) elicited increases in cAMP in the s-LN_v but not the l-LN_v (Fig. 5.4A-D). ATP application to brains that did not express the P2X2 channel in the $Rh6^+$ cells *(;PDF-lexA/+;UAS-Epac1-cAMPs; UAS-P2X2/+)* did not evoke substantial changes in Epac-1camps FRET. A small significant difference in ATP compared with vehicle is due to bleaching of YFP and not actual change in FRET. Actual FRET responses were only observed in the LN_v from this genotype when a known excitatory agonist, nicotine (10^{-4} M) was applied. As only Ca^{2+} and cAMP increases in response to $Rh6^+$ photoreceptor excitation were observed in the s-LN_v, the HB-eyelet is likely targeting the s-LN_v with cholinergic input from the HB-eyelet at the aMe.

External photoreceptors are sufficient to mediate time-of-day dependent phase advances and delays of circadian locomotor rhythms (Kistenpfennig et al., 2012). The HB-eyelet is one of many independent external photoreceptors. External photoreceptors are distinguished from the molecular light sensor, cryptochrome, which is expressed by many clock neurons including the LN_v (Yoshii et al., 2010). Flies mutant for *Cry* expression can entrain to light cycles (Helfrich-Förster et al., 2001) and maintain the ability to both phase-advance and delay circadian locomotor rhythms in response to light pulses in subjective night (ZT 15 and 21 respectively) (Kistenpfennig et al., 2012).Therefore, we wondered whether

the Rh6^{+} photoreceptors, mainly the HB-eyelet, could mediate such time dependent phase-shifts.

We tested whether acute excitation of the Rh6^{+} photoreceptors was sufficient to phase shift circadian locomotor rhythms. For acute excitation of the Rh6^{+} photoreceptors, we selected a temperature activated ion channel rather than light activated channels to avoid exciting other groups of photoreceptors despite the potential drawback to temperature pulses (see below). TRPA1 is a cation channel found in *Drosophila* that is activated at 28°C *in vivo* (Viswanath et al., 2003). The channel is found in very few neurons in the central brain and is not expressed in clock neurons (Hamada et al., 2008).Here, the channel was targeted to the Rh6^{+} photoreceptors by the Rh6-gal4 driver (*;Rh6-gal4/UAS TRPA1;).* Single element controls were crossed to the wildtype w^{1118} strain and used as negative controls. As a positive control, the TPRA1 channel was targeted to the PDF neurons (*PDF-gal4;UAS-TRPA1/+;).* An additional positive control was included to confirm the temperature activation of TRP, where TRPA1 was expressed in all cholinergic neurons (*;Cha-gal4/UAS-TRPA1;).* Previous studies have shown that flies expressing TRPA1 widely throughout the nervous system seize at 35°C (Hamada et al., 2008). Flies were loaded in DAM Trikinetics monitors that allowed for measurement of daily locomotor activity. All flies were exposed to 5 days in a light dark (LD) cycle at 22°C, a temperature at which the TRPA1 channel is not activated. On the night of the last LD cycle flies were exposed to a 32°C heat pulse for 3 hours surrounding ZT 15 (a time during which light pulses cause delays), or ZT 21 (a time during which light pulses cause advances). Control groups did not experience a heat pulse. We selected a 32°C heat pulse to minimize confounding entrainment effects due to temperature. Previous studies established that flies can entrain behavioral rhythms to temperature cycles in constant lighting, and temperature pulses of 37°C can elicit phase delays in the early subjective evening (Yoshii et al., 2005; Kaushik et al., 2007).

Confirming that the given heat pulses resulted in TRPA1 activation, flies expressing TPRA1 in cholinergic neurons *(;Cha-gal4/UAS-TRPA1;)* were incapacitated by the heat pulses at both time points and the majority died (data not

shown). For the remaining genotypes, the offset resulting from the heat pulse was calculated by subtracting the phase of a behavioral locomotor rhythm marker of a pulsed group from the phase of the corresponding unpulsed group. For a circadian phase marker, we tracked the evening offset in locomotor activity, when flies become inactive after two large daytime bouts of activity. This method was used by Kistenpfennig et al. to observe that external photoreceptors are sufficient to mediate light-induced, time-dependent phase shifts of circadian locomotor rhythms (Kistenpfennig et al., 2012).

The heat pulse centered on ZT 15 resulted in a substantial delay in all genotypes whether or not TRP was actually expressed (Fig. 5.5A&B). A previous study showed that temperatures above 37°C were able to phase delay circadian locomotor rhythms but only in the early evening (Kaushik et al., 2007). Correspondingly, our data suggests that 32°C for 3 hours is sufficient to phase delay locomotor rhythms in the early evening as well. However, heat pulses centered on ZT 21 showed a trend to elicit positive phase shifts (advances) from flies expressing TRP in the Rh6^{+} photoreceptors, although the phase shifts form ;*Rh6-gal4/UAS-TRPA1;* flies were not significantly different from ;*Rh6-gal4/+;* negative control flies ($p=0.059$) (Fig5.5A). Heat pulsed flies expressing TRP in the PDF neurons exhibited the same trend (*Pdf-gal4;UAS-TRPA1/+;)*, and phase advances were significantly different from both of the signal element controls (Fig 5.5B). Rh6-cell excitation appears to be able to phase advance circadian locomotor rhythms although replication of the behavioral assay with greater numbers is needed. The effects of Rh6 cell excitation at ZT 21 mimic the more pronounced effects of direct activation of the PDF neurons (Fig 5.5B) or a light pulse given at the same time. Therefore, it is likely that Rh6^{+} photoreceptors are sufficient to phase advance circadian behavioral locomotor rhythms.

Adult studies suggest that the s-LN$_v$ utilize CRY-independent photoreceptor in entrainment (Helfrich-Förster et al., 2001), as PER rhythms cycle robustly in the s-LN$_v$ unlike the majority of other clock neuron classes when Cry is absent. In this last experiment, we address mechanisms of molecular clock resetting in the s-LN$_v$ by Rh6^{+} photoreceptor excitation, as it may be more sensitive than a behavioral assay

in detecting an effect of light input to the clock. We observed the phase of PER rhythms in the s-LN_v after excitation of Rh6-cells at a time when light would evoke behavioral phase-advances. We did not measure PER cycling in the l-LN_v as it has been shown that the l-LN_v cease molecular clock cycling shortly after entering constant conditions (Shafer et al., 2002). Again, we utilized TRPA1 expression and temperature pulses to acutely activate the $Rh6^+$ photoreceptors at ZT 21 (*;Rh6-gal4/UAS-TRPA1;).* Single element controls were crossed to the wildtype w^{1118} strain and measured as negative controls. As a positive control, the TRPA1 channel was expressed in the PDF neurons (*PDF-gal4;UAS-TRPA1/+;).* Groups of flies were subjected to the same 3hr, 32°C heat pulse centered on ZT 21 on the last night of a 12:12LD cycle from 22°C (see above). Three days into constant darkness (DD), groups of flies from each genotype were fixed at CT 0, 6, 12, and 18, and subsequently stained against PER and PDF.

Previous reports show that PER rhythms in the s-LN_v are highest at CT 0, decline through the day, trough at ZT 12 and begin to increase by CT 18 on DD3 (Yao and Shafer, 2014). Using PDF as a marker for the cell body of PDF neurons, we calculated the mean pixel intensity of PER staining in the s-LN_v cell bodies from each of the genotypes and time points. We did not find the cycle of the PER rhythm in the experimental genotype where $Rh6^+$ photoreceptors were activated to be consistently different from each of the heat pulsed single element control genotype (Fig 5.6E). The cycling of PER in the single element control *;Rh6-gal4/+;* appears less tightly regulated than any of the other genotypes observed (Fig. 5.6C), which may explain the lack of a significant difference between it and the experimental cross in the phase advance of behavioral rhythms (Fig.5.5A). Compared to heat pulsed *;UAS-TRPA1/+;* negative control flies, direct excitation of the PDF neurons does appear to advance PER cycling (*Pdf-gal4;UAS-TRPA1/+;*), as the trough is seen to move from CT 12 in the heat pulse negative control, to CT6 in the heat pulsed experimental line (Fig.5.B&D). Although direct excitation of PDF neurons results in a shift of PER rhythm, input on to the clock neurons from the $Rh6^+$ photoreceptors may act through other molecular clock proteins, such as TIM (Keene et al., 2011) and may take longer to become apparent (Helfrich-Förster et al., 2001).

5.5 DISCUSSION

The clock neuron network utilizes information transmitted by external photoreceptors to synchronize circadian rhythms in phase with environmental cycles. Until our current study, it was not established if and how the cluster of external photoreceptors known as the HB-eyelet, communicated to clock neurons. In larvae, PDF^+ ventrolateral clock neurons are excited by Bolwig's light sensing organ, the larval form of the HB-eyelet. However, in the adult, the ventrolateral PDF^+ neurons differentiate and double to include 4 s-LN_v and 4 l-LN_v in each hemisphere. Here, we show that although both LN_v projections are found in the aMe, the cholinergic terminals of the adult eyelet target only the s-LN_v. The cAMP and Ca^{2+} signaling that we observed in the s-LN_v evoked by HB-eyelet input likely induces phase-shifts through unknown interactions with the cycling molecular clock. A resulting phase shift in overt circadian behavioral rhythms is likely then transmitted by neuronal signaling to dorsal clocks neurons by the dorsal projections of the s-LN_v.

The first evidence that the HB-eyelet is both cholinergic and histaminergic arises from immunohistochemical observations dating back to the 1990's (Pollack and Hofbauer, 1991; Nässel, 1999; Yasuyama and Meinertzhagen, 1999). Since then, the staining has not been repeated in finer detail with modern staining techniques and microscopy. It is unclear whether each of the HB-eyelet neurons expresses one or both of these neurotransmitters, or whether there are distinct targets or roles of different HB-eyelet neurons. The larval light-sensing organ, Bolwig's nerve, is immunoreactive to ChAT antibodies, (Malpel et al., 2002) and through development the nerve also takes on anti-histamine staining in the adult (Pollack and Hofbauer, 1991). In the larva, the neurons of Bolwig's organ can be separated by rhodopsin 5 (Rh5) and 6 (Rh6) expression (Sprecher et al., 2007; Sprecher and Desplan, 2008). Only Rh5-neurons are required for the larval photophobicity response, whereas either subtype of Bolwig's neurons are sufficient to entrain the circadian clock neuron network (Keene et al., 2011). In this study, we show that the cholinergic communication by the eyelet to the ventrolateral clock neuron persists into

adulthood. As we do not observe responsiveness of the LN_v to histamine, the role of the histaminergic HB-eyelet may in adulthood may not play a role in circadian photoreception at all, but may target one of the myriad other projections located in densely innervated aMe.

Due to constraints of the Rh6-Gal4 drivers used in this study, we are unable to independently investigate the role of the HB-eyelet and R8 retinal-photoreceptors. We are confident that the excitatory increases in cAMP and Ca^{2+} observed after P2X2/ATP excitation of the $Rh6^+$-cells is due to input from the HB-eyelet (Fig. 3 & 4). First, GRASP signal localized only to the aMe (Fig. 5.2B1) and GFP-staining of Rh6-gal4 driver expression was seen directly adjacent to the s-LN_v cell bodies (Fig.5.2C-E). Second, the retinal photoreceptors express histamine solely as a neurotransmitter. In *Drosophila*, neurons directly downstream of photoreceptors show inhibitory responses to light exposure or histamine application (Hardie, 1987). Therefore, the cholinergic-like response that we have observed from activating $Rh6^+$ photoreceptors is likely direct excitation from the HB-eyelet to the s-LN_v.

Histamine receptors, to date, have only been localized to one of the 9 types of clock neurons: the l-LN_v (Hong et al., 2006). However, we did not detect a calcium or cAMP response in either set of LN_v when histamine was applied. Effects of inhibitory neurotransmitters on calcium levels have been measured on dissociated larval LNv. When visualized with Fura-2, a highly sensitive calcium responsive dye injected into cells of interest, application of glutamate to isolated larval LN_v causes calcium levels to decrease (Hamasaka et al., 2007). There is less evidence to suspect a change in cAMP levels by activating chloride currents. There are examples of cAMP signaling regulating the activity of chloride channels, but it may also be possible for chloride currents to alter cAMP levels by inactivating voltage dependent adenylyl cyclases. With different sensors we might have seen direct response to histamine by the LNv.

Despite our comprehensive attempts to visualize putative effects of histamine, we were limited by the relatively low sensitivity of our sensors. A recently improved suite of GCaMP sensors has been optimized to detect smaller calcium fluxes with higher temporal resolution than previous GCaMP constructs

(Akerboom et al., 2012). Also potentially useful in future investigations, are Cl^- sensors developed in mammalian systems for the detection of direct chloride currents rather than potential downstream effects on Ca^{2+} and cAMP (Waseem et al., 2010). Perhaps the most promising tool is a new fluorescent voltage sensor, vetted in the *Drosophila* l-LN_v, that has the potential to discern local voltage changes with near single action potential resolution (Cao et al., 2013). Our studies focused on the soma of the LN_v neurons so that we could knowingly record activity from single neurons. However, histaminergic input from retinal photoreceptors onto the l-LN_v may occur only locally at the net-like terminal projections in the optic lobe. Future attempts at visualizing histaminergic inhibitory input may be successful with alternative sensors imaged at the l-LN_v projections.

The cAMP sensor, Epac-1cAMPs, has typically shown greater sensitivity to excitatory agonists than GCaMP3.0 (Lelito and Shafer, 2012a). However, we did not see an effect of histamine alone, or co-applied with an excitatory agonist (Fig. 5.1). It is possible that the dose of nicotine that we tested induced a saturating amount of cAMP overwhelming the sensor (Fig. 5.1E-H). Titrating down the nicotine dose to induce the lowest observable increases in cAMP may be the most successful route to visualizing an inhibitory effect of histamine to the LNv. Despite the caveats to our imaging experiments, we interpret the obvious responsivity of the LN_v to cholinergic stimulation and the apparent lack of responsivity to histamine to implicate the cholinergic HB-eyelet neurons, and not the histaminergic R8 photoreceptors, as a candidate for relaying visual system input to the clock via the LNv.

Most animals exhibit a shift in the phase of their circadian locomotor activity in response to brief light exposure presented in subjective evening. In *Drosophila*, these phase shifts can be mediated strictly by external photoreceptors: the compound eyes, ocelli and HB-eyelets (Kistenpfennig et al., 2012). Historically, circadian phase-responses have been difficult to measure in flies compared to mammals. Flies have a much shorter life span and unstable phase markers relative to mammalian wheel running activity. This makes phase-shift calculations noisier and less precise than those obtained in mammalian phase response experiments. In this study we implicate a specific subset of these photoreceptors, the $Rh6^+$

photoreceptors, in being sufficient to phase-advance circadian locomotor rhythms when activated in the late evening. The phase advancing trend that we show by excitation of $Rh6^+$ photoreceptors mimics the effect of directly activating PDF neurons (Fig. 5.5). Based on our circuit interrogation study, when we activate the $Rh6^+$-cells via P2X2/ATP, we induce increases in Ca^{2+} and cAMP from the s-LN_v neurons. Therefore, when we activate those same $Rh6^+$-cells with TRP/temperature activation, we are likely exciting the s-LN_v, eliciting phase changes in the s-LN_v molecular clocks and synchronizing phase information is likely transmitted to dorsal clock neurons by s-LN_v neural activity.

Excitation of PDF neurons directly in late evening was more effective at inducing a behavioral rhythm phase shift (Fig. 5.5B). The effect was likely more pronounced than activating $Rh6^+$-cells for several reasons: 1) The PDF-gal4 is an X-chromosome driver that is dosage compensated in males, the sex used for behavioral rhythm assays. For this reason, TRP expression may have been higher in these populations, and sensitivity of TRP activation by temperature may also have been higher; 2) In addition to being a weaker second chromosome driver, the Rh6-gal4 driver was used to excite the $Rh6^+$ photoreceptors which then transmit a signal to clock neurons. Excitation of Rh6-cells via P2X2 may be sufficient to elicit changes in cAMP and Ca^{2+} in the s-LN_v, but the TRPA1 method of excitation may not be sufficient provoke post-synaptic s-LN_vs signaling that alters the molecular clock or elicits s-LN_v communication to dorsal clock neurons. In addition, this particular Rh6-gal4 driver appeared to have an innate sensitivity temperature unlike any of the other single element controls that experienced the same heat pulse (Fig. 5.5 B & C). Future work using this assay might exploit the use of the alternative Rh6-gal4 driver that may have enhanced expression levels and less innate sensitivity to heat.

Signaling by external photoreceptors to the timing of light cycles is sufficient for shifting the phase of behavioral rhythms and therefore shifting the cell autonomous molecular clocks of clock neurons. Despite our efforts to implicate $Rh6^+$ photoreceptor input in affecting the molecular clock proteins, how external photoreceptor input turns the cogs of the molecular clock remains unknown. Here we examined the most likely candidate that $Rh6^+$ photoreceptor input would affect:

the PERIOD (PER) protein. In mammals, light input to clock neurons elicits increases in *per* transcript dependent on Ca^{2+}/cAMP Response Element-binding Protein (CREB) activation (Shearman et al., 1997; Shigeyoshi et al., 1997; Tischkau et al., 1999). However, excitation of $Rh6^{+}$-cells did not appear to alter PER cycling in the way that direct excitation of PDF neurons did in the same assay (Fig 5.6 A & C). The absence of an observable effect of activating Rh6 cells may be due to the same reasons described for the behavioral assaying using targeted TRP expression. Alternatively, the TIMELESS (TIM) protein of the molecular clock may be the target of external photoreceptor input whose modulation results in phase changes to the molecular clock. The molecular light sensor CRY that is expressed in some clock neurons including the LNv, targets TIM for degradation when activated by light (Lin et al., 2001; Koh et al., 2006; Peschel et al., 2006). Also, light induced TIM degradation requires the light-responsiveness (expression of photopigments) of the larval eyelet (Keene et al., 2011). Future investigations of TIM levels after HB-eyelet excitation may elucidate the resetting mechanism by external photoreceptors in adult flies.

Our current model is that the HB-eyelet phase shifts behavioral rhythms in adult flies by directly exciting the s-LN_v. The cAMP and Ca^{2+} signaling events evoked in the s-LN_v by HB-eyelet input likely influences the phase of the molecular clock through modulation clock gene transcription or clock protein degradation, as has been demonstrated in the larval clock network or in mammalian clocks (Tischkau et al., 2003; Keene et al., 2011). The phase changes to the autonomous molecular clocks of the s-LN_v are then likely communicated to the rest of the clock network. Input from the HB-eyelet to the dorsally projecting s-LN_v would be a mechanism, in parallel to various other light input mechanisms in the fly, for synchronizing global clock network output with external light cycles.

5.6 FIGURES

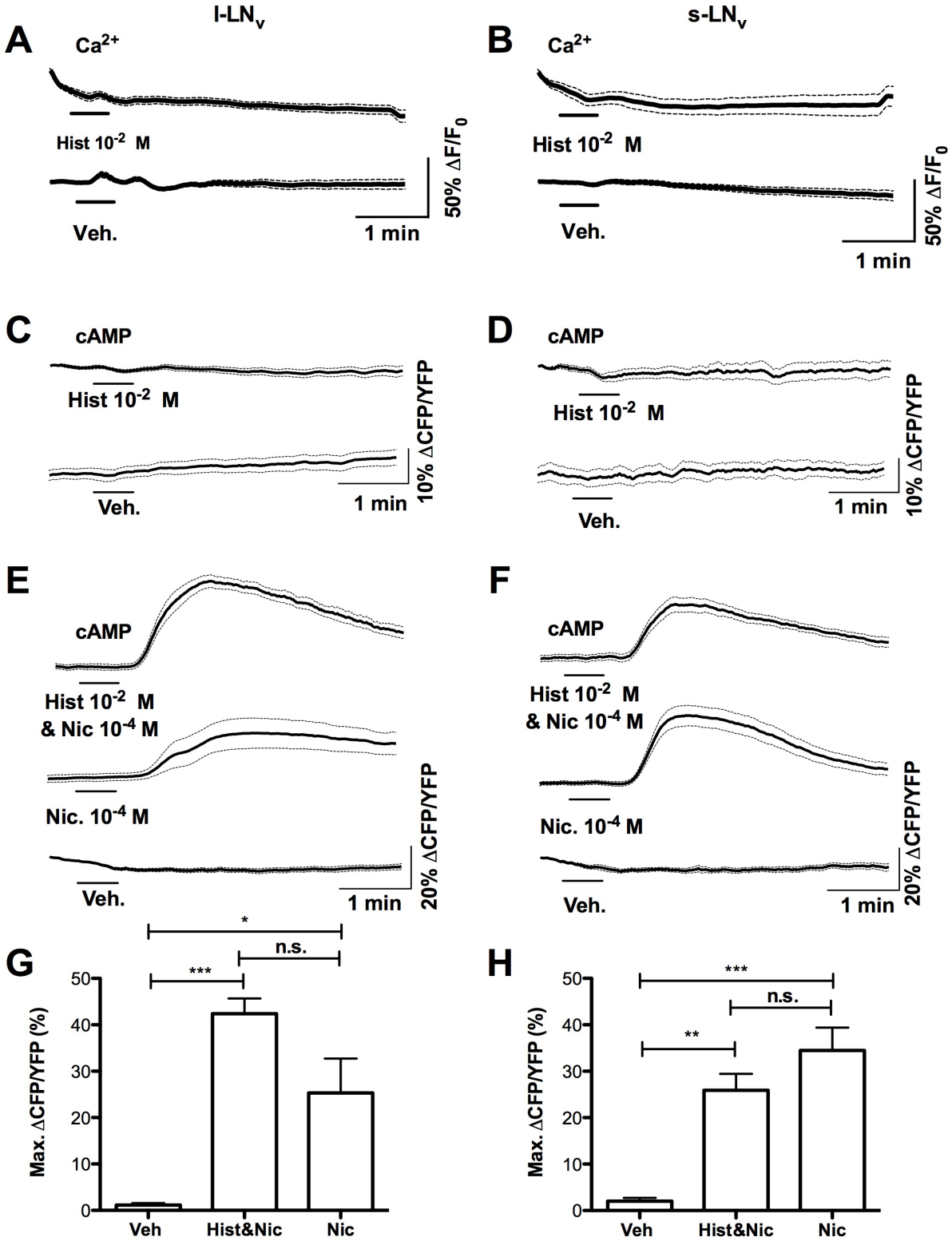
l-LN$_v$
s-LN$_v$
A
B
Ca^{2+}
Hist 10^{-2} M
Veh.
1 min
50% ΔF/F$_0$
C
D
cAMP
10% ΔCFP/YFP
E
F
Hist 10^{-2} M & Nic 10^{-4} M
Nic. 10^{-4} M
20% ΔCFP/YFP
G
H
Max. ΔCFP/YFP (%)
*
n.s.
***
**
Veh
Hist&Nic
Nic

Figure 5.1. The small and large ventrolateral clock neurons are insensitive to histamine. A&B) The GCaMP3.0 calcium sensor is expressed in the PDF$^+$ ventrolateral clock neurons (*Pdf-gal4;UAS-GCaMP3.0;*). Average GCaMP3.0 traces (±SEM) recorded from the LN_v cell bodies before, during and after perfusion with histamine (10^{-2} M) or blank saline (vehicle, Veh.) over the explanted brain in between continuous HL3 saline perfusion flow. Neither the l-LN_v (A) or the s-LN_v (B) exhibited changes in calcium that were different than vehicle perfusion although bleaching of the sensor is seen before introduction of a stimulus. C-H) The Epac1-cAMPs cAMP sensor is expressed in the PDF$^+$ clock neurons (*Pdf-gal4;UAS-Epac-cAMPs;*). C-F) Average Epac-1cAMPs traces (±SEM) recorded from the LN_v cell bodies before, during and after perfusion of histamine or vehicle. Histamine perfusion did not evoke changes in cAMP levels relative to a vehicle perfusion in the l-LN_v (C) or the s-LN_v (D). Co-application of histamine (10^{-2} M) with an excitatory agonist (10^{-4} M nicotine) resulted in robust increases in cAMP from the l-LN_v (E) and s-LN_v (F). Maximum changes in the inverse FRET ratio (CFP/YFP) of the Epac-1cAMPs sensor evoked by co-application were not significantly different from nicotine (10^{-4} M) perfused alone (G-H). Stimulus bars represent 30 seconds of perfusion of the compound indicated below the line, switched from a constant saline flow.

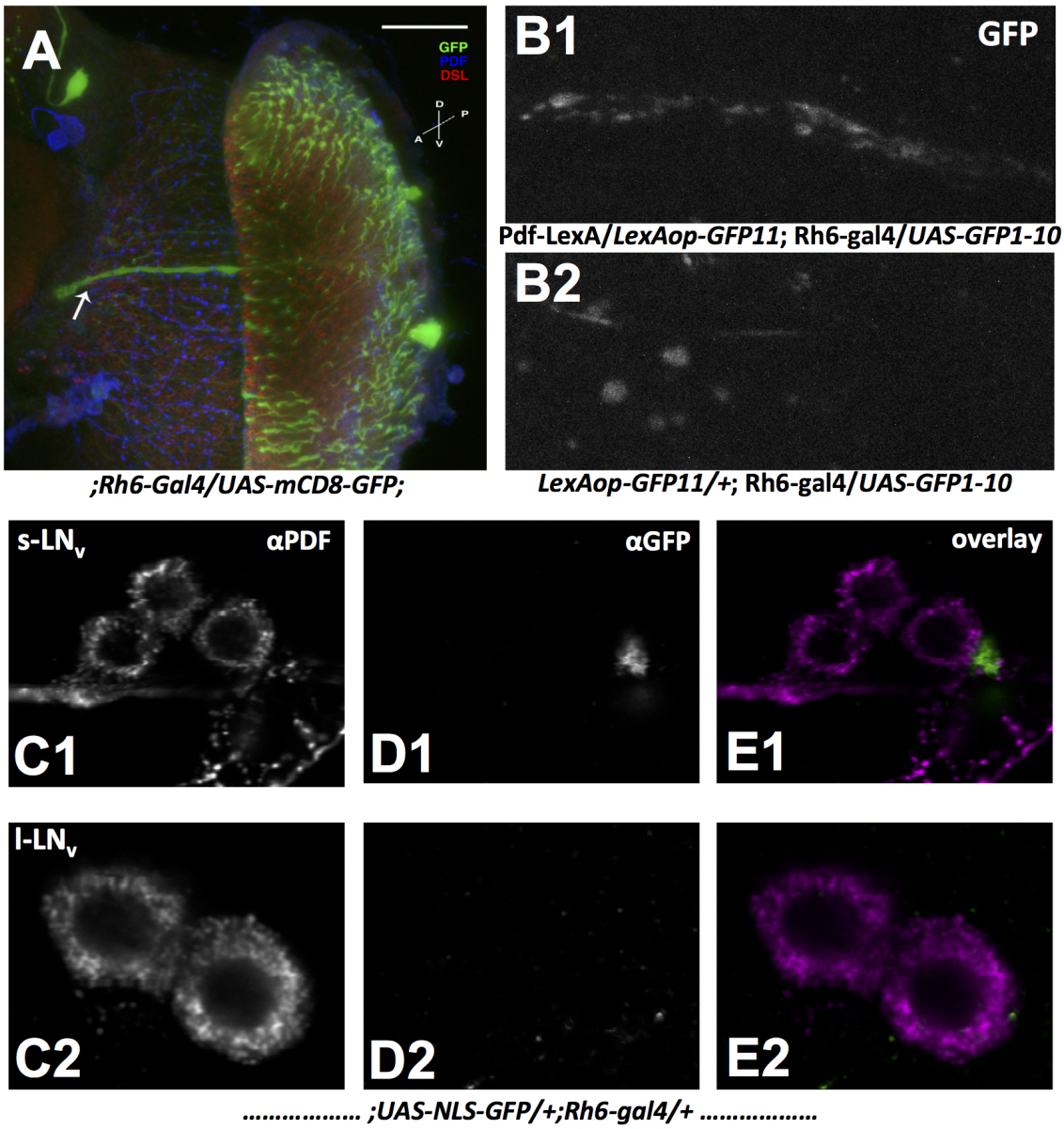

Figure 5.2. The Rh6-Gal4 driver labels the HB-eyelet neurons that project to the accessory medulla but does not express in PDF neurons. A) Confocal stack of the optic lobe labeling pattern of an Rh6-gal4 driver (*;Rh6-gal4/UAS-mCD8-GFP;*). Arrow shows the HB-eyelet cluster of photoreceptive neurons projecting to the accessory medulla. The projections from the R8 retinal-photoreceptors tile the optic lobe. B1) Observing freshly dissected brains, GRASP (GFP Reconstitution Across Synaptic Partners) signal is detected in the location of the aMe in a narrow band resembling the HB-eyelet tract in flies expressing half of a GFP molecule in the PDF neurons and the complementary GFP structure in the Rh6+ photoreceptors *(;Pdf-lexA/LexAop-GFP11;Rh6-gal4/UAS-GFP1-10*). B2) We detected only un-patterned background autofluorescence in the aMe region of flies expressing only half of the

GFP structure *(;LexAop-GFP11/+;Rh6-gal4/UAS-GFP1-10*). C-E) Brains of flies from the genotype (*;UAS-NLS-GFP/+; Rh6-gal4/+)* were co-stained for GFP and PDF to check for overlapping expression pattern of Rh6-gal4 with PDF expression. PDF staining is observed brightly in the cytoplasm but not the nucleus of the s-LN_v (C1) and l-LN_v (C1). Column D shows GFP emission collected from the region of the s-LN_v (D1) and l-LN_v (D2). GFP is not detected in any of the LN_v nuclei but is found adjacent to the s-LN_v cell bodies (column E, overlay).

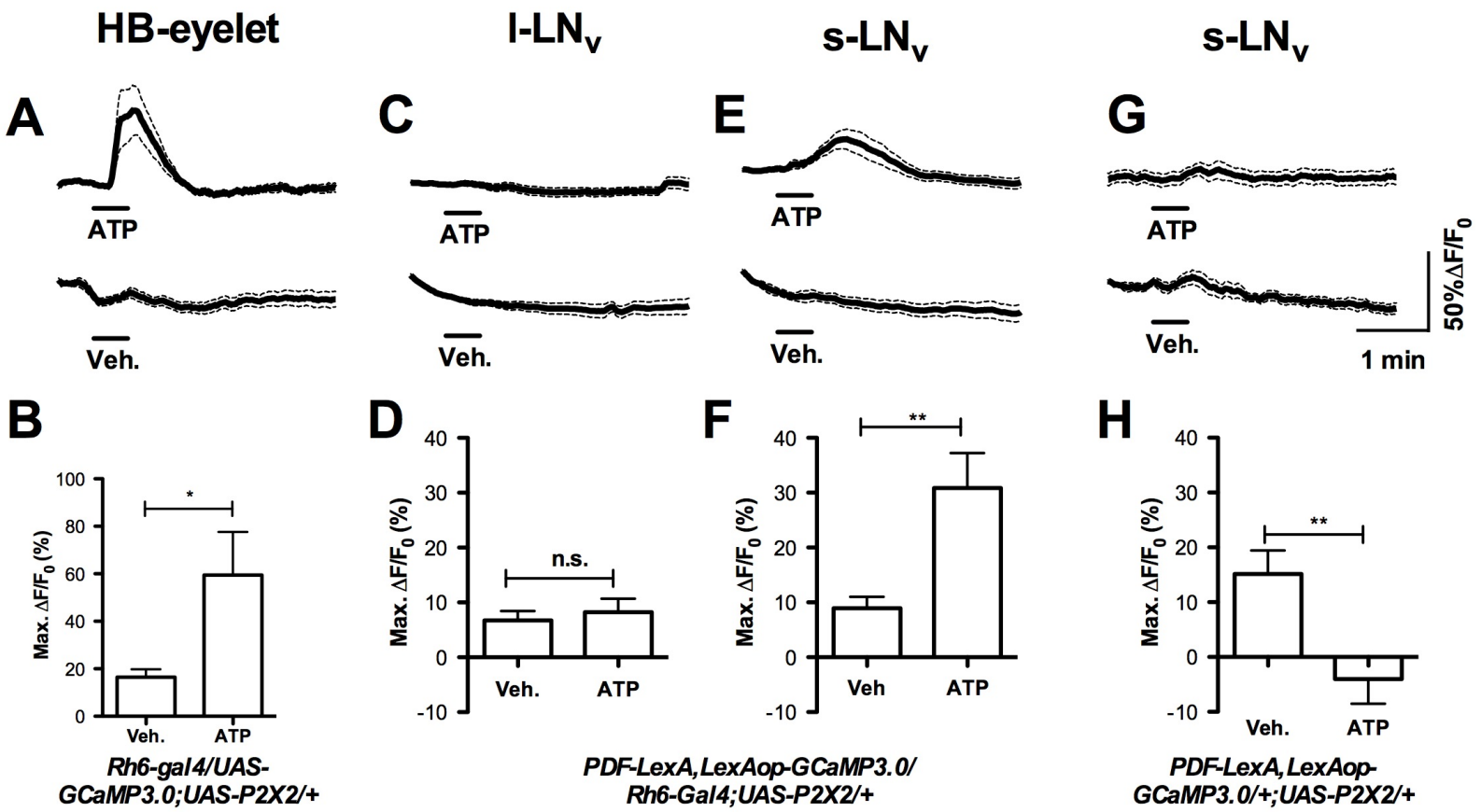

Figure 5.3. The s-LN$_v$ response to HB-eyelet excitation with increases in calcium. Average GCaMP3.0 traces (±SEM) recorded from the LN$_v$ cell bodies before, during and after perfusion with ATP (1 mM) or blank saline (vehicle, Veh.) over the explanted brain in between continuous HL3 saline perfusion flow (A,C,E,G). Scale bar applies to all traces shown and represents 1 minute and a 50% change in GCaMP3.0 fluorescence over baseline. Mean maximum percent changes in

fluorescence (±SEM) of the GCaMP3.0 calcium sensor above baseline (Max. $\Delta F/F_0$) evoked by ATP or vehicle perfusion (B,D,F,H). A-B) Calcium increases are observed in the HB-eyelet in response to ATP but not vehicle perfusion (*Rh6-gal4/UAS-GCaMP3.0;UAS-P2X2/+).* The l-LN_v did not exhibit obvious Ca^{2+} responses to the excitation of $Rh6^+$ photoreceptors (C-D), whereas the s-LN_v (E-F) show changes in calcium significantly increased in response to ATP compared to vehicle perfusion (*Pdf-lexA,LexA-GCaMP3.0/Rh6-gal4; UAS-P2X2/+).* Perfusion of ATP over brains lacking P2X2 expression in the HB-eyelet resulted in a slight decrease in calcium from levels in the s-LN_v relative to vehicle perfusion (G-H). Stimulus bars represent 30 seconds of perfusion switched from a constant saline flow.

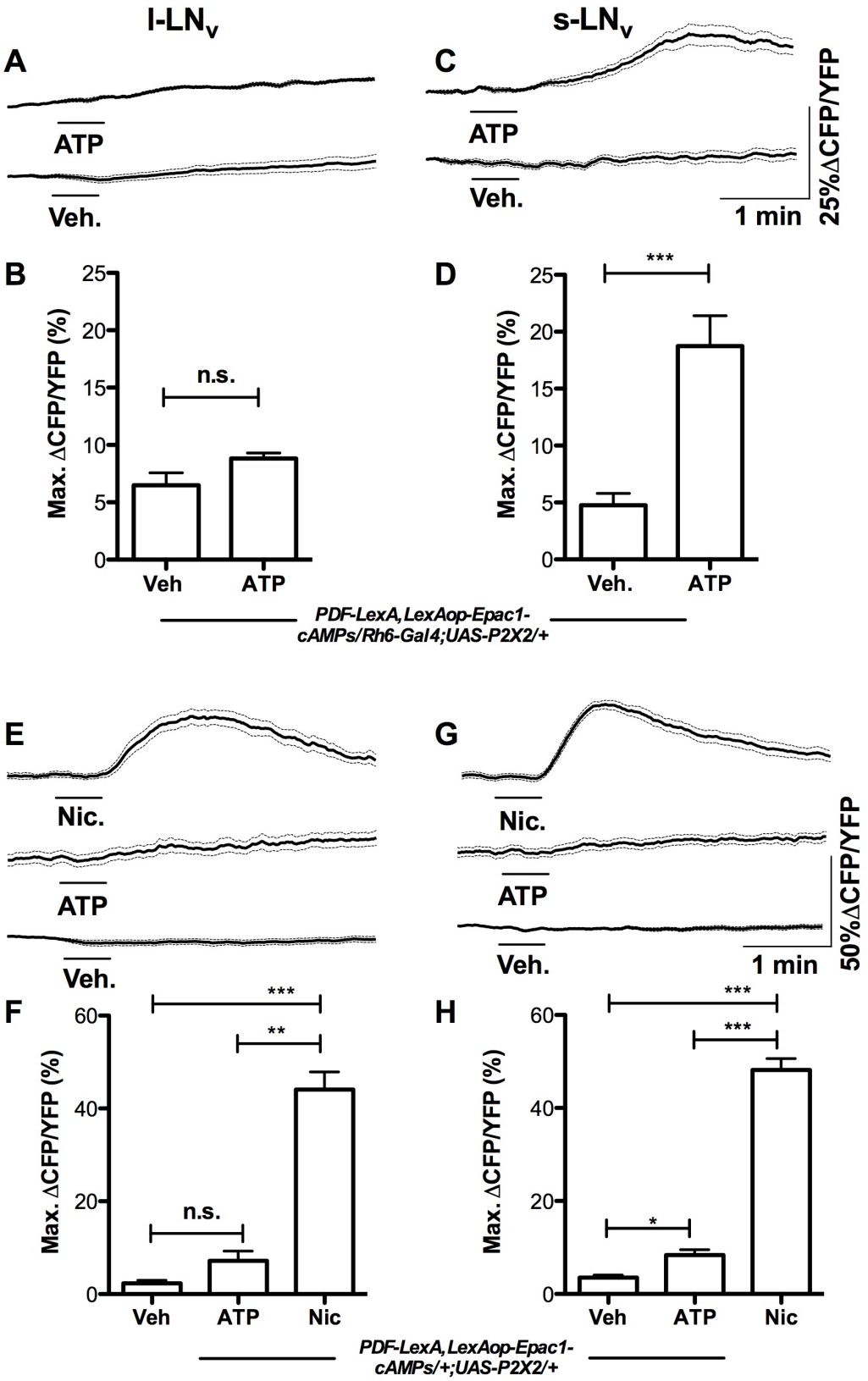
l-LNv
s-LNv
A
C
ATP
Veh.
1 min
25%ΔCFP/YFP
B
D
Max. ΔCFP/YFP (%)
n.s.
***
Veh
ATP
PDF-LexA,LexAop-Epac1-cAMPs/Rh6-Gal4;UAS-P2X2/+
E
G
Nic.
50%ΔCFP/YFP
F
H
**
*
Nic
PDF-LexA,LexAop-Epac1-cAMPs/+;UAS-P2X2/+

Figure 5.4. The s-LN_v respond to HB-eyelet excitation with increases in cAMP. Average inverse FRET traces (±SEM) recorded from the LN_v cell bodies before, during and after stimulus perfusion over the explanted brain in between continuous HL3 saline perfusion flow (A,C,E,G). Stimulus bars represent 30 seconds of perfusion of the compound indicated below the line, switched from a constant saline flow. Mean maximum percent changes from baseline in the inverse FRET ratio (±SEM) recorded from the Epac-1cAMPs sensor (Max. ΔCFP/YFP) evoked by ATP or vehicle perfusion (B,D,F,H). Scale bar in C applies to A, represents 1 minute and a 25% change in in the inverse FRET ratio (CFP/YFP). A-B) The l-LN_v did not exhibit obvious cAMP responses to the excitation of $Rh6^+$ photoreceptors (A-B), whereas the s-LN_v (C-D) show changes in cAMP significantly increased in Rh6-cell excitation (;*Pdf-lexA,LexA-Epac-1cAMPs/Rh6-gal4; UAS-P2X2/+).* Perfusion of ATP over brains lacking P2X2 expression in the HB-eyelet resulted in a no change in cAMP levels from the l-LN_v (E-F) and a slight increase in the inverse FRET ratio from levels in the s-LN_v relative to vehicle perfusion (G-H). Actual FRET responses were observed from this genotype in the l-LN_v (E-F) and the s-LN_v (G-H) only when the excitatory agonist, nicotine (10^{-4} M) was perfused. Stimulus bars represent 30 seconds of perfusion switched from a constant saline flow.

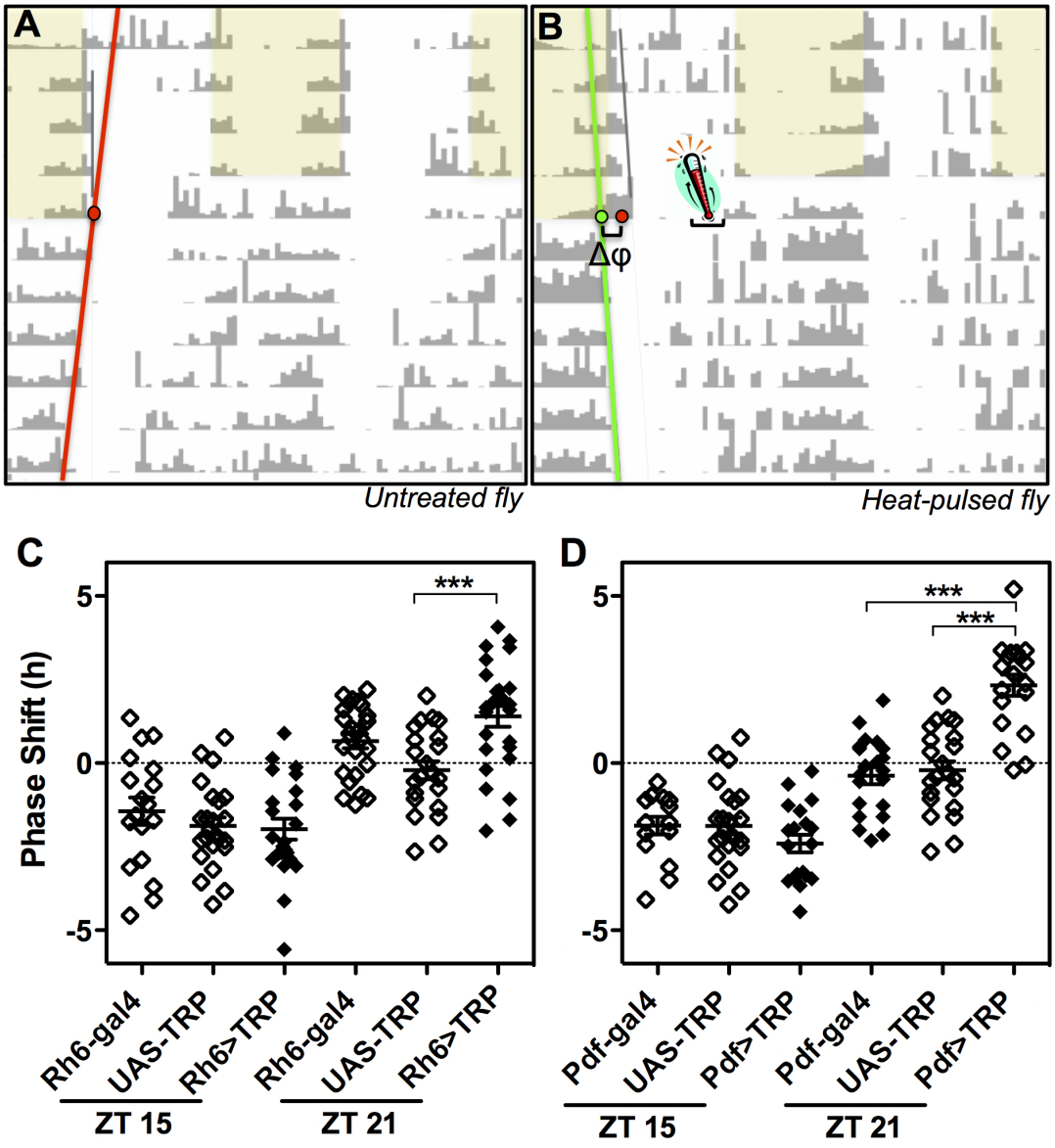

Figure 5.5. Two-time point circadian locomotor rhythm phase response to acute excitation of Rh6⁺ photoreceptors or PDF neurons. Flies were housed in Drosophila Activity Monitors at 22˚C and subjected to a 12-hour light:dark (LD) cycle for 5 days (A-B shaded region). On the last night in LD, a group from each genotype tested was given a 3-hour heat pulse (HP) centered on ZT 15 or ZT 21 (B). A control group from each genotype did not experience a HP (A). The flies were allowed to free-run in constant darkness and constant temperature of 22˚C (DD) for 10 days following the last day in LD. The phase of the evening offset was calculated by fitting a line to the evening offsets from the 10 consecutive days in DD: where this line intersects the x-axis on the last day in LD is the time at which the phase is

measured (A, red dot). The phase of the evening offset was averaged for unpulsed control groups. The phase of the evening offset was measured for each fly in the treated groups in the same way as described above, and was subtracted by the average phase (Δφ) measured from the corresponding unpulsed control genotype to calculate the phase-shift induced by the HP (B). A) Phase shifts (±SEM) induced by a heat pulse at ZT 15 and ZT 21 on single element controls (*;Rh6-gal4/+;* "Rh6-gal4" and *;UAS-TRPA1/+;* "UAS-TRP") and the experimental genotype (*;Rh6-gal4/UAS-TRPA1;* "Rh6>TRP"). C) Phase shifts (±SEM) induced by a heat pulse at ZT 15 and ZT 21 on single element controls (*Pdf-gal4;*;"Pdf-gal4" and *;UAS-TRPA1/+;* "UAS-TRP") and the experimental genotype (*Pdf-gal4;UAS-TRPA1/+;* "Pdf>TRP"). Heat pulses centered on ZT 15 induced a phase delay regardless of TRP expression. Heat pulses centered on ZT 21 appeared to phase advance both experimental genotypes ("Rh6>TRP", "Pdf>TRP") but phases shifts measured for "Rh6>TRP" flies were not significantly different from those of the Gal4 driver ($p=0.0590$). Asterisks (***) indicate significance of $p<0.0001$.

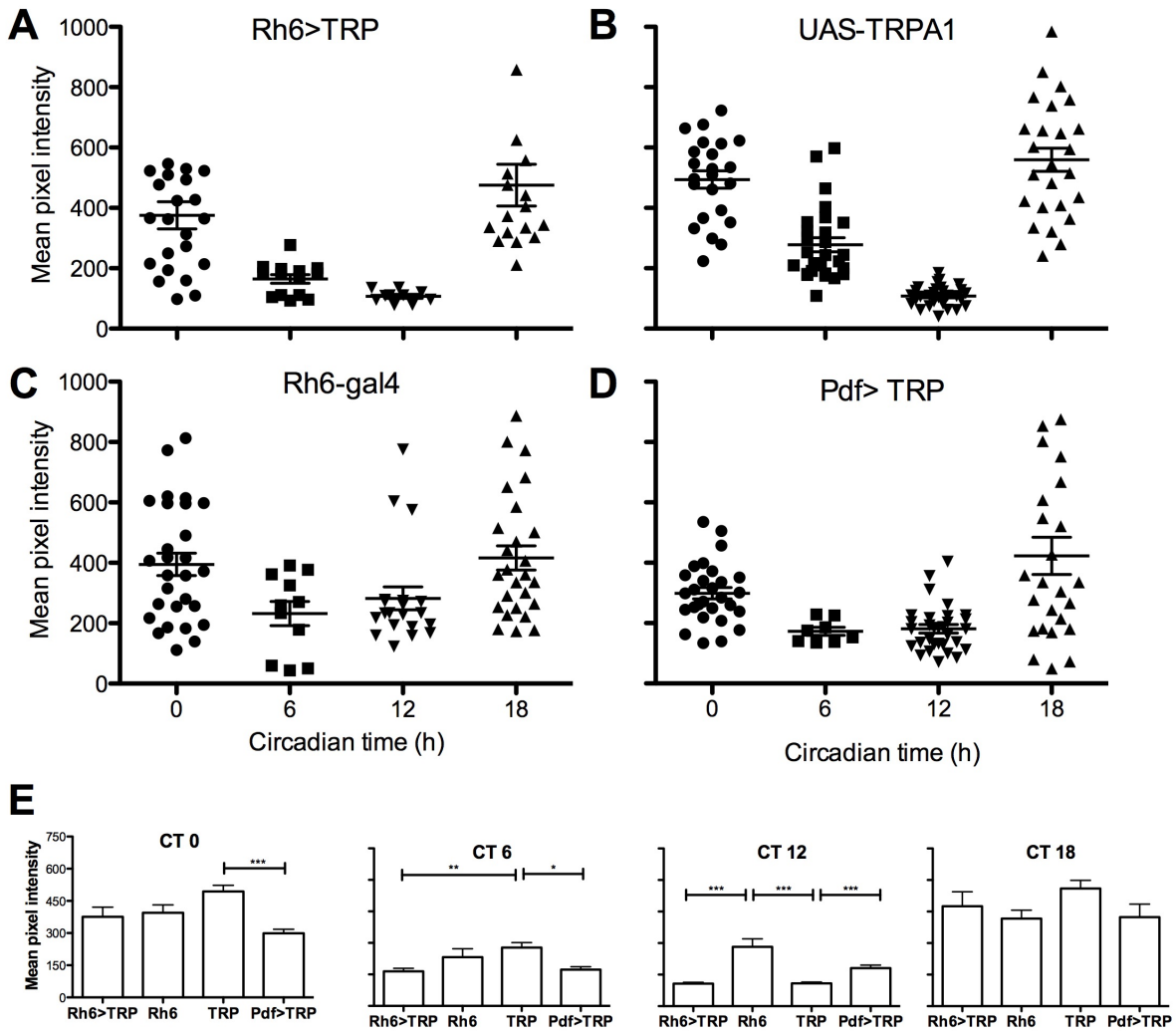

Figure 5.6. Effects of acute excitation of Rh6$^+$ photoreceptors or PDF neurons at an advance zone on PER cycling in the s-LN$_v$. Flies were subjected to a 12-hour light:dark (LD) cycle at 22˚C for 5 days. On the last night in LD, all genotypes were given a 3-hour heat pulse (HP) centered on ZT 21. The flies were allowed to free-run in constant darkness and constant temperature 22˚C (DD) for 3 days following the last day in LD. On the 3rd day in DD, groups of flies from each genotype were fixed at CT 0, 6, 12 or 18. Subsequently, they were co-stained for PDF and PER. PDF was used as a marker for s-LN$_v$ cell bodies, and PER intensity was measured within the region of the cell body. Mean pixel intensity (±SEM) of PER staining is plotted from each genotype A) *;Rh6-gal4/UAS-TRPA1;* "Rh6>TRP"; B) *;UAS-TRPA1/+;* "UAS-TRPA1"; C) *;Rh6-gal4/+;* "Rh6-gal4"; and *Pdf-gal4;UAS-TRPA1/+;* "Pdf>TRP". PER staining from previous studies has been shown to cycle from a peak at CT0, declining throughout subjective day, measuring lowest at CT 12 and rising again at

CT 18, exemplified best in B) “UAS-TRPA1”. PER staining from the s-LN_v of “PDF>TRP” was significantly different from “UAS-TRPA1” at all time points except CT 18 (E). However, PER levels from the s-LN_v of “Rh6>TRP” were only significantly different from “UAS-TRPA1” at ZT 6 and “Rh6-gal4” at ZT 12 (E).

5.7 REFERENCES

Akerboom J, Chen T-W, Wardill TJ, Tian L, Marvin JS, Mutlu S, Calderón NC, Esposti F, Borghuis BG, Sun XR, Gordus A, Orger MB, Portugues R, Engert F, Macklin JJ, Filosa A, Aggarwal A, Kerr RA, Takagi R, Kracun S, Shigetomi E, Khakh BS, Baier H, Lagnado L, Wang SS-H, Bargmann CI, Kimmel BE, Jayaraman V, Svoboda K, Kim DS, Schreiter ER, Looger LL. Optimization of a GCaMP calcium indicator for neural activity imaging. *J. Neurosci.* 32: 13819–13840, 2012.

Allada R, Emery P, Takahashi JS, Rosbash M. Stopping time: the genetics of fly and mouse circadian clocks. *Annu. Rev. Neurosci.* 24: 1091–1119, 2001.

Allada R, White NE, So WV, Hall JC, Rosbash M. A mutant Drosophila homolog of mammalian Clock disrupts circadian rhythms and transcription of period and timeless. *Cell* 93: 791–804, 1998.

Andretic R, Hirsh J. Circadian modulation of dopamine receptor responsiveness in Drosophila melanogaster. *Proc. Natl. Acad. Sci. U. S. A.* 97: 1873–1878, 2000.

Anwyl R. Metabotropic glutamate receptors: electrophysiological properties and role in plasticity. *Brain Res. Brain Res. Rev.* 29: 83–120, 1999.

Ashburner M, Roote J. Laboratory culture of Drosophila. In: *Drosophila protocols*, edited by Sullivan W, Ashburner M, Hawley S. Cold Spring Harbor, NY: Cold Spring Harbor Laboratory Press, 2000.

Aton SJ, Colwell CS, Harmar AJ, Waschek J, Herzog ED. Vasoactive intestinal polypeptide mediates circadian rhythmicity and synchrony in mammalian clock neurons. *Nat. Neurosci.* 8: 476–483, 2005.

Bae K, Lee C, Sidote D, Chuang KY, Edery I. Circadian regulation of a Drosophila homolog of the mammalian Clock gene: PER and TIM function as positive regulators. *Mol. Cell. Biol.* 18: 6142–6151, 1998.

Beavo JA, Brunton LL. Cyclic nucleotide research -- still expanding after half a century. *Nat. Rev. Mol. Cell Biol.* 3: 710–718, 2002.

Beckwith EJ, Lelito KR, Hsu Y-WA, Medina BM, Shafer O, Ceriani MF, de la Iglesia HO. Functional conservation of clock output signaling between flies and intertidal crabs. *J. Biol. Rhythms* 26: 518–529, 2011.

Benzer S. From the gene to behavior. *JAMA J. Am. Med. Assoc.* 218: 1015–1022, 1971.

Borland G, Smith BO, Yarwood SJ. EPAC proteins transduce diverse cellular actions of cAMP. *Br. J. Pharmacol.* 158: 70–86, 2009.

Börner S, Schwede F, Schlipp A, Berisha F, Calebiro D, Lohse MJ, Nikolaev VO. FRET measurements of intracellular cAMP concentrations and cAMP analog permeability in intact cells. *Nat. Protoc.* 6: 427–438, 2011.

Bossy B, Ballivet M, Spierer P. Conservation of neural nicotinic acetylcholine receptors from Drosophila to vertebrate central nervous systems. *EMBO J.* 7: 611–618, 1988.

Brand AH, Perrimon N. Targeted gene expression as a means of altering cell fates and generating dominant phenotypes. *Dev. Camb. Engl.* 118: 401–415, 1993.

Busza A, Emery-Le M, Rosbash M, Emery P. Roles of the two Drosophila CRYPTOCHROME structural domains in circadian photoreception. *Science* 304: 1503–1506, 2004.

Campbell SS, Tobler I. Animal sleep: a review of sleep duration across phylogeny. *Neurosci. Biobehav. Rev.* 8: 269–300, 1984.

Cao G, Nitabach MN. Circadian control of membrane excitability in Drosophila melanogaster lateral ventral clock neurons. *J. Neurosci.* 28: 6493–6501, 2008.

Cao G, Platisa J, Pieribone VA, Raccuglia D, Kunst M, Nitabach MN. Genetically targeted optical electrophysiology in intact neural circuits. *Cell* 154: 904–913, 2013.

Ceriani MF, Darlington TK, Staknis D, Más P, Petti AA, Weitz CJ, Kay SA. Light-dependent sequestration of TIMELESS by CRYPTOCHROME. *Science* 285: 553–556, 1999.

Chen T-W, Wardill TJ, Sun Y, Pulver SR, Renninger SL, Baohan A, Schreiter ER, Kerr RA, Orger MB, Jayaraman V, Looger LL, Svoboda K, Kim DS. Ultrasensitive fluorescent proteins for imaging neuronal activity. *Nature* 499: 295–300, 2013.

Chou WH, Huber A, Bentrop J, Schulz S, Schwab K, Chadwell LV, Paulsen R, Britt SG. Patterning of the R7 and R8 photoreceptor cells of Drosophila: evidence for induced and default cell-fate specification. *Dev. Camb. Engl.* 126: 607–616, 1999.

Chung BY, Kilman VL, Keath JR, Pitman JL, Allada R. The GABA(A) receptor RDL acts in peptidergic PDF neurons to promote sleep in Drosophila. *Curr. Biol. CB* 19: 386–390, 2009.

Crocker A, Sehgal A. Octopamine regulates sleep in drosophila through protein kinase A-dependent mechanisms. *J. Neurosci.* 28: 9377–9385, 2008.

Crocker A, Shahidullah M, Levitan IB, Sehgal A. Identification of a neural circuit that underlies the effects of octopamine on sleep:wake behavior. *Neuron* 65: 670–681, 2010.

Curtin KD, Huang ZJ, Rosbash M. Temporally regulated nuclear entry of the Drosophila period protein contributes to the circadian clock. *Neuron* 14: 365–372, 1995.

Dahdal D, Reeves DC, Ruben M, Akabas MH, Blau J. Drosophila pacemaker neurons require g protein signaling and GABAergic inputs to generate twenty-four hour behavioral rhythms. *Neuron* 68: 964–977, 2010.

Daniels RW, Gelfand MV, Collins CA, DiAntonio A. Visualizing glutamatergic cell bodies and synapses in Drosophila larval and adult CNS. *J. Comp. Neurol.* 508: 131–152, 2008.

Darlington TK, Wager-Smith K, Ceriani MF, Staknis D, Gekakis N, Steeves TD, Weitz CJ, Takahashi JS, Kay SA. Closing the circadian loop: CLOCK-induced transcription of its own inhibitors per and tim. *Science* 280: 1599–1603, 1998a.

Darlington TK, Wager-Smith K, Ceriani MF, Staknis D, Gekakis N, Steeves TD, Weitz CJ, Takahashi JS, Kay SA. Closing the circadian loop: CLOCK-induced transcription of its own inhibitors per and tim. *Science* 280: 1599–1603, 1998b.

Dingledine R, Borges K, Bowie D, Traynelis SF. The glutamate receptor ion channels. *Pharmacol. Rev.* 51: 7–61, 1999.

DiPilato LM, Cheng X, Zhang J. Fluorescent indicators of cAMP and Epac activation reveal differential dynamics of cAMP signaling within discrete subcellular compartments. *Proc. Natl. Acad. Sci. U. S. A.* 101: 16513–16518, 2004.

Dowse HB, Hall JC, Ringo JM. Circadian and ultradian rhythms in period mutants of Drosophila melanogaster. *Behav. Genet.* 17: 19–35, 1987.

Dunlap JC. Molecular bases for circadian clocks. *Cell* 96: 271–290, 1999.

Dushay MS, Konopka RJ, Orr D, Greenacre ML, Kyriacou CP, Rosbash M, Hall JC. Phenotypic and genetic analysis of Clock, a new circadian rhythm mutant in Drosophila melanogaster. *Genetics* 125: 557–578, 1990.

Duvall LB, Taghert PH. The circadian neuropeptide PDF signals preferentially through a specific adenylate cyclase isoform AC3 in M pacemakers of Drosophila. *PLoS Biol.* 10: e1001337, 2012.

Emery P, So WV, Kaneko M, Hall JC, Rosbash M. CRY, a Drosophila clock and light-regulated cryptochrome, is a major contributor to circadian rhythm resetting and photosensitivity. *Cell* 95: 669–679, 1998.

Emery P, Stanewsky R, Helfrich-Förster C, Emery-Le M, Hall JC, Rosbash M. Drosophila CRY is a deep brain circadian photoreceptor. *Neuron* 26: 493–504, 2000.

Feinberg EH, Vanhoven MK, Bendesky A, Wang G, Fetter RD, Shen K, Bargmann CI. GFP Reconstitution Across Synaptic Partners (GRASP) defines cell contacts and synapses in living nervous systems. *Neuron* 57: 353–363, 2008.

Fiala A, Spall T, Diegelmann S, Eisermann B, Sachse S, Devaud J-M, Buchner E, Galizia CG. Genetically expressed cameleon in Drosophila melanogaster is used to visualize olfactory information in projection neurons. *Curr. Biol. CB* 12: 1877–1884, 2002.

Fogle KJ, Parson KG, Dahm NA, Holmes TC. CRYPTOCHROME is a blue-light sensor that regulates neuronal firing rate. *Science* 331: 1409–1413, 2011.

Friggi-Grelin F, Coulom H, Meller M, Gomez D, Hirsh J, Birman S. Targeted gene expression in Drosophila dopaminergic cells using regulatory sequences from tyrosine hydroxylase. *J. Neurobiol.* 54: 618–627, 2003.

Gengs C, Leung H-T, Skingsley DR, Iovchev MI, Yin Z, Semenov EP, Burg MG, Hardie RC, Pak WL. The target of Drosophila photoreceptor synaptic transmission is a histamine-gated chloride channel encoded by ort (hclA). *J. Biol. Chem.* 277: 42113–42120, 2002.

Gervasi N, Tchénio P, Preat T. PKA dynamics in a Drosophila learning center: coincidence detection by rutabaga adenylyl cyclase and spatial regulation by dunce phosphodiesterase. *Neuron* 65: 516–529, 2010.

Gloerich M, Bos JL. Epac: defining a new mechanism for cAMP action. *Annu. Rev. Pharmacol. Toxicol.* 50: 355–375, 2010.

Gordon MD, Scott K. Motor control in a Drosophila taste circuit. *Neuron* 61: 373–384, 2009.

Greenspan RJ. *Fly pushing, the theory and practice of Drosophila genetics*. 2nd ed. Cold Spring Harbor, NY: Cold Spring Harbor Press, 2004.

Grima B, Chélot E, Xia R, Rouyer F. Morning and evening peaks of activity rely on different clock neurons of the Drosophila brain. *Nature* 431: 869–873, 2004.

Gu H, O'Dowd DK. Cholinergic synaptic transmission in adult Drosophila Kenyon cells in situ. *J. Neurosci.* 26: 265–272, 2006.

Guerrero G, Isacoff EY. Genetically encoded optical sensors of neuronal activity and cellular function. *Curr. Opin. Neurobiol.* 11: 601–607, 2001.

Gummadova JO, Coutts GA, Glossop NRJ. Analysis of the Drosophila Clock promoter reveals heterogeneity in expression between subgroups of central oscillator cells and identifies a novel enhancer region. *J. Biol. Rhythms* 24: 353–367, 2009.

Hamada FN, Rosenzweig M, Kang K, Pulver SR, Ghezzi A, Jegla TJ, Garrity PA. An internal thermal sensor controlling temperature preference in Drosophila. *Nature* 454: 217–220, 2008.

Hamasaka Y, Nässel DR. Mapping of serotonin, dopamine, and histamine in relation to different clock neurons in the brain of Drosophila. *J. Comp. Neurol.* 494: 314–330, 2006.

Hamasaka Y, Rieger D, Parmentier M-L, Grau Y, Helfrich-Förster C, Nässel DR. Glutamate and its metabotropic receptor in Drosophila clock neuron circuits. *J. Comp. Neurol.* 505: 32–45, 2007.

Hamasaka Y, Wegener C, Nässel DR. GABA modulates Drosophila circadian clock neurons via GABAB receptors and decreases in calcium. *J. Neurobiol.* 65: 225–240, 2005.

Hamblen-Coyle MJ, Wheeler DA, Rutila JE, Rosbash M, Hall JC. Behavior of period-altered circadian rhythm mutants ofDrosophila in light: Dark cycles (Diptera: Drosophilidae). *J. Insect Behav.* 5: 417–446, 1992.

Hao H, Allen DL, Hardin PE. A circadian enhancer mediates PER-dependent mRNA cycling in Drosophila melanogaster. *Mol. Cell. Biol.* 17: 3687–3693, 1997.

Hardie RC. Is histamine a neurotransmitter in insect photoreceptors? *J. Comp. Physiol. [A]* 161: 201–213, 1987.

Hardie RC. A histamine-activated chloride channel involved in neurotransmission at a photoreceptor synapse. *Nature* 339: 704–706, 1989a.

Hardie RC. A histamine-activated chloride channel involved in neurotransmission at a photoreceptor synapse. *Nature* 339: 704–706, 1989b.

Hardin PE, Hall JC, Rosbash M. Feedback of the Drosophila period gene product on circadian cycling of its messenger RNA levels. *Nature* 343: 536–540, 1990.

Helfrich-Förster C, Edwards T, Yasuyama K, Wisotzki B, Schneuwly S, Stanewsky R, Meinertzhagen IA, Hofbauer A. The extraretinal eyelet of Drosophila: development, ultrastructure, and putative circadian function. *J. Neurosci.* 22: 9255–9266, 2002.

Helfrich-Förster C, Homberg U. Pigment-dispersing hormone-immunoreactive neurons in the nervous system of wild-type Drosophila melanogaster and of several mutants with altered circadian rhythmicity. *J. Comp. Neurol.* 337: 177–190, 1993.

Helfrich-Förster C, Winter C, Hofbauer A, Hall JC, Stanewsky R. The circadian clock of fruit flies is blind after elimination of all known photoreceptors. *Neuron* 30: 249–261, 2001.

Helfrich-Förster C, Yoshii T, Wülbeck C, Grieshaber E, Rieger D, Bachleitner W, Cusamano P, Rouyer F. The lateral and dorsal neurons of Drosophila melanogaster: new insights about their morphology and function. *Cold Spring Harb. Symp. Quant. Biol.* 72: 517–525, 2007.

Helfrich-Förster C. The period clock gene is expressed in central nervous system neurons which also produce a neuropeptide that reveals the projections of circadian pacemaker cells within the brain of Drosophila melanogaster. *Proc. Natl. Acad. Sci. U. S. A.* 92: 612–616, 1995.

Helfrich-Förster C. Differential control of morning and evening components in the activity rhythm of Drosophila melanogaster--sex-specific differences suggest a different quality of activity. *J. Biol. Rhythms* 15: 135–154, 2000.

Helfrich-Förster C. The circadian system of Drosophila melanogaster and its light input pathways. *Zool. Jena Ger.* 105: 297–312, 2002.

Helfrich-Förster C. The neuroarchitecture of the circadian clock in the brain of Drosophila melanogaster. *Microsc. Res. Tech.* 62: 94–102, 2003.

Helfrich-Förster C. The circadian clock in the brain: a structural and functional comparison between mammals and insects. *J. Comp. Physiol. A Neuroethol. Sens. Neural. Behav. Physiol.* 190: 601–613, 2004.

Helfrich-Förster C. Neurobiology of the fruit fly's circadian clock. *Genes Brain Behav.* 4: 65–76, 2005.

Hendricks JC, Sehgal A, Pack AI. The need for a simple animal model to understand sleep. *Prog. Neurobiol.* 61: 339–351, 2000.

Hermann C, Yoshii T, Dusik V, Helfrich-Förster C. Neuropeptide F immunoreactive clock neurons modify evening locomotor activity and free-running period in Drosophila melanogaster. *J. Comp. Neurol.* 520: 970–987, 2012.

Hofbauer A, Buchner E. Does Drosophila have seven eyes? *Naturwissen* 76: 335–336, 1989.

Hong S-T, Bang S, Paik D, Kang J, Hwang S, Jeon K, Chun B, Hyun S, Lee Y, Kim J. Histamine and its receptors modulate temperature-preference behaviors in Drosophila. *J. Neurosci.* 26: 7245–7256, 2006.

Huber A, Schulz S, Bentrop J, Groell C, Wolfrum U, Paulsen R. Molecular cloning of Drosophila Rh6 rhodopsin: the visual pigment of a subset of R8 photoreceptor cells. *FEBS Lett.* 406: 6–10, 1997.

Hyun S, Lee Y, Hong S-T, Bang S, Paik D, Kang J, Shin J, Lee J, Jeon K, Hwang S, Bae E, Kim J. Drosophila GPCR Han is a receptor for the circadian clock neuropeptide PDF. *Neuron* 48: 267–278, 2005.

Im SH, Taghert PH. PDF receptor expression reveals direct interactions between circadian oscillators in Drosophila. *J. Comp. Neurol.* 518: 1925–1945, 2010.

Jan LY, Jan YN. L-glutamate as an excitatory transmitter at the Drosophila larval neuromuscular junction. *J. Physiol.* 262: 215–236, 1976a.

Jan LY, Jan YN. Properties of the larval neuromuscular junction in Drosophila melanogaster. *J. Physiol.* 262: 189–214, 1976b.

Jenett A, Rubin GM, Ngo T-TB, Shepherd D, Murphy C, Dionne H, Pfeiffer BD, Cavallaro A, Hall D, Jeter J, Iyer N, Fetter D, Hausenfluck JH, Peng H, Trautman ET, Svirskas RR, Myers EW, Iwinski ZR, Aso Y, DePasquale GM, Enos A, Hulamm P, Lam SCB, Li H-H, Laverty TR, Long F, Qu L, Murphy SD, Rokicki K, Safford T, Shaw K, Simpson JH, Sowell A, Tae S, Yu Y, Zugates CT. A GAL4-driver line resource for Drosophila neurobiology. *Cell Rep.* 2: 991–1001, 2012.

Johard HAD, Yoishii T, Dircksen H, Cusumano P, Rouyer F, Helfrich-Förster C, Nässel DR. Peptidergic clock neurons in Drosophila: ion transport peptide and short neuropeptide F in subsets of dorsal and ventral lateral neurons. *J. Comp. Neurol.* 516: 59–73, 2009.

Johnson C, Elliot J, Foster RG, Ken-Ichi H, Kronauer R. Fundemental properties of circadian rhythms. In: *Chronobiology: biological timekeeping*, edited by Dunlap JC, Loros JJ, Decoursey PJ. Massachusetts: Sinauer Associates, Inc., 2004.

Kaneko M, Hall JC. Neuroanatomy of cells expressing clock genes in Drosophila: transgenic manipulation of the period and timeless genes to mark the perikarya of circadian pacemaker neurons and their projections. *J. Comp. Neurol.* 422: 66–94, 2000.

Kaneko M, Helfrich-Förster C, Hall JC. Spatial and temporal expression of the period and timeless genes in the developing nervous system of Drosophila: newly identified pacemaker candidates and novel features of clock gene product cycling. *J. Neurosci.* 17: 6745–6760, 1997.

Kaushik R, Nawathean P, Busza A, Murad A, Emery P, Rosbash M. PER-TIM interactions with the photoreceptor cryptochrome mediate circadian temperature responses in Drosophila. *PLoS Biol.* 5: e146, 2007.

Keene AC, Mazzoni EO, Zhen J, Younger MA, Yamaguchi S, Blau J, Desplan C, Sprecher SG. Distinct visual pathways mediate Drosophila larval light avoidance and circadian clock entrainment. *J. Neurosci.* 31: 6527–6534, 2011.

Keene AC, Sprecher SG. Seeing the light: photobehavior in fruit fly larvae. *Trends Neurosci.* 35: 104–110, 2012.

Kim EY, Edery I. Balance between DBT/CKIepsilon kinase and protein phosphatase activities regulate phosphorylation and stability of Drosophila CLOCK protein. *Proc. Natl. Acad. Sci. U. S. A.* 103: 6178–6183, 2006.

Kistenpfennig C, Hirsh J, Yoshii T, Helfrich-Förster C. Phase-shifting the fruit fly clock without cryptochrome. *J. Biol. Rhythms* 27: 117–125, 2012.

Kloss B, Price JL, Saez L, Blau J, Rothenfluh A, Wesley CS, Young MW. The Drosophila clock gene double-time encodes a protein closely related to human casein kinase Iepsilon. *Cell* 94: 97–107, 1998.

Koh K, Zheng X, Sehgal A. JETLAG resets the Drosophila circadian clock by promoting light-induced degradation of TIMELESS. *Science* 312: 1809–1812, 2006.

Kolodziejczyk A, Sun X, Meinertzhagen IA, Nässel DR. Glutamate, GABA and acetylcholine signaling components in the lamina of the Drosophila visual system. *PloS One* 3: e2110, 2008.

Konopka RJ, Benzer S. Clock mutants of Drosophila melanogaster. *Proc. Natl. Acad. Sci. U. S. A.* 68: 2112–2116, 1971.

Kula-Eversole E, Nagoshi E, Shang Y, Rodriguez J, Allada R, Rosbash M. Surprising gene expression patterns within and between PDF-containing circadian neurons in Drosophila. *Proc. Natl. Acad. Sci. U. S. A.* 107: 13497–13502, 2010.

Lai S-L, Lee T. Genetic mosaic with dual binary transcriptional systems in Drosophila. *Nat. Neurosci.* 9: 703–709, 2006.

Lear BC, Zhang L, Allada R. The neuropeptide PDF acts directly on evening pacemaker neurons to regulate multiple features of circadian behavior. *PLoS Biol.* 7: e1000154, 2009.

Lee C, Bae K, Edery I. PER and TIM inhibit the DNA binding activity of a Drosophila CLOCK-CYC/dBMAL1 heterodimer without disrupting formation of the heterodimer: a basis for circadian transcription. *Mol. Cell. Biol.* 19: 5316–5325, 1999.

Lee C, Etchegaray JP, Cagampang FR, Loudon AS, Reppert SM. Posttranslational mechanisms regulate the mammalian circadian clock. *Cell* 107: 855–867, 2001.

Lelito KR, Shafer OT. Reciprocal cholinergic and GABAergic modulation of the small ventrolateral pacemaker neurons of Drosophila's circadian clock neuron network. *J. Neurophysiol.* 107: 2096–2108, 2012a.

Lelito KR, Shafer OT. Imaging cAMP Dynamics in the Drosophila Brain with the Genetically Encoded Sensor Epac1-Camps. In: *Genetically Encoded Functional Indicators*, edited by Martin J-R. Humana Press, p. 149–168.

Levine JD, Casey CI, Kalderon DD, Jackson FR. Altered circadian pacemaker functions and cyclic AMP rhythms in the Drosophila learning mutant dunce. *Neuron* 13: 967–974, 1994.

Lima SQ, Miesenböck G. Remote control of behavior through genetically targeted photostimulation of neurons. *Cell* 121: 141–152, 2005.

Lin FJ, Song W, Meyer-Bernstein E, Naidoo N, Sehgal A. Photic signaling by cryptochrome in the Drosophila circadian system. *Mol. Cell. Biol.* 21: 7287–7294, 2001.

Lissandron V, Rossetto MG, Erbguth K, Fiala A, Daga A, Zaccolo M. Transgenic fruit-flies expressing a FRET-based sensor for in vivo imaging of cAMP dynamics. *Cell. Signal.* 19: 2296–2303, 2007.

Lissandron V, Terrin A, Collini M, D'alfonso L, Chirico G, Pantano S, Zaccolo M. Improvement of a FRET-based indicator for cAMP by linker design and stabilization of donor-acceptor interaction. *J. Mol. Biol.* 354: 546–555, 2005.

Littleton JT, Ganetzky B. Ion channels and synaptic organization: analysis of the Drosophila genome. *Neuron* 26: 35–43, 2000.

Malpel S, Klarsfeld A, Rouyer F. Larval optic nerve and adult extra-retinal photoreceptors sequentially associate with clock neurons during Drosophila brain development. *Dev. Camb. Engl.* 129: 1443–1453, 2002.

Martinek S, Inonog S, Manoukian AS, Young MW. A role for the segment polarity gene shaggy/GSK-3 in the Drosophila circadian clock. *Cell* 105: 769–779, 2001.

Mazzoni EO, Desplan C, Blau J. Circadian pacemaker neurons transmit and modulate visual information to control a rapid behavioral response. *Neuron* 45: 293–300, 2005.

McCarthy EV, Wu Y, Decarvalho T, Brandt C, Cao G, Nitabach MN. Synchronized bilateral synaptic inputs to Drosophila melanogaster neuropeptidergic rest/arousal neurons. *J. Neurosci.* 31: 8181–8193, 2011.

McDonald MJ, Rosbash M, Emery P. Wild-type circadian rhythmicity is dependent on closely spaced E boxes in the Drosophila timeless promoter. *Mol. Cell. Biol.* 21: 1207–1217, 2001.

Mealey-Ferrara ML, Montalvo AG, Hall JC. Effects of combining a cryptochrome mutation with other visual-system variants on entrainment of locomotor and adult-emergence rhythms in Drosophila. *J. Neurogenet.* 17: 171–221, 2003.

Mertens I, Vandingenen A, Johnson EC, Shafer OT, Li W, Trigg JS, De Loof A, Schoofs L, Taghert PH. PDF receptor signaling in Drosophila contributes to both circadian and geotactic behaviors. *Neuron* 48: 213–219, 2005.

Miesenböck G, Kevrekidis IG. Optical imaging and control of genetically designated neurons in functioning circuits. *Annu. Rev. Neurosci.* 28: 533–563, 2005.

Miesenböck G. The optogenetic catechism. *Science* 326: 395–399, 2009.

Naidoo N, Song W, Hunter-Ensor M, Sehgal A. A role for the proteasome in the light response of the timeless clock protein. *Science* 285: 1737–1741, 1999.

Nakagawa T, Vosshall LB. Controversy and consensus: noncanonical signaling mechanisms in the insect olfactory system. *Curr. Opin. Neurobiol.* 19: 284–292, 2009.

Nakai J, Ohkura M, Imoto K. A high signal-to-noise Ca(2+) probe composed of a single green fluorescent protein. *Nat. Biotechnol.* 19: 137–141, 2001.

Nässel DR, Holmqvist MH, Hardie RC, Håkanson R, Sundler F. Histamine-like immunoreactivity in photoreceptors of the compound eyes and ocelli of the flies Calliphora erythrocephala and Musca domestica. *Cell Tissue Res.* 253: 639–646, 1988.

Nässel DR. Histamine in the brain of insects: a review. *Microsc. Res. Tech.* 44: 121–136, 1999.

Nikolaev VO, Bünemann M, Hein L, Hannawacker A, Lohse MJ. Novel single chain cAMP sensors for receptor-induced signal propagation. *J. Biol. Chem.* 279: 37215–37218, 2004.

Nikolaev VO, Lohse MJ. Monitoring of cAMP synthesis and degradation in living cells. *Physiol. Bethesda Md* 21: 86–92, 2006.

O'Neill JS, Maywood ES, Chesham JE, Takahashi JS, Hastings MH. cAMP-dependent signaling as a core component of the mammalian circadian pacemaker. *Science* 320: 949–953, 2008.

Pantazis A, Segaran A, Liu C-H, Nikolaev A, Rister J, Thum AS, Roeder T, Semenov E, Juusola M, Hardie RC. Distinct roles for two histamine receptors (hclA and hclB) at the Drosophila photoreceptor synapse. *J. Neurosci.* 28: 7250–7259, 2008.

Parisky KM, Agosto J, Pulver SR, Shang Y, Kuklin E, Hodge JJL, Kang K, Kang K, Liu X, Garrity PA, Rosbash M, Griffith LC. PDF cells are a GABA-responsive wake-promoting component of the Drosophila sleep circuit. *Neuron* 60: 672–682, 2008.

Park D, Griffith LC. Electrophysiological and anatomical characterization of PDF-positive clock neurons in the intact adult Drosophila brain. *J. Neurophysiol.* 95: 3955–3960, 2006.

Park JH, Hall JC. Isolation and chronobiological analysis of a neuropeptide pigment-dispersing factor gene in Drosophila melanogaster. *J. Biol. Rhythms* 13: 219–228, 1998.

Park JH, Helfrich-Förster C, Lee G, Liu L, Rosbash M, Hall JC. Differential regulation of circadian pacemaker output by separate clock genes in Drosophila. *Proc. Natl. Acad. Sci. U. S. A.* 97: 3608–3613, 2000.

Peschel N, Veleri S, Stanewsky R. Veela defines a molecular link between Cryptochrome and Timeless in the light-input pathway to Drosophila's circadian clock. *Proc. Natl. Acad. Sci. U. S. A.* 103: 17313–17318, 2006.

Pfeiffer BD, Ngo T-TB, Hibbard KL, Murphy C, Jenett A, Truman JW, Rubin GM. Refinement of tools for targeted gene expression in Drosophila. *Genetics* 186: 735–755, 2010.

Pichaud F, Desplan C. A new visualization approach for identifying mutations that affect differentiation and organization of the Drosophila ommatidia. *Dev. Camb. Engl.* 128: 815–826, 2001.

Van den Pol AN. The hypothalamic suprachiasmatic nucleus of rat: intrinsic anatomy. *J. Comp. Neurol.* 191: 661–702, 1980.

Pollack I, Hofbauer A. Histamine-like immunoreactivity in the visual system and brain of Drosophila melanogaster. *Cell Tissue Res.* 266: 391–398, 1991.

Ponsioen B, Zhao J, Riedl J, Zwartkruis F, van der Krogt G, Zaccolo M, Moolenaar WH, Bos JL, Jalink K. Detecting cAMP-induced Epac activation by fluorescence resonance energy transfer: Epac as a novel cAMP indicator. *EMBO Rep.* 5: 1176–1180, 2004.

Price JL, Blau J, Rothenfluh A, Abodeely M, Kloss B, Young MW. double-time is a novel Drosophila clock gene that regulates PERIOD protein accumulation. *Cell* 94: 83–95, 1998.

Pulver SR, Pashkovski SL, Hornstein NJ, Garrity PA, Griffith LC. Temporal dynamics of neuronal activation by Channelrhodopsin-2 and TRPA1 determine behavioral output in Drosophila larvae. *J. Neurophysiol.* 101: 3075–3088, 2009.

Pyza E, Meinertzhagen IA. Daily rhythmic changes of cell size and shape in the first optic neuropil in Drosophila melanogaster. *J. Neurobiol.* 40: 77–88, 1999.

Renn SC, Park JH, Rosbash M, Hall JC, Taghert PH. A pdf neuropeptide gene mutation and ablation of PDF neurons each cause severe abnormalities of behavioral circadian rhythms in Drosophila. *Cell* 99: 791–802, 1999.

Rieger D, Stanewsky R, Helfrich-Förster C. Cryptochrome, compound eyes, Hofbauer-Buchner eyelets, and ocelli play different roles in the entrainment and masking pathway of the locomotor activity rhythm in the fruit fly Drosophila melanogaster. *J. Biol. Rhythms* 18: 377–391, 2003.

Rietveld WJ, Minors DS, Waterhouse JM. Circadian rhythms and masking: an overview. *Chronobiol. Int.* 10: 306–312, 1993.

Rutila JE, Suri V, Le M, So WV, Rosbash M, Hall JC. CYCLE is a second bHLH-PAS clock protein essential for circadian rhythmicity and transcription of Drosophila period and timeless. *Cell* 93: 805–814, 1998.

Salvaterra PM, Kitamoto T. Drosophila cholinergic neurons and processes visualized with Gal4/UAS-GFP. *Brain Res. Gene Expr. Patterns* 1: 73–82, 2001.

Sarthy PV. Histamine: a neurotransmitter candidate for Drosophila photoreceptors. *J. Neurochem.* 57: 1757–1768, 1991.

Schild D, Restrepo D. Transduction mechanisms in vertebrate olfactory receptor cells. *Physiol. Rev.* 78: 429–466, 1998.

Schuster R, Phannavong B, Schröder C, Gundelfinger ED. Immunohistochemical localization of a ligand-binding and a structural subunit of nicotinic acetylcholine receptors in the central nervous system of Drosophila melanogaster. *J. Comp. Neurol.* 335: 149–162, 1993.

Sehgal A, Rothenfluh-Hilfiker A, Hunter-Ensor M, Chen Y, Myers MP, Young MW. Rhythmic expression of timeless: a basis for promoting circadian cycles in period gene autoregulation. *Science* 270: 808–810, 1995.

Shafer OT, Helfrich-Förster C, Renn SCP, Taghert PH. Reevaluation of Drosophila melanogaster's neuronal circadian pacemakers reveals new neuronal classes. *J. Comp. Neurol.* 498: 180–193, 2006a.

Shafer OT, Helfrich-Förster C, Renn SCP, Taghert PH. Reevaluation of Drosophila melanogaster's neuronal circadian pacemakers reveals new neuronal classes. *J. Comp. Neurol.* 498: 180–193, 2006b.

Shafer OT, Kim DJ, Dunbar-Yaffe R, Nikolaev VO, Lohse MJ, Taghert PH. Widespread receptivity to neuropeptide PDF throughout the neuronal circadian

clock network of Drosophila revealed by real-time cyclic AMP imaging. *Neuron* 58: 223–237, 2008.

Shafer OT, Rosbash M, Truman JW. Sequential nuclear accumulation of the clock proteins period and timeless in the pacemaker neurons of Drosophila melanogaster. *J. Neurosci.* 22: 5946–5954, 2002.

Shakiryanova D, Levitan ES. Prolonged presynaptic posttetanic cyclic GMP signaling in Drosophila motoneurons. *Proc. Natl. Acad. Sci. U. S. A.* 105: 13610–13613, 2008.

Shang Y, Griffith LC, Rosbash M. Light-arousal and circadian photoreception circuits intersect at the large PDF cells of the Drosophila brain. *Proc. Natl. Acad. Sci. U. S. A.* 105: 19587–19594, 2008.

Shang Y, Haynes P, Pírez N, Harrington KI, Guo F, Pollack J, Hong P, Griffith LC, Rosbash M. Imaging analysis of clock neurons reveals light buffers the wake-promoting effect of dopamine. *Nat. Neurosci.* 14: 889–895, 2011.

Shaw PJ, Cirelli C, Greenspan RJ, Tononi G. Correlates of sleep and waking in Drosophila melanogaster. *Science* 287: 1834–1837, 2000.

Shearman LP, Zylka MJ, Weaver DR, Kolakowski LF Jr, Reppert SM. Two period homologs: circadian expression and photic regulation in the suprachiasmatic nuclei. *Neuron* 19: 1261–1269, 1997.

Sheeba V, Fogle KJ, Kaneko M, Rashid S, Chou Y-T, Sharma VK, Holmes TC. Large Ventral Lateral Neurons Modulate Arousal and Sleep in Drosophila. *Curr. Biol.* 18: 1537–1545, 2008a.

Sheeba V, Gu H, Sharma VK, O'Dowd DK, Holmes TC. Circadian- and light-dependent regulation of resting membrane potential and spontaneous action potential firing of Drosophila circadian pacemaker neurons. *J. Neurophysiol.* 99: 976–988, 2008b.

Shiga Y, Tanaka-Matakatsu M, Hayashi S. A nuclear GFP/β-galactosidase fusion protein as a marker for morphogenesis in living Drosophila. *Dev. Growth Differ.* 38: 99–106, 1996.

Shigeyoshi Y, Taguchi K, Yamamoto S, Takekida S, Yan L, Tei H, Moriya T, Shibata S, Loros JJ, Dunlap JC, Okamura H. Light-induced resetting of a mammalian circadian clock is associated with rapid induction of the mPer1 transcript. *Cell* 91: 1043–1053, 1997.

Simpson JH, Stephen F. Genetic dissection of neural circuits and behavior. In: *Advances in genetics*, edited by Goodwin SF. San Diego, CA: Academic Press (Elsevier), 2009.

De Souza NJ, Dohadwalla AN, Reden J. Forskolin: a labdane diterpenoid with antihypertensive, positive inotropic, platelet aggregation inhibitory, and adenylate cyclase activating properties. *Med. Res. Rev.* 3: 201–219, 1983.

Spaulding SW. The ways in which hormones change cyclic adenosine 3',5'-monophosphate-dependent protein kinase subunits, and how such changes affect cell behavior. *Endocr. Rev.* 14: 632–650, 1993.

Sprecher SG, Desplan C. Switch of rhodopsin expression in terminally differentiated Drosophila sensory neurons. *Nature* 454: 533–537, 2008.

Sprecher SG, Pichaud F, Desplan C. Adult and larval photoreceptors use different mechanisms to specify the same Rhodopsin fates. *Genes Dev.* 21: 2182–2195, 2007.

Stanewsky R, Kaneko M, Emery P, Beretta B, Wager-Smith K, Kay SA, Rosbash M, Hall JC. The cryb mutation identifies cryptochrome as a circadian photoreceptor in Drosophila. *Cell* 95: 681–692, 1998.

Stanewsky R. Genetic analysis of the circadian system in Drosophila melanogaster and mammals. *J. Neurobiol.* 54: 111–147, 2003.

Stewart BA, Atwood HL, Renger JJ, Wang J, Wu CF. Improved stability of Drosophila larval neuromuscular preparations in haemolymph-like physiological solutions. *J. Comp. Physiol. [A]* 175: 179–191, 1994.

Stoleru D, Peng Y, Agosto J, Rosbash M. Coupled oscillators control morning and evening locomotor behaviour of Drosophila. *Nature* 431: 862–868, 2004.

Suri V, Qian Z, Hall JC, Rosbash M. Evidence that the TIM light response is relevant to light-induced phase shifts in Drosophila melanogaster. *Neuron* 21: 225–234, 1998.

Taghert PH, Shafer OT. Mechanisms of clock output in the Drosophila circadian pacemaker system. *J. Biol. Rhythms* 21: 445–457, 2006.

Talsma AD, Christov CP, Terriente-Felix A, Linneweber GA, Perea D, Wayland M, Shafer OT, Miguel-Aliaga I. Remote control of renal physiology by the intestinal neuropeptide pigment-dispersing factor in Drosophila. *Proc. Natl. Acad. Sci. U. S. A.* 109: 12177–12182, 2012.

Tei H, Okamura H, Shigeyoshi Y, Fukuhara C, Ozawa R, Hirose M, Sakaki Y. Circadian oscillation of a mammalian homologue of the Drosophila period gene. *Nature* 389: 512–516, 1997.

Tian L, Hires SA, Mao T, Huber D, Chiappe ME, Chalasani SH, Petreanu L, Akerboom J, McKinney SA, Schreiter ER, Bargmann CI, Jayaraman V, Svoboda

K, Looger LL. Imaging neural activity in worms, flies and mice with improved GCaMP calcium indicators. *Nat. Methods* 6: 875–881, 2009.

Tischkau SA, Barnes JA, Lin FJ, Myers EM, Barnes JW, Meyer-Bernstein EL, Hurst WJ, Burgoon PW, Chen D, Sehgal A, Gillette MU. Oscillation and light induction of timeless mRNA in the mammalian circadian clock. *J. Neurosci.* 19: RC15, 1999.

Tischkau SA, Mitchell JW, Tyan S-H, Buchanan GF, Gillette MU. Ca2+/cAMP response element-binding protein (CREB)-dependent activation of Per1 is required for light-induced signaling in the suprachiasmatic nucleus circadian clock. *J. Biol. Chem.* 278: 718–723, 2003.

Tomchik SM, Davis RL. Dynamics of learning-related cAMP signaling and stimulus integration in the Drosophila olfactory pathway. *Neuron* 64: 510–521, 2009.

Ultsch A, Schuster CM, Laube B, Schloss P, Schmitt B, Betz H. Glutamate receptors of Drosophila melanogaster: cloning of a kainate-selective subunit expressed in the central nervous system. *Proc. Natl. Acad. Sci. U. S. A.* 89: 10484–10488, 1992.

Veleri S, Brandes C, Helfrich-Förster C, Hall JC, Stanewsky R. A self-sustaining, light-entrainable circadian oscillator in the Drosophila brain. *Curr. Biol. CB* 13: 1758–1767, 2003.

Veleri S, Rieger D, Helfrich-Förster C, Stanewsky R. Hofbauer-Buchner eyelet affects circadian photosensitivity and coordinates TIM and PER expression in Drosophila clock neurons. *J. Biol. Rhythms* 22: 29–42, 2007.

Vincent P, Gervasi N, Zhang J. Real-time monitoring of cyclic nucleotide signaling in neurons using genetically encoded FRET probes. *Brain Cell Biol.* 36: 3–17, 2008.

Viswanath V, Story GM, Peier AM, Petrus MJ, Lee VM, Hwang SW, Patapoutian A, Jegla T. Opposite thermosensor in fruitfly and mouse. *Nature* 423: 822–823, 2003.

Völkner M, Lenz-Böhme B, Betz H, Schmitt B. Novel CNS glutamate receptor subunit genes of Drosophila melanogaster. *J. Neurochem.* 75: 1791–1799, 2000.

Wang JW, Wong AM, Flores J, Vosshall LB, Axel R. Two-photon calcium imaging reveals an odor-evoked map of activity in the fly brain. *Cell* 112: 271–282, 2003.

Waseem T, Mukhtarov M, Buldakova S, Medina I, Bregestovski P. Genetically encoded Cl-Sensor as a tool for monitoring of Cl-dependent processes in small neuronal compartments. *J. Neurosci. Methods* 193: 14–23, 2010.

Wegener C, Hamasaka Y, Nässel DR. Acetylcholine increases intracellular Ca2+ via nicotinic receptors in cultured PDF-containing clock neurons of Drosophila. *J. Neurophysiol.* 91: 912–923, 2004.

Weiner J. Time, love, memory: a great biologist and his quest for the origins of behavior. New York: Vintage Books, 2000.

Wheeler DA, Hamblen-Coyle MJ, Dushay MS, Hall JC. Behavior in light-dark cycles of Drosophila mutants that are arrhythmic, blind, or both. *J. Biol. Rhythms* 8: 67–94, 1993.

Willoughby D, Cooper DMF. Live-cell imaging of cAMP dynamics. *Nat. Methods* 5: 29–36, 2008.

Wu JS, Luo L. A protocol for dissecting Drosophila melanogaster brains for live imaging or immunostaining. *Nat. Protoc.* 1: 2110–2115, 2006.

Wu MN, Ho K, Crocker A, Yue Z, Koh K, Sehgal A. The effects of caffeine on sleep in Drosophila require PKA activity, but not the adenosine receptor. *J. Neurosci.* 29: 11029–11037, 2009.

Xia Z, Liu Y. Reliable and global measurement of fluorescence resonance energy transfer using fluorescence microscopes. *Biophys. J.* 81: 2395–2402, 2001.

Yao Z, Macara AM, Lelito KR, Minosyan TY, Shafer OT. Analysis of functional neuronal connectivity in the Drosophila brain. *J. Neurophysiol.* 108: 684–696, 2012.

Yao Z, Shafer OT. The Drosophila circadian clock is a variably coupled network of multiple peptidergic units. *Science* 343: 1516–1520, 2014.

Yasuyama K, Kitamoto T, Salvaterra PM. Immunocytochemical study of choline acetyltransferase in Drosophila melanogaster: an analysis of cis-regulatory regions controlling expression in the brain of cDNA-transformed flies. *J. Comp. Neurol.* 361: 25–37, 1995.

Yasuyama K, Meinertzhagen IA. Extraretinal photoreceptors at the compound eye's posterior margin in Drosophila melanogaster. *J. Comp. Neurol.* 412: 193–202, 1999.

Yasuyama K, Salvaterra PM. Localization of choline acetyltransferase-expressing neurons in Drosophila nervous system. *Microsc. Res. Tech.* 45: 65–79, 1999.

Yin JC, Tully T. CREB and the formation of long-term memory. *Curr. Opin. Neurobiol.* 6: 264–268, 1996.

Yoshii T, Hermann C, Helfrich-Förster C. Cryptochrome-positive and -negative clock neurons in Drosophila entrain differentially to light and temperature. *J. Biol. Rhythms* 25: 387–398, 2010.

Yoshii T, Heshiki Y, Ibuki-Ishibashi T, Matsumoto A, Tanimura T, Tomioka K. Temperature cycles drive Drosophila circadian oscillation in constant light that otherwise induces behavioural arrhythmicity. *Eur. J. Neurosci.* 22: 1176–1184, 2005.

Yoshii T, Todo T, Wülbeck C, Stanewsky R, Helfrich-Förster C. Cryptochrome is present in the compound eyes and a subset of Drosophila's clock neurons. *J. Comp. Neurol.* 508: 952–966, 2008.

Yu W, Zheng H, Houl JH, Dauwalder B, Hardin PE. PER-dependent rhythms in CLK phosphorylation and E-box binding regulate circadian transcription. *Genes Dev.* 20: 723–733, 2006.

Yuan Q, Lin F, Zheng X, Sehgal A. Serotonin modulates circadian entrainment in Drosophila. *Neuron* 47: 115–127, 2005.

Zheng X, Sehgal A. Speed control: cogs and gears that drive the circadian clock. *Trends Neurosci.* 35: 574–585, 2012.

Zylka MJ, Shearman LP, Weaver DR, Reppert SM. Three period homologs in mammals: differential light responses in the suprachiasmatic circadian clock and oscillating transcripts outside of brain. *Neuron* 20: 1103–1110, 1998.

CHAPTER 6
CONCLUDING REMARKS

Since their discovery, the PDF neurons have been suspected to communicate with the visual system and relay circadian information to the rest of the brain (Helfrich-Förster and Homberg, 1993; Helfrich-Förster, 1995, 1997). Over the years, evidence increasingly implicates the small PDF^+ neurons, and not the larges, as the master pace-making cells in constant darkness (Helfrich-Förster et al., 1998; Renn et al., 1999; Blanchardon et al., 2001; Grima et al., 2004; Stoleru et al., 2004). In this thesis, I further delineate the differences in functional connectivity and receptivity between of the s-LN_v and l-LN_v. This work is the first to thoroughly examine the receptivity of the s-LN_v to neurotransmitters important for circadian rhythms, and to establish a means of circuit interrogation of neurons suspected to modulate the s-LN_v. Using this technique, I have shown conclusively, that the s-LN_v and not the l-LN_v are recipients of excitatory neuromodulation from the extra-retinal eyelet. This establishes a working model, wherein the mechanism of light entrainment and phase-shifts to the circadian clock by external photoreceptors is excitation of the s-LN_v master pacemaker cells (Figure 6.1).

6.1 THE SMALL VENTROLATERAL NEURONS INTEGRATE ENIRONMENTAL AND INTERNAL INPUTS

The small ventrolateral clock neurons have the unique anatomy of connecting the dorsal brain to the ventral clock neurons(Helfrich-Förster, 1997). Their cell bodies and ventral projections reside in the accessory medulla (aMe), a center of visual system projections and other inputs that may modulate clock neuron activity. Previously, it was not well understood how the s-LN_v are modulated

because it is difficult to record electrophysiologically from their small cell bodies (Cao and Nitabach, 2008). To overcome this issue, I employed non-invasive, genetically encoded sensors of neuronal activity to visualize the responsivity of the s-LN_v. Because these techniques were relatively new, I also examined the responsivity of the l-LN_v to known excitatory and inhibitory neuromodulators to test the sensitivity of the sensors. Using genetically encoded sensors, I was able to show the similarities and differences in the way the s-LN_v and l-LN_v are modulated.

Acetylcholine

Acetylcholine is predicted to excite the s-LN_v based on the electrophysiological responses observed in the l-LN_v and the larval LN_v clock neurons(Wegener et al., 2004; McCarthy et al., 2011). The source is predicted to be the cholinergic terminals of the HB-eyelet as a pathway for circadian photoreception(Yasuyama and Meinertzhagen, 1999). I first showed that known excitatory responses of the l-LN_v to cholinergic agonists were detectable using GCaMP and Epac sensors(McCarthy et al., 2011). As predicted, the l-LN_v showed increases in Ca^{2+} in response to cholinergic agonists, but additionally they also displayed increases in cAMP. The s-LN_v, also as predicted, exhibited increases in cAMP and Ca^{2+} to an nAChR agonist even in the presence of tetrodotoxin, a sodium channel blocker used to prevent neuronal communication (Soderlund, 2005). Therefore, the s-LN_v are directly responsive to ACh via nAChRs (Chapter 3; Lelito and Shafer, 2012).

Knowing that I could now detect excitatory responses in the s-LN_v and that the s-LN_v expressed nAChRs, I tested whether the cholinergic HB-eyelet could excite the s-LN_v (Yasuyama and Meinertzhagen, 1999). To keep the brain and cells intact during circuit interrogation, I employed genetically encoded activators (see section 6.4) to excite the HB-eyelet and genetically encoded Ca^{2+} and cAMP sensors to record from the PDF neurons (Nikolaev et al., 2004; Shafer et al., 2008; Tian et al., 2009). As predicted, the s-LN_v responded to HB-eyelet excitation with increases in Ca^{2+} and cAMP, in a manner consistent with nAChR activation(Chapter 5). To our surprise, however, the l-LN_v did not respond to HB-eyelet activation. At the least, the

cholinergic terminals of the HB-eyelet specifically target the s-LN_v. There is still a possibility that the histaminergic terminals of the HB-eyelet modulate the l-LN_v, which have been shown to express a histamine receptor. Neuronal excitation of the s-LN_v by the HB-eyelet could be a direct pathway of light to the clock network, but until now, the HB-eyelet has not been shown to be critical to circadian photoreception.

I found that activation of the HB-eyelet induces a trend to advance behavioral rhythms in the late evening. Never before has such a discrete set of neurons been implicated in visual system phase shifting and entrainment. Previous studies that found only a minor role of the HB-eyelet in circadian photoreception based their findings on the effect of progressive elimination of visual system components on entrainment (Helfrich-Förster et al., 2002; Rieger et al., 2003). The caveat to these experiments is that the clock neuron network likely undergoes substantial restructuring in mutants missing large portions of the visual system. For example, in *disco* mutants where one optic lobe and compound eye degenerates, the projections of the LN_v can also become abnormal: projections from the l-LN_v, which normally project laterally across the posterior optic tract, project dorsally from the posterior optic tract towards the ocelli (Helfrich-Förster et al., 2007). It is suggested that in the absence of light input from the compound eye, the l-LN_v restructure to receive light information from the ocelli. In light of this, it may be difficult to draw conclusions regarding entrainment ability in visual system mutants where clock neurons may develop differentially to compensate for the loss of critical visual system inputs.

Assuming that the clock network developed normally in visual system mutants tested by Rieger et al. (2003), their results still determined that the HB-eyelet played only a modest role in entrainment, counter to predictions. The combinatorial visual system mutant studies to elucidate the role of the HB-eyelet in entrainment were done in very bright, 500 lux, white light. Because the visual system appears to have such overlapping circadian function, it may be difficult to separate the effects of the different mutations in conditions where other visual system pathways may be sufficient for entrainment. Even still, impairment of

entrainment was only observed after silencing the HB-eyelet if flies were subjected to dim light entrainment *and* carried a mutation in a phototransduction cascade (Veleri et al., 2007). Our approach differed from previous studies in that I used discrete TRP mediated activation of the HB-eyelet when I assayed for phase-shifts, thereby avoiding activation of other light input pathway by light exposure. In this work, I was able to show that activation of the HB-eyelet neurons mimicked the effect of directly activating the PDF neurons to mediate a phase-advance of circadian rhythms in the late night. Our work suggests that the HB-eyelet is an independent pathway for light transmission that alters the gears of the molecular clock.

The use of a particular visual system mutant to eliminate HB-eyelet function comes into question based on my finding that the HB-eyelet excites the s-LN_v. Rieger et al. (2003) used a histidine decarboxylase mutation in combination with a CRY mutation to eliminate the function of the compound eye, ocelli, CRY and HB-eyelet (*hdc^{jk910}; cry^{b}*). It was compared to mutants that maintained the HB-eyelet but lack compound eyes, ocelli, and CRY (*so^{1}; cry^{b}*). HDC is an enzyme that converts histidine into histamine, and the mutation blocks the function of histaminergic photoreceptors (presumably, the compound eyes, ocelli, and HB-eyelet). *hdc^{jk910}; cry^{b}* mutants exhibited significantly less entrainment than *so^{1}; cry^{b}* mutants, but under 12:12 LD cycle, 13% of flies tested still entrained. When subjected to increasing photoperiods, *hdc^{jk910}; cry^{b}* mutants increasingly lengthened their period, suggesting that flies retained the ability to track the photoperiod, albeit poorly. In these experiments, the actual function of the HB-eyelet was not tested to confirm that its output was blocked. The original study of the *hdc^{jk910}* mutant showed that histamine immunoreactivity in photoreceptors was eliminated, and mutant flies lost an optimotor behavioral response(Melzig et al., 1996). However, in larvae the optimotor response persisted. Authors speculated that the larval optimotor response was controlled by another neurotransmitter, ACh, which was not affected by the *hdc^{jk910}* mutation. Yasuyama and Meinertzhagen (1999) later showed that the HB-eyelet is reactive to antibodies raised against choline acetyltransferase as well as histamine. I argue that the cholinergic function of the HB-eyelet is still intact in *hdc^{jk910},cry^{b}* mutants and could explain why entrainment wasn't completely

eliminated and why increasing photoperiods still elicited lengthening of the behavioral period.

Several researchers speculate about the existence of an unknown photopigment expressed by the dorsal clock neurons, the so-called "cryptic DN-photoreceptors" (Rieger et al., 2003, 2006; Veleri et al., 2003). Rieger et al. (2003) attributes the remaining 13% entrainment and period lengthening under extreme photoperiods to the cryptic DN photoreceptors that are not eliminated in the *hdc*^{jk910}*,cry*^{b} mutant. In this particular mutant, I attribute the remaining entrainment ability to the cholinergic terminals of the HB-eyelet that I have shown can excite the s-LN_v. However, there is still evidence for cryptic DN photoreceptors. In flies that carry a mutation for CRY and a transcription factor required for the development of external photoreceptors (*;;glass*^{60j}*,cry*^{b}), cycling of TIM in some dorsal neurons can still be entrained to light cycles (Veleri et al., 2003; Rieger et al., 2006). These flies still exhibit a normal circadian rhythm, but because CRY and all external photoreceptors are eliminated, the locomotor rhythm cannot be entrained to light cycles (Helfrich-Förster et al., 2001). The fact that the molecular clocks of the DNs are still entrained is evidence for another unidentified photoreceptor.

Histamine

Until now, it was unclear which neurotransmitter, ACh or histamine, the HB-eyelet employed to communicate to the LN_v. I show that the HB-eyelet excites the s-LN_v, likely in a cholinergic manner (Chapter 5). The currently available sensors made it difficult to implicate or exclude a role for histamine in circadian photoreception. I was not able to observe a response of either PDF neuron subtype to histamine using Ca^{2+} or cAMP sensors. The evidence supporting histamine receptivity in the l-LN_v is weak. Sera raised against HisCl1 receptors localizes to the l-LN_v but it was not tested in a HisCl1 mutant to determine if the staining persisted or remained in the l-LN_v (Hong et al., 2006). Assuming that the receptor staining is *bona fide*, histamine is a widespread neurotransmitter employed for mechanoreceptors and interneurons in *Drosophila* (Buchner et al., 1993). It is entirely possible that histamine transmission by the HB-eyelet has very little role in

circadian photoreception. The HB-eyelet projects into a very dense neuropil (aMe), and the inhibitory input could mediate some other light-mediated behavior or physiological response in a completely different set of neurons. For example, loss of histamine production leads to the loss of a visually mediated locomotor behavior in adult flies (Melzig et al., 1996). It is possible the histaminergic HB-eyelet/l-LN_v circuit mediates this behavior. Future investigations are needed to determine whether there is a role of the histaminergic HB-eyelet terminals in circadian photoreception.

The role of light input from histaminergic retinal photoreceptors appears to enhance sensitivity to extreme photoperiods and to mediate masking (Rieger et al., 2003). Masking may not be a passive startle response to abrupt environmental changes. Masking, or immediate changes in activity associated with environmental changes, allows animals to respond to changes in the environment with appropriate behaviors without waiting for the circadian clock to synchronize (Rietveld et al., 1993). For example, if an animal changes geographic locations and experiences a new light cycle, masking behaviors immediately adapt to the new light cycle, while the circadian clock may take days to synchronize. Interestingly, the l-LN_v are the most proximal clock neuron class to retinal photoreceptor input (Helfrich-Förster, 2005). The l-LN_v also mediate wakefulness and arousal and may be the part of the photoreceptive pathway that induces masking behaviors (Parisky et al., 2008; Shang et al., 2008; Sheeba et al., 2008a). In addition to potentially playing a role in masking, the pathway and mechanism by which histaminergic signaling leads to increased entrainment sensitivity is unknown. Although I did not observe a response of the l-LN_v to application of the retinal photoreceptor neurotransmitter, histamine, the retinal signaling pathway still deserves more thorough investigation.

GABA

GABA counteracts the arousal producing effects mediated by PDF neuron activity (Agosto et al., 2008; Parisky et al., 2008; Chung et al., 2009). Although GABA inhibition of the l-LN_v has been shown electrophysiologically to occur by GABA-gated chloride channels (Agosto et al., 2008; Chung et al., 2009), it was unknown

whether the s-LN_v are also inhibited by GABA. Ca2+ levels visualized by Fura-2 in dissociated larval LN_v were decreased by $GABA_BR$ agonists (Hamasaka et al., 2005), suggesting that the adult s-LN_v may be modulated in the same way. I showed that although GABA applied alone had no effects on Ca^{2+} levels, cholinergic excitatory responses could be blocked when co-applied with GABA. Fura-2 has a higher sensitivity to Ca^{2+} than GCaMP; therefore, I might have expected GCaMP to miss small decreases in Ca^{2+} associated with GABA inhibition. Using GCaMP, the technique of co-application of a putative inhibitory neuromodulator applied with an excitatory agonist allow us to visualized the inhibitory effects of GABA on the l-LN_v. Application of this technique is limited because not all cells interrogated will have a known excitatory neurotransmitter (See section 6.3).

The s- and l-LN_v differed dramatically in their cAMP response to GABA. Compared to the s-LN_v, the l-LN_v exhibited higher magnitude cAMP decreases that occurred at a later onset and remained low after application of the stimulus. The l-LN_v are thought to be critical regulators of arousal that receive direct inhibition from GABAergic sleep circuits (Shang et al., 2008; Sheeba et al., 2008a; Chung et al., 2009). Because of this, cAMP levels may be more affected by GABA in the l-LN_v than the s-LN_v. Our data suggests that the l-LN_v express $GABA_BRs$ based on their longer latency cAMP responses. In support of this, a recent study showed that $GABA_B$-R2 expression in the l-LN_v was required for sleep maintenance in the late night (Gmeiner et al., 2013). I also predict that the s-LN_v express ionotropic $GABA_ARs$ as their response to GABA was faster acting and more transient, although I lack direct evidence to conclude this. Our study extends the model of GABAergic inhibition to include negative regulation of cAMP signaling in both types of LN_v.

6.2 CONSERVED ROLE OF CAMP IN CIRCADIAN CLOCK RESETTING AND CLOCK NETWORK SYNCHRONIZATION

In Mammals, cAMP signaling plays a crucial role in circadian timekeeping and resetting of the circadian clock. cAMP production is rhythmic, and sustained cAMP fluctuations drive molecular clock cycling in the master clock in constant darkness (O'Neill et al., 2008). Time-dependent phase-delays and advances produced by light

exposure elicit cAMP changes in the master clock neurons (Tischkau et al., 2000). Light excitable retinohypothamalic neurons excite clock neurons via NMDA receptors. Evoked intracellular signaling leads to rapid transcription of *mPer1* that is dependent on a cAMP-responsive element (CRE) within the gene's promoter region (Albrecht et al., 1997; Shearman et al., 1997; Travnickova-Bendova et al., 2002; Wilsbacher et al., 2002). The mechanism by which light-induced cAMP signaling induces time dependent phase-delays and advances is not fully understood in mammals.

My thesis work contributes to the evidence that cAMP is also a critical signal for timekeeping and re-setting in the *Drosophila* clock neuron network. I showed that cholinergic, GABAergic, glutamatergic inputs modulate cAMP levels in the LN_v. These inputs represent environmental and internal modulation of the LN_v that are critical to maintenance and entrainment of circadian rhythms. I showed that at least some cholinergic input that modulates cAMP comes from the HB-eyelet, an extra-retinal photoreceptor (Chapter 5). I also showed that GABA negatively regulates cAMP levels in PDF neurons (Chapter 3). Although it is not completely understood, GABA input comes from sleep centers in the brain that potentially integrate an animal's need for sleep with circadian sleep/wake patterning. In a collaborative study, I showed that glutamatergic signaling (mGluRA) from the dorsal clock neurons reduced PDF-induced cAMP responses in larval LN_v via metabotropic glutamate receptors (Collins et al. *submitted*). Expression of mGluRA in the LN_v was shown to be required for synchronized molecular clock cycling within the LN_v. In total, these inputs likely represent the integration of environmental and internal communication to the LN_v that converge on cAMP levels. Modulation of cAMP signaling is now emerging as a conserved target by which neuronal communication can modify circadian timekeeping.

6.3 UTILITY AND LIMITATIONS OF GENETICALLY ENCODED SENSORS

Genetically encoded tools to detect excitatory responses are relatively well developed. Using the GCaMP Ca^{2+}sensor and Epac1-cAMPs cAMP sensor, I was able to see increases in Ca^{2+} and cAMP in response to applied neuromodulators and

response to activation of discrete subsets of neurons. The advantage of bath application is that relatively large doses can be used to assay for responsivity. In our hands, cAMP responses induced by cholinergic agonists could be detected by Epac1Camps in the LN_v at an order of magnitude lower concentration than GCaMP3.0 (Chapter 3; Lelito and Shafer, 2012). This suggests that Epac1-cAMPs may be slightly more sensitive that GCaMP3.0 in instances when excitatory modulation induces Ca^{2+} and cAMP changes. In experiments when eyelet activation elicited visible excitatory responses in the larval LN_v or adult s-LN_v, only 12 and 4 eyelet neurons, respectively, were activated per hemisphere (Chapter 4,5; Yao et al., 2012). This bodes well for the success of these sensors in circuit interrogation when only very few putative upstream neurons are activated. Today, even more sensitive genetically encoded sensors have been developed: GCaMP6.0 for example, has an even higher affinity for Ca^{2+} and a wider range of fluorescence dynamics (Akerboom et al., 2012). It remains to be seen whether excitatory modulation evoked by the activation of a single neuron can be detected with the current generation of sensors.

In opposition to their success at detecting excitatory responses, GCamp3.0 and Epac were relatively limited in detecting inhibitory responses. GABA is known to inhibit spontaneous firing in the l-LN_v, but GABA alone did not change Ca^{2+} levels sufficiently for detection by GCaMP3.0. Ca^{2+} changes in response to inhibitory neuromodulation have been shown, for example in dissociated larval LN_v, GABA induces decreases in Ca^{2+} as visualized by Fura-2 (Hamasaka et al., 2005). Even the newest versions of GCaMPs (6.0) are optimized to detect excitatory activity, with baseline fluorescence so low that decreases in Ca^{2+} expected from inhibitory neuromodulation would be difficult to observe (Akerboom et al., 2012). Using GCaMP3.0, co-application of GABA with nicotine was successful in showing inhibition of an excitatory Ca^{2+} response (Chapter 3; Lelito and Shafer, 2012). In the case of GABA, the response was also associated with decreases in cAMP. In the event that cAMP is coupled with an inhibitory response, the Epac1-CaMPs reporter works well to detect inhibitory neuromodulation, however in the event it is not, an inhibitory modulation will still be difficult to detect.

There are instances when a known inhibitory neuromodulator has no effect on Ca^{2+} levels, no ability to block excitatory Ca^{2+} increases, and has no effect on cAMP. This was the case with glutamate (data not shown) that was previously shown to block spontaneous firing in the l-LN_v. In further experimenting with the co-application technique, I was able to show effects of glutamate on cAMP levels in the s-LN_v using the Epac-1camps sensor (Collins et al., *submitted*). First, I generated a dose-response for the s-LN_v cAMP levels to applied PDF neuropeptide. Applied PDF is known to elicit increases in cAMP from the s-LN_v (Shafer et al., 2008). I selected the lowest dose of PDF that elicited an increase in cAMP to apply to explanted brains from animals where the metabotropic glutamate receptor (mGluRA) was knocked down in PDF neurons. In this case, the LN_v cAMP response to PDF was potentiated, even though no inhibition of the cAMP response could be detected by co-applying the same low dose of PDF with glutamate. Sensitizing the LN_v by knocking down the glutamate receptor was required to visualize the effect of glutamate signaling on cAMP using the Epac1-cAMPs sensor. It is not yet known whether this type of experiment will reveal the predicted inhibitory neuromodulation of the l-LN_v by histamine.

Until recently, genetically encoded voltage indicators (GEVI) were not responsive enough to be useful in biological experimentation. However, in 2013, Cao and colleagues optimized the ArcLight GEVI for use in the *Drosophila* brain. ArcLight is a fusion of GFP to the voltage-sensing domain from a voltage sensitive phosphatase isolated from a sea squirt (Murata et al., 2005). Depolarization of the membrane induces a loss in GFP emission, therefore, depolarization is inversely proportional to decreases in fluorescence. Cao et al. vetted the sensor in the l-LN_v with simultaneous electrode recording of neural activity. For the first time, a GEVI showed single action potential firing relatively faithfully. Spontaneous firing, which was completely undetectable by GCaMP3.0 expression, was detectable with ArcLight (Cao et al., 2013). In agreement with the limited electrophysiology of the s-LN_v (Cao and Nitabach, 2008), Cao et al. showed that the spontaneous membrane activity in the s-LN_v was higher when recorded in the fly's subjective morning than evening. With addition improvements to ArcLight's dynamic range and speed, this sensor

could be used to visualize voltage changes locally along a neuron to understand the specific voltage inputs underlying excitation or inhibition in electrophysiologically inaccessible neurons. Although it has only been used to visualize baseline membrane activity and spontaneous firing, it may be useful in the detection of inhibitory neuromodulation, in cases where Ca^{2+} and cAMP sensors fall short. The response of the LN_v to histamine would be the first response to evaluate.

6.4 UTILITY AND LIMITATIONS OF GENETICALLY ENCODED ACTIVATORS OF NEURAL ACTIVTY FOR CIRCIUT BREAKING IN THE CIRCADIAN CLOCK NETWORK

The greatest challenge of genetically encoded circuit interrogation of the clock network was ensuring that the activation mechanism did not influence the clock neurons. Many *Drosophila* researchers have taken advantage of the light activated opsins to excite neurons, channelrhodopsin (ChR) being the most popular (reviewed by Olsen and Wilson, 2008). In our studies, I sought to examine the connectivity between a specific subgroup of visual system neurons and circadian clock neurons. Both visual system neurons and clock neurons are innately sensitive to light and activation of ChR by light may stimulate multiple light pathways. Opening of the ChR channel is also activated by wavelengths of light that are necessary to image from genetically encoded sensors of neuronal activity. With a confocal microscope, simply imaging from sensors would lead to excitation of any neurons expressing the opsin. Recently, red-shifted opsins have been developed that are potentially compatible with genetically encoded fluorescent sensors of neural activity (Lin et al., 2013). For the current study, however, our conclusion was that use of light-mediated neuronal activation was not feasible for our live imaging or behavioral experiments investigating clock neuron network connectivity with the visual system.

A heat activated cation channel, TRPA1, was also available for excitation of neurons during live-imaging and behavioral assays (Hamada et al., 2008). Movement induced by heat was a problem for researchers attempting to live-image from TRPA1 expressing neurons. Therefore, heat-mediated neuronal activation was

not used in our studies for genetically encoded circuit interrogation. Use of the TRPA1 channel was our preferred method for discrete activation of neurons in freely moving flies (Chapter 5). I had to be cautious using temperature activation as previous studies established a role for temperature in entrainment and phase-shifting, specifically in the early subjective evening (Kaushik et al., 2007; Yoshii et al., 2009). I attempted to activate TRP by giving temperature pulses lower than those required to phase-shift in the early evening, but even the lower temperature pulses induced a phase-delay in the early evening. At other times of day, when the clock is not sensitive to temperature, I did not observe phase-shifts in response to heat. When I used TRPA1 and a heat pulse in the late evening to excite the HB-eyelet neurons, I was then able to show a trend of HB-eyelet excitation to induce phase-delays. The experiment using heat activated TRPA1 to directly excite the PDF neurons was even more conclusive: activation of the PDF neurons in late evening induced a delay in circadian locomotor rhythms, but heat alone (without TRPA1 expression) did not. In our experiments, use of TRPA1 is only compatible for neuronal activation in freely moving flies, and temperature does preclude its utility at certain times of day. Investigation of the clock network, which is innately sensitive to light and temperature, has presented unique challenges.

Ligand activation of the P2X2 cation channel was the most successful method of neuronal activation in explanted brains (Chapter 4, 5; Yao et al., 2012). The P2X2 channel is not endogenously expressed by *Drosophila* (Littleton and Ganetzky, 2000), and therefore, when ATP is perfused over explanted brains, only neurons expressing the P2X2 channel are excited. The method of neuronal activation avoids using light or temperature mediated neuronal activation, signals to which the clock neuron network is highly sensitive. Importantly, our group did not find that ATP elicited any changes in Ca^{2+} or cAMP without the targeted expression of P2X2. I used the genetically encoded circuit interrogation technique to show that activation of the larval eyelet induced excitatory Ca^{2+} responses in the LN_v, and activation of the adult eyelet induced excitatory Ca^{2+} and cAMP responses in the s-LN_v (Chapter 4, 5; Yao et al., 2012). The expansion of the *Drosophila* circuit breaking toolkit to include P2X2, TRPA1, GCaMP and Epac1-cAMPs was essential for the complete functional

analysis of the eyelet/ LN_v connectivity, but it required integration into a light and heat sensitive network.

I was limited by available expression systems to selectively activate specific subsets of neurons. In the assay in which the larval eyelet (Bolwig's nerve) was excited, the eyelets were the only set of neurons expressing P2X2 (Chapter 4; Yao et al., 2012). However, in the adult, the same driver targeting the eyelet expresses in another set of neurons, a subset of the R8 retinal photoreceptors (Chapter 5). I ruled out R8 contribution to excitatory responses in the s-LN_v because R8 photoreceptors utilize the inhibitory neurotransmitter histamine, and their projections are not near the cells that were excited. In the behavioral assays where the eyelet-driver was used in activation, I could not distinguish between potential indirect effects from stimulating the R8 retinal photoreceptors and the excitatory effects of the eyelet on the s-LN_v. In order to maximize the utility of this genetically encoded circuit interrogation technique in the *Drosophila* nervous system, a wider range of more discrete Gal4 and LexA drivers are needed.

6.5 PHARMACOLOGICAL TOOLS REQUIRE VETTING FOR USE WITH GENETICALLY ENCODED SENSORS AND ACTIVATORS

Most pharmacological tools available for analysis of receptors and connectivity were first validated with electrophysiological recordings of membrane voltage and channel currents. Pharmacological tools are used to ask many important questions about a circuit including: 1) What receptors are required for a particular response?; 2) Is the response to a particular neuromodulator direct (endogenously expressed receptor?); and 3) Is a connection between two neurons mono- or poly-synaptic? In order for these questions to be addressed using genetically encoded circuit interrogation, pharmacological tools need to be re-accessed for their compatibility with genetically encoded sensors and activators.

The genetically encoded sensors GCaMP and Epac1-cAMPs sensors reflect changes in molecules that are often dependent on changes in voltage. This presents a problem particularly when one seeks to determine whether a neuron of interest expresses a receptor endogenously. Traditionally, tetrodotoxin (TTX), a blocker

voltage gated sodium channels, would be used to prevent neuronal communication (Soderlund, 2005); responses that persisted in the presence of TTX would be responses mediated by activation of receptors on the neuron of interest. Large influxes of Ca^{2+} that are detected by genetically encoded Ca^{2+} sensor GCaMP are likely to depend on voltage gated influx of Ca^{2+}, and the use of TTX would block many Ca^{2+} responses whether they were direct or indirect. Evidence to support this comes from a study of larval LN_v responses to cholinergic agonists using Fura-2 (Wegener et al., 2004). The response of dissociated LN_v to ACh could be blocked completely by imaging the neurons in Na^+-free saline, or in Ca^{2+}-free saline or in the presence of non-specific Ca^{2+} channel blockers ($MnCl_2$ or $LaCl_3$). Therefore, the source of Ca^{2+} that was detected by Fure-2 after ACh excitation by voltage dependent Ca^{2+} influx. Wegener's data also suggests that even the very sensitive Ca^{2+} dye, Fura-2, could not detect Ca^{2+} changes (if any) associated with Ca^{2+} ion flow through activated nicotinic cation channels expressed by the LN_v. Therefore, TTX will not only block the intended secondary neuron communication, but also will block voltage changes on the neuron of interest that are required for visualizing a direct Ca^{2+} response with GCaMP.

It was very important for my work to establish whether the responses of the s-LN_v to nicotine and GABA were mediated by direct expression of receptors by the s-LN_v (Chapter 3; Lelito and Shafer, 2012). The LN_v are known to have sodium channels sensitive to TTX. The spontaneous firing of l-LN_v from brains that have been enzymatically digested and pierced with a recording-electrode shows sensitivity to TTX (Sheeba et al., 2008b). At the request of the reviewers of our manuscript describing the ACh and GABA responses of the LN_vs, I used TTX to determine whether the responses were direct. According to my explanation above, I should have discovered that the responses to nicotine were blocked in the presence of TTX, but nicotinic responses persisted (Fig.6.2 A-B). In our explanted brain preparation, the brain and the surrounding lamina are left intact. I hypothesized that the TTX molecule might not fully penetrate and block sodium channels. I used an alternative blocker of sodium channels, mexilitine, and as predicted from my explanation above, blocked nicotine induced increases in Ca^{2+} and cAMP in the s-and

l-LN_v (Fig.6.2 C-F). Therefore, in addition to having unintended interactions with genetically encoded sensors, it may be difficult for TTX to penetrate through the intact explanted brain.

I encountered similar molecule penetration issues when attempting to use an antagonist of nicotinic channels to test for the requirement of nAChRs in mediating the response of the s-LN_v to cholinergic agonists. Dissociated larval LN_v were shown to be sensitive to alpha bungarotoxin (a-BTX) (Dahdal et al., 2010). Ca^{2+} responses to ACh as visualized by GCaMP1.6 in the LN_v were blocked by 500 nM a-BTX. However, after 10-minute incubations of explanted adult brains in BTX (5 ug/mL), the response of the s-LN_v and l-LN_v to nicotine persisted in our trials (data not shown). I suspect that the relatively large BTX peptide does not circulate into the intact adult brain preparation to block nicotinic channels in deeply situated neurons. I assayed another antagonist of nAChRs, d-tubocurarine, for it's ability to block an the response to nicotine in the adult LN_v in intact brains. Concentrations of d-tubocurarine above 50 uM were sufficient to block nearly 100% of Ca^{2+} responses in the LN_v to nicotine (10^{-4} M) (Fig. 6.3). Although d-tubocurarine worked well in conjunction with GCaMP Ca^{2+} imaging, I also sought to use d-tubocurarine in conjunction with the genetically encoded neuronal activator, P2X2. I found that d-tubocurarine concentrations higher than 50 uM blocked ATP- activation of P2X2 channel, but that 50 uM permitted P2X2 activation by ATP (Fig. 6.3).

Integration of traditionally used pharmacological agents requires screening for compatibility with genetically encoded circuit interrogation techniques. To my knowledge, the use of TTX with genetically encoded sensors has only lead authors to conclude that the response they recorded was direct; in other words, the response to the neuromodulator of interest persisted in the presence of TTX in each instance (Shang et al., 2011; Lelito and Shafer, 2012; Pírez et al., 2013). This is just one example of hasty integration of pharmacology with genetically encoded sensors. With the more prevalent use of genetically encoded circuit interrogation techniques in place of electrophysiology, I encourage the field of *Drosophila* neurobiology to recognize the need for reassessment of pharmacological tools for use with genetically encoded tools.

6.6 FIGURES

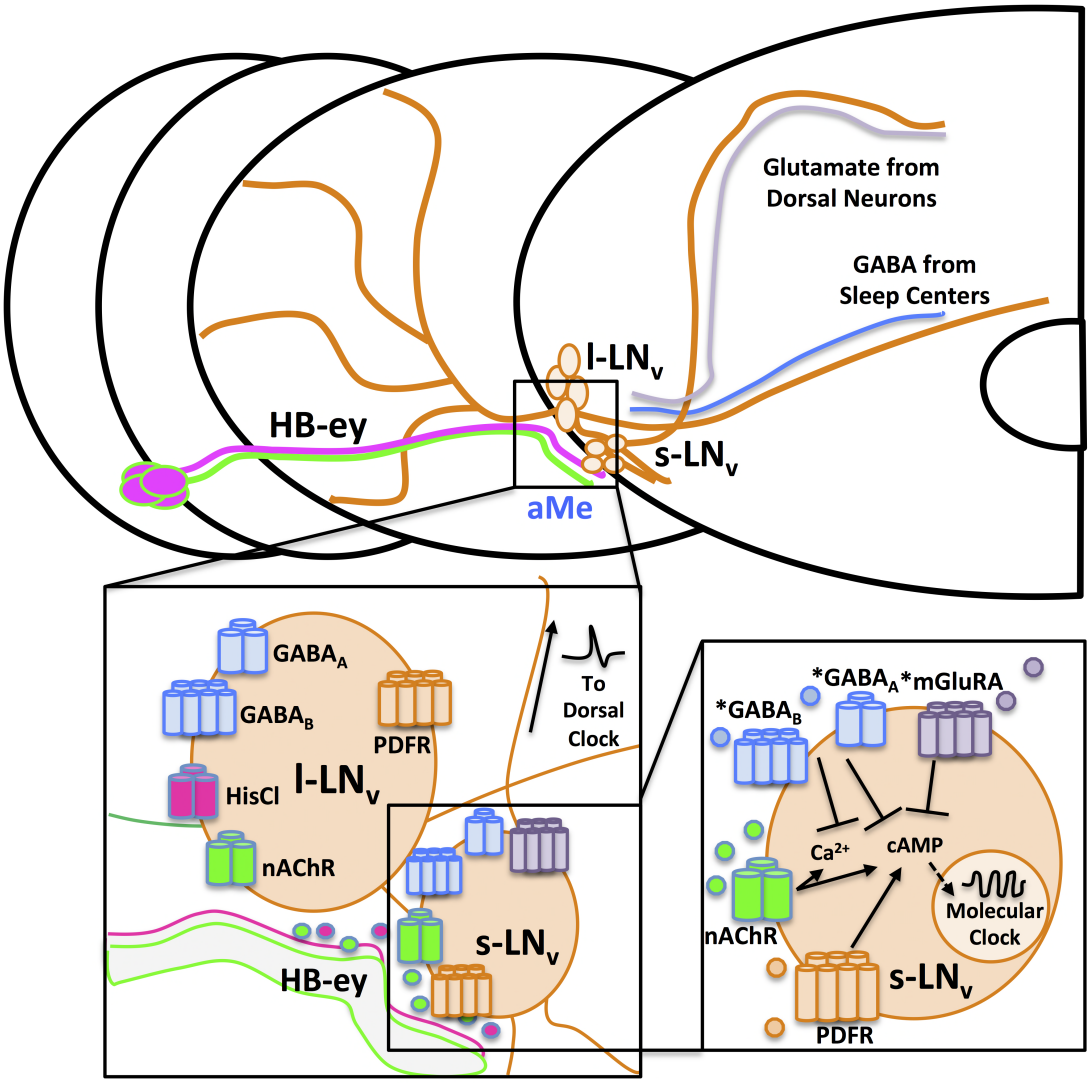

Figure 6.1. Model of LN_v modulation by external and internal neural signaling. External photoreceptors, or non-Cryptochrome photoreception, are sufficient to entrain and phase-shift behavioral rhythms of *Drosophila*. The extra-retinal eyelet, or HB-eyelet (HB-ey), projects closely to the s-LN_v and l-LN_v clock neuron projections in the accessory medulla (aMe) or second optic neuropil. The HB-eyelet is predicted to release acetylcholine and histamine as neurotransmitters, and the LN_v express receptors for each of these neurotransmitters (HisCl, nAChR). However, our studies show that only nicotine, a cholinergic agonist, causes measurable changes in the neuronal activity of the LN_v. I was not able to visualize a response to histamine with our sensors. When I stimulate the HB-eyelet, I observe only excitatory increases in $Ca^{2+}$and cAMP, consistent with nicotinic receptor activation.

These responses were only visualized in the small ventrolateral neurons, and not the larges. I also show that cAMP levels are decreased by GABA in both LN_v; however, which GABA receptor mediates this inhibitory response is not known (asterisks). The s-LN_v respond to PDF neuropeptide stimulation with increases in cAMP. I show that glutamate signaling via metabotropic glutamate receptors negatively regulates the PDF-cAMP response in larval LN_v, the precursors to the adult s-LN_v. Modulation of cAMP levels by PDF, ACh, GABA, and glutamate in the LN_v is potentially a conserved mechanism whereby neuronal signaling results in changes to the molecular clock of pacemaker neurons.

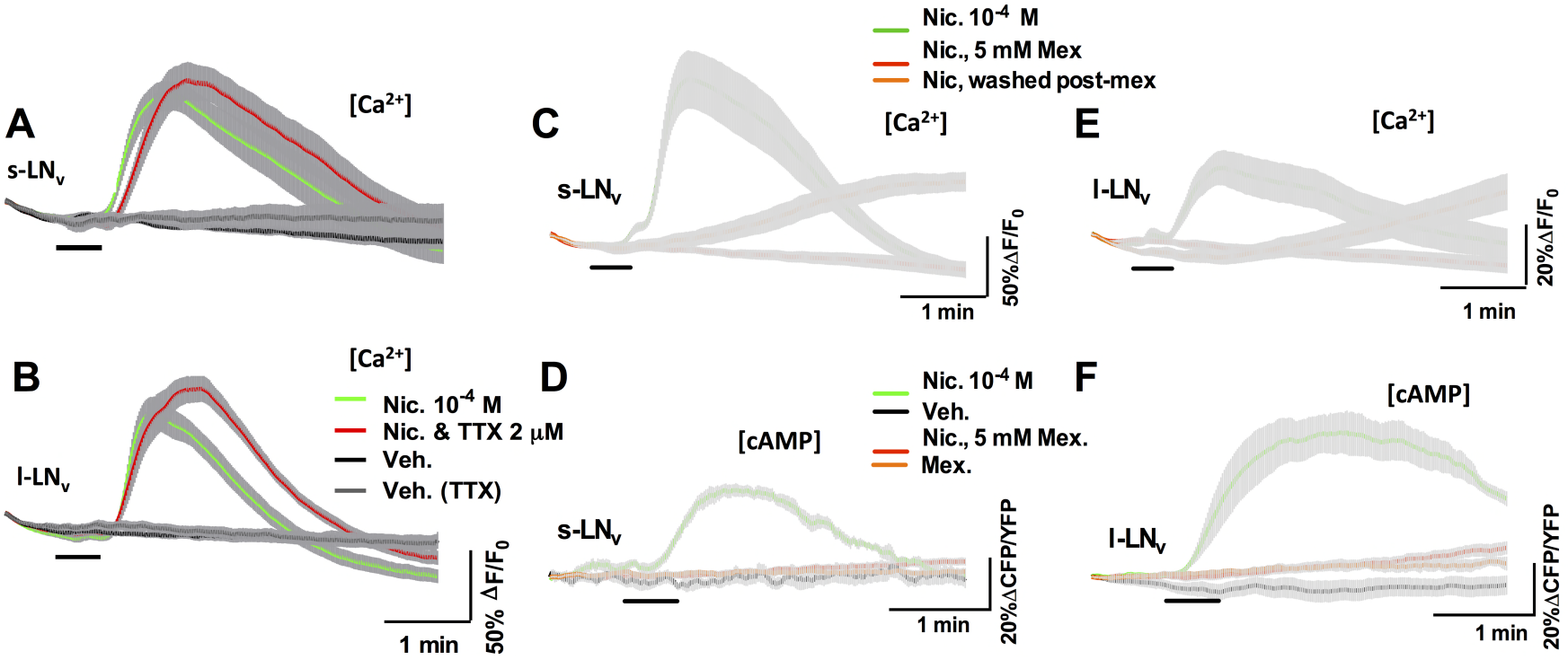

Figure 6.2. Use of sodium channel blockers blockers with GCaMP and Epac1-cAMPs. Live-imaging of cholinergic responses of the LN_v in the presence of different sodium channel blockers, TTX (tetrodotoxin) and Mexilitine (Mex.). Flies used for this experiment expressed GCaMP3.0 or Epac1-cAMPs in the PDF neurons (*Pdf-Gal4; UAS-GCaMP3.0/+;* or *Pdf-Gal4; UAS-Epac1-cAMPs (50A)/+;*). TTX had no effect on excitatory Ca^{2+} (Ca^{2+}) responses to nicotine in the s- (A) or l-LN_v (B), whereas mexilitine blocked nicotinic Ca^{2+} and cAMP responses completely in the s- (C,D) and l-LN_v (E,F).

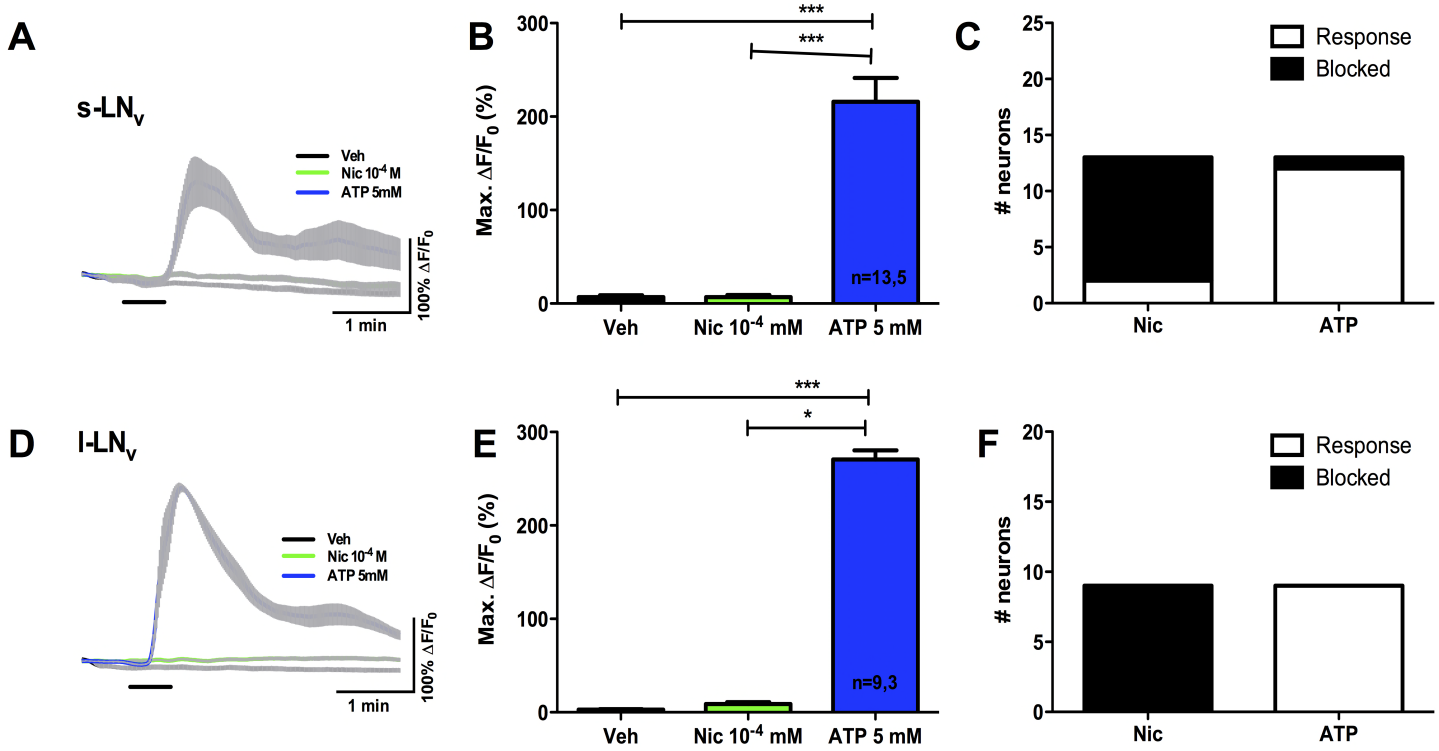

Figure 6.3. Compatibility of d-tubocurarine, a nicotinic acetylcholine receptor antagonist, with GCaMP imaging and P2X2/ATP neuronal activation. All experiments were done using 50 uM d-tubocurarine, a blocker of nicotinic channels, in the perfusion and stimulating compound. Flies used for this experiment expressed P2X2 and GCaMP3.0 in the PDF neurons (*Pdf-Gal4; UAS-GCaMP3.0/+; UAS-P2X2/+*). In the presence of d-tubocurarine, 5 mM ATP was able to elicit an increase in Ca^{2+} by P2X2 (blue) activation in the s-and l-LN_v whereas 10^{-4} M nicotine was not (green)(A-F). Higher doses of tubocurarine also blocked the ATP response.

6.7 REFERENCES

Agosto J, Choi JC, Parisky KM, Stilwell G, Rosbash M, Griffith LC. Modulation of GABAA receptor desensitization uncouples sleep onset and maintenance in Drosophila. *Nat. Neurosci.* 11: 354–359, 2008.

Akerboom J, Chen T-W, Wardill TJ, Tian L, Marvin JS, Mutlu S, Calderón NC, Esposti F, Borghuis BG, Sun XR, Gordus A, Orger MB, Portugues R, Engert F, Macklin JJ, Filosa A, Aggarwal A, Kerr RA, Takagi R, Kracun S, Shigetomi E, Khakh BS, Baier H, Lagnado L, Wang SS-H, Bargmann CI, Kimmel BE, Jayaraman V, Svoboda K, Kim DS, Schreiter ER, Looger LL. Optimization of a GCaMP calcium indicator for neural activity imaging. *J. Neurosci. Off. J. Soc. Neurosci.* 32: 13819–13840, 2012.

Albrecht U, Sun ZS, Eichele G, Lee CC. A differential response of two putative mammalian circadian regulators, mper1 and mper2, to light. *Cell* 91: 1055–1064, 1997.

Blanchardon E, Grima B, Klarsfeld A, Chélot E, Hardin PE, Préat T, Rouyer F. Defining the role of Drosophila lateral neurons in the control of circadian rhythms in motor activity and eclosion by targeted genetic ablation and PERIOD protein overexpression. *Eur. J. Neurosci.* 13: 871–888, 2001.

Buchner E, Buchner S, Burg MG, Hofbauer A, Pak WL, Pollack I. Histamine is a major mechanosensory neurotransmitter candidate in Drosophila melanogaster. *Cell Tissue Res.* 273: 119–125, 1993.

Cao G, Nitabach MN. Circadian control of membrane excitability in Drosophila melanogaster lateral ventral clock neurons. *J. Neurosci. Off. J. Soc. Neurosci.* 28: 6493–6501, 2008.

Cao G, Platisa J, Pieribone VA, Raccuglia D, Kunst M, Nitabach MN. Genetically targeted optical electrophysiology in intact neural circuits. *Cell* 154: 904–913, 2013.

Chung BY, Kilman VL, Keath JR, Pitman JL, Allada R. The GABA(A) receptor RDL acts in peptidergic PDF neurons to promote sleep in Drosophila. *Curr. Biol. CB* 19: 386–390, 2009.

Dahdal D, Reeves DC, Ruben M, Akabas MH, Blau J. Drosophila pacemaker neurons require g protein signaling and GABAergic inputs to generate twenty-four hour behavioral rhythms. *Neuron* 68: 964–977, 2010.

Gmeiner F, Kołodziejczyk A, Yoshii T, Rieger D, Nässel DR, Helfrich-Förster C. GABA(B) receptors play an essential role in maintaining sleep during the second half of the night in Drosophila melanogaster. *J. Exp. Biol.* 216: 3837–3843, 2013.

Hamada FN, Rosenzweig M, Kang K, Pulver SR, Ghezzi A, Jegla TJ, Garrity PA. An internal thermal sensor controlling temperature preference in Drosophila. *Nature* 454: 217–220, 2008.

Hamasaka Y, Wegener C, Nässel DR. GABA modulates Drosophila circadian clock neurons via GABAB receptors and decreases in calcium. *J. Neurobiol.* 65: 225–240, 2005.

Helfrich-Förster C, Edwards T, Yasuyama K, Wisotzki B, Schneuwly S, Stanewsky R, Meinertzhagen IA, Hofbauer A. The extraretinal eyelet of Drosophila: development, ultrastructure, and putative circadian function. *J. Neurosci. Off. J. Soc. Neurosci.* 22: 9255–9266, 2002.

Helfrich-Förster C, Homberg U. Pigment-dispersing hormone-immunoreactive neurons in the nervous system of wild-type Drosophila melanogaster and of several mutants with altered circadian rhythmicity. *J. Comp. Neurol.* 337: 177–190, 1993.

Helfrich-Förster C, Stengl M, Homberg U. Organization of the circadian system in insects. *Chronobiol. Int.* 15: 567–594, 1998.

Helfrich-Förster C, Winter C, Hofbauer A, Hall JC, Stanewsky R. The circadian clock of fruit flies is blind after elimination of all known photoreceptors. *Neuron* 30: 249–261, 2001.

Helfrich-Förster C, Yoshii T, Wülbeck C, Grieshaber E, Rieger D, Bachleitner W, Cusamano P, Rouyer F. The lateral and dorsal neurons of Drosophila melanogaster: new insights about their morphology and function. *Cold Spring Harb. Symp. Quant. Biol.* 72: 517–525, 2007.

Helfrich-Förster C. The period clock gene is expressed in central nervous system neurons which also produce a neuropeptide that reveals the projections of circadian pacemaker cells within the brain of Drosophila melanogaster. *Proc. Natl. Acad. Sci. U. S. A.* 92: 612–616, 1995.

Helfrich-Förster C. Development of pigment-dispersing hormone-immunoreactive neurons in the nervous system of Drosophila melanogaster. *J. Comp. Neurol.* 380: 335–354, 1997.

Helfrich-Förster C. Neurobiology of the fruit fly's circadian clock. *Genes Brain Behav.* 4: 65–76, 2005.

Hong S-T, Bang S, Paik D, Kang J, Hwang S, Jeon K, Chun B, Hyun S, Lee Y, Kim J. Histamine and its receptors modulate temperature-preference behaviors in Drosophila. *J. Neurosci. Off. J. Soc. Neurosci.* 26: 7245–7256, 2006.

Kaushik R, Nawathean P, Busza A, Murad A, Emery P, Rosbash M. PER-TIM interactions with the photoreceptor cryptochrome mediate circadian temperature responses in Drosophila. *PLoS Biol.* 5: e146, 2007.

Lelito KR, Shafer OT. Reciprocal cholinergic and GABAergic modulation of the small ventrolateral pacemaker neurons of Drosophila's circadian clock neuron network. *J. Neurophysiol.* 107: 2096–2108, 2012.

Lin JY, Knutsen PM, Muller A, Kleinfeld D, Tsien RY. ReaChR: a red-shifted variant of channelrhodopsin enables deep transcranial optogenetic excitation. *Nat. Neurosci.* 16: 1499–1508, 2013.

Littleton JT, Ganetzky B. Ion channels and synaptic organization: analysis of the Drosophila genome. *Neuron* 26: 35–43, 2000.

McCarthy EV, Wu Y, Decarvalho T, Brandt C, Cao G, Nitabach MN. Synchronized bilateral synaptic inputs to Drosophila melanogaster neuropeptidergic rest/arousal neurons. *J. Neurosci. Off. J. Soc. Neurosci.* 31: 8181–8193, 2011.

Melzig J, Buchner S, Wiebel F, Wolf R, Burg M, Pak WL, Buchner E. Genetic depletion of histamine from the nervous system of Drosophila eliminates specific visual and mechanosensory behavior. *J. Comp. Physiol. [A]* 179: 763–773, 1996.

Murata Y, Iwasaki H, Sasaki M, Inaba K, Okamura Y. Phosphoinositide phosphatase activity coupled to an intrinsic voltage sensor. *Nature* 435: 1239–1243, 2005.

Nikolaev VO, Bünemann M, Hein L, Hannawacker A, Lohse MJ. Novel single chain cAMP sensors for receptor-induced signal propagation. *J. Biol. Chem.* 279: 37215–37218, 2004.

O'Neill JS, Maywood ES, Chesham JE, Takahashi JS, Hastings MH. cAMP-dependent signaling as a core component of the mammalian circadian pacemaker. *Science* 320: 949–953, 2008.

Olsen SR, Wilson RI. Cracking neural circuits in a tiny brain: new approaches for understanding the neural circuitry of Drosophila. *Trends Neurosci.* 31: 512–520, 2008.

Parisky KM, Agosto J, Pulver SR, Shang Y, Kuklin E, Hodge JJL, Kang K, Kang K, Liu X, Garrity PA, Rosbash M, Griffith LC. PDF cells are a GABA-responsive wake-promoting component of the Drosophila sleep circuit. *Neuron* 60: 672–682, 2008.

Pírez N, Christmann BL, Griffith LC. Daily rhythms in locomotor circuits in Drosophila involve PDF. *J. Neurophysiol.* 110: 700–708, 2013.

Renn SC, Park JH, Rosbash M, Hall JC, Taghert PH. A pdf neuropeptide gene mutation and ablation of PDF neurons each cause severe abnormalities of behavioral circadian rhythms in Drosophila. *Cell* 99: 791–802, 1999.

Rieger D, Shafer OT, Tomioka K, Helfrich-Förster C. Functional analysis of circadian pacemaker neurons in Drosophila melanogaster. *J. Neurosci. Off. J. Soc. Neurosci.* 26: 2531–2543, 2006.

Rieger D, Stanewsky R, Helfrich-Förster C. Cryptochrome, compound eyes, Hofbauer-Buchner eyelets, and ocelli play different roles in the entrainment and masking pathway of the locomotor activity rhythm in the fruit fly Drosophila melanogaster. *J. Biol. Rhythms* 18: 377–391, 2003.

Rietveld WJ, Minors DS, Waterhouse JM. Circadian rhythms and masking: an overview. *Chronobiol. Int.* 10: 306–312, 1993.

Shafer OT, Kim DJ, Dunbar-Yaffe R, Nikolaev VO, Lohse MJ, Taghert PH. Widespread receptivity to neuropeptide PDF throughout the neuronal circadian clock network of Drosophila revealed by real-time cyclic AMP imaging. *Neuron* 58: 223–237, 2008.

Shang Y, Griffith LC, Rosbash M. Light-arousal and circadian photoreception circuits intersect at the large PDF cells of the Drosophila brain. *Proc. Natl. Acad. Sci. U. S. A.* 105: 19587–19594, 2008.

Shang Y, Haynes P, Pírez N, Harrington KI, Guo F, Pollack J, Hong P, Griffith LC, Rosbash M. Imaging analysis of clock neurons reveals light buffers the wake-promoting effect of dopamine. *Nat. Neurosci.* 14: 889–895, 2011.

Shearman LP, Zylka MJ, Weaver DR, Kolakowski LF Jr, Reppert SM. Two period homologs: circadian expression and photic regulation in the suprachiasmatic nuclei. *Neuron* 19: 1261–1269, 1997.

Sheeba V, Fogle KJ, Kaneko M, Rashid S, Chou Y-T, Sharma VK, Holmes TC. Large Ventral Lateral Neurons Modulate Arousal and Sleep in Drosophila. *Curr. Biol.* 18: 1537–1545, 2008a.

Sheeba V, Gu H, Sharma VK, O'Dowd DK, Holmes TC. Circadian- and light-dependent regulation of resting membrane potential and spontaneous action potential firing of Drosophila circadian pacemaker neurons. *J. Neurophysiol.* 99: 976–988, 2008b.

Soderlund D. Sodium Channels. In: *Comprehensive Molecular Insect Science*, edited by Gibert L, Latrou K, Gill S. Amsterdam: Elsevier, 2005.

Stoleru D, Peng Y, Agosto J, Rosbash M. Coupled oscillators control morning and evening locomotor behaviour of Drosophila. *Nature* 431: 862–868, 2004.

Tian L, Hires SA, Mao T, Huber D, Chiappe ME, Chalasani SH, Petreanu L, Akerboom J, McKinney SA, Schreiter ER, Bargmann CI, Jayaraman V, Svoboda K, Looger LL. Imaging neural activity in worms, flies and mice with improved GCaMP calcium indicators. *Nat. Methods* 6: 875–881, 2009.

Tischkau SA, Gallman EA, Buchanan GF, Gillette MU. Differential cAMP Gating of Glutamatergic Signaling Regulates Long-Term State Changes in the Suprachiasmatic Circadian Clock. *J. Neurosci.* 20: 7830–7837, 2000.

Travnickova-Bendova Z, Cermakian N, Reppert SM, Sassone-Corsi P. Bimodal regulation of mPeriod promoters by CREB-dependent signaling and CLOCK/BMAL1 activity. *Proc. Natl. Acad. Sci. U. S. A.* 99: 7728–7733, 2002.

Veleri S, Brandes C, Helfrich-Förster C, Hall JC, Stanewsky R. A self-sustaining, light-entrainable circadian oscillator in the Drosophila brain. *Curr. Biol. CB* 13: 1758–1767, 2003.

Veleri S, Rieger D, Helfrich-Förster C, Stanewsky R. Hofbauer-Buchner eyelet affects circadian photosensitivity and coordinates TIM and PER expression in Drosophila clock neurons. *J. Biol. Rhythms* 22: 29–42, 2007.

Wegener C, Hamasaka Y, Nässel DR. Acetylcholine increases intracellular Ca2+ via nicotinic receptors in cultured PDF-containing clock neurons of Drosophila. *J. Neurophysiol.* 91: 912–923, 2004.

Wilsbacher LD, Yamazaki S, Herzog ED, Song E-J, Radcliffe LA, Abe M, Block G, Spitznagel E, Menaker M, Takahashi JS. Photic and circadian expression of luciferase in mPeriod1-luc transgenic mice invivo. *Proc. Natl. Acad. Sci. U. S. A.* 99: 489–494, 2002.

Yao Z, Macara AM, Lelito KR, Minosyan TY, Shafer OT. Analysis of functional neuronal connectivity in the Drosophila brain. *J. Neurophysiol.* 108: 684–696, 2012.

Yasuyama K, Meinertzhagen IA. Extraretinal photoreceptors at the compound eye's posterior margin in Drosophila melanogaster. *J. Comp. Neurol.* 412: 193–202, 1999.

Yoshii T, Vanin S, Costa R, Helfrich-Förster C. Synergic entrainment of Drosophila's circadian clock by light and temperature. *J. Biol. Rhythms* 24: 452–464, 2009.